Interacting with consciousness: An investigation into the neural signatures of conscious processing using the global-local auditory task

A THESIS SUBMITTED TO
THE UNIVERSITY OF KENT AT CANTERBURY
IN THE SUBJECT OF COMPUTER SCIENCE
FOR THE DEGREE OF
DOCTOR OF PHILOSOPHY

By
Jennifer Ann Cooke

September 2016

Abstract

Can conscious processing be inferred from electrophysiological measurements?

Bekinschtein et al. (2009) devised the global-local auditory oddball task as a way of investigating electrophysiological (EEG) responses to hierarchical violations in auditory regularity. It was argued that the detection of local violations in auditory regularity (arising within a short temporal window) occurs independently of consciousness, whilst the detection of global violations in auditory regularity (arising within a longer temporal window) occurs only with the presence of consciousness. For this to be the case, global and local effects must be assumed to be independent and thus share an additive relationship. Crucially, if a relationship is additive, then cognitive subtraction allows each effect to be understood in isolation. Within this thesis, we explore the notion that global and local effects may not be independent but actually share a multiplicative relationship, based on the principle that the brain is a non-linear system (Friston et al., 1996). We examine this by re-analysing the data of the original attention study by Bekinschtein et al. (2009) using a factorial design analysis. What is more, we extend this work to consider the presence of an interaction between global and local effects when consciousness is manipulated using healthy sedation. Our findings reveal an interaction between global and local effects that occurs within the region of the global effect and varies depending on the presence of direct attention, expectancy and sedation. The manifestation of an interaction between global and local effects is discussed in detail in relation to a predictive coding framework, whereby multiple levels of prediction exist within the brain (Auksztulewicz & Friston, 2015). Furthered analysis, directly comparing the findings of varied attention to the findings with healthy sedation is presented and discussed with a view to the brain's predictive nature. Methodological issues that were encountered, as well as a method we developed for re-aligning time-series data, are presented and explored in detail within the later Chapters of this thesis. Our research suggests that global and local effects may not be considered as independent and therefore the presence of a global effect is not sufficient to constitute a functionally isolated marker of conscious processing (as initially proposed by Bekinschtein et al. [2009]). Further research is necessary to better define the nature of an interaction between global and local effects in relation to conscious experience.

Table of Contents

List of Figures

List of Tables

Acknowledgements

I would first and foremost like to thank my supervisor Professor Howard Bowman for encouraging my interest in Computer Science during his module on Cognitive Neural Networks. Without his tutelage, I would not have had the confidence to pursue doctoral study in the School of Computing. Moreover, I would also like to thank my co-supervisor Dr Caroline Li for her support and instruction over the past five years.

Of paramount importance is my express gratitude to Dr Tristan Bekinschtein, who devised the global-local auditory task at the Cognition and Brain Sciences Unit (CBU) in Cambridge and who very kindly shared his data with us. I would also like to extend this gratitude to Dr Srivas Chennu, also at the CBU, who provided us with much needed guidance and professional insight. Without their hard work, this PhD would not exist.

Many thanks must also go to the School of Computing administration team, for their enduring support over the past five years. In particular, Sonnary Dearden, Sarah Whitfield, Angie Allen, Julie Teulings, Angela Doe and Sandra Shine, whose kindness and warm professionalism have been integral to my ability to fulfil my duties here in the department.

It would also be remiss of me not to mention and thank my fellow PhD students, with whom I have shared an office and the occasional beer, Dr Abdulmajeed Alsufyani, Dr Jumana Ahmad, Dr Marco Filletti, Alexia Zoumpoulaki, Dr Luise Gootjes-Dreesbach, George Parish, William Jones, Adrien Witon and my close friend and colleague Dr Amirali Shirazibeheshti. You have all been such a great source of support to me throughout my PhD and I can only hope that I will be fortunate enough to work with such talented individuals in the future.

Lastly, but certainly not least, I would like to dedicate this thesis to my long suffering parents, Frank and Margaret Cooke, who have instilled within me the value of hard work and the importance of a good education. You have always been there to love and encourage me through all of my academic endeavours, and for that I am eternally

grateful. This thesis, and all of my hard work over the past 5 years, I dedicate to you as both my greatest source of support and my greatest source of inspiration. Most importantly, I grant you my word, that now I will find myself a '*proper*' job.

1. Introduction

The extent to which conscious processing can be inferred from neurophysiological measurements is a pivotal question for modern neuroscience. We introduce this thesis as an investigation into the neural markers of conscious processing when evaluating electrophysiological responses from the human brain. Our fundamental motivation centers on the clinical relevance of such neural markers to Disorders of Consciousness (DoC), where the presence of conscious processing may be detected using neuroimaging techniques, specifically Electroencephalography (EEG). Within this thesis, we pay particular attention to the statistical analysis of EEG data using the statistical parametric mapping (SPM) approach, and also the presence of a statistical interaction between two effects that arises in response to a multi-level auditory oddball task. In the subsequent Chapters of this thesis, we explore the presence of such an interaction and discuss how it may support recent evidence that points to the existence of hierarchical predictive systems within the human brain.

The brain

The brain is arguably the most complex structure in the human body, consisting of an estimated 78 to 94 billion neurons (Azevedo, Carvalho & Grinberg, 2009). A neuron is a nerve cell, which processes and transmits electrical and chemical signals. When groups of neurons connect together, this is known as a neural network. Neurons within the brain and the spinal cord are the core component of the Central Nervous System (CNS), which transmits signals throughout the entire body. Each neuron has three main components: soma, dendrites and axon. The soma is the body of the nerve cell that contains the nucleus, whilst the dendrites are branch-like structures, which receive input from other connecting neurons. The axon acts as a channel through which electrical impulses are propagated and subsequently diffused across a synapse (small gap between neurons) to be received by other connecting neurons (see Figure 1.1). The number of connections made by a single neuron can be as many as 10,000 (Alonso-Nanclares, Gonsalez-Soriano, Rodriguez & DeFelipe, 2008).

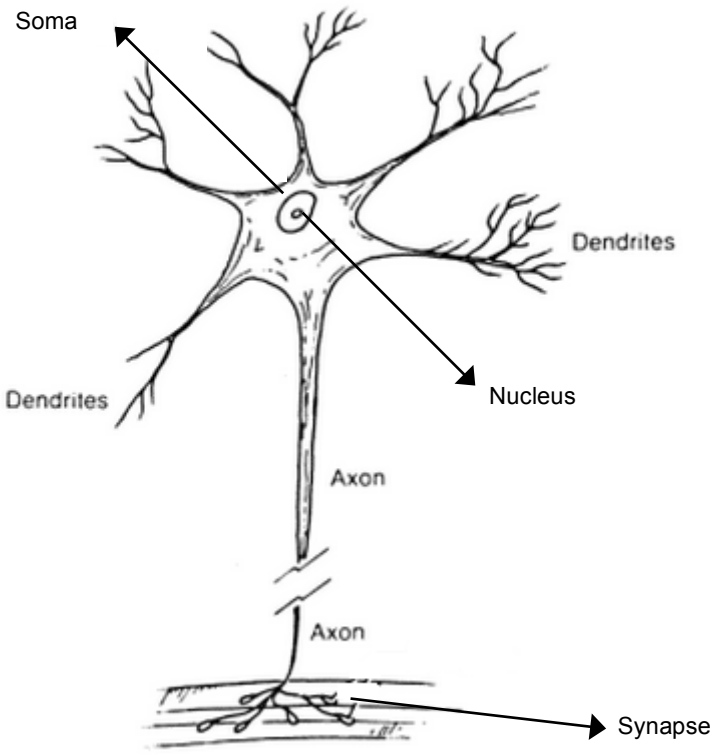

Figure 1.1. Illustration of a neuron.

The cerebral cortex is the outer layer of the brain where the aforementioned electrophysiological signals are transmitted. The neocortex constitutes 94% of the total cerebral cortex. The neocortex is made up of six layers (layers I-VI) and is approximately 2-4mm thick. More than half of the neocortex (around 55%) is involved in visual processing, whilst 11% is allocated to somatosensory processing, 8% to motor processing, and 3% to auditory processing (Felleman & Van Essen, 1991).

The high density of neural networks within the brain means that information is processed in a parallel architecture, as opposed to a serial architecture (O'Reilly & Munakata, 2000). As a result, there is an unknown number of computations taking place in the brain at any given time; this makes modelling neural processes very complicated. In order to evaluate patterns of activity in the brain, it is necessary to undertake controlled experiments using neuroimaging techniques that can capture neural activity in response to specific stimuli.

Neuroimaging techniques

Psychology has typically relied on behavioural measurements as a means of determining cognition. However, the advent of modern neuroimaging techniques, such as functional Magnetic Resonance Imaging (fMRI), Electroencephalography (EEG), Magnetoencephalography (MEG) and Positron Emission Tomography (PET), has changed the landscape of research in cognitive science. Whist behavioural measurements can provide evidence about the way in which individuals act upon their thought processes, measuring neural activity can provide the possibility of observing the thought processes themselves; this really provides a deeper insight into the functional mechanisms underlying human behaviour and in particular, human consciousness.

The use of EEG to investigate neural activity in clinical contexts is rising, most likely because it is a cheaper, less invasive and portable alternative to fMRI. First introduced by Berger in 1929, EEG is a method for detecting electrophysiological responses from the brain by placing electrodes on the scalp (Tudor, Tudor & Tudor, 2005). Inference can be drawn from data collected using EEG in relation to the way an individual is processing a task. The nature of such processing may inform researchers about the conscious state of an individual; what is more, it opens the possibility that one may be able to determine a neural marker of conscious processing.

Consciousness

Western philosophers, including Decartes and Locke, have typically debated the properties of consciousness. Some key concerns include the way in which language can be used to define the concept of consciousness and whether consciousness can be defined mechanistically. The concept of consciousness has also been debated within the field of Psychology, where types of consciousness have been established, that is, access consciousness (to have access to one's own thoughts) and phenomenological consciousness (to experience without access to the information) (Block, 2005). It has been argued that access consciousness can be defined mechanistically, whilst phenomenological consciousness cannot, and therefore represents the 'hard problem of consciousness' (Chalmers, 1995). Consequently, neuroimaging techniques, which detect

patterns of neural activity relating to processes such as perception and attention may inform the way in which we understand the conscious processing of information in humans. Nevertheless, one should also be mindful of the possible limitations of quantitative research in relation to the subjective experience of consciousness. Many consider the cohesive phenomenon of the subjective conscious experience to transcend the sum of its component parts (ie. cognitive mechanisms); thus, to this day, a universally accepted definition of consciousness remains a point for debate.

Objectives

This thesis will explore how conscious experience interfaces with prediction in the human brain, and in particular, multiple levels of prediction. Our main focus will be on how interaction between levels of prediction manifest in the brain's electrical response to an auditory oddball task. In addition, we will investigate how these responses are modulated by the presence or absence of direct attention and wakefulness.

Thesis structure

At this point, we will outline the content of this thesis by briefly introducing each Chapter:

Chapter 1. We introduce a background to our research and discuss DoC, as well as theories of consciousness in the context of cognitive neuroscience and electroencephalography (EEG). We arrive finally at our experimental hypotheses, which are informed by the existing research we outline in this Chapter.

Chapter 2. Before presenting our research, we discuss in detail, the statistics that underlie our analyses shown in Chapters 3, 4, 5 & 6. The meaning of an interaction is explored and supported with preliminary findings.

Chapter 3. A re-analysis of an existing EEG dataset (collected by Bekinschtein et al., 2009) in relation to attention and the processing of an auditory oddball task (namely the global-local task, which is explained in more detail within Chapters 1 & 3) is presented,

taking into account interactions between effects, which have not previously been explored in detail. Findings are discussed within a predictive coding framework of human cognition (the theory of which is also outlined in Chapters 1 & 3).

Chapter 4. We expand upon the findings in Chapter 3 to conduct a simple effects analysis, further exploring the nature of an interaction between effects in relation to attention.

Chapter 5. Having considered attention, we transition to consider consciousness as wakefulness and explore the implications of healthy sedation on responses to the auditory oddball task. Again, an interaction between effects is explored using EEG responses, and simple effects analysis reveals the nature of this interaction in the sedated vs. the recovered brain.

Chapter 6. Findings from the study of attention (in Chapters 3 & 4) are directly compared to the findings of the study with sedation (Chapter 5) in an exploratory analysis. Findings are tentatively presented with focus specifically on a discussion around the possible implications of an interaction between effects that varies by the direction of attention, the level of sedation and the composition of the auditory task. We consider once again how findings may be interpreted within a predictive coding framework, and also the complex hierarchical nature of brain responses, which complicates the detection of an isolated neural marker of human consciousness.

Chapter 7. Within the final research Chapter, we present a method for re-aligning time-series data (EEG data) when discontinuity within the time-series occurs. This Chapter addresses a methodological issue that we encountered within the early stages of data pre-processing and is included for reasons of transparency, but also because we feel the method has a wider utility to the field of EEG research.

Discussion. We outline, in sum, the findings of our research and discuss their relevance to the wider clinical context of DoC. Key findings are highlighted, along with a review of our central hypotheses and an overall conclusion to the work. We close by presenting possible future directions for the research.

Contributions and collaborations

The research presented in this thesis benefited from collaboration within our research group based in the School of Computing at the University of Kent. All data for the analyses presented within this thesis was collected and provided by our external collaborators at the Cognition and Brain Sciences Unit (CBU) in Cambridge, namely Dr Tristan Bekinschtein and Dr Srivas Chennu. Chapters 3 and 4 contain analyses conducted by myself in collaboration with my colleague Dr Amirali Shirazibeheshti, which is currently undergoing preparation for submission and publication.

Dr Ram Adapa and Dr David Menon from the Division of Anaesthesia at the University of Cambridge supervised drug administration, which contributed to the study in Chapter 5. My colleague, Dr Amirali Shirazibeheshti, conducted the pre-processing and data preparation for the analysis in Chapter 5, with statistical analysis performed by myself.

2. Defining consciousness with a clinical purpose: states of minimal consciousness, psychological theory and neural markers in cognitive neuroscience

The human conscious experience has been debated for centuries; a once philosophical discussion around abstract concepts has now become a scientific exploration into the human brain (Baars, 1988; Crick & Koch, 1990; Koch, 2004). In an attempt to better understand the most fundamental part of the human psyche, Cognitive Neuroscience and Philosophical thought have evolved to focus on patterns of brain activity as a means of establishing the source, or at least a marker, of human consciousness.

To further explore this topic, we firstly present the clinical context of Disorders of Consciousness (DoC) and discuss the relevance of studying conscious processing for this purpose. We then focus on the neuroimaging technique of Electroencephalography (EEG) as a method for detecting neural correlates of consciousness in the human brain. Subsequently, we introduce an auditory oddball task, devised by Bekinschtein, Dehaene, Rohaut, Tadel, Cohen, & Naccache (2009) (the global-local task), which has been used to investigate specific EEG components in connection with conscious processing. Lastly, we present and discuss relevant theories from Philosophy and Psychology that inform the scientific study of human consciousness in this context, and consider the most recent findings in relation to the global-local task to arrive at a set of central hypotheses upon which this thesis is based.

Disorders of Consciousness (DoC)

One way to examine human conscious processing is to consider pathologies of consciousness, specifically patients with Disorders of Consciousness (DoC). Patients with a DoC most commonly have sustained some form of traumatic head injury (referred to as Traumatic Brain Injury [TBI]). However, in some cases patients may be rendered unable to communicate through a loss of physical function as the result of

neurodegeneration. Diseases such as Amyotrophic Lateral Sclerosis (ALS) (a form of Motor Neuron Disease [MND]) can lead to 'locked-in' syndrome whereby patients lose motor function gradually whilst retaining mental faculty. Sadly, patients within this state may maintain some level of capacity to think about, and experience, the world around them whilst having very little or no means of physical or verbal communication (Boly, Faymonville, Schnakers, Peigneux, Lambermont, Phillips, Lancellotti, Luxen, Lamy, Moonen, Maquet & Laureys, 2008; Giacino, Ashwal, Childs, Cranford, Jennett, Katz, Kelly, Rosenberg, Whyte, Zafonte & Zasler, 2002).

By definition, a DoC is characterized as any medical condition that inhibits consciousness, most commonly a coma state inflicted by traumatic brain injury (TBI). Conditions that transiently interrupt consciousness are not considered to be DoC, for example epilepsy or dementia. With regard to clinical diagnosis, patients with a DoC are placed into one of two main categories: Vegetative State (VS), that is awake but not aware, or Minimally Conscious State (MCS), which is awake and transiently aware. Due to the obvious incapability of patients to self-report, practitioners rely heavily on Neuroimaging techniques such as functional Magnetic Resonance Imaging (fMRI) along with behavioural observations to make inference about a patient's conscious state. The highly subjective nature of diagnosis may be open to error as behaviour can vary substantially between patients and there is no widely accepted indicator of conscious processing against which responses can be compared. Furthermore, the criterion for diagnosis varies across countries and even within countries in some cases (eg. North America); thus, the successful diagnosis and treatment of these cases can be difficult to achieve.

Currently, around 40% of patients are misdiagnosed as VS when they are actually minimally conscious (Giacino et al., 2002). It may be the case that practitioners underestimate a patient's level of consciousness and as a result, do not to meet their needs, particularly regarding pain management (Boly, Faymonville, Peigneux, Lambermont, Damas, Luxen, Lamy, Moonen, Maquet & Laureys, 2005; Boly et al., 2008). Successful diagnosis currently relies heavily upon the expertise of the medical professional, which can be highly variable. Therefore, the consideration of neural markers in electrophysiology may bridge the gap between the conscious experience and that which can be objectively measured in order to reduce the likelihood of misdiagnosis

in these cases. With advancing technology it is possible to use Electroencephalography (EEG) to record brain activity, or lack thereof, in people within low awareness states (ie. minimally conscious patients); this could potentially provide an objective measure of conscious processing that would facilitate a dramatic improvement in quality of life for these patients. If one were to achieve this, then it becomes plausible that computational systems linked to brain activation could facilitate communication with individuals who may have formally been diagnosed as unconscious.

Electroencephalography (EEG), Event-Related Potentials (ERPs) and neural markers of conscious processing

Within this thesis, we explore conscious processing by considering electrophysiological responses in the brain, as measured by Electroencephalography **(**EEG). EEG involves placing electrodes on the scalp to detect electrical dipoles in the brain that are generated by collections of neuronal activity; much of the activation captured by this method comes from the cortex (outer layer of the brain). In comparison to neuroimaging techniques, such as functional Magnetic Resonance Imaging (fMRI), EEG has less spatial specificity but higher temporal resolution, meaning that although pinpointing regions in space may be less accurate with EEG than with fMRI, one can establish a more precise recording with respect to time. Furthermore, techniques for source localisation have been developed for EEG, whereby signals can be inverted to estimate their source(s) within the brain (Phillips, Mattout, Rugg, Maquet & Friston, 2005).

The placement of multiple electrodes on the scalp is referred to as an electrode array; such arrays can differ in size given the system one is using. EGI Geodesic sensor nets are commonly used in clinical research due to their ease of application. Figure 2.1 is the EGI Geodesic sensor net electrode array, demonstrating electrode placement on the scalp.

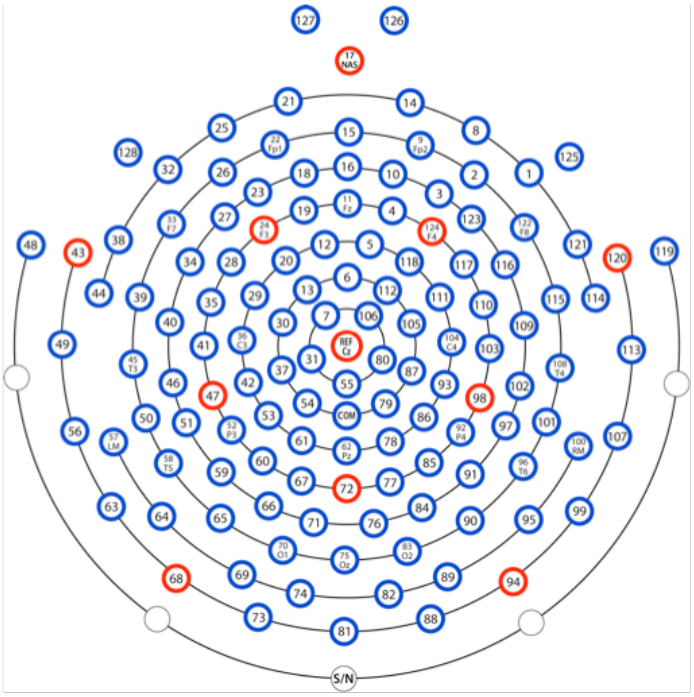

Figure 2.1. HydroCel™ Geodesic Sensor Net 128-Channel map (electrode array), illustrating electrode placement on the scalp. Note, in subsequent Chapters crown electrodes were eliminated from statistical analysis meaning that channel labels were re-assigned as per Appendix 2.

Within this thesis, we are particularly interested in Event-Related Potentials (ERPs) that have been linked to conscious processing. ERPs are the averaged EEG signal across a large number of identical trials that have been time locked to the onset of a particular stimulus. Thus, what is captured with an ERP is the signal evoked by a certain event (see Figure 2.2). There are certain peaks and troughs within the signal that have been characterised in relation to a number of cognitive processes; these are referred to as components. For example, the N400 is a negative peak occurring approximately 400ms after stimulus presentation, which has been linked to semantic language processing (Holcomb, 1993). Importantly, EEG responses may include a varying amount of electrical noise due to surrounding electrical equipment. What is more, movements from the individual themselves, such as eye-blinks, head or jaw movements will also result in patterns of activity within the data; these are referred to as artefacts. Artefacts are predominantly characterised and removed from data before it is analysed in an attempt to ensure that findings relate to the stimuli presented. Techniques such as Principal Components Analysis (PCA) and Independent Components Analysis (ICA) can be used to isolate and remove artefacts before filtering is applied to smooth the data.

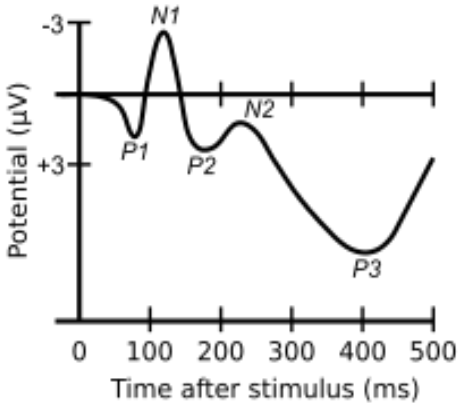

Figure 2.2. Example averaged ERP waveform. Note that positive voltages are plotted down within this figure and the reverse is true within Figure 2.3 (positive voltages are plotted up).

Two ERP components that have been linked to conscious processing are Mismatch Negativity (MMN) and the P300 (P3) (Bekinschtein et al., 2009). MMN (also known as the mismatch response) is thought to signify the recognition of incongruency, that is, the detection of deviant stimuli (Tiitinen, May, Reinikainen & Näätänen, 1994; Näätänen, Tervaniemi, Sussman, Paavilainen & Winkler, 2001). MMN occurs around frontal electrode Fz, approximately 150ms after stimulus presentation, and has been considered a pre-attentive response signalling the detection of deviancy (see Figure 2.3) (Bekinschtein et al., 2009). The implication of a pre-attentive response is that it is considered to occur independently of consciousness (awareness) (Tiitinen at al., 1994; Näätänen et al., 2001).

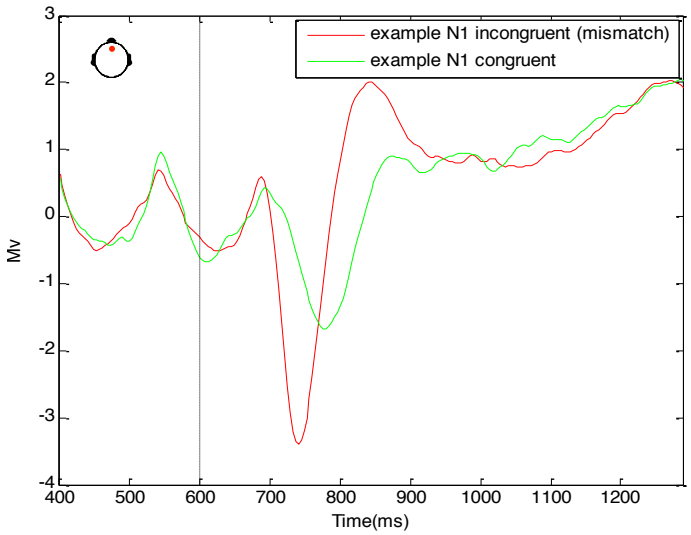

Figure 2.3. Example of N1 response to congruent stimulus (green line) and mismatch response to incongruent stimulus (red line) at electrode Fz. MMN can be measured as the difference between congruent and incongruent N1 responses. Stimulus presented at 600ms (therefore MMN is expected around 750ms). Note that positive voltages are plotted up within this figure and the reverse is true within Figure 2.2 (positive voltages are plotted down).

Arguably, there are two subcomponents within the MMN complex: an early negative component around frontal electrodes (ie. Fz), and a subsequent positive component appearing at central electrodes (ie. around Cz) (Näätänen, Paavilainen, Titinen, Jiang & Alho, 1993). The early negative component occurs initially in response to deviant stimuli, followed by the positive sub-component, which is considered in some cases to be linked to the P300 as a P3a response (Freidman, Cycowicz & Gaeta, 2001; Polich, 2007). This secondary positive response has been associated with the capture of wandering attention (Freidman, Cycowicz & Gaeta, 2001; Näätänen et al., 1993).

Furthermore, the P300 (P3) is a positive peak occurring around 250-700ms after stimulus presentation (see Figure 2.2). There are considered to be two subcomponents of the P3, namely the aforementioned P3a, and the P3b (Polich, 2007; Freidman, Cycowicz & Gaeta, 2001). The P3a is a short-lived positive peak around 250ms after stimulus presentation occurring at frontal/central electrode sites. As previously mentioned, it has been associated with the capture of attention, particularly by deviant stimuli (Polich, 2007; Freidman, Cycowicz & Gaeta, 2001). The P3b is a broad positive peak occurring at centro-posterior electrodes (principally Cz and Pz) and is associated with the updating and regulation of working memory (Morgan, Klein, Boehm, Shapiro, & Linden, 2008; Polich, 2007). Thus, the P3b is thought to involve higher-level cognitive processing, which has been linked to conscious perception (Bekinschtein et al., 2009). As a consequence, in opposition to the proposed pre-attentive nature of the MMN, typically consciousness is considered necessary for the presence of a P3b response (Bekinschtein et al., 2009).

In the next section, we introduce the global-local auditory task, which examines the presence of the MMN and P300 components in relation to the conscious processing of auditory regularity.

The global-local auditory task paradigm

Bekinschtein et al. (2009) devised an auditory irregularity paradigm, namely the global-local task, which can be used to examine the MMN and the P3b in relation to conscious processing. It was designed with the intention of detecting a neural marker of consciousness in patients with DoC, as it was argued that the presence of a P3b response may require a level of cognition that is only attainable when conscious (Bekinschtein et al., 2009).

The global-local task is comprised of both global and local violations of auditory regularity, meaning that deviancy can occur on two levels (local and/or global). This gives rise to four experimental conditions: global deviant local deviant (GDLD), global standard local standard (GSLS), global standard local deviant (GSLD) and global deviant local standard (GDLS) (see (a) (b) (c) and (d) in Figure 2.4).

During the task, tones are presented via headphones in quintuples, which are sets of five tones where the fifth tone is either the same or a different frequency to the preceding four tones (see Figure 2.4). In order to counter-balance the type of frequent stimulus presented (that is, the global regularity), two block types are introduced: XXXXX (XX) and XXXXY (XY) (see Figure 2.4). XX refers to a block where locally standard quintuples are the global regularity (ie. frequent stimulus), and XY refers to a block where locally deviant quintuples are the global regularity (see Figure 2.4). Tone frequency was also counter balanced (see box in bottom left of Figure 2.4).

At the beginning of a block, 20-30 frequently occurring quintuples are played to establish global regularity in an adaption phase (see Figure 2.4). After regularity has been established, globally standard quintuples (frequent stimulus) are delivered pseudorandomly 80% of the time, whereas globally deviant quintuples (infrequent stimulus) are presented only 20% of the time (see Figure 2.4).

Given that block type and tone frequency are both counter-balanced, altogether there are four possible block types: the aforementioned XX and XY, but also YY and YX, where standard and deviant tone frequencies are reversed. Each of these four blocks are

repeated and presented in a random order, so that 8 blocks are delivered in one experimental session.

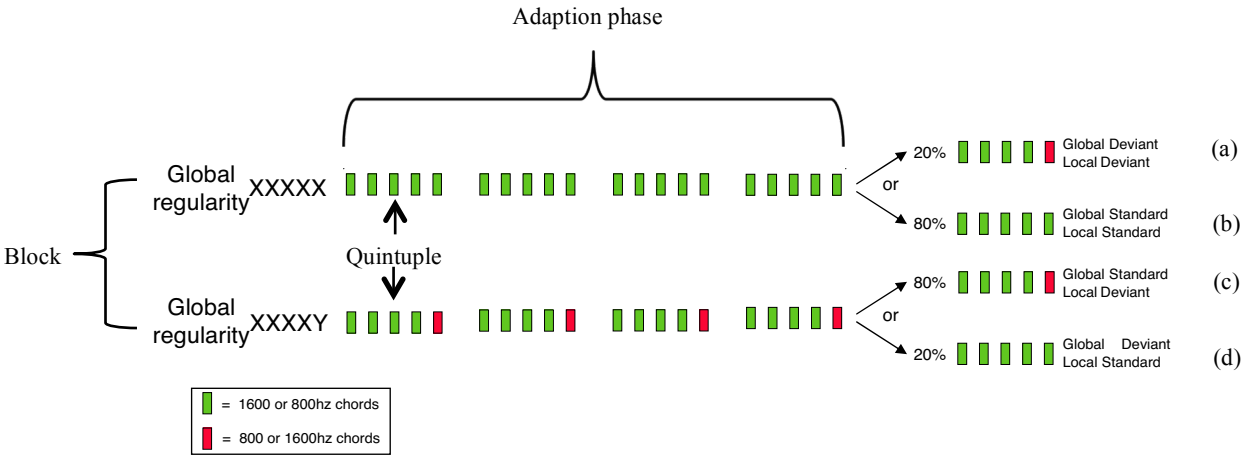

Figure 2.4. The global-local auditory task (Bekinschtein et al., 2009).

It was proposed by Bekinschtein et al. (2009) that local violations in auditory regularity would generate MMN, as a pre-attentive response to deviancy, which suggests that it may occur even in the absence of consciousness (as previously discussed). Thus, the presence of a local effect (local deviant response – local standard response) was considered to be independent of conscious processing (Bekinschtein et al., 2009).

In contrast, it was argued that global violations in auditory regularity require the maintenance of perceptual representations across time, given that global violations involve determining whether the current quintuple is deviant in the context of all quintuples within the block (Bekinschtein et al., 2009). Thus, detecting global deviance was argued to require consciousness, as it relies upon higher-level cognitive systems such as working memory (Bekinschtein at al., 2009).

The suggestion that the local effect may be independent of consciousness whilst the global effect may be dependent on consciousness appears to imply that the two effects are orthogonal. In order to sustain an orthogonal relationship between global and local effects then the relationship between the two should be additive, in other words, the two effects sit on top of one another (ie. are summed). However, some have proposed that the brain as an immensely interconnected non-linear system, the implication of which is

likely to be that we cannot consider activity to be a simple sum of all inputs (Friston, Price, Fletcher, Moore, Frackowiak & Dolan, 1996). Consequently, it may be the case that activity arises as a non-linear combination of inputs, suggesting the existence of a series of multiplicative relationships, whereby a complex network of interactions between areas (rather than parallel processes) constitutes the activity we observe on the scalp.

Typical analysis of the global-local task has, if only implicitly, assumed orthogonality of effects, ie. the performance of cognitive subtractions: local/global deviant – local/global standard. The trouble with cognitive subtraction, as proposed by Friston et al. (1996), is that it implies linearity that may not exist. Furthermore, it is argued that the most appropriate way to address possible non-linearity in neuroimaging data is to implement a factorial design analysis, which can account for interactions between effects (Friston et al., 1996). For this reason, we argue that it may be unlikely that global and local responses exist in isolation as independent effects.

It is important at this point to state that whilst it has been argued that brain responses are not simply the linear summation of all inputs (Friston et al., 1996), one cannot directly assume that this is reflected in a statistical analysis conducted at the scalp-level. It is therefore the case that the interpretation of findings made hereafter within this thesis are tentative and based heavily on the existing literature.

Bekinschtein et al. (2009) also explored the possibility that consciousness, or a lack thereof, may not be the only reason for the absence of a P3b response (or global response) to the global-local task. They investigated how varying states of attention in healthy controls may impact upon responses, as a lack of attention towards the task could result in a failure to detect global patterns of irregularity (Bekinschtein et al., 2009). Participants in this study were placed in to one of three attention conditions. The first group were asked to focus their attention on the task by counting the number of globally deviant tones they heard (active group). The second group were asked to perform a cognitively taxing visual task on a computer whilst the auditory task was played to them (interference group), and a third group were told to relax and "let their minds wander" whilst the auditory task was played to them (passive group) (Bekinschtein et al., 2009).

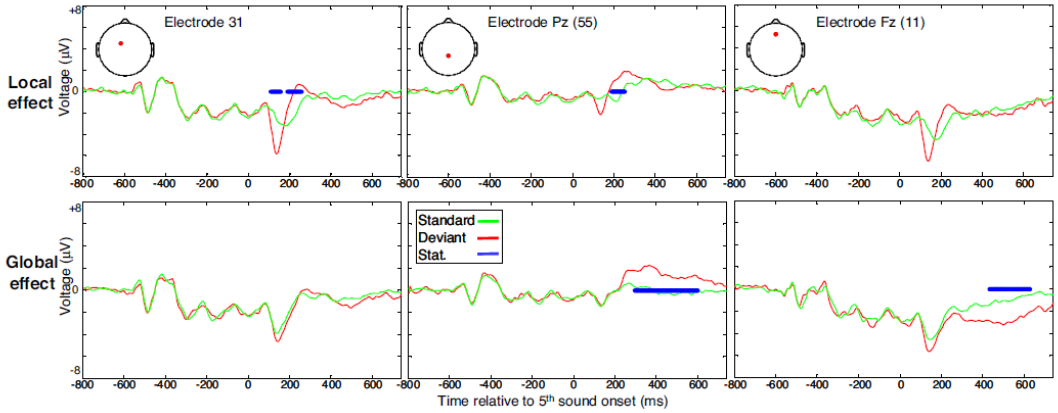

Figure 2.5. ERPs for global and local effects from the active counting group in Bekinschtein et al. (2009), at electrodes 31 (top & bottom left), Pz (top & bottom middle) and Fz (top & bottom right). Local effect is defined as local deviant – local standard, whilst the global effect is defined as global deviant – global standard. Blue lines labelled as Stat. indicate a region of statistical significance as defined by a t-test between standard (green lines) and deviant (red lines) conditions.

It was found that participants who completed the cognitively taxing visual task (interference) elicited no global effect (P3b) whatsoever, but did elicit a local effect (MMN). This suggests that fixing attention elsewhere led to participants failing to detect global violations of auditory regularity, whilst still detecting local violations (Bekinschtein et al., 2009). Those in the mind wandering group (passive) elicited a low amplitude global effect (P3b) but a marked local effect (MMN), implying that wandering attention may have been captured by instances of global deviancy in some cases, whilst local deviancy was more easily detected regardless of a wandering attentional state (Bekinschtein et al., 2009). Those whose attention was directed towards the task (active) elicited a large amplitude global effect (P3b) as well as a marked local effect (MMN) (see top left & middle bottom panel in Figure 2.5), suggesting that when attention is directed towards the task it enhances the size of the global response as attentional engagement with the task may increase the saliency of global deviance when individuals are actively counting the instances of global deviance they hear (Bekinschtein et al., 2009). The findings suggest that whilst MMN appears robust against manipulations of attention, the size of the P3b may be subject to varying attentional states (Bekinschtein et al., 2009).

In the following section we expand upon the current discussion to further explore considerations of auditory violation in relation to the MMN within the field of consciousness science.

Mismatch Negativity (MMN) within consciousness science

Beyond the work of Bekinschtein et al. (2009), others have considered the nature of varying responses to patterns of auditory irregularity. Näätänen (1992) and Näätänen, Jacobsen & Winkler (2005) argue that the habituation of neurons to the repetition of sounds can reduce N1 response size; this was referred to as a process of passive adaption (Näätänen, Jacobsen & Winkler, 2005). Moreover, passive adaption to standard patterns of sound (ie. identical tones or frequent patterns) has been considered to enhance the size of the mismatch response to deviance (ie. a deviant tone or infrequent patterns) relative to standard stimuli, if one is to consider such responses as reflecting echoic memory processes (Näätänen, Jacobsen & Winkler, 2005; Haenschel, Vernon, Dwivedi, Gruzelier & Baldeweg, 2005). Others have disputed the link between adaption and memory, suggesting that it may not be congruent with the physiology and time-scale of early responses in the brain (May & Tiitinen, 2010).

Furthermore, Haenschel et al. (2005) have suggested that pre-attentive echoic memory traces may be created when identical tones or consistent patterns of sound are presented; such memory traces are strengthened with increased repetition, which can subsequently increase the size of the MMN response to deviant stimuli relative to standard stimuli.

Recent work has reconsidered MMN in the context of predictions that the brain may make regarding incoming auditory information (Friston, 2010; Auksztulewicz & Friston, 2015). The theory of predictive coding suggests that hierarchical predictions within the brain are informed by the amount of prediction error between a predicted outcome and the actual outcome (Friston, 2010). Prediction error is argued to propagate up through a multi-layered hierarchy that reflects a temporal pathway of increasing cognitive complexity within the brain. Crucially, prediction error informs precision and allows for the adjustment of predictions to minimise error (Friston, 2010; Auksztulewicz & Friston, 2015).

Within the theory of predictive coding, MMN arguably reflects the amount of prediction error occurring and it has been shown that the size of the mismatch response to local deviance may decrease with repetition, when hierarchical violations of auditory regularity are introduced (as with the global-local task); this is because global

predictions of auditory regularity may adjust to incorporate new local patterns of sound (Wacongne, Labyt, Wassenhove, Bekinschtein, Naccache & Dehaene, 2011; Chennu, Noreika, Gueorguiev, Blenkmann, Kochen, Ibáñez, Owen & Bekinschtein, 2013).

Auksztulewicz & Friston (2015) have recently demonstrated that attention plays a vital role in predictive coding, that is, direct attention to incoming auditory information can enhance the size of MMN, suggesting that attentional engagement may be important earlier in the auditory processing pathway than previously thought. The findings somewhat speak against the supposedly pre-attentive nature of the MMN (Auksztulewicz & Friston, 2015; Tiitinen at al., 1994; Näätänen et al., 2001). Moreover, it has been suggested that attention and prediction may impact on early EEG responses (ie. MMN) in different ways, namely that attention may enhance the size of MMN, whilst prediction (that is expectation acquired through repetition) may diminish the size of the MMN. Distinguishing attention and prediction in the way proposed by Auksztulewicz & Friston (2015) is accounted for by weighting prediction errors by precision associated with attentional modulation; meaning that the size of responses will change as a function of attentional focus. It may therefore be the case that attention and expectancy (as formed through repetition) play a key role in the manifestation of MMN (Bekinschtein et al., 2009; Chennu et al., 2013; Auksztulewicz & Friston, 2015).

Theories of consciousness from Philosophy and Psychology

Momentarily moving away from neural markers of consciousness, within the current section we will introduce some of the relevant theories from Philosophy and Psychology that have informed the scientific study of consciousness to this point.

It has been argued that there are two neural correlates of consciousness, access consciousness (AC) and phenomenological consciousness (PC) (Block, 2005). In Block's (2005) view, AC refers to the ability to access one's own thoughts, feelings and emotional states. Arguably, the information is made readily available to a variety of cognitive processes including memory and reasoning (Block, 2005). Notably, it is proposed that an individual has *access* to the content of AC and is therefore immediately aware of the information it contains (Block, 1996). Importantly, although one has access

to the contents of AC, the cognitive systems that underlie processes such as memory, work implicitly and are therefore independent of conscious access. In other words, we are not conscious of information being committed to long-term memory, nevertheless in order for the information to be committed to long-term memory, it must first be made available to the relevant cognitive processes via AC (Block, 2005).

The notion of an abstract space in which information is made available to cognitive systems has also been explored within the literature on the Global Workspace (GWS) (Baars, 1988, 1996; Dehaene, Kerszberg, & Changeux, 1998). Dehaene, Kerszberg, & Changeux (1998) suggest that the information to which an individual has conscious access, is information that has conceptually succeeded in a winner-take-all competition between itself and other information (see Figure 2.6). Success in the competition is determined by the preferences and expectations of the individual (Dehaene, Kerszberg, & Changeux, 1998). Unlike Block's (2005) view of AC, GWS does not assume the autonomy of AC and PC, therefore conscious experience consists of the contents of GWS (Dehaene, Kerszberg, & Changeux, 1998).

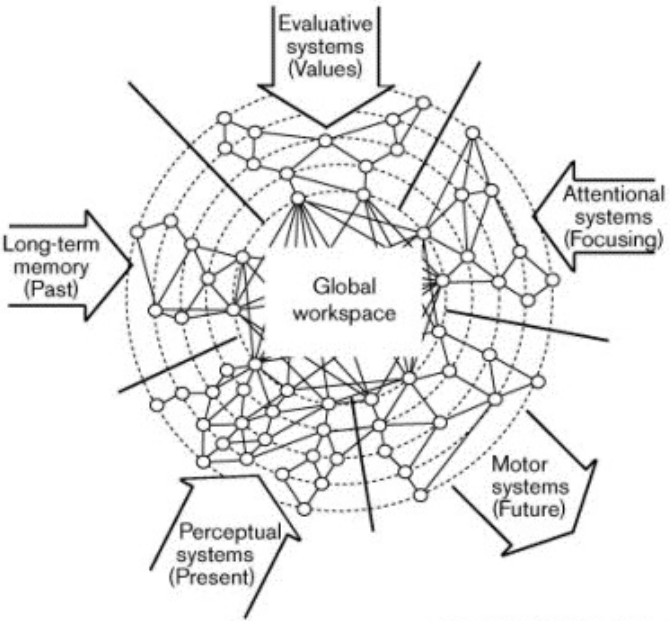

Figure 2.6. Model of Global Workspace (Gisiger, Dehaene, & Changeux. 2000).

The success of salient information within a competition over conscious access is based upon the concept that valance adds an inherent value to information (stimuli) that

monopolises attention allowing for conscious perception. Notably, Dehaene, Kerszberg, & Changeux (1998) propose conscious perception to be an integrative process involving high order cognition.

Interestingly, Block (2005) also argues for the existence of phenomenological consciousness (PC); PC refers to information held in consciousness that one does not have access to. Block (2005) suggests that information in PC was at one time accessible (ie. when perceived) and that it may be accessed again under the necessary circumstances. The existence of PC may explain why individuals are able to recognise information they were not aware they knew to a degree of accuracy above that of pure chance. Alternatively, there is some debate surrounding whether one can refer to PC as consciousness at all if indeed its contents cannot be accessed (Block, 2005). It has been argued that PC can only be defined by the existence of AC, given that it's definition relies upon an inherent inaccessibility (Dennett, 1978). Put another way, a conscious state that exists without access, could be considered as conceptually void if that to which one is conscious is that to which one has access (Dennett, 1978).

Furthermore, Rosenthal (2005) suggests that to be conscious is to be immediately aware of one's own internal state. Although, to be aware of one's own internal state can be viewed as part of the internal state itself, thus, immediacy is guaranteed (Rosenthal, 2005). Moreover, it is proposed that internal states may be conscious at one time, yet not at another (Block, 2005; Rosenthal, 2005). Consequently, when reporting one's own state of mind, the outcome will reflect the information to which one has access at the current time. The availability of information therefore, may vary over time (Rosenthal, 2005; Block, 2005). Nevertheless, Block (2005) maintains that AC and PC are dissociable concepts, which can be demonstrated via experimentation.

Within this thesis, we specifically consider the concepts of attention, perception and awareness in relation to the study of consciousness. Thus, within the next section we will explain in more detail what is meant by each concept.

Attention, perception and awareness

Within this thesis, we initially approach the term consciousness by considering the cognition that is thought to sub-serve it, namely attention and perception (Koch, 2004; Bekinschtein et al., 2009). In addition to this, we subsequently consider consciousness from a clinical perspective, as a static state upon a spectrum of wakefulness, whereby states at the lower end of the spectrum arguably correspond to a reduced availability of cognitive systems (Boly, Garrido, Gosseries, Bruno, Boveroux, Schnakers, Massimini, Litvak, Laureys, & Friston, 2011). Alternatively, occupying states higher on the spectrum may correspond to greater availability of cognitive systems (Boly et al., 2011). By considering consciousness from both a cognitive and clinical perspective, we attempt to make sense of how manipulations of attention may impact upon the information one perceives, in relation to how reducing wakefulness may influence the availability of cognitive resources, all with respect to the global-local auditory task.

The term attention within this thesis specifically refers to directed attention in relation to an auditory listening task (the global-local task). Directed attention can be considered akin to selective attention as a top-down process whereby individuals voluntarily focus their attention on a particular task or stimulus (Baluch & Itti, 2011; Bekinschtein et al., 2009; Auksztulewicz & Friston, 2015). Conversely, attentional capture (or bottom-up attention) in this thesis, refers to the involuntary seizing of attentional resources by an incongruent external stimulus (Freidman, Cycowicz & Gaeta, 2001). For clarity, when actively engaging with the auditory oddball task, we term this as ‘direct attention’ to represent attention having been directed towards the auditory task. Alternatively, when participants were instructed to let their minds wander during the passive condition, we term this as ‘passive attention’ to represent attention being passive in relation to the auditory task.

As previously mentioned, attentional engagement with the auditory oddball task has been linked to an enhanced MMN response (Auksztulewicz & Friston, 2015). What is more, direct attention has also been linked to echoic memory and the accumulation of echoic memory traces (Haenschel et al., 2005). Most recently, direct attention has been argued to afford a degree of precision with respect to evoked responses in the brain, and this may suggest that direct attention modulates response size within the auditory

processing pathway earlier than previously considered (Auksztulewicz & Friston, 2015; Chennu et al., 2013).

Closely related to attention is the concept of perception. Within this thesis, we consider perception in relation to the detection (indexed by ERP deflections) of global violations in auditory regularity. Our consideration of perception is based on the work of Bekinschtein et al. (2009), who suggest that the presence of a P3b response signifies conscious perception. This notion is based on models of conscious access that have been explored and stipulate that the active maintenance of perceptual representations across time require consciousness (Del Cul, Baillet & Dehaene, 2007; Sergent, Baillet, Dehaene, 2005). The active maintenance of perceptual representations across time can be thought of as storing information in working memory; this means that perceptual information is temporarily stored and accessed for the purpose of performing the required task (eg. counting the number of globally deviant tones heard) (Baddeley & Hitch, 1974; Bekinschtein et al., 2009).

Most importantly, within this thesis, we use the terms consciousness and awareness interchangeably to refer to perception with access to conscious contents but also to refer to the underlying static state of awareness upon a spectrum of wakefulness. Notably, this is not to suggest that consciousness is defined as wakefulness in these terms, only that awareness may exist as a static state upon a spectrum of wakefulness, as previously considered by Boly et al. (2011). It could be argued that one's position upon a spectrum of wakefulness may underlie the ability to engage cognitive systems, such as attention and memory. Therefore, we draw together the considerations of consciousness as perception from Bekinschtein et al. (2009), and the clinical perspective of consciousness as a static state upon a spectrum of wakefulness discussed by Boly et al. (2011). Interestingly, an alternative perspective from the field of visual attention suggests that the concepts of awareness and attention are actually highly dissociable. Lamme (2004) has argued that the two concepts may co-exist but do not necessarily co-vary.

Overall, within this thesis we consider attention as a mechanism that may serve the conscious perception of information. Meanwhile, we also consider a static state of consciousness, arguably served by a level of wakefulness, which may facilitate one's ability to access and engage cognitive resources, such as attention. It should be noted

that we acknowledge the highly debatable nature of the term consciousness and therefore make cautious efforts here, and within subsequent Chapters, to be clear in any reference made to the term. In the following section, we briefly extend our discussion of the relationship between attention, perception and awareness to consider examples from the literature.

Perception without awareness and attention without perception

One example of perception without awareness is blindsight (Bauer, 1984; Sperry, 1961). Blindsight is the ability to demonstrate an accurate percept of a stimulus, even though it cannot be recollected or identified (Bauer, 1984). This phenomenon has been studied extensively in various populations, including prosopagnosics (those unable to recognize faces) and split brain patients (Bauer, 1984; Sperry, 1961). A study on hemi-spatial neglect within stroke patients found that when objects were presented to the neglected visual field, patients were unable to report them. However, when asked to guess which object had been presented, their accuracy in guessing the correct object was above that of pure chance, suggesting that patients may have unconsciously perceived objects but were not aware of having done so (Berti & Rizzolatti, 1992).

Moreover, it has been argued that an example of attention without perception is change blindness (Humphreys, Hodsoll, & Campbell, 2005). Change blindness occurs when an individual is attending to an ongoing task, but fails to detect a change (or number of changes) to the stimuli or the surrounding environment (Humphreys, Hodsoll, & Campbell, 2005). It has been proposed within the literature on visual attention, that what one consciously perceives is that which falls within a spotlight of attention (Prinzmetal, Nwachuku, Bodanski, Blumenfeld, & Shimizu, 1997), suggesting that direct attention may evoke salience that affords the conscious perception of stimuli. As mentioned previously, the notion of direct attention affording precision has recently been shown to enhance early EEG responses to auditory irregularities as well (Auksztulewicz & Friston, 2015). The extent to which one perceives information outside the spotlight of attention is debatable and has been explored within studies on visual attention (Yuval-Greenberg, Merriam & Heeger, 2014; Seydell-Greenwald, Greenberg & Rauschecker,

2014). In the following section, we refine our discussion to consider what it may mean to be conscious versus what it may mean to be unconscious.

Conscious versus unconscious

Within Cognitive Neuroscience, the term unconscious has been defined as, "any neuronal activity that does not give rise to conscious sensation", and evidence suggests that sensorimotor systems in the primate brain function in the absence of reportable conscious experience (Koch & Crick, 2001, p.893; Crick & Koch, 2003). Notably, to be unconscious, as defined by Koch & Crick (2001), differs from PC discussed by Block (2005), as PC is considered to be a *conscious* state without access to its contents. The extent to which the unconscious brain can be distinguished from PC is debatable (Dennett, 1978).

From a slightly different standpoint, Milner & Goodale (1995) refer to unconscious systems as "online systems", comparable to software, which process information in real-time. Milner & Goodale (1995) put forward that much of what occurs inside the brain happens independently of conscious awareness and therefore can be classified as unconscious. According to Milner & Goodale (1995), it is these unconscious cognitive systems that allow humans to deal with everyday situations, such as reading, writing, and decision-making. It has been argued that these online systems are primitive, and as such, operate faster than conscious awareness; they are often referred to as pre-conscious systems (Milner & Goodale, 1995). Koch & Crick (2001) have suggested that these systems can be viewed as 'the zombie within', or the covert functional mechanisms that underlie the conscious state of awareness.

With respect to DoC, one may consider being unawake as unconscious (Boly et al., 2005, 2008). Therefore, one is unable to access the contents of consciousness when not in a wakeful state. In this way, consciousness can be reduced to a definition of wakefulness, whereby awake means conscious whilst unawake means unconscious. For the clinical purpose of assessing minimally conscious patients, wakefulness is further considered to be either with awareness (minimally conscious state) or without awareness (vegetative state). Once again, within this thesis we consider consciousness from both a

clinical and a cognitive perspective, in order to better understand the nature of conscious processing and the neural activity associated with it.

Within the final section of this Chapter, we lastly consider the existing research on the global-local task and arrive at the central hypothesis of this thesis.

Existing research on the global-local task

Pegado et al. (2010) probed the lifetime of echoic memory traces by implementing the global-local task and manipulating the stimulus onset asynchrony (SOA) of tones. Blocks of tones were presented as one of three SOA conditions (600ms, 1000ms or 2000ms) and responses were recorded using a high-density electrode array. They found that as SOA between tones increased from 600ms to 1000ms (the first of their SOA increases), the size of the MMN decreased, that is, the size of the difference between responses to standard and deviant tones, corresponding to the notion that echoic memory may be pre-attentive and fast decaying (see top left & middle left panel in Figure 2.7). Furthermore, they observed a delay in P3a/P3b responses with increased SOA, which was argued to indicate that greater time between tones might have made the detection of global violations more complex, given that arguably they depend upon the aggregation of auditory information across time (see middle [Cz] & right [Pz] columns in Figure 2.7). Interestingly, the size of the early mismatch response to deviance was largest when SOA was at a maximum (ie. 2000ms) (see bottom left panel in Figure 2.7). Pegado et al. (2010) argue that when the interval between tones is at a maximum then the presence of a tone in itself manifests as deviance because of the fast decaying nature of echoic memory (represented by the MMN within this study).

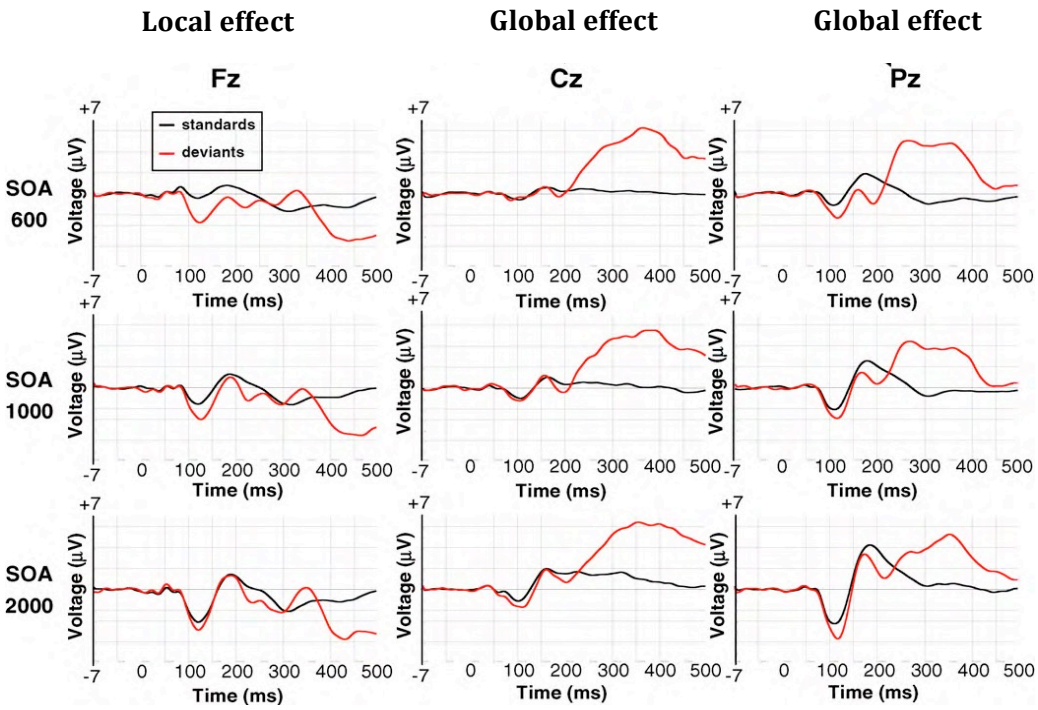

Figure 2.7. Grand average ERPs from Pegado et al. (2010) plotted for midline electrodes for each SOA: 600ms (top row), 1000ms (middle row) and 2000ms (bottom row).

Moreover, Wacongne et al. (2011) examined how top-down expectation, as opposed to bottom-up stimulus presentation, influenced auditory processing of the global-local task. An adapted version of the task, including auditory omissions was used in an attempt to reveal the brains predictive nature (see Figure 2.8). Blocks were administered in a similar way to the original work of Bekinschtein et al. (2009), with frequent vs. infrequent stimuli presented after an adaption phase that established regularity. However, an additional infrequent omission condition was present (10% of the time) within these blocks, as well as the introduction of an omission block within which only quintuples containing an omission were presented as a control (see Figure 2.8).

In regards to attention and evoked responses, Wacongne et al. (2011) firstly addressed the issue of counting vs. attention, which related to the original work of Bekinschtein et al.'s (2009) (ie. participants had been asked to count the number of globally deviant tones they heard within the original study of Bekinschtein et al. [2009]). It was argued that responses within the original active counting group may have been the result of the cognitive process of counting and not attentional investment in the task. Therefore, Wacongne et al. (2011) addressed this issue within their work by requesting that participants simply listen to the tones as opposed to counting the number of global deviants they heard.

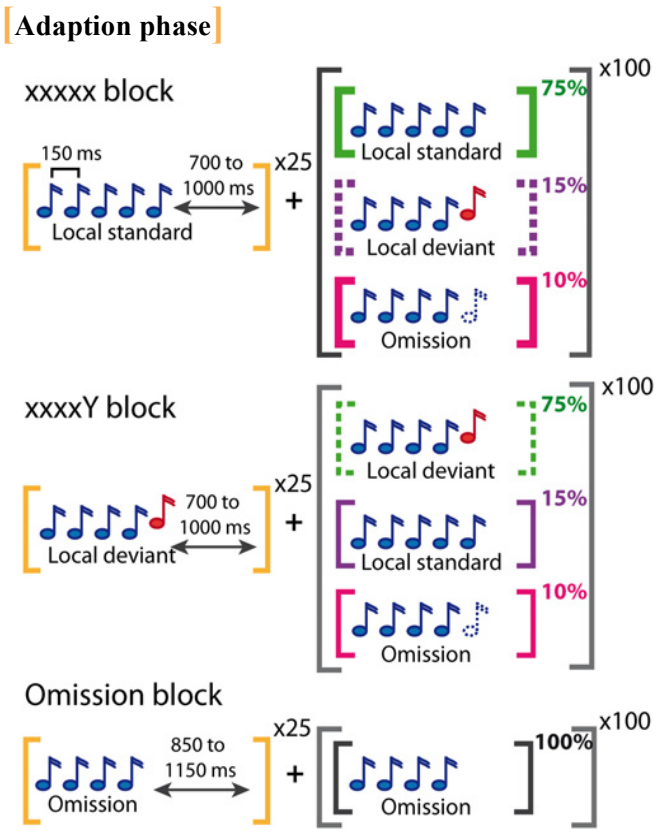

Figure 2.8. Amended global-local task including auditory omissions (Wacongne et al., 2011). Adaption phase consists of 25 quintuples which are one of three possible block types: local standard (XX), local deviant (XY) or omission; this establishes a frequent pattern. After the adaption phase, for blocks XX and XY, 100 quintuples are presented randomly according to the following: the frequent quintuple (75%), the infrequent quintuple (15%) or the omission (10%). For the omission block, only sequences of four tones with the fifth tone omitted are played, within the adaption phase and thereafter.

Wacongne et al. (2011) found that the MMN was sensitive to local violations in auditory regularity, that is, as the expectation of local deviance increased (ie. within XY blocks), the size of the early mismatch response decreased (see purple dashed line in A & green dashed line in B on Figure 2.9), suggesting that when local deviance is the global regularity, then the response to local deviance is attenuated through heightened global expectation for local irregularity. It was argued that this is because prediction error within the predictive hierarchy is minimised with repetition (Wacongne et al., 2011). Crucially, Wacongne et al. (2011) observed an interaction between global and local effects within an early time window, which may suggest that global and local processes are not independent within this region.

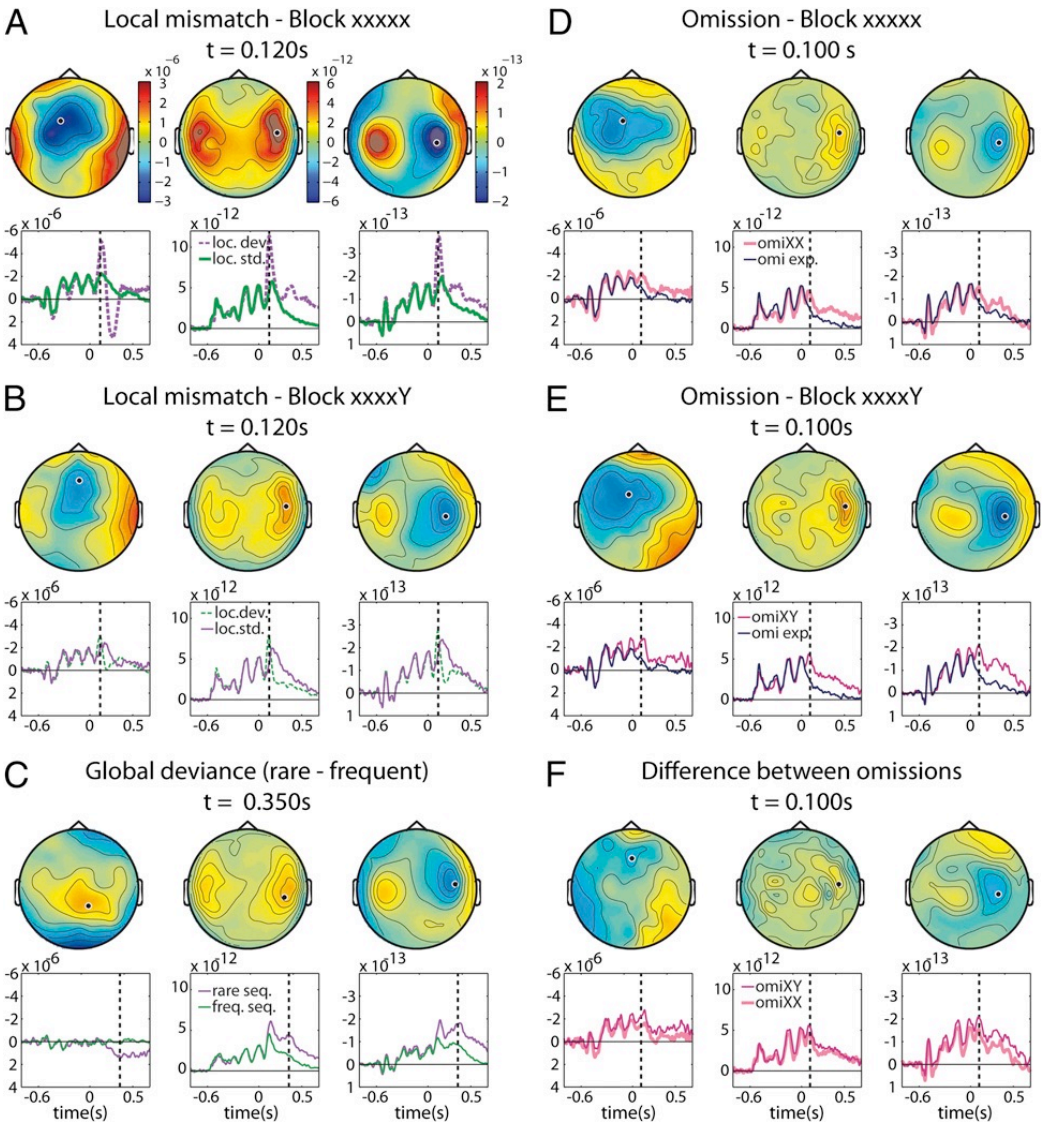

Figure 2.9. Grand average ERPs and accompanying scalpmaps for Wacongne et al. (2011) at various electrode sites. A: local responses (standard vs. deviant) in blocks XX, B: local responses (standard vs. deviant) in blocks XY, C: global deviance (rare seq.) vs. global standard (freq. seq.) responses plotted together, D: responses to omission of the fifth tone in a quintuple in an XX block, E: responses to omission of the fifth tone in a quintuple in an XY block, F: responses to omissions in blocks XX and XY plotted together to show the difference.

Furthermore and interestingly, Wacongne et al. (2011) found that the early mismatch response to omissions occurred at approximately the same time for both XX blocks and XY blocks (see left panels of D & E in Figure 2.9), indicating that the global regularity of the block did not impact the onset of local responses. However, the size of early mismatch responses to omissions was larger for XY blocks compared to XX blocks (see left panels of D, E & F in Figure 2.9), suggesting that the biggest mismatch response was elicited when there was both a violation to the expectation of deviance and a violation to the expectation that a tone would be presented. Wacongne et al. (2011) propose that this is evidence of a hierarchical predictive system within which higher-

order predictions (ie. global expectations) cancel out lower-order predictions (ie. local expectations) as a function of expectancy. In other words, as global expectancy for deviance increases (as in XY blocks), the size of local responses (ie. the MMN) decreases. It is argued that such predictions are the result of top-down systems and not passive adaption and this is evidenced by the presence of early mismatch responses to auditory omission (Wacongne et al., 2011).

Notably, Wacongne et al. (2011) do not fully consider the implications of an early interaction between global and local effects, which could inform the relationship between global and local expectations. Instead, it is proposed that the detection of auditory irregularity is organised into stages: firstly, MMN is argued to reflect the operations of a conceptually limited prediction system that is based solely on the probabilities of the component tones and their transitions. Secondly, the later P3b (global response) is argued to be a temporally extended and distributed response that represents deviance in the overall sequence and not individual component tones. Therefore, emphasis by Wacongne et al. (2011) is placed on separate processes occurring at different levels of the hierarchy. It may be the case that Wacongne et al.'s (2011) interpretation of a predictive hierarchy is limited by not considering the impact of an interaction between global and local effects.

Chennu et al. (2013) have expanded upon the notion of top-down expectation to also consider the role of attentional focus in the processing of hierarchical violations in auditory regularity using the global-local task. This work stems from predictive coding accounts, which propose that attention emerges from increased precision in probabilistic inference, meaning that the focus of attention may facilitate perception (Chennu et al., 2013; Friston 2010). Within this study, attention was therefore directed either towards tones (local regularity) or towards sequences (global regularity) in an attempt to manipulate expectation at successive levels of the predictive hierarchy. A third attention condition, namely the interference condition, was also included whereby participants were required to engage in a cognitively taxing visual task whilst tones were presented to them. In addition, deviancy within this study was expanded upon to include interaural tone presentation to provide an additional level of auditory complexity; thus deviant tones were presented both monaurally (to the same ear) and interaurally (to the opposite ear) in equal frequency (see Figure 2.10 & Table 2.1).

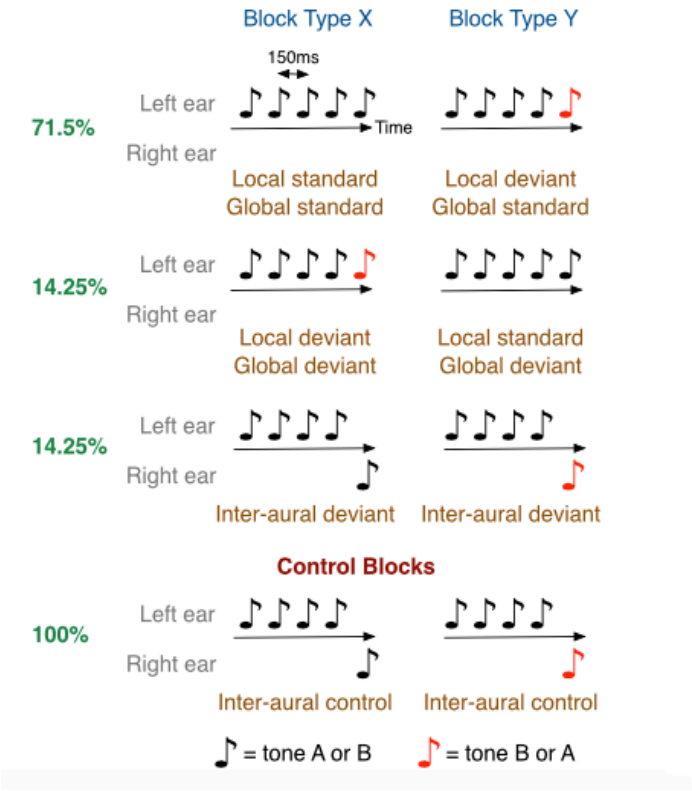

Figure 2.10. Adapted global-local task (Chennu et al., 2013). Auditory stimuli consisted of sequences of five tones of type A or B and were presented in experimental blocks of type X or Y. In X blocks, standard sequences (71.5%) were monaural repetitions of the same tone type, interspersed with rare deviant sequences with the fifth tone differing in either type (monaural; 14.25%) or laterality (interaural; 14.25%). Y blocks were similar, except that the standard sequences had a fifth tone differing in type. This effectively created an orthogonal contrast between temporally local versus global deviance in the pattern of tones. Additionally, interaural deviant sequences generated both global and local deviance. These were contrasted with control blocks consisting only of interaural deviant sequences.

Table 2.1. Structure of experimental blocks from Chennu et al. (2013)

Laterality	Tone type	Block type	Global standard	Global deviant	Interaural deviant
Left	A	X	AAAAA	AAAAB	AAAA*A*
Left	B	X	BBBBB	BBBBA	BBBB*B*
Left	A	Y	AAAAB	AAAAA	AAAA*B*
Left	B	Y	BBBBA	BBBBB	BBBB*A*
Right	A	X	AAAAA	AAAAB	AAAA*A*
Right	B	X	BBBBB	BBBBA	BBBB*B*
Right	A	Y	AAAAB	AAAAA	AAAA*B*
Right	B	Y	BBBBA	BBBBB	BBBB*A*

The eight different blocks listed were presented in random order, interspersed with two control blocks. Together, these eight blocks counterbalanced laterality, tone type, and local and global deviance in five-tone sequences.

Interestingly, Chennu et al. (2013) found that despite monaural and interaural deviants occurring in equal frequency, they produced varying responses with respect to local violations in auditory regularity. Specifically, in the attend tones condition interaural

deviants did not generate a larger MMN compared with monaural deviants, possibly because participants were only focused on the local tonal features of the stimuli and not the sequence as a whole (Chennu et al., 2013). Furthermore, the early mismatch response to deviance in the attend tones condition was significantly smaller than the attend sequences condition (see ERPs in B in Figure 2.11). It is argued that when attending to tones (as opposed to sequences), the task-conditional expectation for local deviance increases, which attenuates responses to local violations in auditory regularity as prediction error is minimised (Chennu et al., 2013).

In contrast, for the attend sequences and interference conditions, interaural deviancy generated a larger MMN comparing to monaural deviancy (see ERPs in A & C in Figure 2.11), although responses were smaller when attention was diverted suggesting that attention to sequences may somewhat enhance responses to local deviancy comparing to when attention is fixated elsewhere.

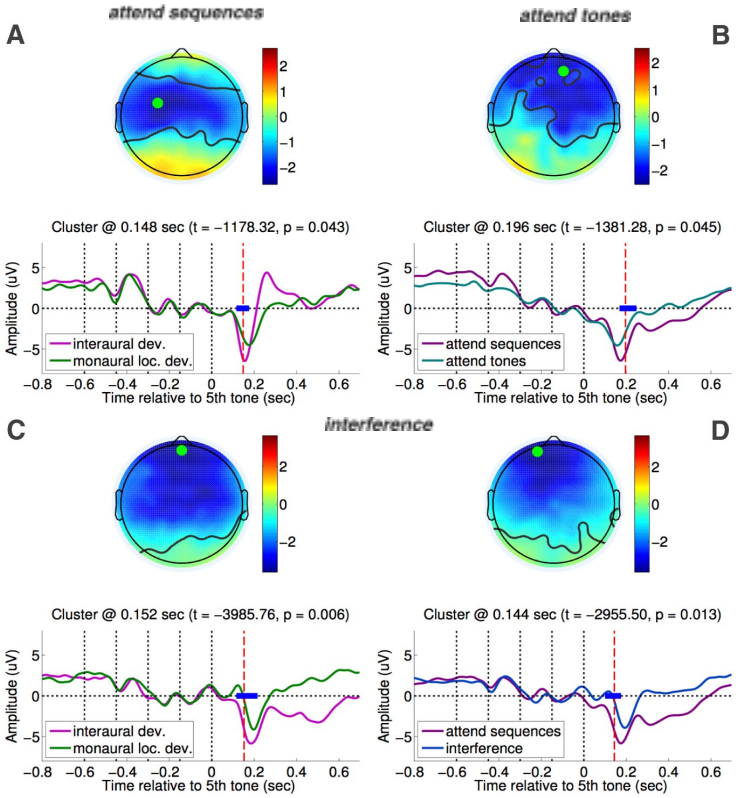

Figure 2.11. ERPs and accompanying scalpmaps for local effects, from Chennu et al (2013). Locally deviant responses are shown at various electrode sites, some located within spatiotemporally significant clusters. Periods of significance are marked with a bold blue line. A: local responses in the attend sequences condition for interaural (pink line) vs. monaural (green line) deviance. B: local responses in the attend tones (blue line) vs. attend sequences (pink line) conditions. C: local responses in the interference condition for interaural (pink line) vs. monaural (green line) deviance. D: local responses in the interference (blue line) vs. the attend sequences (purple line) conditions.

With respect to global violations of auditory regularity, the evoked responses (P3 responses) to interaural deviance for the attend tones and attend sequences conditions were larger than those elicited to monaural deviants (see A & D in Figure 2.12). The interference condition elicited no marked global effect (see C in Figure 2.12). Chennu et al. (2013) argue that for auditory task directed attention conditions (ie. attend tones and attend sequences conditions), larger responses to interaural deviance may index a greater amount of cortical activation that is generated by a rare shift in the laterality of a tone (Chennu et al., 2013). One should note yet again that both monaural and interaural deviance was equally rare, therefore a larger interaural global effect cannot be explained by differences in stimulus probability. What is more, the same interaural deviance when presented in separate control blocks, consisting of only interaural deviance, did not generate a global effect (see B in Figure 2.12), suggesting that as expectation for interaural deviance increased, the global response to deviance was attenuated.

Consequently, Chennu et al. (2013) propose that the global effect (P3) indexes auditory irregularity at the level of sequences (globally) and not the level of individual tones (locally), given that global responses were not sensitive to changes in local tonal features but variations in the sequence as a whole.

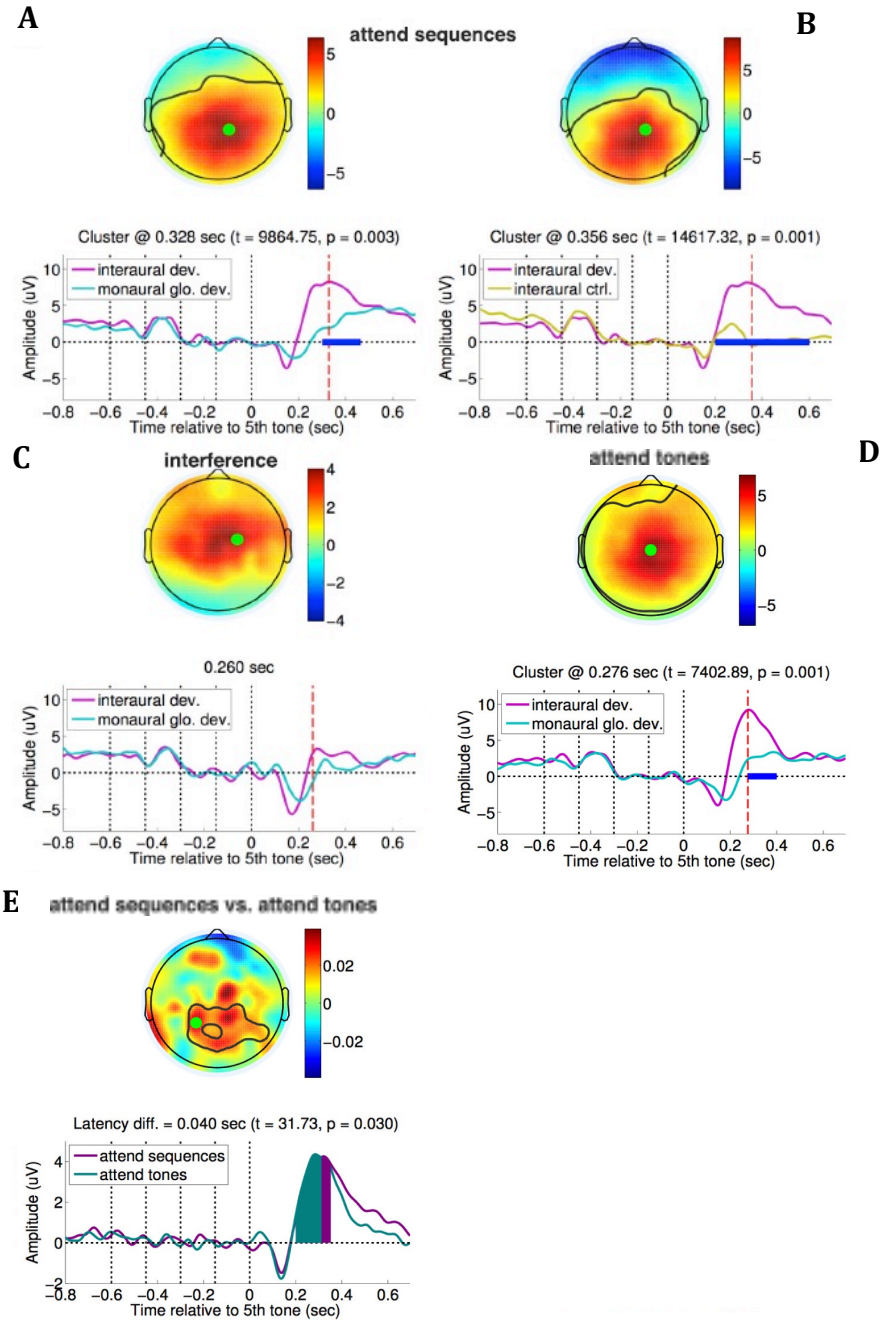

Figure 2.12. ERPs and accompanying scalpmaps for global effects, from Chennu et al (2013). Globally deviant responses are shown at various electrode sites, some located within spatiotemporally significant clusters. Periods of significance are marked with a bold blue line. A: global responses to interaural (pink line) vs. monaural deviance (blue line) in the attend sequences condition. B: global responses to interaural deviance where attention is directed towards sequences (pink line) or from the control block where only interaural deviance is presented (green line) C: centrally located responses to interaural (pink line) vs. monaural deviance (blue line) in the interference condition. D: global responses to interaural (pink line) vs. monaural deviance (blue line) in the attend tones condition. E: global responses to global deviance in the attend sequences (purple line) vs. the attend tones (green line) conditions.

Interestingly, there was no significant difference between the amplitude of the P3 response in the attend tones vs. the attend sequences conditions (see E in Figure 2.12). However, a small but significant difference was observed between the latency and duration of the P3 between these two conditions (see E in Figure 2.12), which manifested in an interaction between attention (attend tones vs. attend sequences) and deviance presentation (monaural vs. interaural) (Chennu et al., 2013). Most importantly, any divergence in the P3 response is argued by Chennu et al. (2013) to reflect the main impact of the attentional manipulation, that is, although stimuli were identical in both attend sequences and attend tones conditions, the precision of the attentional bias was not. Therefore, within the attend sequences condition, long-range temporal focus on global patterns of regularity resulted in increased attentional precision relatively late in the predictive hierarchy. In turn, this generated more protracted P3 responses, likely to indicate the integration of more complex predictive contexts (ie. sequences). By way of contrast, in the attend tones condition, the short-term interest in local tone features resulted in shorter, sharper P3 responses, suggestive that in this context the necessary predictive information available earlier in the processing hierarchy benefited more from attentional precision (ie. tones) (Chennu et al., 2013).

Altogether, it is argued that attention is not necessary for the detection of local deviance (see blue line in D in Figure 2.11), although response size was dependent upon whether the deviant tone was presented monaurally or interaurally for the attend sequences and interference conditions (see period of significance in A & C in Figure 2.11). At the local level, the focus of attention (towards either the local or global features of the task) may have attenuated the early mismatch response when attention was paid to the short-term local features as opposed to the long-range global features of the task (see blue line in B in Figure 2.11). Moreover, responses at the global level were contingent upon attentional engagement with the auditory task (see A, C & D in Figure 2.12), whilst the shape and duration of such responses appears to have varied based on the focus of attention between global and local features of the task (see E in Figure 2.12). Theses finding suggest that whilst bottom-up stimulus predictability may attenuate early responses to local deviance, top-down attentional precision may enhance them (Chennu et al., 2013). Furthermore, the focus of top-down attention appears to modulate responses to hierarchical violations in auditory regularity that involve more complex processing and the integration and maintenance of auditory information across time.

Within the final section of this Chapter, we bring together the ideas and findings presented to this point to discuss the central hypotheses of our research.

Central hypotheses

We propose that in order to further examine the relationship between global and local effects in relation to attention and expectancy, one must dissect the interaction between global and local effects that is eluded to, but not directly addressed, within the existing research to this point (Wacongne et al., 2011; Chennu et al., 2013). An interaction between global and local effects would mean that the two cannot be considered independent and this may offer further explanation as to how expectancy is impacting upon responses at multiple levels of a predictive hierarchy.

Our interpretation of a predictive hierarchy is based primarily on Chennu et al.'s (2013) work, given their consideration of both global and local predictive contexts. Critically, although we do make reference to a possible predictive hierarchy, we do not necessarily presume the relationship between levels of such a hierarchy to be linear. In actual fact, we propose that local and global levels of the hierarchy may share a multiplicative relationship, which would have important implications for the implementation and interpretation of statistical analysis. However, assuming non-linearity between levels does not necessarily contradict the existing concept of a processing pathway that is hierarchical. What is more, our interpretation of precision as linked to attention is also based on the recent work of Auksztulewicz & Friston (2015), who (as previously stated) suggest that attention affords precision to enhance early negative responses to auditory deviance.

With consideration of the above, the following are the central hypotheses around which this thesis is based:

1 ***We propose that an interaction between global and local effects within the region of the global effect may exist***, based on the principle that the brain is highly inter-connected and non-linear (Friston et al., 1996). If this is the case, then global and local effects share a multiplicative relationship, as opposed to an additive relationship, which renders the cognitive subtraction of effects as unsuitable. We propose, based on the work of Friston et al. (1996), that a factorial design analysis is

the most appropriate way to address this issue, given that it considers the possibility of interactions between effects. Moreover, an interaction between global and local effects has already been reported within the region of the local effect (Wacongne et al., 2011), possibly suggesting that the global context of auditory regularity impacts on early responses to local deviancy.

2 ***We propose that the interaction between global and local effects within the region of the global effect will be subject to changes in attention and wakefulness,*** as the presence of a global effect has already been argued to depend on the direction of attentional focus (Bekinschetin et al., 2009; Chennu et al., 2013), we expand upon this to consider the impact of healthy sedation on directed attention in relation to the global-local auditory task.

3 ***We propose that the interaction between global and local effects within the region of the global effect will also be subject to changes in expectancy***, which result from an internal predictive hierarchy that consists of both global and local predictive contexts. Based on the proposed nature of the relationship between global and local effects we do not necessarily assert that there is a linear relationship between different levels within the predictive hierarchy. Moreover, the predictive coding framework put forward by Friston (2010) is based upon Bayesian inference. Thus, as mentioned above, an early interaction between global and local effects (within the region of the local effect) reported by Wacongne et al. (2011) can be interpreted as the global predictive context impacting upon early responses to local auditory deviance. It may therefore be the case that the local composition of global regularity (that is whether a quintuple is locally deviant or locally standard) impacts upon the manifestation of global responses later on in the predictive hierarchy.

To comprehensively address these questions, in the first instance, we re-analyse the original EEG data of Bekinschtein et al. (2009) using a factorial design analysis to account for interactions between global and local effects. Subsequent to this, we examine the impact of reduced wakefulness, as opposed to attention, on an interaction between global and local effects when attention was always directed towards the task. Lastly, we directly compare manipulations of attention to manipulations of wakefulness, in an attempt to better understand the relationship between attention, expectancy and

wakefulness, particularly considering the clinical relevance that neural markers of conscious processing may have to DoC.

Thus, within the following Chapter we firstly present a background to the statistical methods used to conduct the subsequent analyses we have proposed. In addition, we further explain what is meant by an interaction between global and local effects and provide support for an interaction with preliminary investigations.

3. Measuring consciousness: Inferential statistics and Statistical Parametric Mapping (SPM) for electrophysiology

Inferential statistics are widely adopted throughout the scientific community in order to answer specific research questions or hypotheses. This is achieved by performing experiments on samples, drawn from a population, and posing the predicted outcome against a likelihood of no difference (also referred to as the null hypothesis). From this, certain types of statistical inference can be drawn from the sample and generalised to the population. Given that one is assessing samples that have been randomly drawn from the population as a whole, it is reasonable to consider the likelihood that the predicted outcome may arise purely by chance. To ensure that this is less often the case, a widely accepted threshold (known as an alpha level) of 5% is employed (Fisher, 1925). This corresponds to ensuring that the predicted outcome may only be due to chance 5% of the time (each time being each statistical test).

In this Chapter, we will outline and explain the fundamental concepts of hypothesis testing and statistical analysis within Cognitive Neuroscience (particularly T-tests and Linear Regression Modeling). Moreover, we will also discuss the Statistical Parametric Mapping approach to the analysis of EEG time-series data, which relies on the application of Random Field Theory (RFT) (Kilner, Kiebel & Friston, 2004; Friston, Holmes, Worsley, Poline, Frith & Frackowiak, 1995; Kilner & Friston, 2010). Within the later sections of this Chapter, we will also discuss statistical interactions and present some preliminary observations, which lead to our full-factorial re-analysis of responses to the global-local task with varied attention (Bekinschtein et al., 2009).

Hypotheses and T-tests

A T-test examines the difference between two sets of data in order to determine whether or not this difference is statistically significant. If the null hypothesis is true, in other words if there is no difference, then (assuming normality) the test statistic is unlikely to fall into the extremes of the T-distribution. Thus, essentially what is measured within a T-test is the extremity of an effect with respect to a T-distribution. Within a T-test, assumptions are made about the population distribution from which the data was drawn. Specifically, the assumption of normality must be met, ie. the population distribution should be normal (Gaussian). The outcome of the T-test will vary depending on the dispersion of variance and the type of hypothesis used.

One-tailed hypotheses. A one-tailed hypothesis refers to a directional hypothesis, which predicts the direction of the experimental outcome. For example, Condition A will perform better than Condition B, or Condition A will perform worse than Condition B. The occurrence of a directional hypothesis means that the alpha level of 5% must be applied to either the positive or the negative (depending on the direction) extreme of the probability distribution. The difference between conditions is considered statistically significant if the test statistic falls within the most extreme 5% of the probability distribution, which is either positive or negative but not both.

Two-tailed hypotheses. Comparatively, a two-tailed hypothesis refers to a non-directional hypothesis, which assumes only that there is a difference between groups. For example, Condition A will perform differently to Condition B, or visa versa. In this case, the alpha level is split equally (at 2.5%) between the positive and negative extremes of the probability distribution. The difference between conditions is considered statistically significant if the test statistic falls within the highest or lowest 2.5% of the probability distribution.

One-sample T-test. A one-sample T-test assesses whether a data set (sample) is statistically different from zero. This is achieved using the following equation:

(1) $$T = \frac{\bar{x} - \mu_0}{s/\sqrt{n}}$$

Where μ_0 is the null hypothesis (zero), $\bar{x}$ is the sample mean, s is the standard deviation of the sample, while n is the sample size. T is calculated by subtracting the sample mean from zero and dividing the result by the standard deviation of the sample that is divided by the square root of the sample size. This means that the size of the sample and the dispersion of values contribute to the size of the T-statistic.

Independent two-sample T-test. An Independent two-sample T-test assesses whether two independent but identically distributed samples (drawn from normally distributed populations) are statistically different from one another. This is also known as a Student's T-test, as variance within both samples is assumed to be equal ($\sigma_1 = \sigma_2$). The calculation is as follows:

(2) $$T = \frac{\bar{\bar{X}}_1 - \bar{X}_2}{sx_1x_2 \cdot \sqrt{\frac{1}{n}}}$$

Where,

(3) $$sx_1x_2 = \sqrt{\left(s_{x_1}^2 + s_{x_2}^2\right)}$$

$\bar{\bar{X}}_1$ is the sample mean of group 1 and $\bar{\bar{X}}_2$ is the sample mean of group 2. sx_1x_2 represents the grand standard deviation of groups 1 and 2, while n is the sample size (assumed to be the same for both groups). The denominator of equation (2) is the standard error of the difference between the two means. Moreover, equation (3) shows the summation of the standard deviation squared for groups 1 and 2.

The difference between two independent sample means is divided by the standard error of the difference between the two means. Note that the standard error is the standard deviation of the sampling distribution of the means.

This is only possible when the variance within the two samples is equal ($\sigma_1 = \sigma_2$). When variance within the two samples is not equal ($\sigma_1 \neq \sigma_2$) and/or the sample sizes may be unequal ($n_1 \neq n_2$), then the variant, Welch's T-test, should be used as follows:

(4) $$T = \frac{\bar{\bar{X}}_1 - \bar{X}_2}{s_{\bar{x}_1 - \bar{x}_2}}$$

Where,

(5) $$s_{\bar{x}_1 - \bar{x}_2} = \sqrt{\frac{s_1^2}{n_1} + \frac{s_2^2}{n_2}}$$

In this case, the sample variance is calculated separately for each group, as shown in equation (5), and therefore the denominator in equation (4) is not the grand standard deviation as before.

Paired two-sample T-test. A paired two-sample T-test creates meaningful pairs between cases across the two samples, in order to assess whether there is a statistical difference between these pairs. This is achieved using the following equation:

(6) $$T = \frac{\bar{\bar{X}}_D - \mu_0}{s_D / \sqrt{n}}$$

Where $\bar{\bar{X}}_D$ is the mean of the differences calculated between pairs. μ_0 is the null hypothesis (zero), s_D is the standard deviation of the differences and n is the sample size.

The null hypothesis is subtracted from the mean of the differences and the solution is divided by the standard deviation of the difference itself divided by the square root of the sample size.

Degrees of freedom (df). When conducting statistical tests such as T-tests and F-tests, the degrees of freedom (*df*) are of paramount importance. The *df* in a statistical calculation are the number of values that are free to vary. More specifically, the number

of ways in which these values can vary independently, without violating the constraints of the test, is referred to as the number of degrees of freedom. The number is estimated by taking the sample size (ie. number of contributing values) and subtracting the number of parameters used within the test (ie. number of experimental factors). For example, with an independent two-sample T-test, the *df* are: $n - 2$, where n is the sample size. For Welch's T-test, as the sampling distributions may be different or unknown for the two samples, the *df* are calculated using a different method.

Linear Regression Modeling and Analysis of Variance (ANOVA)

When it is necessary to assess the difference between more than two means, the most commonly used method is linear regression, or an Analysis of Variance (ANOVA). This is likely to arise when experiments contain more than two factors or one factor with more than two levels. Akin to a T-value that relates to a T-distribution within a T-test, an ANOVA provides an F-value that relates to an F-distribution. Using an ANOVA, it is possible to determine whether or not the differences between means are significant, and a judgment can be made about whether or not to reject the null hypothesis (that there is no difference).

ANOVAs are based on the assumptions of the General Linear Model (GLM), which as with the Student T-test, assumes that populations are normally distributed and that all samples are independent of one another. In the context of linear regression, one refers to independent variables (IVs) and dependent variables (DVs). An independent variable (IV) is an experimental factor (or factors), manipulated by the experimenter to test a hypothesis. IVs are also known as predictor variables, explanatory variables, factors or regressors. A dependent variable (DV) is an outcome variable or in other words, the observed data. In some cases, there may be more than one DV and in this instance, multivariate linear regression should be applied. In the simplest form, an ANOVA will consist of only one IV with two levels, and one DV, which creates an F-test equivalent to an independent two-sample T-test, in the next section we will explore in more depth how linear regression is implemented.

Linear Regression Modeling. The aim of linear regression in ANOVA is to explain the relationship between the IV(s) and the DV(s) using linear predictor functions and model parameters that are estimated from the observed data (DV). Linear regression modeling seeks to explain how much variance within the DV is attributable to each IV and how much cannot be explained by the present model (ie. is error variance). One assumes that all IVs are independent and therefore do not share a significant amount of variance within the model. However, when IVs do share a significant amount of variance, this can reduce the statistical power of the test.

The amount of variance within the DV that can be attributed to a given IV within an ANOVA is referred to as the effect size (β). The effect size within an ANOVA is a standardised parameter of the model that is estimated from the observed data. Furthermore, any variance that is not successfully predicted by the model will be attributed to error (or residual variance).

The following equation is used to fit the linear regression model:

(8) $$y = \beta x_1 + \beta x_2 \ldots + \varepsilon$$

Where y is the observed data, β is the effect size and x_1 and x_2 are factors. Ordinary least squares (OLS) is used to estimate β-values as the observed data is considered to be a linear combination of IVs plus error.

Analysis of Variance (ANOVA) and the F-statistic. In order to assess the statistical significance between factors (IVs) along with any existing interactions, an ANOVA is implemented within which an F-value is obtained using the following ratio/equation:

(10) $$F = \frac{explained\ variance\ (effect)}{unexplained\ variance\ (error)}$$

When unexplained variance is high and explained variance is low, the F-statistic will be small, meaning the effect is less likely to be significant. In contrast, when explained

variance is high and unexplained variance is low, the F-statistic will be large, meaning that the effect is more likely to be significant.

P-values and significance. Whether or not the test statistic is considered significant is typically determined using a p-value. A p-value is the probability, assuming the null hypothesis is true (ie. there is no difference between means), that if one were to re-sample from the same population they would observe another extreme effect. Thus, when the p-value is low, the likelihood of accepting the null hypothesis (that there is no difference) is high. Conversely, when the p-value is high, the likelihood of rejecting the null hypothesis is high (meaning that there is a difference). The universally accepted threshold for determining at what level a p-value becomes significant is a value of less than 0.05 (Fisher, 1925); one may also refer to this probability threshold as the alpha level (α-level).

Type I errors. A type I error is assigning significance to effects which have arisen by chance, also known as a false positive, and can be considered as the incorrect rejection of the null hypothesis (that there is no difference). This can occur when the α-level is set very high, allowing for lower F-values to constitute a significant effect. However, this more commonly occurs when high numbers of the same test are conducted (as in the analysis of neuroimaging data), which can be described as an inflation of the family-wise error rate when considering the statistical analysis of EEG data (Friston et al., 1996).

Type II errors. A type II error is failing to detect significance when it indeed exists, also known as a false negative, and can be explained as the incorrect acceptance of the null hypothesis. This can occur when incorrect measures are used to detect an effect, but may also occur under other circumstances, such as when there is a large amount of error variance and/or a small sample size. If the statistical test is under-powered then this may give rise to false negatives.

Statistical interactions and the importance of factorial design analysis

An ANOVA not only addresses the main effects associated with each factor but also any interactions that might exist between factors. An interaction forms when the relationship between two (or more) variables is multiplicative. In the case of an ANOVA with two IVs with two levels (2x2 design), an interaction can be described as a relationship whereby the difference between two levels of one factor varies as one moves between the two levels of another factor, in other words, the relationship between variables is not additive. Figures 3.1 & 3.2 are illustrations of, respectively, a full cross-over interaction between two factors (with no main effect) and no interaction between two factors:

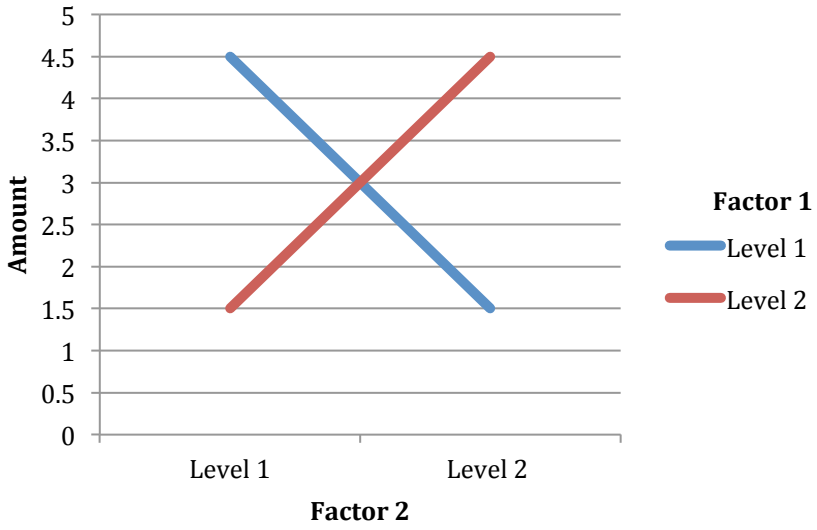

Figure 3.1. An example illustration of a full cross-over interaction between two factors with two levels.

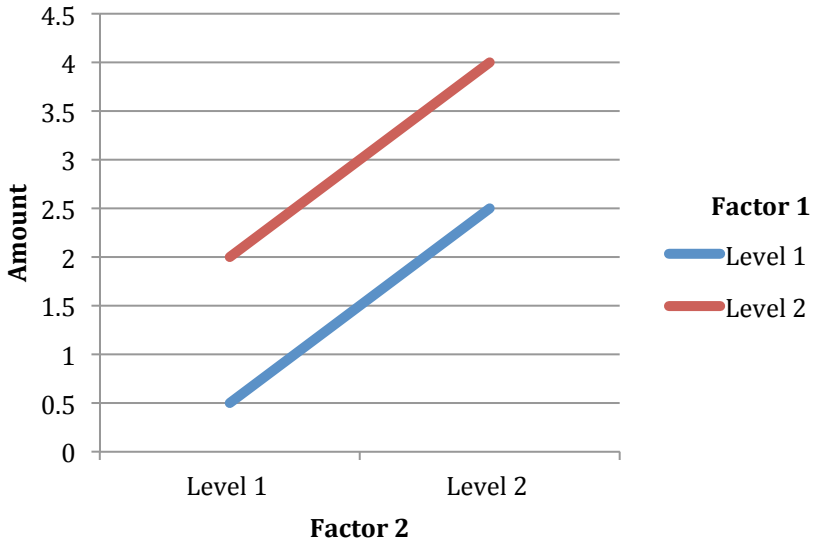

Figure 3.2. An example illustration of no interaction between two factors with two levels.

Assuming a multiplicative relationship between factors is something addressed by Friston et al. (1996) (as mentioned within the previous Chapter) in their work regarding the principle of pure insertion. Friston et al. (1996) propose that experiments should accommodate factorial designs so that analysis will consider main effects and interactions between effects as it is unlikely that effects exist in isolation when considering the brain. Within this thesis, we place specific emphasis on the necessity of implementing factorial designs for EEG analysis, as they account for possible interactions between effects that are not captured by simple effect subtractions (Friston et al. 1996). As discussed within the previous Chapter, Bekinschtein et al. (2009) appear to assume that global and local effects are independent of one another and therefore do not interact; however, we question this assumption and explore the presence and nature of an interaction between global and local effects within this thesis. Crucially, an interaction between global and local effects could indicate that the size of the global effect is dependent on the level of the local effect and visa versa; this will be explained in more depth subsequently.

In the following Chapters, we will investigate the existence of this interaction by re-analysing the data of Bekinschtein et al.'s (2009) study using a full factorial design analysis (as discussed previously). We also extend this investigation to an additional study exploring the effects of sedation on responses to the global-local task, before comparing the two and considering the implications for future research. Firstly however, within the next sections of this Chapter, we will briefly discuss the preliminary observations which led us to examine the interaction, and subsequently the Statistical Parametric Mapping (SPM) approach to analysing electrophysiological (EEG) data, which involves non-stationary cluster based statistics (Kilner, Kiebel & Friston, 2004).

Preliminary observations. On first obtaining the data of two control participants, from the dataset acquired by Bekinschtein et al. (2009), we performed a preliminary observation to assess any differences there may be between experimental conditions. Thus, we generated ERPs by averaging across all trials in each condition for each participant.

Figures 3.3 and 3.4 are the ERPs of one control participant, at frontal electrode Fz (focus of the local effect). The onset of the last tone of the trial is 600ms, which is the

determinant of global regularity (whether standard or deviant). Just after 600ms, MMN appears (local effect) for the global deviant local deviant condition (GDLD) but not so clearly for the global deviant local standard condition (GDLS) (see Figure 3.3). Arguably, this is because there is no local violation of regularity in the case of GDLS. Moreover, around 900ms there is a larger positive peak for GDLD comparing to GDLS, which may suggest that the response to global deviance varies between GDLD and GDLS conditions (see Figure 3.3).

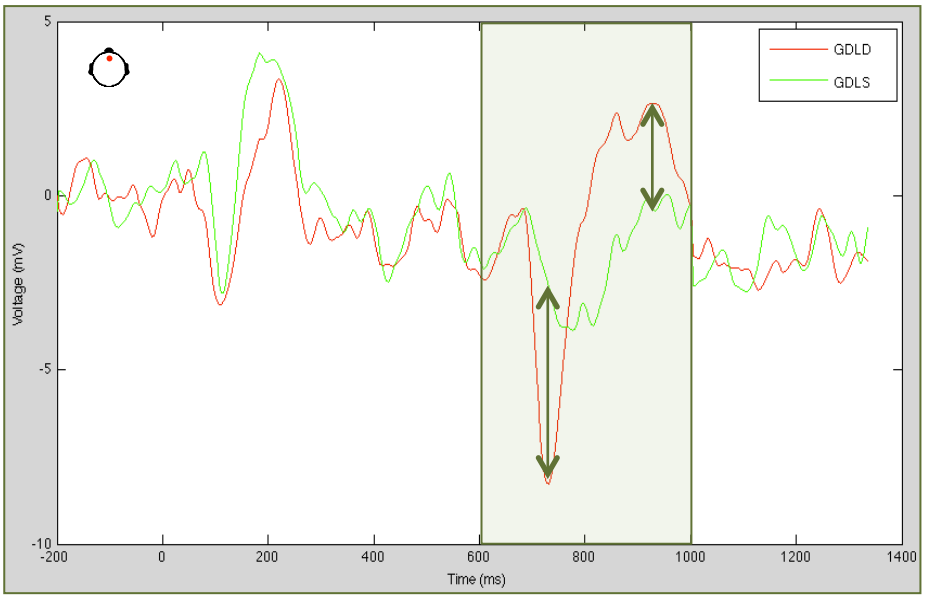

Figure 3.3. ERPs for global deviant local deviant (red line) vs. global deviant local standard (green line) at Fz (one control participant).

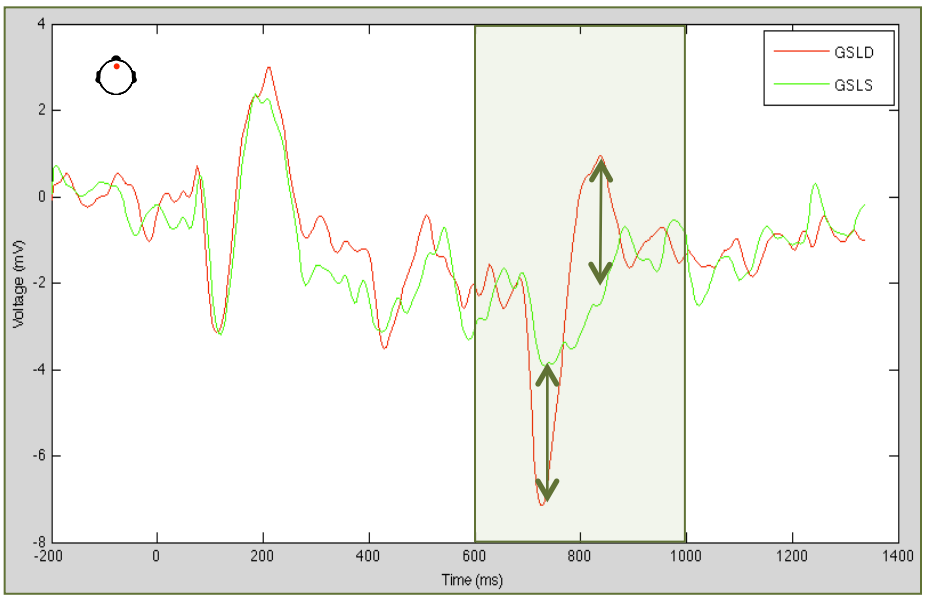

Figure 3.4. ERPs for global standard local deviant (red line) vs. global standard local standard (green line) at Fz (one control participant).

Accordingly, Figure 3.4 shows a similar mismatch response is elicited to local deviance when it is the globally regular pattern of sound (GSLD). Importantly, local deviance elicits a mismatch response (MMN) when local deviance is also globally deviant (GDLD), but also when local deviance is the globally regular pattern of sound (GSLD). In contrast, locally standard tones elicit no marked mismatch response (MMN), most likely because there is no local violation of regularity in this case.

Figures 3.5 and 3.6 show the same ERPs at midline-posterior electrode Pz, which is arguably the focus of the global effect (Bekinschtein et al., 2009). One can see in Figure 3.5 that around 800ms there is a positive peak within the GSLD condition, which is not matched in the global standard local standard condition (GSLS). The positive peak may be a somewhat delayed response to local deviance, which extends to the regions associated with global regularity. The fact that the same response is not generated for GSLS, as with GSLD, may indicate that the size of responses to global standards depends upon the level of local regularity (ie. whether the tone is locally deviant or locally standard).

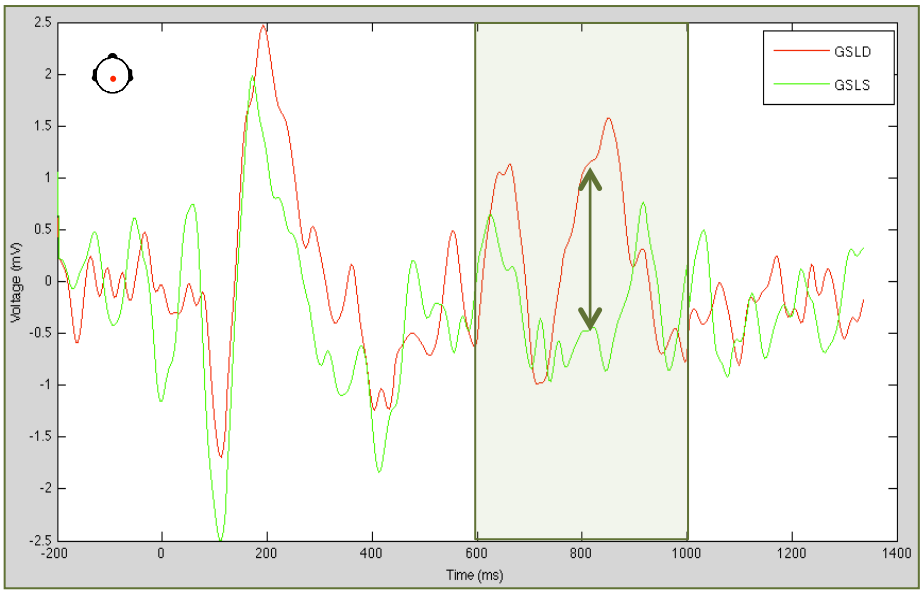

Figure 3.5. ERPs for global standard local deviant (red line) vs. global standard local standard at Pz (one control participant).

Figure 3.6 shows a much larger response to global deviance when there is also local deviance (GDLD) comparing to when there is global deviance that is marked by a

locally standard quintuple (GDLS). One may argue that global deviance that is also locally deviant (GDLD) violates both global and local assumptions of regularity, generating a large response at both levels. However, global deviance that is marked by a locally standard quintuple (GDLS) only violates global regularity, whilst maintaining local assumptions of regularity (ie. 5 identical tones within a quintuple). Therefore, global deviance that is marked by a locally standard quintuple (GDLS), may be more difficult to detect than GDLD, as it solely requires the higher-level cognition involved in the monitoring of global regularity.

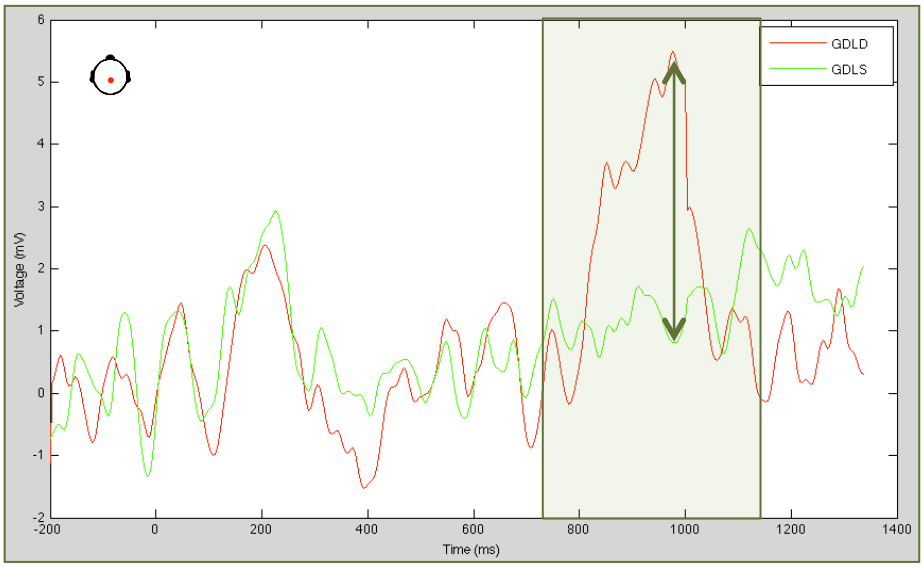

Figure 3.6. ERPs for global deviant local deviant (red line) vs. global deviant local standard (green line) at Pz (one control participant).

From our preliminary observations, we conclude that there is evidence to suggest that global and local processing of auditory irregularities do not operate independently, as proposed by Bekinschtein et al. (2009). Therefore, the cognitive subtraction of global and local effects may be discounting the possibility of a multiplicative relationship. Within the next section, we will explain in more detail the proposed interaction between global and local effects.

The global x local interaction. Figures 3.7 illustrates the relationship between global and local effects one might expect if there were no interaction. The result is an additive relationship, where the difference between GDLS and GSLS ((1) in Figure 3.7) is the same as the difference between GDLD and GSLD ((2) in Figure 3.7).

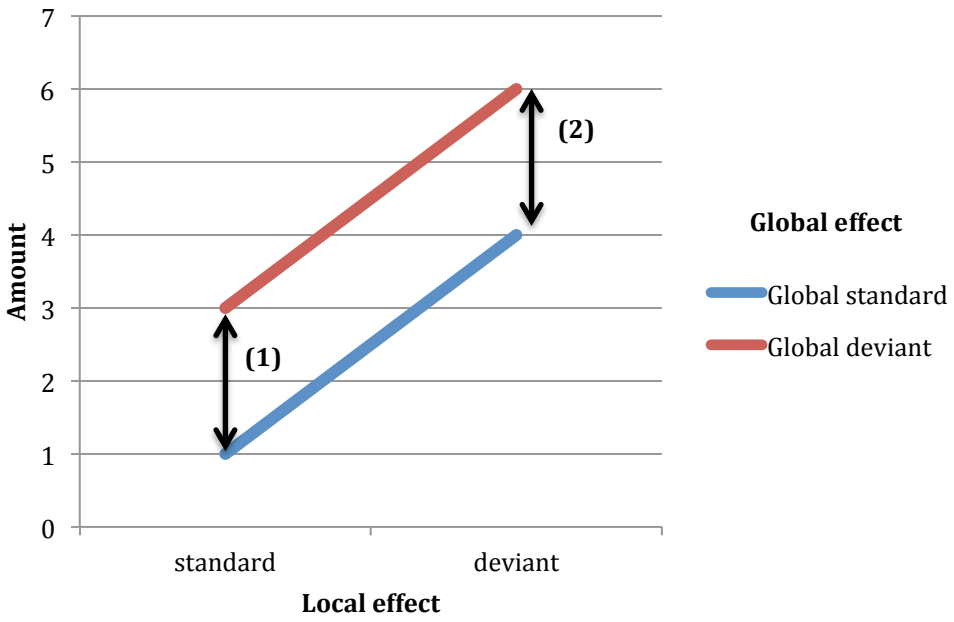

Figure 3.7. An illustration of additive global and local effects (no interaction).

Figure 3.8 illustrates a multiplicative relationship, inspired by the patterns seen in Figures 3.5 and 3.6, between global and local effects that would be indicative of an interaction.

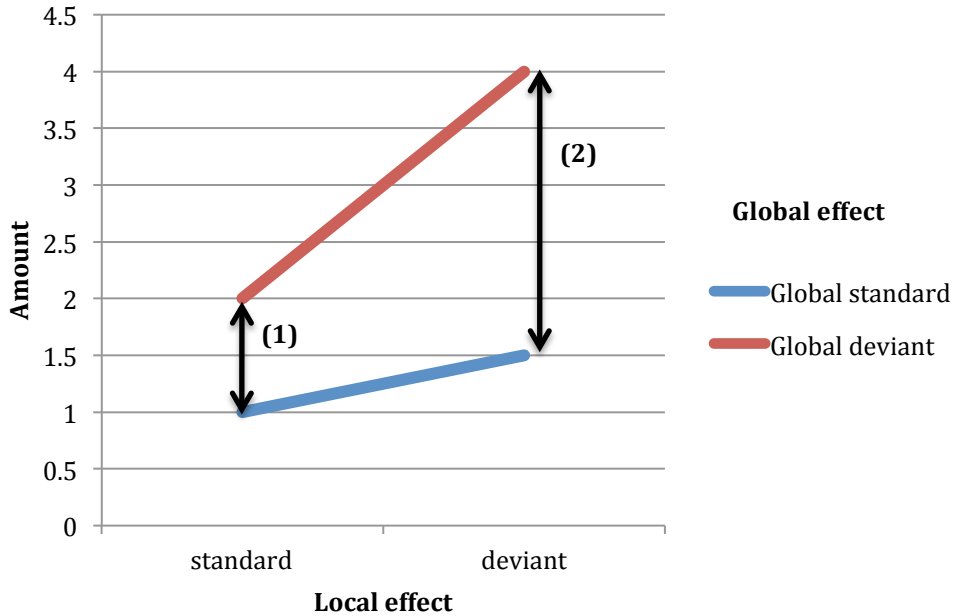

Figure 3.8. An illustration of multiplication global and local effects (the interaction).

One can see the difference between global standard and global deviant ((1) and (2) in Figure 3.8) is no longer equal across local standard and local deviant. Global deviant is larger overall (see red line in Figure 3.8) than global standard (see blue line in Figure 3.8), although, GDLD is much larger than GDLS. Put another way, GSLD is small, comparing to GDLD, therefore the difference between GDLD and GSLD ((2) in Figure 3.8) is much bigger than the difference between GDLS and GSLS ((1) in Figure 3.8).

At this point it is important to clarify that it is the change in the size of the differences that constitutes an interaction between effects. If this is the case then it stands against Bekinschtein et al.'s (2009) proposal of the global and local effects as orthogonal (ie. independent). The presence of an interaction may mean that the global effect cannot be considered a functionally isolated marker of conscious processing, because it is subject to changes in local regularity. Critically, for global and local effects to share an additive relationship, the size of the difference between levels of the global effect will be the same for both levels of the local effect (illustrated as (1) and (2) in Figure 3.7), and visa versa, meaning that one effect is merely sitting (ie. summed) on-top of the other. Where there is a multiplicative relationship between effects, the aforementioned differences will be unequal (illustrated as (1) and (2) in Figure 3.8).

As mentioned within the previous Chapter, we consider the presence of an interaction within the framework of predictive coding. Friston (2010) suggests that when predictions are violated, a large response is elicited comparing to when there is less or no predictive violation, based on the level of prediction error arising. Multiple layers of prediction are argued to exist within a hierarchical structure inside the cortex (Friston, 2010). The presence of a hierarchy implies that the complexity of predictions increases at each stage, which can allow for the encoding of more complex patterns (Friston, 2010). Within this thesis, we consider how an interaction between global and local effects may reflect a hierarchical predictive system in which the local context of global irregularity impacts global responses, whilst the global context of local deviance may also impact early local responses.

Within the final section of this Chapter, we will present the method of Statistical Parametric Mapping (SPM) for electroencephalography (EEG), which was subsequently used to conduct a factorial design analysis on the original data of Bekinschtein et al. (2009).

Statistical Parametric Mapping (SPM) approach to electroencephalography (EEG)

SPM is a parametric approach to the statistical analysis of neuroimaging data, which follows the assumptions of the General Linear Model (GLM) (Friston et al., 1995; Kilner & Friston, 2010). The GLM assumes normality, that is, that the distribution is Gaussian and also that data points are independent and identically distributed (iid). The method of SPM specifically considers the distribution of the maximum statistic (T or F) under the null hypothesis. In contrast, when assumptions of normality are not met, non-parametric approaches may be applied, such as permutation testing (McIntosh & Lobaugh, 2004).

Although non-parametric methods do not assume normality, methods such as permutation testing become difficult to implement with mixed factorial designs, as one must establish how to appropriately resample. Consequently, our interest in examining the interaction creates difficulty with respect to how one is to appropriately permute samples. Therefore, we chose to adopt the method of SPM in order to appropriately analyse the interaction between global and local effects.

Building on the basics of inferential statistics that were described at the beginning of this Chapter, SPM can handle EEG data by creating a mass of three-dimensional points, namely voxels, which contain two-dimensions in space and one through time from EEG scalp recordings (Friston et al., 1995). These voxels create a two-dimensional scalp, which can be represented through time (ie. a 2D scalpmap is created for each time-point of a trial). T-tests (or F-tests) can be applied on top of this at each voxel in order to assess the statistical significance of responses at different electrodes through the time-series; generating statistical parametric maps (see Figure 3.9).

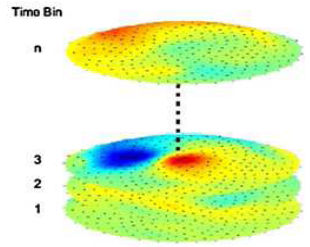

Figure 3.9. Illustration of 3-D statistical parametric maps (T-maps), showing T-values of activation with two dimensions in space represented at each point in time.

One issue with conducting such a high volume of statistical tests is the inflation of the Family-Wise Error Rate (FWER) or false positive rate; this is known as the multiple comparisons problem (Kilner, Kiebel & Friston, 2004). As one is conducting a high volume of statistical tests across the scalp and through time, with a universal a-level of 0.05, 5% of conducted tests will be significant purely by chance (that is 5,000 if 100,0000 tests are conducted). For this reason, a blanket a-level of 0.05 is not considered an acceptable constraint on the likelihood of false positives (Kilner, Kiebel & Friston, 2004), therefore a more stringent method of correction should be applied.

One way of constraining the likelihood of false positives is to correct the a-level, ie. make the threshold for significance more difficult to pass. SPM applies statistical thresholds at two different levels, a cluster-forming threshold and cluster-extent threshold, which will be discussed in more depth in the next Chapter. Both thresholds can be manipulated to allow more or less activation to pass. The first threshold is applied when allowing voxels to form clusters of activation. The second threshold is applied when judging cluster extent, and establishes the necessary number of voxels a cluster must contain in order to reach significance. To adequately constrain the likelihood of false positives, consideration of the a-level at both thresholding stages is necessary.

Bonferroni correction is often considered as an appropriate constraint for the multiple comparisons problem, however it can become overly conservative when applied to neuroimaging data, in particular EEG data (Kilner & Friston, 2010; Kilner, Kiebel & Friston, 2004). Bonferroni correction divides the a-level by the number of tests conducted and therefore arguably becomes unnecessarily conservative with regards to EEG data for two reasons. Firstly, the number of tests conducted will be extremely

large, because they occur at every space-time point; therefore the a-level becomes extremely small, possibly inflating the Type II error rate (likelihood of a false negative) (Kilner, Kiebel & Friston, 2004). Secondly, Bonferroni correction assumes all tests are independent, which is unlikely to be the case with EEG data as there are high correlations in space and in time between data points (Kilner, Kiebel & Friston, 2004). Kilner, Kiebel & Friston (2004), argue that a more adequate solution to the multiple comparisons problem with EEG data is the implementation of Random Field Theory (RFT).

Random Field Theory (RFT). RFT addresses the multiple comparisons problem that arises from applying inferential statistics to EEG data, by assessing the likelihood of the observed data under the assumption that the data is Gaussian noise with a particular smoothness (Kilner, Kiebel & Friston, 2004). The volume of the data and the smoothness of the data play an important role in the calculation of this likelihood, as they contribute to the shape of the data (Kilner & Friston, 2010; Kilner, Kiebel & Friston, 2004). Estimating the smoothness of EEG data within SPM is achieved using a measurement of Full Width Half Maximum (FWHM).

Full Width Half Maximum (FWHM). FWHM estimates the smoothness of EEG data by taking a measure of the width of a peak at half the maximum height and calculating the size of the Gaussian kernel necessary to smooth the data to become the same smoothness as the null data (Gaussian noise). Once smoothness has been estimated, the data is characterized by the term Resolution Elements (RESELS). One RESEL is equal to the FWHM value for all three dimensions of the data ($RESEL = FWHM_x FWHM_y FWHM_z$) (Kilner, Kiebel & Friston, 2004). Importantly, the number of RESELS does not equal the number of voxels, as when estimating smoothness, several highly correlated neighbouring voxels may contribute to a single RESEL (see Figure 3.10). The number of RESELS within the data is important as RFT performs a correction on the number of RESELS and not the number of voxels. In order to establish an appropriate significance threshold that maintains an a-level of 0.05, the expected Euler Characteristic is calculated using the smoothness of the data, along with the volume of data and the size of the search region (region of interest) (Kilner, Kiebel & Friston, 2004).

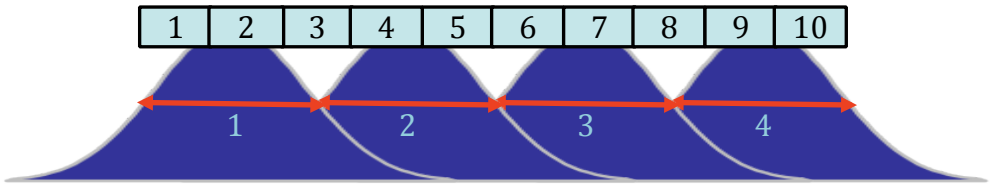

Figure 3.10. Illustration of 10 voxels with FWHM of 2.5 = 4 RESELS.

As RFT can handle variations in the shape of the data, that is non-stationarity (through both space and time), the method is an extremely powerful tool for establishing statistically significant effects with EEG data (Kilner & Friston, 2010; Kilner, Kiebel & Friston, 2004). The final aspect of the SPM method to be discussed within this Chapter is the different levels of topological inference that can be drawn, ie. findings at the level of peaks, clusters and sets of clusters.

Levels of topological inference. The levels of topological inference within SPM are defined as peak-level, cluster-level and set-level. This means that statistical inference can be drawn from the data at any one of these levels.

Peak-level inference. Peak-level inference involves assessing which peaks in the data are statistically significant. By nature, peaks are local maxima in activity and therefore are not necessarily broad through space or through time. They may be of interest if one is examining localized EEG components (see Figure 3.11).

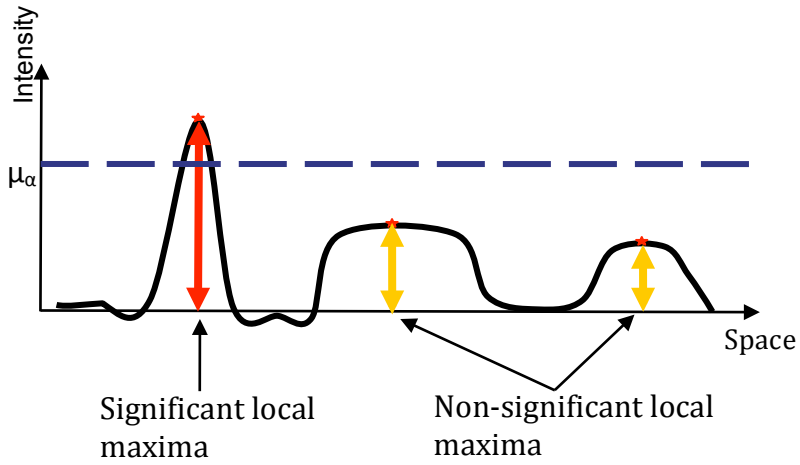

Figure 3.11. Illustration of peak-level topological inference where μ_α is the corrected significance threshold.

Cluster-level inference. Cluster-level inference involves assessing which clusters in the data are statistically significant. Clusters are groups of active voxels (activation) in space and in time. As previously mentioned, clusters are formed by setting a cluster-forming threshold, which determines the level of activation necessary for voxels to exceed the significance threshold and form a cluster. At the cluster-level, inference refers to the cluster-extent, ie. the number of collective voxels necessary to create a significant clusters (see Figure 3.12). Cluster-level inference is of interest if one is examining EEG components that are broader in space and/or time as they concern the extent of activation.

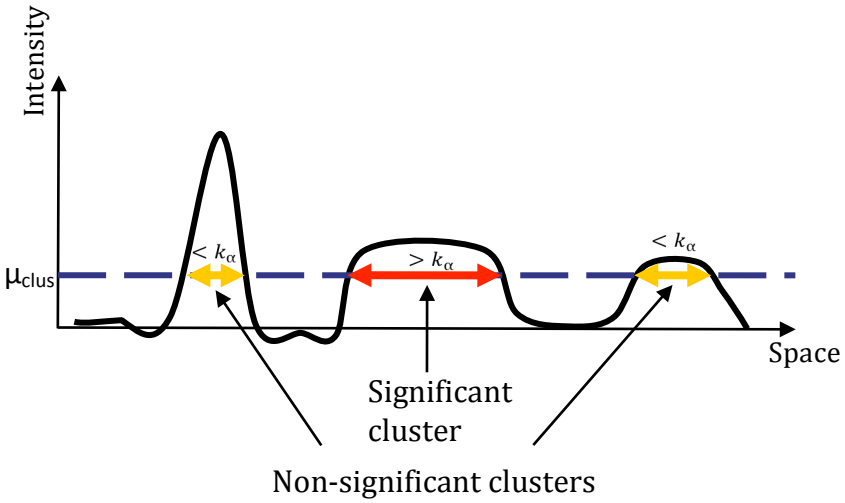

Figure 3.12. Illustration of cluster-level topological inference, where μ_{clus} is the cluster-forming threshold and k_α is the $\boldsymbol{\alpha}$-level extent threshold.

Set-level inference. Set-level inference assesses the total number of significant clusters. That is, the number of significant clusters in the data as opposed to the extent of a given cluster (see Figure 3.13). Set-level is mostly useful as an overall determinant of significance within the data.

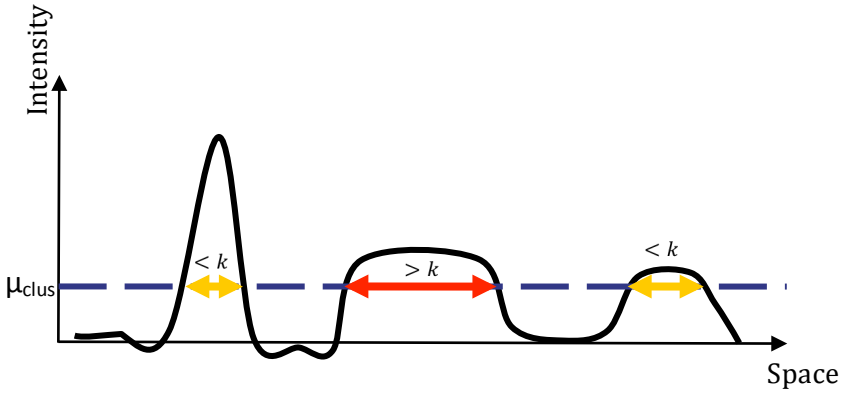

Figure 3.13. Illustration of set-level topological inference where μ_{clus} is the cluster-forming threshold and k is the minimum cluster extent. Above, only the middle cluster is larger than k, therefore the number of clusters reaching significance is 1.

Altogether, SPM employs RFT as a solution to the multiple comparisons problem, given that Bonferroni correction is considered to be overly conservative on neuroimaging data (Kilner, Kiebel & Friston, 2004). Regarding EEG data, SPM generates two-dimensional statistical parametric maps at every time-point in the time-series by conducting T-tests (or F-tests) at every space-time point. RFT assumes that these statistical images are a good approximation of a continuous Gaussian field (ie. that data was collected from a high density electrode array) and estimates the smoothness to characterize the shape of the data. The smoothness estimate, along with the volume of data and the size of the search region (region of interest) are used to calculate the Euler Characteristic. The Euler Characteristic maintains an α-level, typically of 0.05 (which is set externally), and P-values are adjusted in accordance with this threshold. Finally, depending on the experimental hypotheses, statistical inference within SPM can be drawn at the peak, cluster or set level.

Most importantly, SPM allows for the implementation of factorial design analysis on EEG data, which considers interactions between factors (Friston et al., 1996). In the following two Chapters we will present and discuss the re-analysis of original data collected by Bekinschtein et al. (2009), where we have applied a full factorial design analysis in SPM to examine the presence and nature of an interaction between global and local effects.

4 Interacting with consciousness I: a full factorial re-analysis of electrophysiological responses to the global-local task with varied attention

Introduction

In this Chapter, we will present and discuss the results of a mass univariate re-analysis applied to the data collected by Bekinschtein et al. (2009) within the study of attention and the global-local auditory task. The original study was presented in Chapter 2, where the global-local auditory paradigm was outlined (Bekinschtein et al., 2009). Here, we present a comprehensive re-analysis to specifically address the possibility of an interaction between global and local effects.

The presence of an interaction between global and local effects would mean that the two effects cannot be cognitively subtracted to isolate each effect individually (Friston et al., 1996). Consequently, an interaction between global and local effects would suggest that the global effect is not a functionally isolated marker of conscious processing, as initially proposed by Bekinschtein et al. (2009). Previous work by Wacongne et al. (2011) revealed an interaction between global and local effects within an early time window around the frontal region of the local effect, which may indicate that the global context of sound impacts upon the size of local responses; however, this was not explored in any further detail within the paper.

Additionally, it has been found that mismatch responses to local deviance are enhanced by direct attention yet attenuated by increased expectancy (Chennu et al., 2013; Auksztulewicz & Friston, 2015). These findings have been interpreted within a predictive coding framework, whereby direct attention affords precision and therefore enhances effects, whilst stimulus repetition increases expectancy through reducing prediction error (Friston, 2010; Chennu et al., 2013; Auksztulewicz & Friston, 2015). We propose that further analysis is necessary to explore the possibility of an interaction between global and local effects, which expands upon the existing research by

examining the relationship between global and local expectation within a predictive framework. What is more, we will investigate how the presence of an interaction between global and local effects may vary between direct (active) attention and passive (mind wandering) attention, as previous findings suggest that attentional engagement is necessary for long-range temporal focus on global patterns of sound (Chennu et al., 2013); this has previously been linked to the integration of more complex predictive contexts and the involvement of working memory at higher stages of the predictive hierarchy (Chennu et al., 2013; Wacongne, Changeux & Dehaene, 2012; Bekinschtein et al., 2009).

To comprehensively address the presence of an interaction between global and local effects, we adopt the full factorial approach of Statistical Parametric Mapping (SPM) (Kilner, Kiebel & Friston, 2004; Friston et al., 1996). Non-parametric approaches, such as permutation testing, were also considered, although cluster-based permutation methods become complex when considering multi-way factorial designs, which in this case include both between-subjects and within-subjects factors. Therefore, given the design of the study and the nature of the dataset, the parametric approach of SPM was deemed most suitable. Notably, SPM for EEG can handle non-stationarity across both space and time, meaning that the analysis can characterise differing levels of smoothness within the data (through space *and* time) in order to establish an accurate characterisation of the time-series (Kilner & Friston, 2010). SPM for EEG is an extremely powerful and robust technique for establishing statistical significance within EEG data (Kilner, Kiebel & Friston, 2004; Kilner & Friston, 2010).

Design

As outlined, within this Chapter we present a comprehensive re-analysis of the data from the global-local task with respect to varying states of attention (active attention vs. passive attention). More specifically, as explained within Chapter 2, participants either had their attention directed towards the task by counting the number of globally deviant quintuples they heard, or were instructed to "let their minds wander" whilst the task was played to them passively. In both conditions, participants were instructed to keep their eyes closed. For clarity, the global-local auditory task consists of both global and local violations in auditory regularity, meaning that there are two factors (global and local),

each with two levels (standard vs. deviant). Therefore, there are four possible conditions within the study design (global standard local standard [GSLS], global standard local deviant [GSLD], global deviant local standard [GDLS] and global deviant local deviant [GDLD]). Data from an interference condition was not included within the following analysis as it was corrupted during recording.

For clarity, Figure 4.1 illustrates the factorial design of the study/analysis, where attention is a between-subjects factor (active vs. passive) and local (standard and deviant) and global (standard and deviant) are within-subjects factors. Thus, as there are three factors - one between-subjects factor and two within-subjects factors - we apply a three-way mixed ANOVA (attention x global x local) to the data.

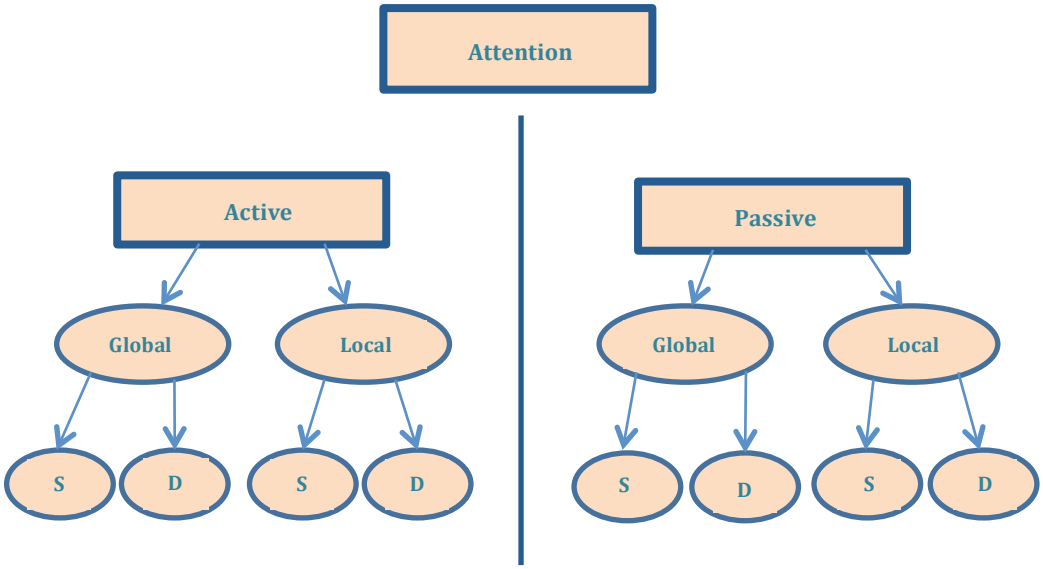

Figure 4.1. Illustration of the three-way mixed ANOVA design. Attention (between-subjects), global and local (within-subjects) are factors, each with two levels: attention (active vs. passive), local (standard[S] vs. deviant[D]) and global (standard[S] vs. deviant[D]).

Typically, auditory oddball paradigms consist of only one level of auditory violation, that is, a local violation of auditory regularity (Näätänen et al., 1993). What is particularly notable about the global-local task is that it introduces a hierarchy of auditory violation, which as previously mentioned, allows for investigation into and across global and local auditory contexts (Bekinschtein et al., 2009).

Explanation of the interaction (global x local)

Within Bekinschtein et al.'s (2009) original work, global and local effects were reported to be significant in the absence of a statistical interaction. However, the possibility of an interaction was addressed by applying two-sample t-tests, which did not in fact account for interactions between the levels of different factors (see Figures 4.2 and 4.3). Moreover, the interaction between global and local effects within the original work was examined by observing regions of significant difference within a certain time window relating to the global and local effects respectively (Bekinschtein et al., 2009). Regions of significant difference were established using a criterion of $p < .01$ for a minimum of 5 consecutive time samples in a trial (quintuple) at a minimum of 10 electrode sites. On this basis it was concluded that the global and local effects did not interact (Bekinschtein et al., 2009).

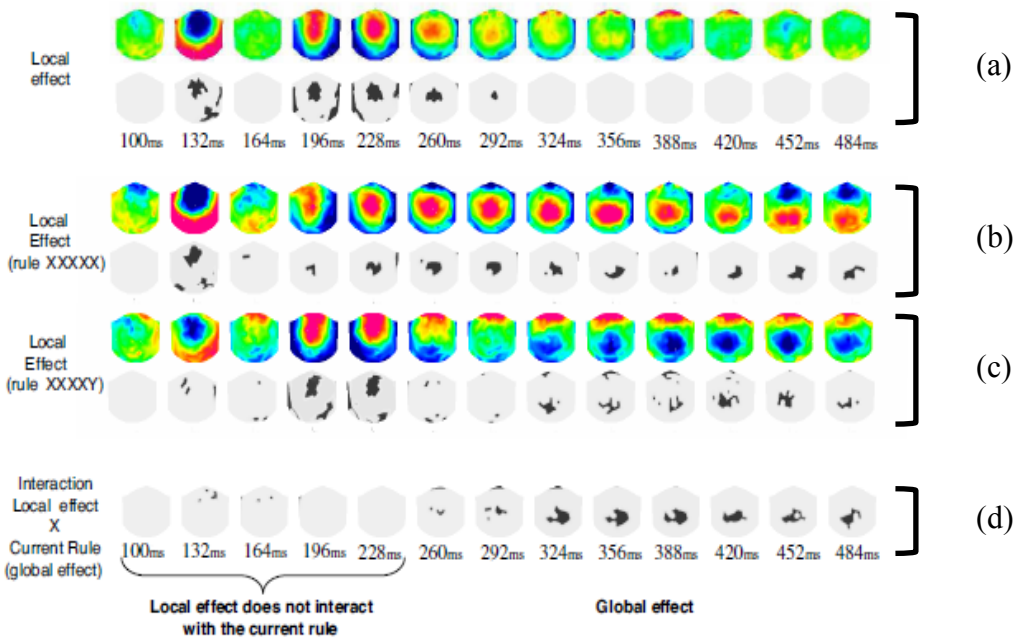

Figure 4.2. Local effect split by current global regularity in the active attention group. (a) shows averaged voltage scalpmaps for the local effect as found by Bekinschtein et al. (2009), along with thresholded t-statistic scalpmaps underneath in black and white to show regions of statistical significance. (b) and (c) contain averaged voltage scalpmaps for the local effect subtractions, plotted separately for the two global rules or block types (GDLD-GSLS [XXXXX] and GSLD-GDLS [XXXXY]) from 100-484ms after the onset of the fifth sound. Correspondingly, thresholded t-statistic scalpmaps are shown underneath in black and white to indicate regions of statistical significance. (d) shows in black and white the thresholded t-statistic scalpmaps, indicating regions of statistical significance, for the interaction between the local effect and the current global rule or block type (current block type: XXXXX or XXXXY), which mathematically corresponds almost exactly to the main effect of the global violation ([GDLD-GSLS]-[GSLD-GDLS] = [GDLD+GDLS]-[GSLS+GSLD]).

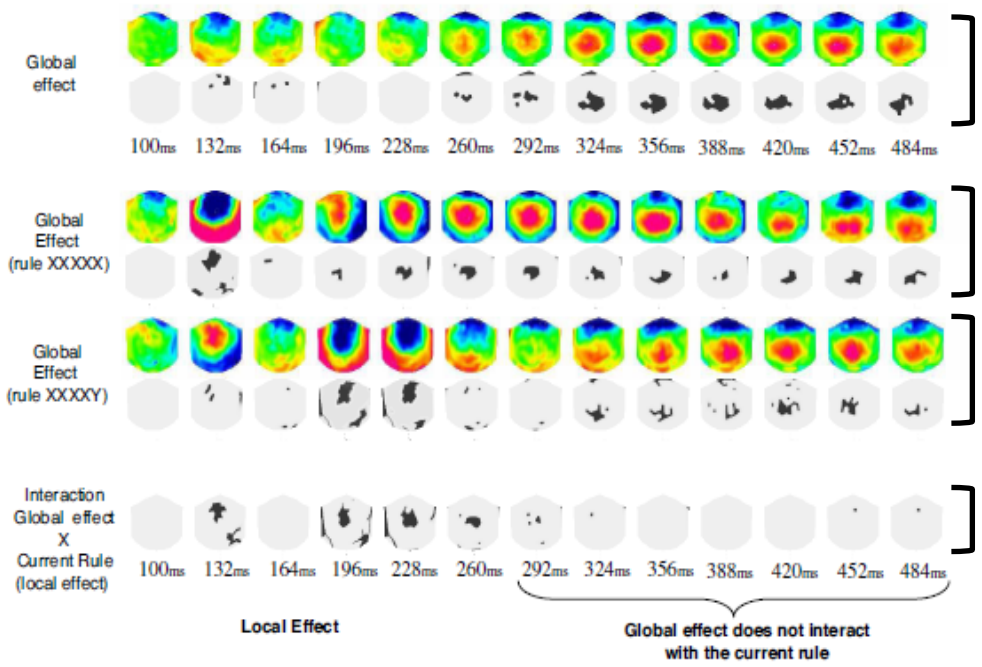

Figure 4.3. Global effect split by current global regularity in the active attention group. (a) shows averaged voltage scalpmaps for the global effect as found by Bekinschtein et al. (2009), along with thresholded t-statistic scalpmaps underneath in black and white to show regions of statistical significance. (b) and (c) contain averaged voltage scalpmaps for the global effect subtractions, plotted separately for the two global rules or block types (GDLD-GSLS [XXXXX] and GDLS-GSLD [XXXXY]) from 100-484ms after the onset of the fifth sound; correspondingly, thresholded t-statistic scalpmaps are shown underneath in black and white to indicate regions of statistical significance. (d) shows in black and white the thresholded t-statistic scalpmaps, indicating regions of statistical significance, for the interaction between the global effect and the current global rule or block type (current block type: XXXXX or XXXXY), which mathematically corresponds almost exactly to the main effect of the local violation: ([GDLD-GSLS]-[GDLS-GSLD] = [GDLD+GSLD]-[GSLS+GDLS]).

The presence of an interaction between global and local effects would suggest that the levels of one factor are influencing the levels of another factor. Since the brain is considered to be a largely non-linear system (Friston et al., 1996), one may accept the necessity to apply full factorial analysis to electrophysiological data in order to reliably reflect non-linearity between responses. Thus, on the basis of the preliminary findings presented in the previous Chapter, we propose that global deviance that is marked by the presence of local deviance (LDGD) may elicit a larger response than global deviance that is marked by a locally standard tone (see (a) and (d) in Figure 4.5). An interaction will only form when considered against a smaller difference between responses where there is no violation of global regularity, that is globally standard conditions (global standard local standard and global standard local deviant) (see (b) and (c) in Figure 4.5).

Accordingly, it may be the case that individuals are more likely to detect global deviance when it is marked by a locally deviant tone because in this case there are both global and local violations in auditory regularity. Conversely, a locally standard tone, even when

marking global deviance, is identical to the four preceding tones and thus may induce a smaller response as there is only a violation of global regularity in this case (and not local regularity). As just stated, in order for this to form an interaction between global and local effects it must sit in contrast to the difference occurring between the globally standard conditions (see (b) and (c) on Figure 4.5). Put another way, the difference between globally standard conditions (global standard local deviant vs. global standard local standard), that is difference 1 in Figure 4.4, should be different from the difference between globally deviant conditions (global deviant local deviant vs. global deviant local standard), that is difference 2 in Figure 4.4. It is this difference of differences which generates an interaction between global and local effects (see Figure 4.4).

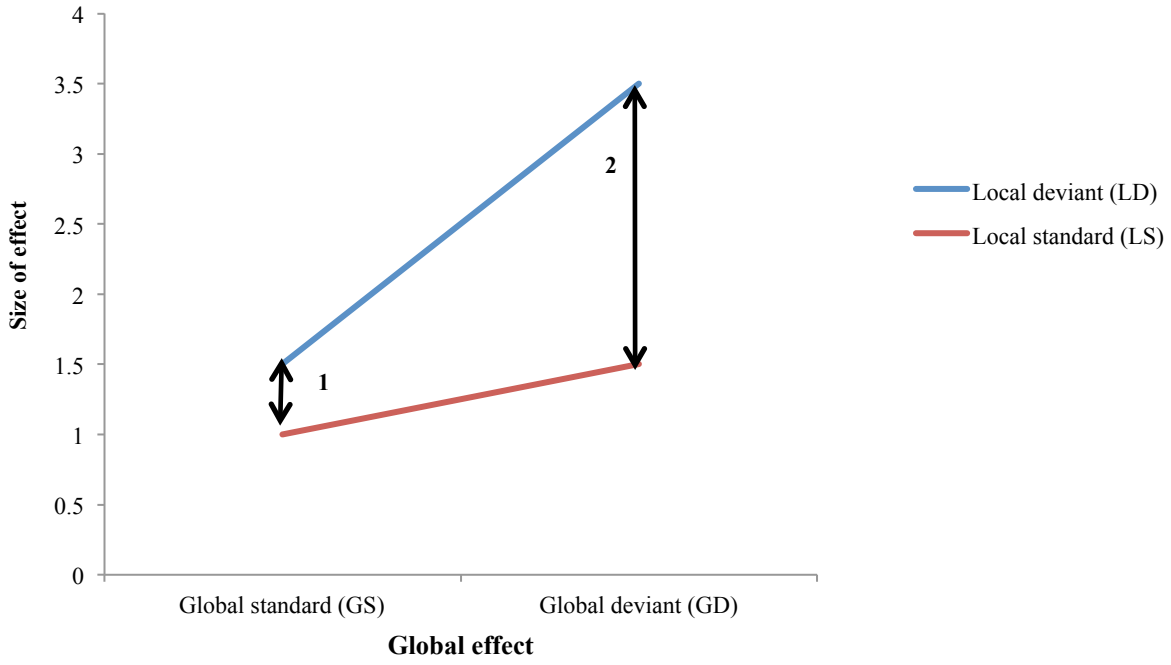

Figure 4.4. Illustration of a possible global x local interaction

Within the next section, we will present the global-local task and all further information regarding methods and materials. Subsequently, we will discuss the analysis and statistical thresholds applied. Thereafter, the results of the three-way mixed ANOVA are presented, followed by a discussion of the findings. The results of a further simple effects analysis, consisting of two two-way ANOVAs, exploring each attention group respectively (active and passive), are presented within the subsequent Chapter.

Methods and Materials

In this section, we will describe the methods and materials used by Bekinschtein et al. (2009) to collect their data sample (for full details of data acquisition see Bekinschtein et al., 2009).

Participants. 25 participants (mean age = 27.0 ± 3.0; sex-ratio = 0.9) tested gave written informed consent. Three participants were not included in the analysis because of excessive movement artefacts. 11 participants were placed in the active group and the remaining 11 were placed in the passive (mind wandering) group.

Auditory task. The following is an illustration of the global-local auditory task, along with definitions of the terms used to describe features of the task.

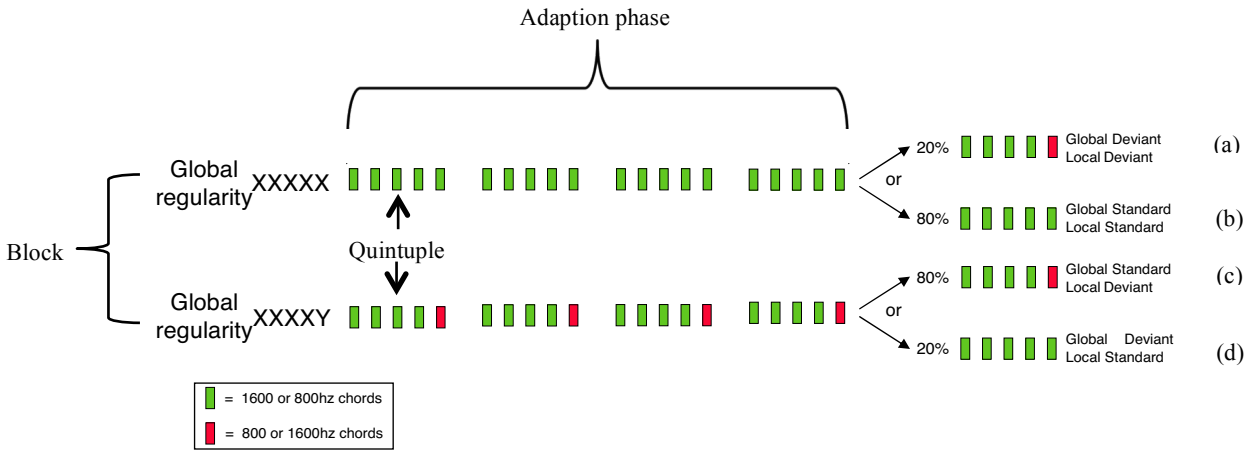

Figure 4.5. Global-local auditory task design from Bekinschtein et al. (2009).

Quintuple: a set of five tones. The fifth tone is either the same frequency as the four preceding it (standard), or of a different frequency (deviant) (see Figure 4.5). Global regularity was established by playing 20-30 frequently occurring quintuples at the beginning of the session, known as the adaption phase (see Figure 4.5). After the adaption phase, globally standard quintuples were delivered randomly 80% of the time (frequent), whilst 20% of the time globally deviant (infrequent) quintuples were presented; thus ensuring that global deviance was in fact the infrequent stimulus.

Block: consists of 120 quintuples. Two block designs are introduced: XXXXX (XX), where global regularity is established as quintuples containing only tones of the same frequency, or XXXXY (XY), where global regularity is established as quintuples

containing a fifth tone of a different frequency to the four preceding tones (see Figure 4.5). The frequency of standard and deviant tones were also counter balanced (see bottom left panel in Figure 4.5).

Session: consists of 8 blocks, where each block type (of which there are two) and tone frequency within the block (of which there are two), were presented twice in a pseudo-randomised order (see Figure 4.5).

Quintuples were made up of 5 complex 50ms duration sounds and were presented via headphones with an intensity of 70dB and an SOA of 150ms between sounds. All tones were prepared with 7ms rise and 7ms fall times. Given that global regularity can be established in two ways, this gave rise to four possible conditions: global deviant local deviant (GDLD), global deviant local standard (GDLS), global standard local deviant (GSLD) and global standard local standard (GSLS) (see (a), (b), (c) and (d) on Figure 4.5). As discussed in Chapter 2, all participants were subjected to all tone combinations. Given that tone frequency and block type were both counter balanced, there are 4 block types in total; XX and XY (as shown in Figure 4.5), but also the reverse: YY and YX, where standard and deviant tone frequencies are swapped. Each block was repeated and presented in a pseudo-random order so that 8 blocks were present in total within one experimental session.

In the active group, participants were instructed to actively count the number of globally deviant quintuples they heard. However, in the passive group, participants were instructed as follows: "During the next 30 minutes different sounds will be played by the headphones for successive periods of approximately 3 minutes. You don't need to pay attention to these sounds. Please close your eyes, and let yourself mind-wander" (Bekinschtein et al., 2009). Again, the visual interference group were omitted from the following analysis as data was corrupted during recording. Participants were either allocated to the active group or the passive group, never both.

Data preparation

Pre-processing. Sampling rate was 250 Hz with a 128-electrode geodesic sensor net (EGI), referenced to vertex (electrode Cz). Participant's eyes were closed in a resting state during data collection. Voltages exceeding ±200 μV, transients exceeding ±100

μV, or electro-oculogram activity exceeding ±70 μV were rejected. Quintuples were segmented from -200ms to +1288ms relative to the onset of the first sound in the quintuple. Bad channels were interpolated. Quintuples with > 25 bad channels were rejected. The remaining quintuples were averaged in synchrony with stimulus onset, digitally transformed to an average reference, band-pass filtered (0.5-20 Hz) and corrected for baseline over a 200ms window before the onset of the last tone (400-600ms). Data was re-referenced to mastoid before converting into SPM. All data was converted to image format within SPM (.NIfTI) for statistical analysis in sensory space (Friston et al., 1995; Kilner & Friston, 2010).

For clarity, below (Figure 4.6) is an illustration of how the quintuple data was segmented for analysis.

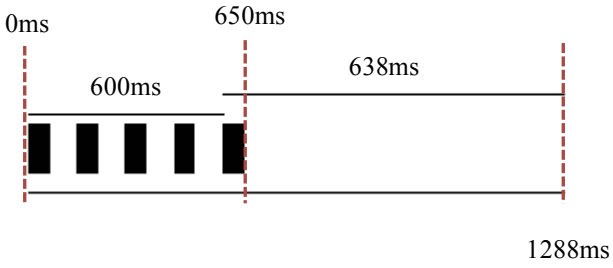

Figure 4.6. Quintuple design illustration and indication of segmentation for statistical analysis

0ms represents the onset of the first tone in a quintuple. The onset of the last tone occurred at 600ms and ended at 650ms. The last tone was either the same frequency as the four preceding (standard) or of a different frequency (deviant).

The time segment between the end of the last tone and 1288ms (638ms, as shown in Figure 4.6) was the quintuple data extracted in each condition for each participant, at all electrodes. This data was entered into SPM for EEG to conduct peak and cluster level analysis on the scalp. We chose 650ms onwards as our quintuple time segment because the components of interest (MMN and P300) do not begin until approximately 200ms post stimulus. For statistical analysis, crown electrodes were eliminated (36 channels eliminated, 93 remained) as they were not areas of interest and would not be contributing to source reconstruction (for channel locations after elimination see Appendix 2).

ERPs were generated in MATLAB 2012b for active and passive groups separately by averaging across all quintuples for all participants in each of the four conditions respectively ((a), (b), (c), (d), as shown in Figure 4.5). An ERP for the main effect of attention was generated by collapsing across all four conditions for active and passive groups separately (see Figure 4.8). ERPS are presented from 400-1288ms for ease of visual presentation.

Statistical analysis

First level analysis (individual analysis). The first level analysis was conducted within participants. In other words, a within-subjects ANOVA was applied to each participant respectively in both active and passive conditions separately.

The ANOVA itself contained two factors: global and local, each with two levels: standard vs. deviant (see Figure 4.1). Therefore, there were 4 possible conditions: GDLD, GDLS, GSLD and GSLS (see (a), (b), (c) and (d) in Figure 4.5).

Quintuples (as discussed in the previous section) for each of the 4 conditions were inputted for each given participant. This was repeated 11 times for the active group and a further 11 times for the passive group, as there were 11 participants within each group (22 in total).

A linear regression model was used to estimate beta values for each of the 4 conditions based on the participant quintuple information. The betas represent the effect size for each condition and would be used to form the input of the second level analysis, which is across participant rather than within participant (ie. a group level analysis). One might consider this as taking forward the average effect of each condition for each participant.

Second level analysis (group analysis). The second level analysis is conducted across participants. At this second stage a three-way mixed ANOVA design was applied on the betas taken from the first level. That is, at the second stage there are still two within-subjects factors (global and local) with two levels (standard vs. deviant), however there is now also a third between-subjects factor of attention (active vs. passive). Participants were either actively engaging with the task by counting the number of global deviants

they heard, or passively listening to the task and allowing their mind's to wander. The presence of a between-subjects factor is why we use a mixed ANOVA for this analysis.

For second level analysis, instead of inputting quintuples, we input the beta values for each condition from each subject. As we include both active and passive groups in the second level analysis, there are 8 conditions (active: GDLD, GDLS, GSLS, GSLD and passive: GDLD, GDLS, GSLS, GSLD) and 22 participants (11 active, 11 passive) to be represented. Each participant (active or passive) had one beta value per condition (estimated at the first level) and so 4 in total.

For the active condition, there were eleven beta values placed in each condition (GDLD, GDLS, GSLD and GSLS), one per active participant, and this was repeated for the passive condition. Therefore, 4 of the 8 conditions relate to the active group (AGDLD, AGDLS, AGSLD and AGSLS), whilst the remaining 4 relate to the passive group (PGDLD, PGDLS, PGSLD and PGSLS). Once again, a linear regression model was used to estimate new beta values, which corresponded to a group level effect. All subsequent analysis presented in this Chapter is the result of group level analysis.

Thresholds. There are two significance thresholds associated with the current analysis. The first is the cluster-forming threshold, which concerns the significance of each voxel. Put another way, the threshold here determines whether or not single voxels are significant. Where a number of voxels are significant, a cluster may form. However, this cluster is not constrained by any significance threshold at this point. The second-level threshold is concerned with the issue of cluster extent. The meaning of extent here applies not only to clusters in space but also clusters through time. At the second-level, the threshold (cluster-extent threshold) controls the size of significant clusters (in space and time) using an alpha level (false positive rate) and by applying Random Field Theory (RFT) (see Chapter 3 for full explanation of RFT).

We set our thresholds in correspondence with the existing literature (Kilner, Kiebel & Friston, 2004; Kilner & Friston, 2010), that is we applied a cluster-forming threshold of $p < .01$(uncorrected) and a cluster extent threshold of $p < .05$. All analysis (unless stated otherwise) was carried out with a cluster-forming threshold of $p < .01$(uncorrected) and a cluster extent threshold of $p < .05$. Specific P-values and F-values for each cluster can be viewed in Appendix 1.1.

Results

Table 4.1 is a summary of the statistically significant effects resulting from our analyses. The following is a large body of work therefore Table 4.1 may act as a good reference point with regard to the overall pattern of effects found.

Table 4.1. *Summary of effects for three-way ANOVA (attention x global x local) and two-way (simple effects) ANOVAs (global x local) for the active and passive groups separately. 'Y' indicates there is statistical significance (ie. at least one significant cluster), 'N' indicates there is no statistical significance.*

	Local (L)	Global (G)	GxL	Attention (A)	AxL	AxG	AxGxL
combined (active + passive)	Y	Y	Y	Y	Y	Y	N
active	Y	Y	N	-	-	-	-
passive	Y	Y	Y	-	-	-	-

Y = cluster extent threshold for combined analysis of $p < .05$, cluster extent threshold for active and passive simple effects of $p < .01$, cluster forming threshold for all analyses of $p < .01$

Three-way ANOVA (attention x global x local)

Attention effect. The effect of attention is significant between 856-1056ms around central/ posterior electrodes Cz and Pz (see Figure 4.7).

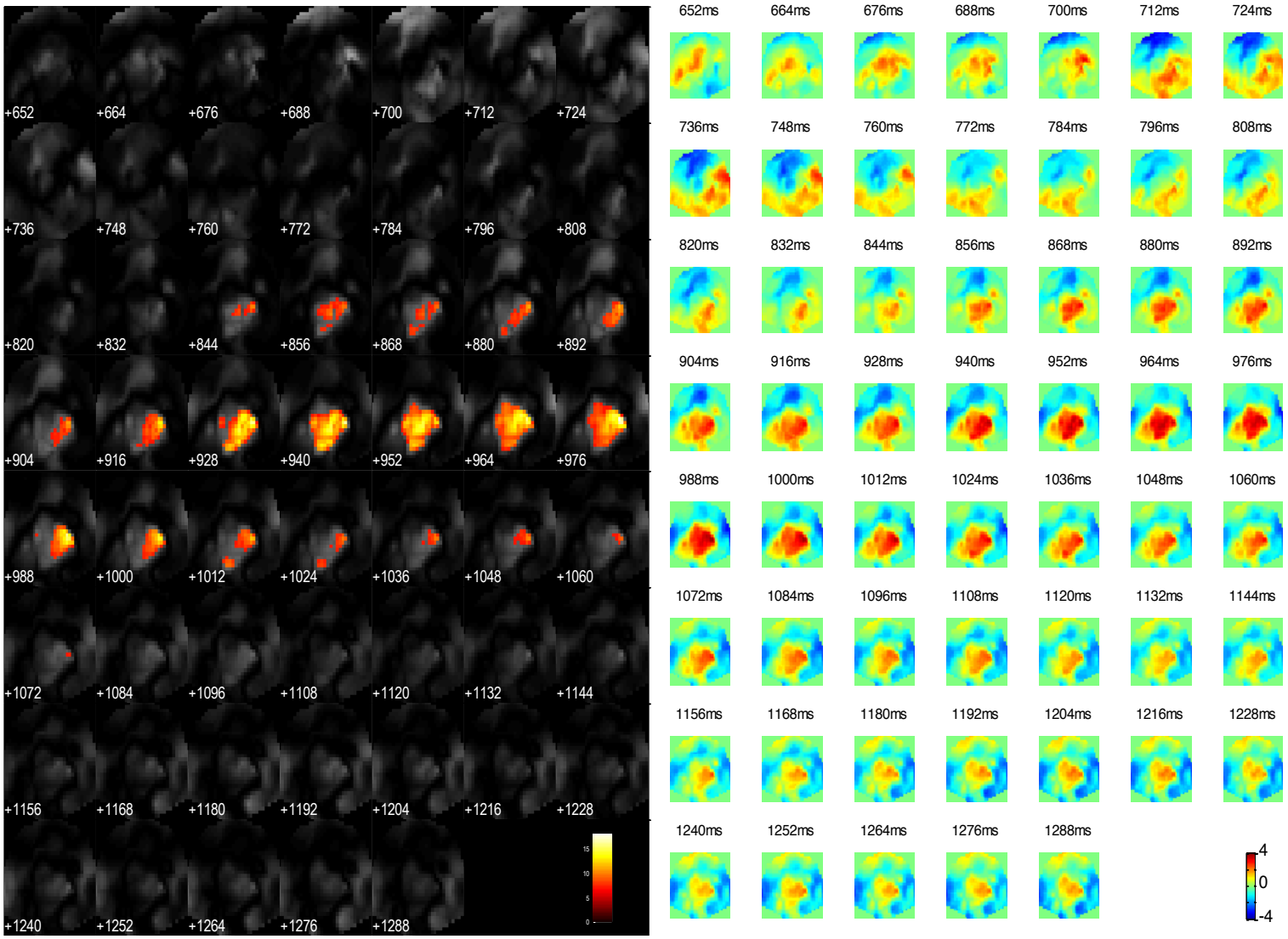

Figure 4.7. Thresholded F-maps ($p < .05$) to show regions of significance for the effect of attention [active-passive] on the scalp through time (left). Unthresholded T-maps to show the polarity of the effect on the scalp through time (right). Front of the scalp is positioned at the top. Note that time within the left panel is presented below the corresponding row of scalpmaps, whilst time within the right panel is presented above the corresponding row of scalpmaps.

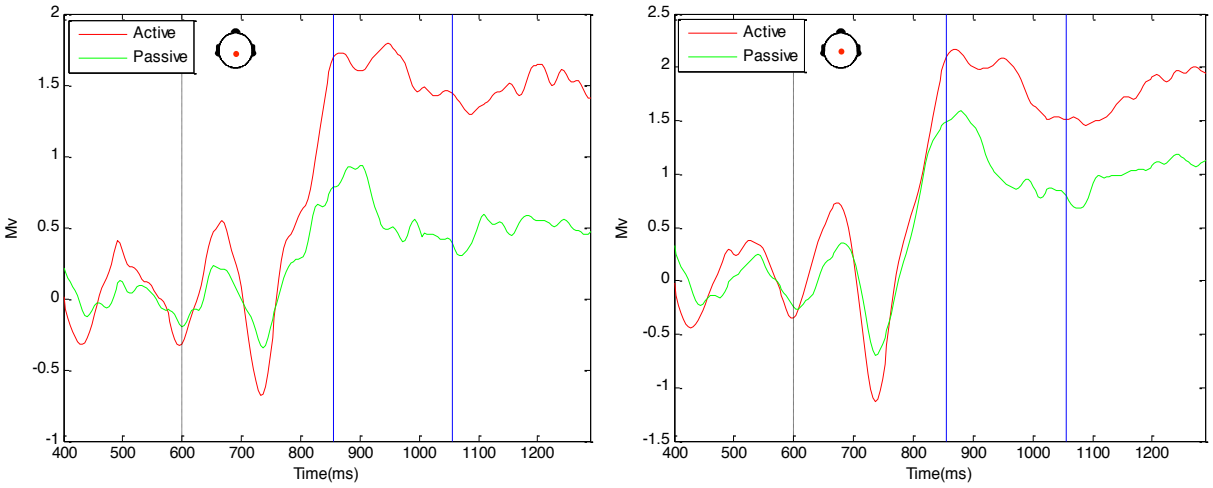

Figure 4.8. Grand average ERPs for the effect of attention at Pz (left) and Cz (right). Blue lines indicate the region of significance. Black dashed line (600ms) indicates the onset of the final tone.

Figure 4.8 shows that responses in the active condition were larger than responses in the passive condition, possibly indicating that active participants were more attentionally engaged in the task than their passive counterparts. Interestingly, the onset of the global effect (P3) is very similar for both active and passive groups, suggesting that varying attention towards the task may not accelerate the onset of a global response. In other words, manipulating attention towards the task does not appear to effect response latency (for scalp topography see Figure 4.7).

Local effect. The local effect is significant between 712-752ms around frontal electrode Fz. Subsequently the local effect is significant in the region of central-posterior electrode Pz between 784-848ms (see Figure 4.9).

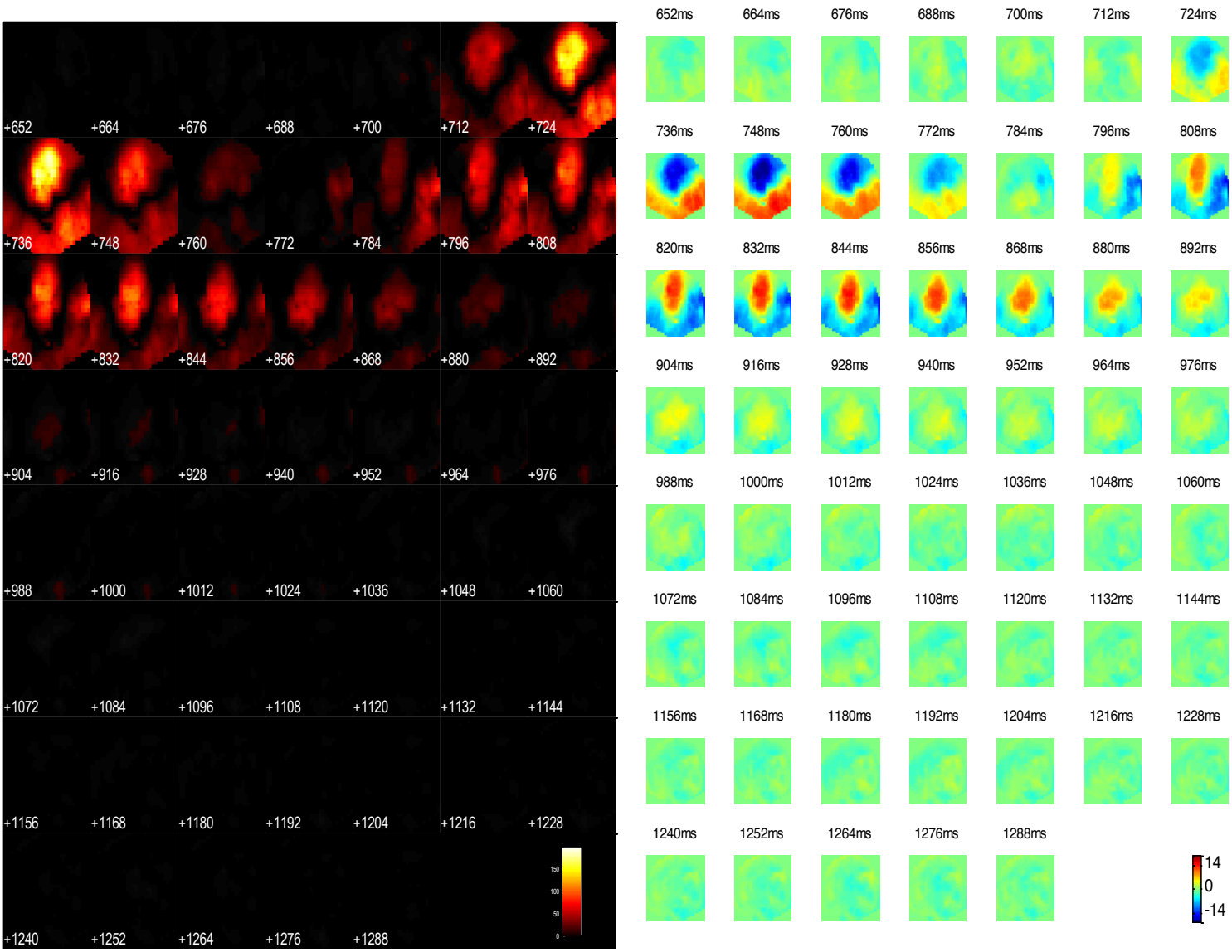

Figure 4.9. Thresholded F-maps ($p < .05$) to show regions of significance for the local effect [LD-LS] on the scalp through time (left). Unthresholded T-maps to show the polarity of the effect on the scalp through time (right). Front of the scalp is positioned at the top. Note that time within the left panel is presented below the corresponding row of scalpmaps, whilst time within the right panel is presented above the corresponding row of scalpmaps.

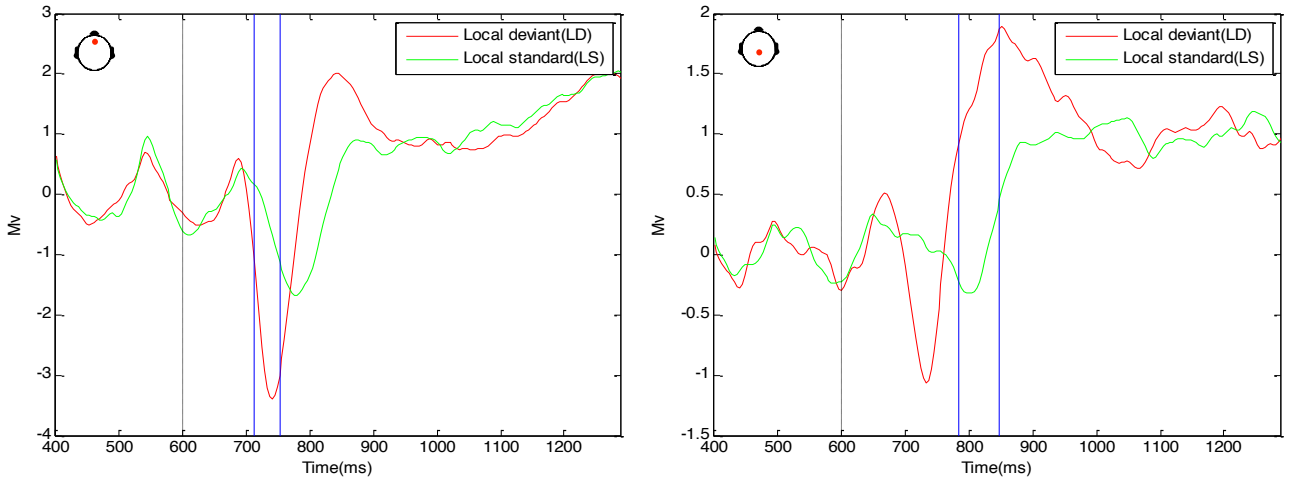

Figure 4.10. Grand average ERPs for the local effect at Fz (left) and Pz (right). Blue lines indicate the region of significance. Black dashed line (600ms) indicates the onset of the final tone.

In Figure 4.9, one can see that during the initial region of significance (712-752ms), the polarity of the response is negative and located frontally, suggesting the significance falls within the region of the mismatch negativity (MMN). What is more, within the second region of significance (784–848ms) the polarity of the response is positive and located centrally, possibly indicative of a P3a response.

It can be seen (in Figure 4.10) that locally deviant tones (red lines) generate a larger response than locally standard tones (green lines). This is consistent with Bekinschtein et al.'s (2009) finding of a local effect, and suggests that local deviance elicits a larger N1 response than locally standard tones.

Furthermore, the local deviant response appears earlier in time compared to the locally standard response, which may suggest that local deviancy accelerates the onset of the local response (see both panels in Figure 4.10; for scalp topography see Figure 4.9).

Global effect. The global effect is significant from 850-1150ms around central electrodes Cz and ch.61 (see Figure 4.11).

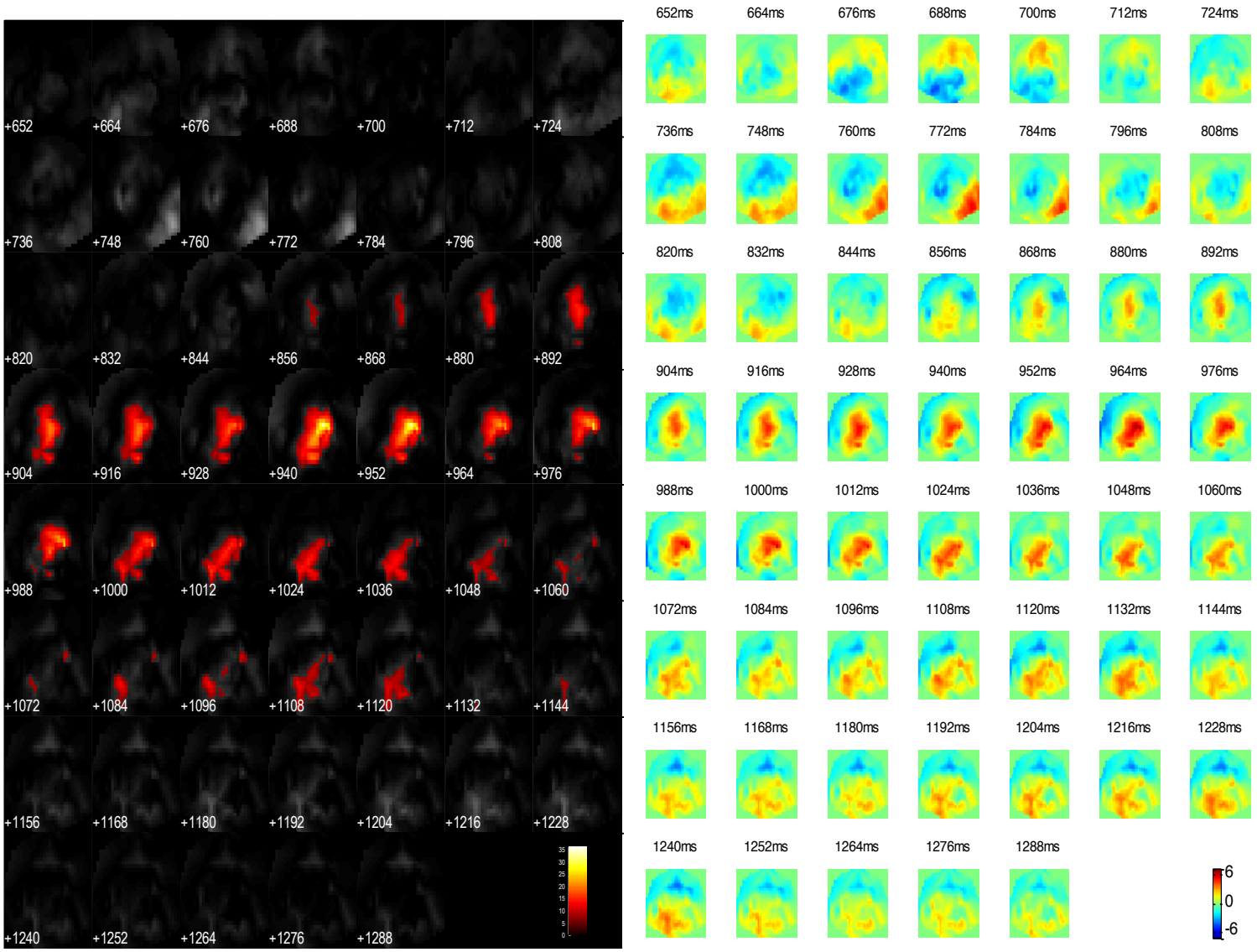

Figure 4.11. Thresholded F-maps ($p < .05$) to show regions of significance for the global effect [GD-GS] on the scalp through time (left). Unthresholded T-maps to show the polarity of the effect on the scalp through time (right). Front of the scalp is positioned at the top. Note that time within the left panel is presented below the corresponding row of scalpmaps, whilst time within the right panel is presented above the corresponding row of scalpmaps.

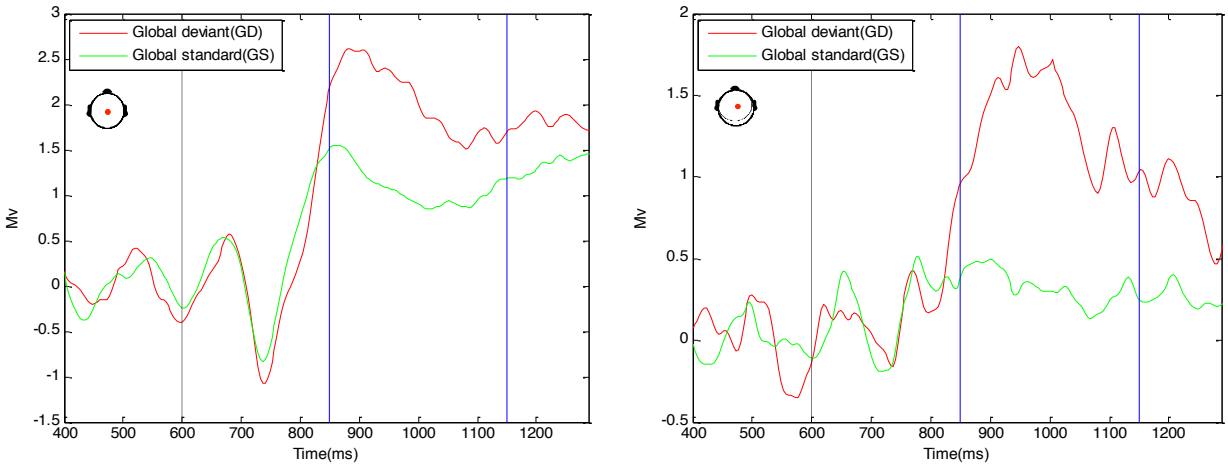

Figure 4.12. Grand average ERPs for the global effect at Cz (left) and ch.61. (right). Blue lines indicate the region of significance. Black dashed line (600ms) indicates the onset of the final tone.

Figure 4.11 shows that the global effect is significant centrally and around 300ms post stimulus onset (900ms in Figures), which is consistent with Bekinschtein et al.'s (2009) previous findings. It can also be seen in Figure 4.12 that global deviance elicits a larger response than global standard, suggesting that globally deviant quintuples elicit a larger response than globally standard quintuples by virtue of their infrequency. Interestingly, there appears to be no significant latency difference between globally deviant and globally standard responses, indicating that global violations of auditory regularity do not accelerate the onset of the P3b.

Interactions

Attention x local. The attention x local interaction is significant between 696-732ms around left frontal electrode ch.19 (see Figure 4.13).

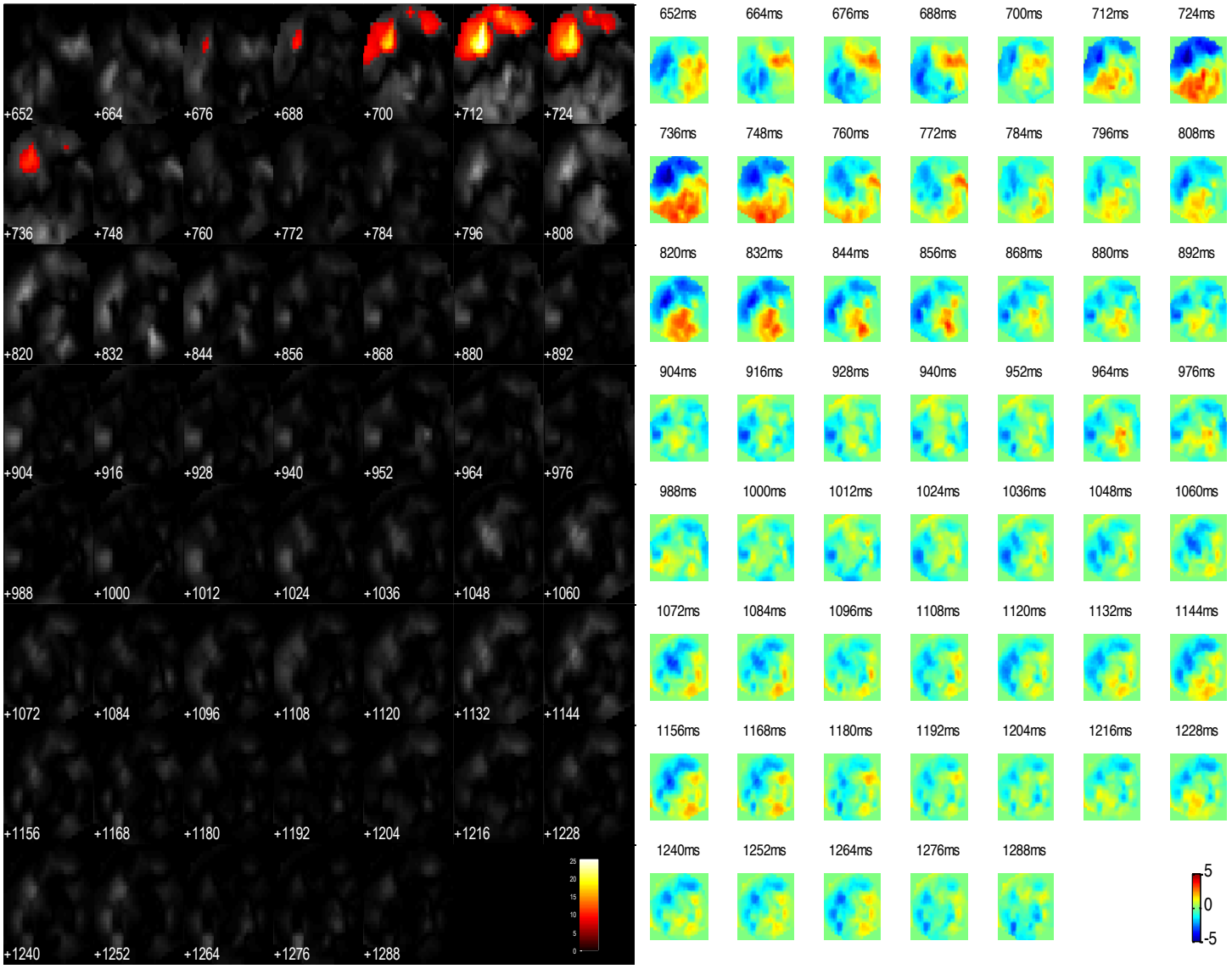

Figure 4.13. Thresholded F-maps ($p < .05$) to show regions of significance for the attention x local interaction [(ALD-ALS)-(PLD-PLS)] on the scalp through time (left). Unthresholded T-maps to show the polarity of the effect on the scalp through time (right). Front of the scalp is positioned at the top. Note that time within the left panel is presented below the corresponding row of scalpmaps, whilst time within the right panel is presented above the corresponding row of scalpmaps.

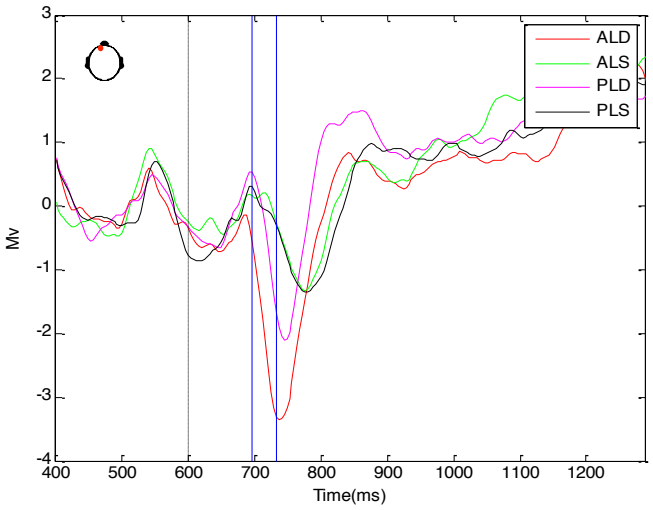

Figure 4.14. Grand average ERPs for the attention x local interaction at ch.19. Blue lines indicate the region of significance. Black dashed line (600ms) indicates the onset of the final tone. (A: active condition, P: passive condition).

The presence of an interaction between attention and local effects suggests that the local effect is changing between active and passive groups in an early time window (see Figure 4.13). The effect is present in the left frontal region around channel 19. In Figure 4.14, one can see that the size of the local effect is smaller within the passive group (ie. difference between magenta and black lines), comparing to that of the active group (ie. difference between red and green lines), possibly because direct attention is enhancing the size of the mismatch response to local deviance, creating a larger difference between local deviant and locally standard responses for the active group comparing to when attention is passive (ie. the passive group). These findings can be related to the work of Chennu et al. (2013), who found that attention to global regularity (ie. auditory sequences) elicited a larger mismatch response to local deviance than attention to local regularity (ie. tones), which further indicates that the local effect is sensitive to manipulations of attention. Interestingly, we found that direct attention is not necessary for the presence of a mismatch response to local deviance (see magenta line in Figure 4.14), which is again consistent with the findings of Chennu et al. (2013). In the presence of direct attention, it appears that the size of the mismatch response to local deviance increases, which has been linked to a degree of precision afforded by attentional engagement with the task (Auksztulewicz & Friston, 2015).

Furthermore, Figure 4.14 reveals a trend towards a larger positive rebound (or P3a response) for the passive group (occurring around 800ms), which may be linked to the

capture of attention by deviant stimuli when passively listening to the task (Freidman, Cycowicz & Gaeta, 2001; Näätänen et al., 1993).

Attention x global. The attention x global interaction is significant from around 900-1072ms around frontal electrode ch.15 and posterior electrode Pz (see Figure 4.15).

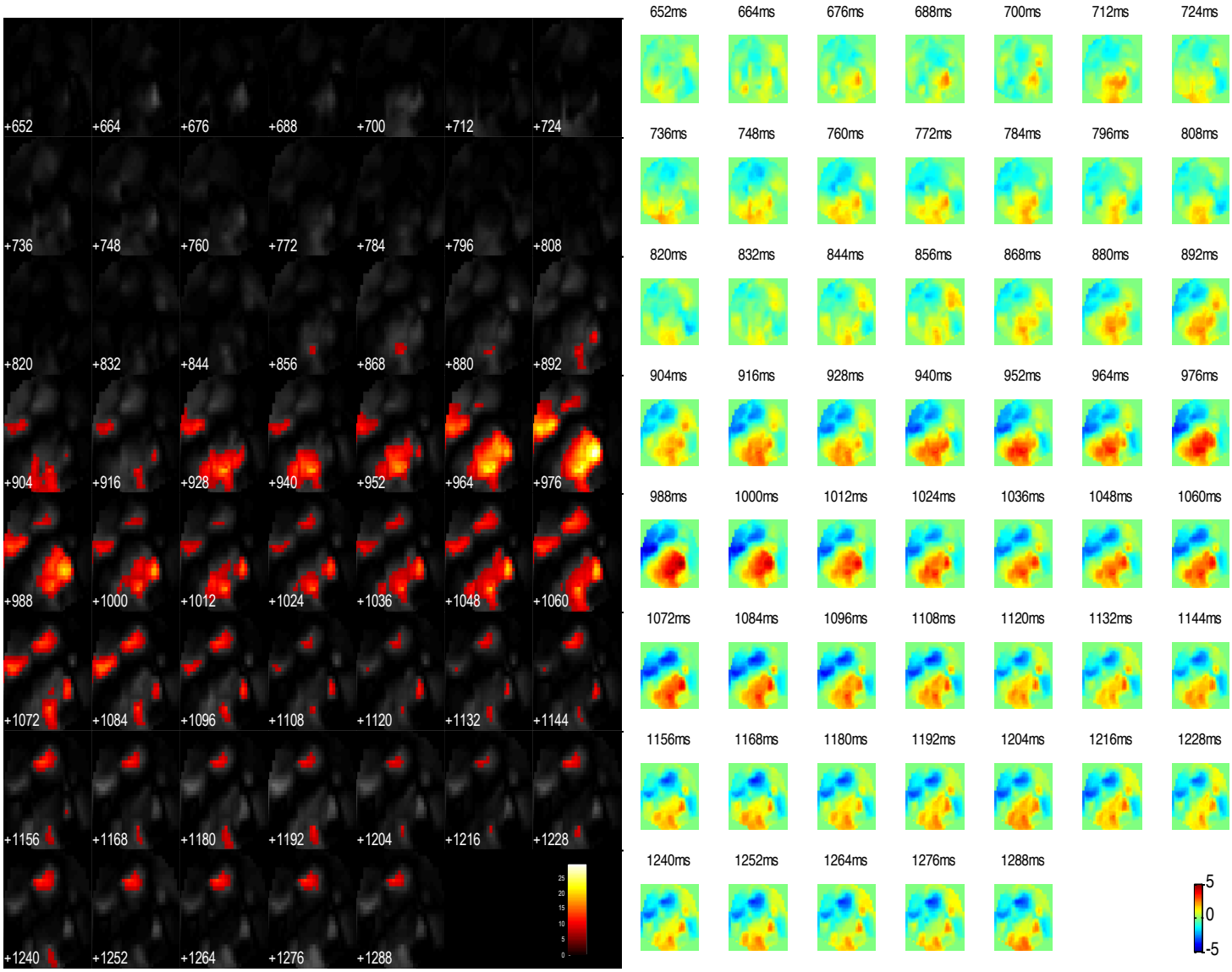

Figure 4.15. Thresholded F-maps ($p < .05$) to show regions of significance for the attention x global interaction [(AGD-AGS)-(PGD-PGS)] on the scalp through time (left). Unthresholded T-maps to show the polarity of the effect on the scalp through time (right). Front of the scalp is positioned at the top. Note that time within the left panel is presented below the corresponding row of scalpmaps, whilst time within the right panel is presented above the corresponding row of scalpmaps.

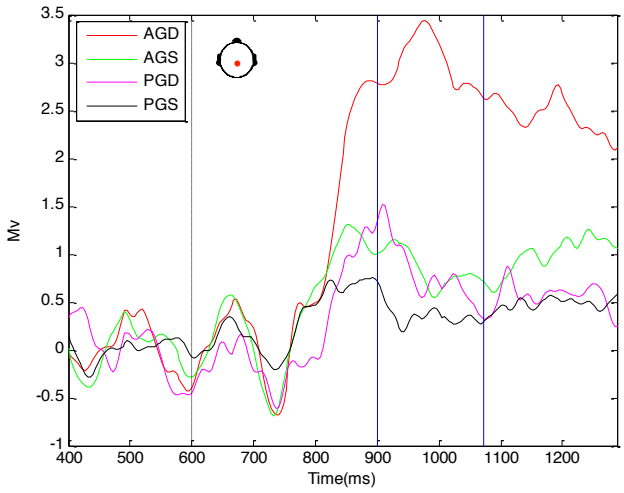

Figure 4.16. Grand average ERPs for the attention x global interaction at Pz. Blue lines indicate the region of significance. Black dashed line (600ms) indicates the onset of the final tone. (A: active condition, P: passive condition).

An interaction between attention and the global effect implies that the global effect is also changing between attention groups (active vs. passive). Figure 4.16 illustrates a large time window of significance (900-1072ms) where it can be seen that the difference between active global deviant (red line) and active global standard (green line) is large comparing to the difference between passive global deviant (magenta line) and passive global standard (black line) which is small. When the disparity of these differences is considered, the attention x global interaction is formed.

Although we observe a possible difference between passive global deviant and passive global standard, neither elicits a large P3b response, suggesting that the absence of direct attention may result in the absence of a large P3b response; this finding is consistent with previous research, which proposes that the global response is contingent upon attentional engagement with the task (Chennu et al., 2013). In contrast, the presence of direct attention may facilitate the detection of global *irregularity* in particular, given that a P3b response is present for active global deviant but not for active global standard. The positive response we observe for the active group is a right lateralised P3b that is consistent with the observed global effect shown previously (see Figures 4.15 and 4.11).

A significant cluster occurring around left lateralised frontal electrode ch.22 at 976ms appears to be the opposite side of the dipole observed at this time (see Appendix 3 for ERP).

Global x local. The global x local interaction is significant from 720–804ms around central electrode Cz. Moreover, the global x local interaction is significant laterally around right frontal electrode ch.90 around 840-984ms (see Figure 4.17).

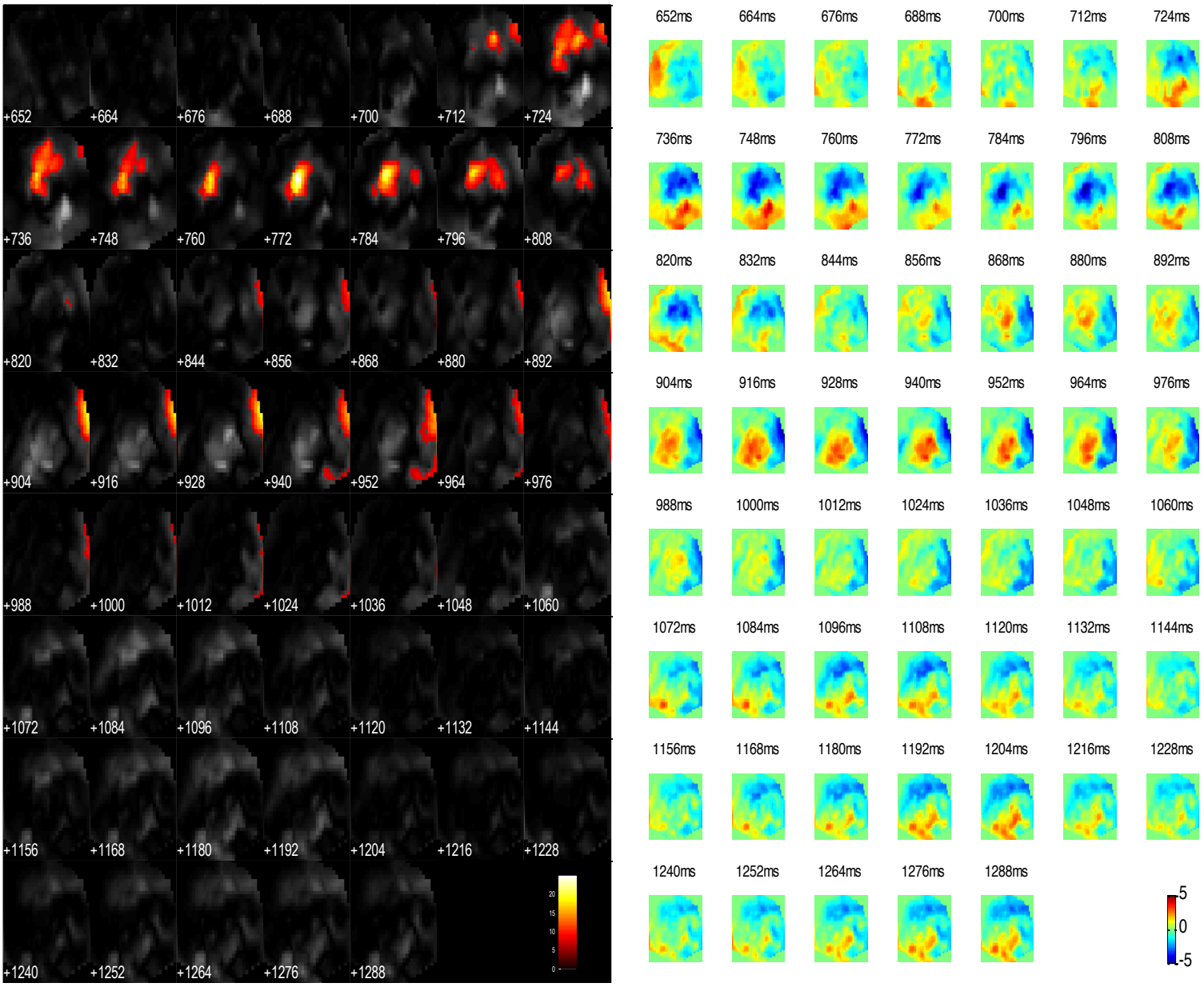

Figure 4.17. Thresholded F-maps ($p < .05$) to show regions of significance for the global x local interaction [(GDLD-GDLS)-(GSLD-GSLS)] on the scalp through time (left). Unthresholded T-maps to show the polarity of the effect on the scalp through time (right). Front of the scalp is positioned at the top. Note that time within the left panel is presented below the corresponding row of scalpmaps, whilst time within the right panel is presented above the corresponding row of scalpmaps.

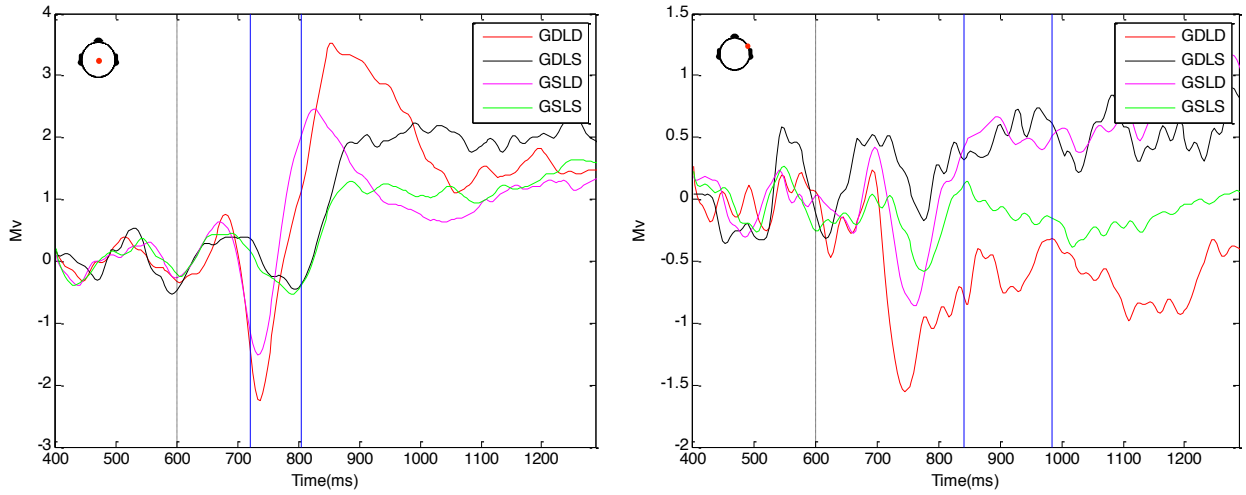

Figure 4.18. Grand average ERPs for the global x local interaction at Cz (left) and ch.90 (right). Blue lines indicate the region of significance. Black dashed line (600ms) indicates the onset of the final tone.

The presence of an interaction between global and local effects suggests that the level of one factor is dependent upon the level of the other factor. Put another way, the two effects (global and local) are not independent and therefore do not share an additive relationship, as implied by Bekinschtein et al. (2009). It appears that the difference between GDLD (red lines) and GDLS (black lines) significantly varies from the difference between GSLD (magenta lines) and GSLS (green lines) (see Figures 4.18 and for clarity on the interaction see Figure 4.4). When the disparity of these differences is considered, the global x local interaction is formed.

In Figure 4.18 one can see that in an early time window (720-804ms) (see left panel in Figure 4.18), the difference between GDLD (red line) and GDLS (black line) is larger than the difference between GSLD (magenta line) and GSLS (green line). As the interaction falls within the time region of the local effect, one may consider the impact of global context upon local responses, as multiple violations in auditory regularity at different levels of the predictive hierarchy (global and local) appear to generate larger responses at the local level. The presence of a global x local interaction which manifests in this way may reveal how top-down expectation of global context impacts upon variations to local regularity.

Furthermore and specifically, GSLD (magenta line) elicits a smaller response, relative to zero, than GDLD (red line) creating a smaller difference between itself and GSLS (green line) when compared to the difference between GDLD (red line) and GDLS (black line).

A reduced initial mismatch response in the case of GSLD may be attributed to an increase in expectancy for local deviance, given that local deviance is the global regularity for GSLD; this finding is consistent with the early interaction between global and local effects observed by Wacongne et al. (2011) (for scalp topography see Figure 4.17).

Additionally, there is a significant interaction laterally on the right side appearing between 840 – 984ms, which is occurring within the time region of the P3b. From the right panel in Figure 4.17, it can be seen that there is a trend towards a central positivity, marking a global effect that may be driving the fringe negativity we observe as significant. Thus, this finding may be indicative of an emerging interaction within the region of the global effect, which did not reach statistical significance within this dataset.

Attention x global x local. The attention x global x local interaction is not statistically significant. This indicates that the global x local interaction was not varying significantly between active and passive groups, although there is a slight trend towards a right lateral positive significance and a central negative significance beyond 650ms (see Figure 4.19).

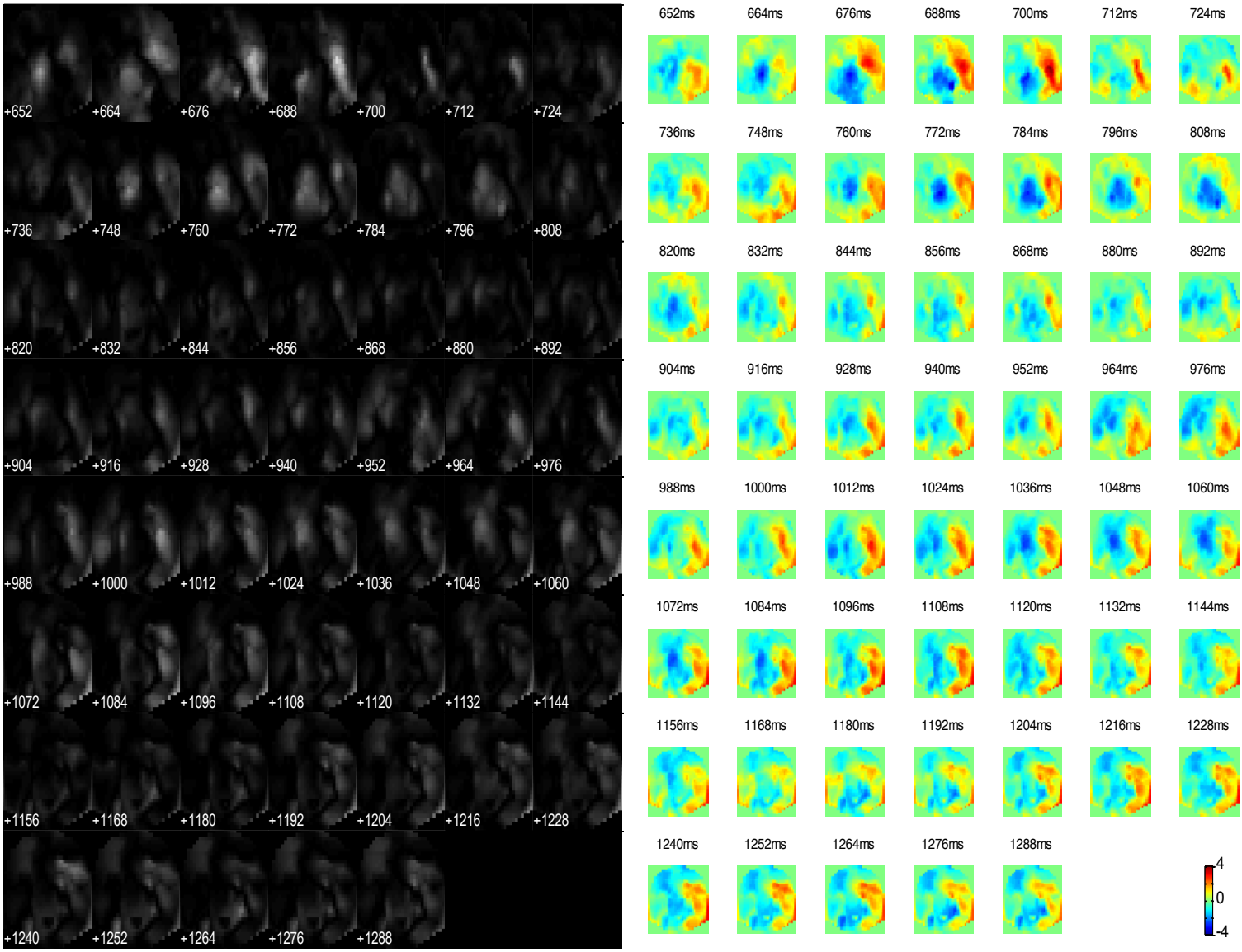

Figure 4.19. Thresholded F-maps ($p < .05$) to show regions of significance for the attention x global x local interaction [((AGDLD-AGDLS)-(AGSLD-AGSLS))-((PGDLD-PGDLS)-(PGSLD-PGSLS))] on the scalp through time (left). Unthresholded T-maps to show the polarity of the effect on the scalp through time (right). Front of the scalp is positioned at the top. Note that time within the left panel is presented below the corresponding row of scalpmaps, whilst time within the right panel is presented above the corresponding row of scalpmaps.

Discussion (attention x global x local)

Firstly, we were successful in replicating the global and local effects found by Bekinschtein et al. (2009) and others in the literature (Wacongne et al., 2011; Wacongne, Changeux & Dehaene, 2012; Pegado et al., 2010; Chennu et al., 2013; Rémi-King, Gramfort, Schurger, Naccache & Dehaene, 2014). In addition to this, we found an interaction between the global and local effects, occurring within the region of the local effect, that has previously been reported by Wacongne et al. (2011) but not explored in detail. The presence of an interaction signifies that global and local effects are not orthogonal (independent). Our findings sit in contrast to Bekinschtein et al.'s (2009) original proposal that the global and local effects are independent, as the size of local responses appear to be dependent upon the global regularity of the block.

More specifically, it appears that global deviance that is marked by a local deviant (GDLD) elicits a larger initial negative mismatch response than a local deviant, which is globally standard (GSLD) (see left panel in Figure 4.18). One might suggest that GDLD violates not only a local expectation of regularity but also a global expectation of regularity, therefore a larger amount of prediction error is contributing to a larger mismatch response comparing to when there is only a local violation in auditory regularity (as with GSLD). This can be interpreted within the predictive coding framework whereby violations in global regularity as well as local regularity generate prediction error not only at the local level but also at the global level of expectation (Chennu et al., 2013; Wacongne et al., 2011; Friston, 2010). The presence of an interaction within the region of the local effect suggests that not only may prediction error propagate from the lower to the higher levels of the predictive hierarchy, but that top-down expectation also feeds back from higher to lower levels of the hierarchy as a function of prediction accuracy (precision) (Friston, 2010).

Moreover, it may be argued that when local deviance is the globally regular pattern of sound, expectation for local deviance increases. As such, the expectation of local deviancy increases and the size of the negative mismatch response reduces over repetition given that prediction error decreases and precision increases. The attenuation of the mismatch response through repetition is a well-documented finding within the literature on auditory deviance processing (Auksztulewicz & Friston, 2015; Pegado et

al., 2010; Chennu et al., 2013; Wacongne et al., 2011; Wacongne, Changeux & Dehaene, 2012).

Furthermore, we found that the manipulation of attention also impacted significantly on global and local effects respectively. That is, participants in the active group, ie. attention directed towards the task, elicited larger overall responses than those in the passive group (allowed to let their minds wander) (see Figure 4.8). This indicates that attentional engagement enhances the size of both global and local effects, most likely because active participants are better able to distinguish between deviant and standard tones by actively listening for the presence of global deviance. Interestingly, Chennu et al. (2013) previously found that manipulating global attentional bias increased the size of the mismatch response. That is, the MMN was largest when participants attended to sequences (ie. the global context of sound) as opposed to tones (ie. local features of the auditory stream). Therefore, attentional engagement with global regularity appears to afford precision that enhances the size of the MMN in response to local deviance (see Figure 4.14). One may consider that the precision afforded by attention not only enhances the size of the mismatch response but is also subject to the focus of attentional bias (Chennu et al., 2013).

Additionally, there appears to be no instance of a P3b response to global deviance when passive (see Figure 4.16), which could signify the absence of direct attention (Chennu et al, 2013). Moreover, given that a P3b response is present for the active group, it appears that the detection of global deviance is contingent upon attentional engagement with task, which is consistent with previous findings that suggest attentional engagement is necessary for long-range temporal focus on global patterns of sound (Chennu et al., 2013). Furthermore, attentional engagement with the task was found to impact upon response onset at the local level, that is attentional engagement with the task increased response onset to local deviancy suggesting that direct attention may increase the processing speed of local violations in auditory regularity (see Figure 4.14). What is more, attentional engagement with the task does not appear to have significantly impacted upon response onset at the global level, suggesting that direct attention does not increase the processing speed of global violations in auditory regularity (see Figure 4.16).

Interestingly, the latency difference between responses to local deviance vs. locally standard tones exceeded that of direct vs. passive attention; that is, locally deviant tones elicited an earlier frontal negative response than locally standard tones (see left panel in Figure 4.10). This finding suggests that local deviance elicits a faster ERP response than locally standard stimuli, suggesting possibly that the brain detects local violations in auditory regularity more quickly than locally regular patterns of sound. What is more, the size of mismatch response to local deviance appears dependent upon the global context in which local deviance is occurring (ie. whether local deviance is also globally deviant or globally standard) (see left panel in Figure 4.18), which contributes to the interaction between global and local effects that we observe within this region.

Moreover, there appears to be a trend towards a difference between responses to global deviance depending upon the level of the local effect (ie. local standard vs. local deviance) around 900ms (see left panel in Figure 18 and T-maps in Figure 4.17), although this was not found to be significant within this dataset. What is more, we found that the interaction between global and local effects was not changing significantly between active and passive groups although there was a trend towards a central negativity around 760ms and a right lateralised positive effect around 650ms onwards (see T-maps in Figure 4.19).

In sum, it is implied that whilst the presence of deviancy in the local context generates earlier responses, regardless of whether attention is engaged with the task or passive, the differentiation of standard and deviant quintuples at the global level appears to be indexed by the presence of direct attention. At the same time, the size of the local effect is subject to both attention and global regularity. Consequently, it appears that whilst direct attention facilitates the presence of a global effect, it enhances the size of the local effect. What is more, the presence of an early interaction within the region of the local effect reveals that global regularity impacts upon the size of local responses to deviance. It may be the case that top-down expectancy from higher levels of the predictive hierarchy is coinciding with expectation at lower levels of the predictive hierarchy to generate responses to deviance which correspond to the amount of prediction error they induce.

It is important to clarify at this point that all participants within the study were awake and therefore able to attend to the task, meaning that consciousness as a static state of

wakefulness was not explored within the current Chapter. The present study examined attentional focus as a function of what one may be conscious *of* when awake and aware. Thus, the discussion within this Chapter has centred around the cognitive processes that underlie conscious perception and not consciousness as a static state upon a spectrum of wakefulness (which will be explored in more detail within subsequent Chapters). In order to further examine the interaction between global and local effects with respect to attention, we conducted a simple effects analysis (presented in the subsequent Chapter) of active and passive groups respectively.

5 Interacting with consciousness II: a simple effects re-analysis of electrophysiological responses to the global-local task with varied attention

Within this Chapter, we will present the simple effects analysis conducted to further examine how attention impacts on responses to the global-local task. A two-way ANOVA was applied to the active and passive groups separately assessing levels of the local effect (standard vs. deviant) against levels of the global effect (standard vs. deviant).

Post-hoc correction

As we are conducting post-hoc analysis of simple effects, consideration must be paid to adequate correction of the alpha level. Given that the cluster-forming threshold at the first-level defines features of the signal it should not change within the post-hoc analysis. However, the cluster-extent threshold at the second-level can be adjusted to manage the significance of clusters, for example if Bonferroni correction is applied the alpha level of 0.05 should be divided by 2 (as two tests are conducted, one for the active group and one for passive group); therefore 0.05/2 = 0.025. We acknowledge that there is some difficulty in accurately correcting for the number of comparisons within time-series data, as one is attempting to correct for post-hoc multiple comparisons made across both time and space simultaneously (Kilner & Friston, 2010). In order to reduce inflation of the alpha level, we have taken the cautious and pragmatic approach of reducing the significance threshold from 0.05 to 0.01 in all of the following cluster-level analyses within this Chapter (P-values and F-values for each cluster can be viewed in Appendix 1.2 and 1.3).

Active group

Two-way ANOVA (global x local)

A two-way ANOVA (global x local) was applied to the active group to examine local (standard vs. deviant) and global (standard vs. deviant) effects.

Active local effect. The local effect is significant between 712–752ms around frontal electrode Fz. Furthermore, there is significance between 784–872ms around central electrode Cz (see Figure 5.1).

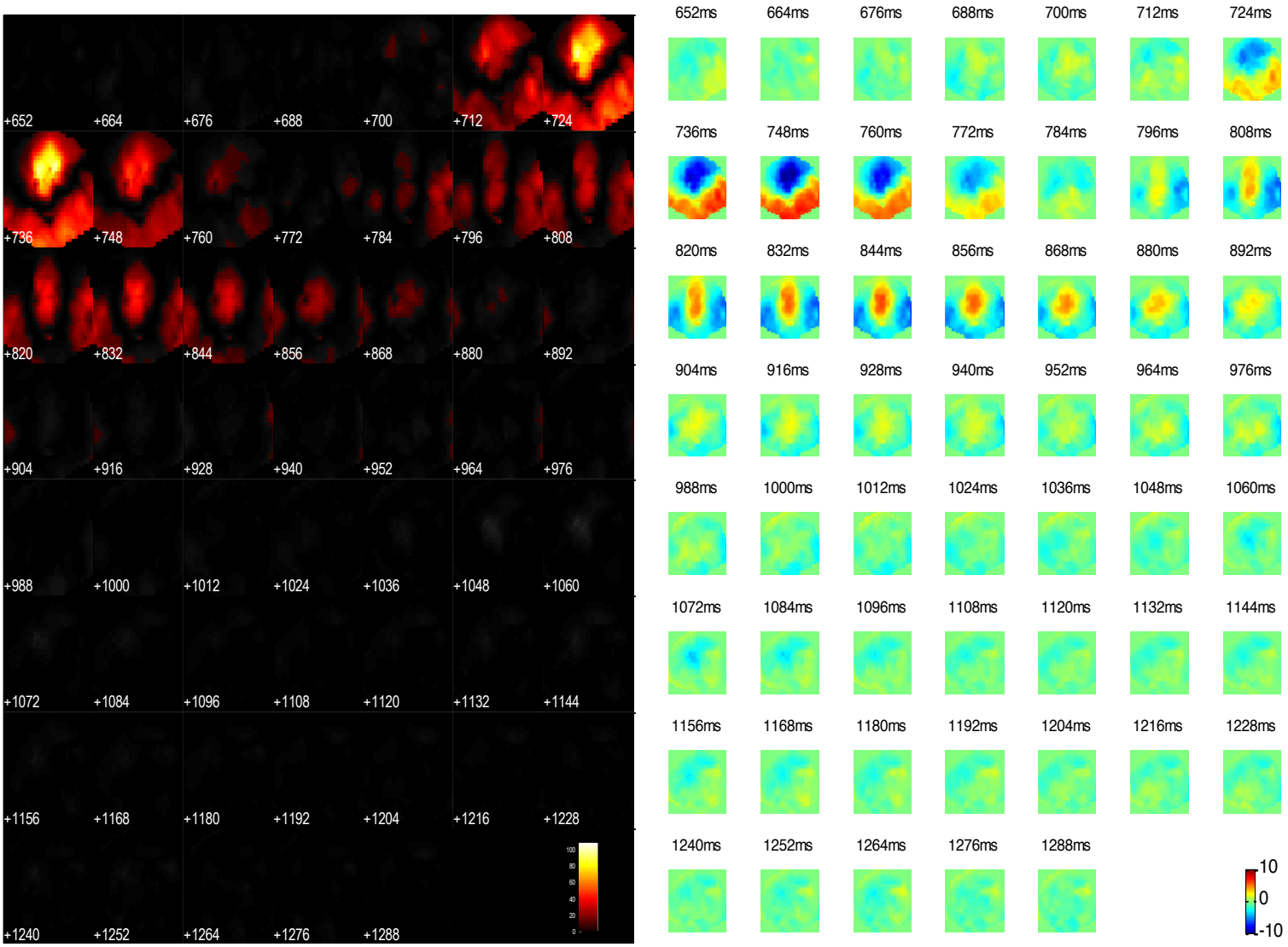

Figure 5.1. Thresholded F-maps ($p < .05$) to show regions of significance for the local effect in the active condition [ALD-ALS] on the scalp through time (left). Unthresholded T-maps to show the polarity of the effect on the scalp through time (right). Front of the scalp is positioned at the top. Note that time within the left panel is presented below the corresponding row of scalpmaps, whilst time within the right panel is presented above the corresponding row of scalpmaps.

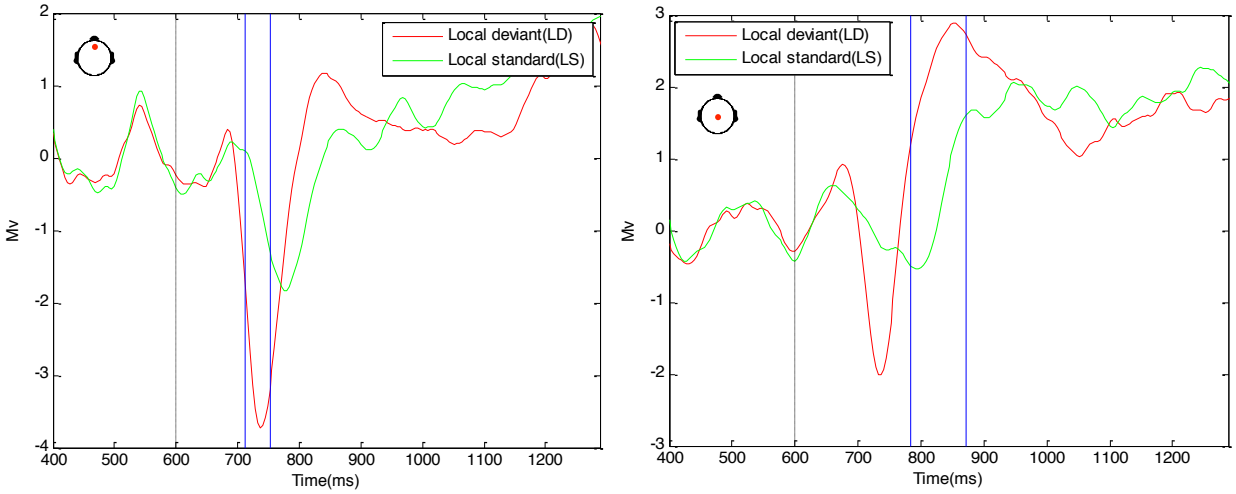

Figure 5.2. Grand average ERPs for the local effect at Fz (left) and Cz (right) in the active condition. Blue lines indicate the region of significance. Black dashed line (600ms) indicates the onset of the final tone.

One can see that for the active group within an early window of significance (712-752ms) at electrode Fz (left panel in Figure 5.2), local deviance (red line) is eliciting a large N1 response, whilst local standard (green line) is not. In the later region of significance at electrode Cz, we find that local deviance (red line) elicits a larger positive response than a locally standard tone (green line) (right panel in Figure 5.2) (for scalp topography see Figure 5.1). The onset of the response to local deviance is earlier than the response to locally standard tones, suggesting that participants are quicker to detect local deviance comparing to local standard.

Active global effect. The global effect is significant from 852-1236ms around posterior central electrode Pz (see Figure 5.3).

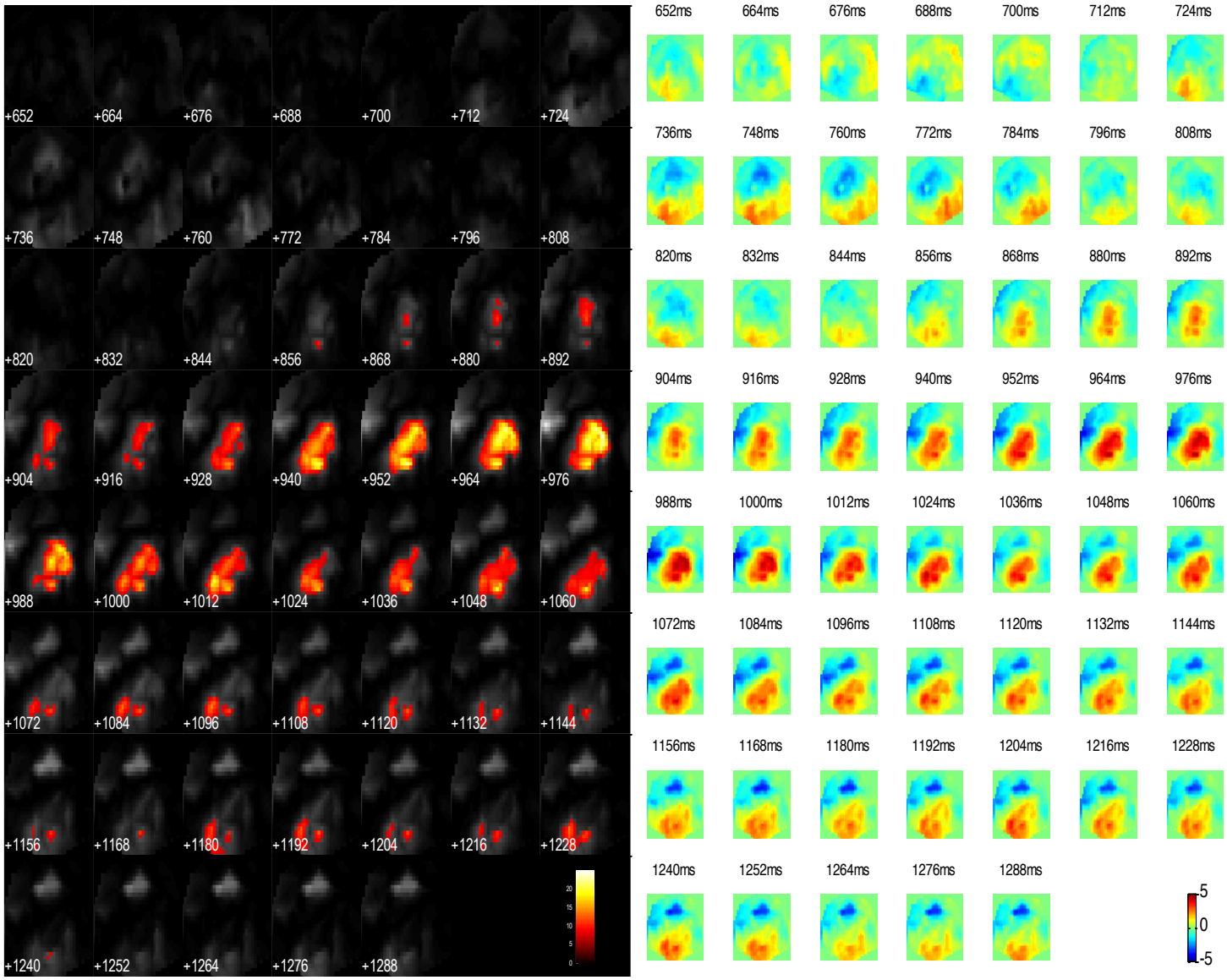

Figure 5.3. Thresholded F-maps ($p < .05$) to show regions of significance for the global effect in the active condition [AGD-AGS] on the scalp through time (left). Unthresholded T-maps to show the polarity of the effect on the scalp through time (right). Front of the scalp is positioned at the top. Note that time within the left panel is presented below the corresponding row of scalpmaps, whilst time within the right panel is presented above the corresponding row of scalpmaps.

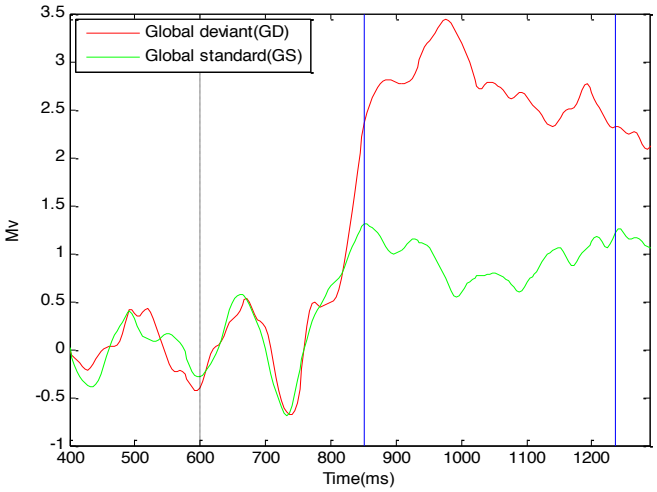

Figure 5.4. Grand average ERP for the global effect at Cz in the active condition. Blue lines indicate the region of significance. Black dashed line (600ms) indicates the onset of the final tone.

It can be seen in Figure 5.4 that globally deviant tones (red line) elicit a larger positive response than locally standard tones (green line), suggesting that global deviance elicits a P3b response, whilst global standard does not (for scalp topography see Figure 5.3). There appears to be no large difference in latency between global deviant and global standard suggesting that the presence of global deviance does not impact response onset.

Active global x local. The global x local interaction is not significant for the active condition. This suggests that, at least in this dataset, the global and local effects are independent of one another within the active group. There is a trend towards significance fronto-centrally around 740ms (see Figure 5.5).

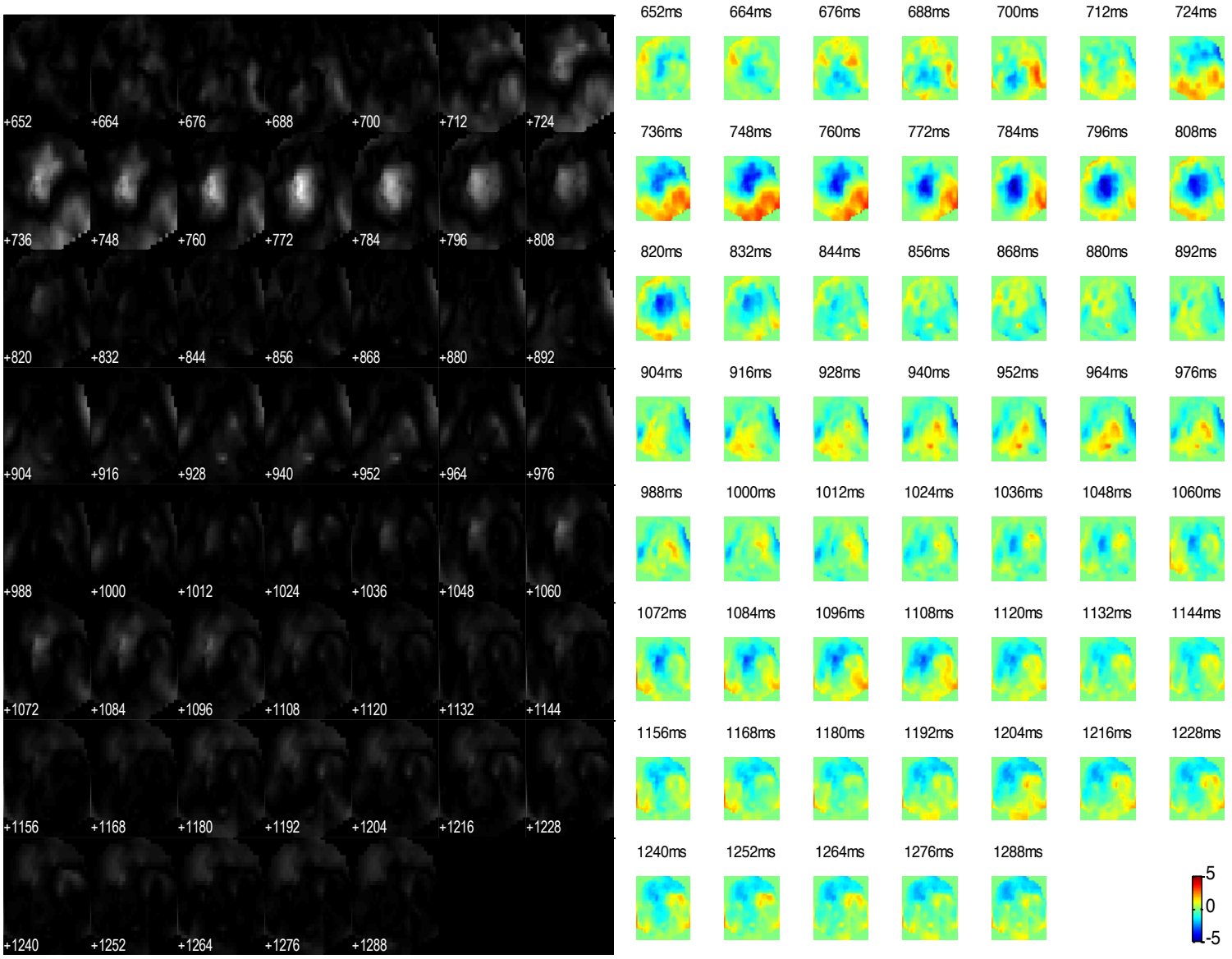

Figure 5.5. Thresholded F-maps (p <.05) to show regions of significance for the global x local interaction in the active condition [(AGDLD-AGDLS)-(AGSLD-AGSLS)] on the scalp through time (left). Unthresholded T-maps to show the polarity of the effect on the scalp through time (right). Front of the scalp is positioned at the top. Note that time within the left panel is presented below the corresponding row of scalpmaps, whilst time within the right panel is presented above the corresponding row of scalpmaps.

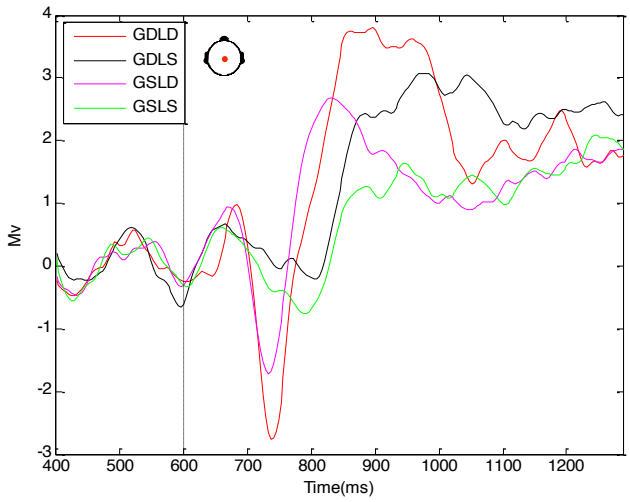

Figure 5.6. Grand average ERP for the global x local interaction in the active condition at Cz. Black dashed line (600ms) indicates the onset of the final tone.

The right panel in Figure 5.5, and Figure 5.6 show a trend towards a significant interaction in an early time region (just after 700ms) given the difference between GDLD (red line) and GDLS (black line) compared to the difference between GSLD (magenta line) and GSLS (green line); this may be indicative of global regularity impacting upon the size of local responses, which would be consistent with the early frontal interaction between global and local effects reported by Wacongne et al. (2011). In particular, locally deviant responses (GDLD [red line] and GSLD [magenta line]) reveal that when local deviance is also globally deviant (GDLD) there is a trend towards a larger negative response comparing to when local deviance is globally standard (GSLD).

Just after 800ms, there is a positive response to GDLD (red line) and GDLS (black line) for the active group, suggesting that those with their attention directed towards the task may have been detecting global deviance as marked by a locally deviant quintuple and global deviance as marked by locally standard quintuples; this is most likely because they were actively listening for global deviance. Meanwhile, no P3b response was observed for globally standard quintuples (GSLD [magenta line] and GSLS [green line]), as they do not violate global regularity. The ability to detect global deviance with both locally standard quintuples and locally deviant quintuples put against the absence of a P3b response when quintuples are globally standard, results in no interaction between global and local effects as the variation of these two differences is not substantial enough to reach statistical significance. Thus, the absence of an interaction

between global and local effects may be a signature of attentional engagement with the task. Moreover, the shape of the P3b responses around 900ms to GDLD (red line) and GDLS (magenta line) are quite different, which may have constituted an interaction had there been a larger sample and therefore greater statistical power.

Summary of results for the active group

Both global and local effects are found in the active group (see Figures 5.1, 5.2, 5.3 and 5.4), although no interaction was observed between them within this dataset (see Figure 5.5). There is a trend within the data towards a difference in P3b response between GDLD and GDLS, although this difference did not vary significantly from the difference between GSLD and GSLS conditions, therefore an interaction was not formed; it may be the case that with greater statistical power, this effect becomes significant. However, within this study, the absence of an interaction between effects indicates that global and local effects are separable when attention was directed towards the task. Participants appear to be detecting global deviance marked both by locally standard and locally deviant quintuples, most likely because they are actively listening for instances of global deviance. Direct attention therefore, may facilitate the detection of global deviance without being subject to differences in the local context. What is more, globally standard quintuples did not elicit a P3b response, as they did not violate expectations of global regularity. Therefore, within the active group, global and local effects appear to be separable because participants are eliciting a P3b response to both GDLD and GDLS conditions.

Passive group

A two-way ANOVA (global x local) was applied to the passive group to examine local (standard vs. deviant) and global (standard vs. deviant) effects.

Two-way ANOVA (global x local)

Passive local effect. The local effect is significant between 720-752ms around frontal electrode Fz. Moreover, the local effect is again significant around frontal electrode Fz between 784-880ms (see Figure 5.7).

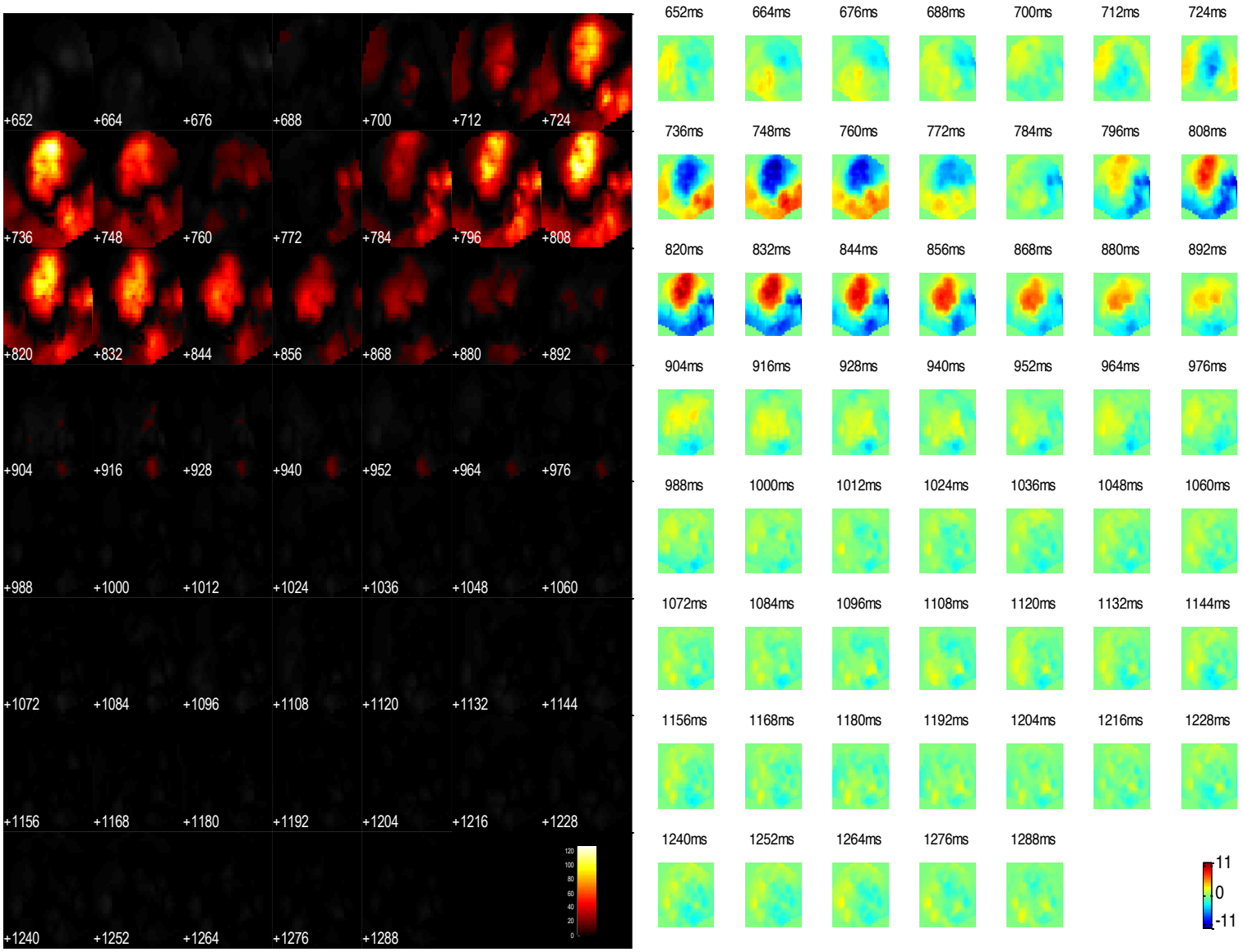

Figure 5.7. Thresholded F-maps ($p < .05$) to show regions of significance for the local effect in the passive condition [PLD-PLS] on the scalp through time (left). Unthresholded T-maps to show the polarity of the effect on the scalp through time (right). Front of the scalp is positioned at the top. Note that time within the left panel is presented below the corresponding row of scalpmaps, whilst time within the right panel is presented above the corresponding row of scalpmaps.

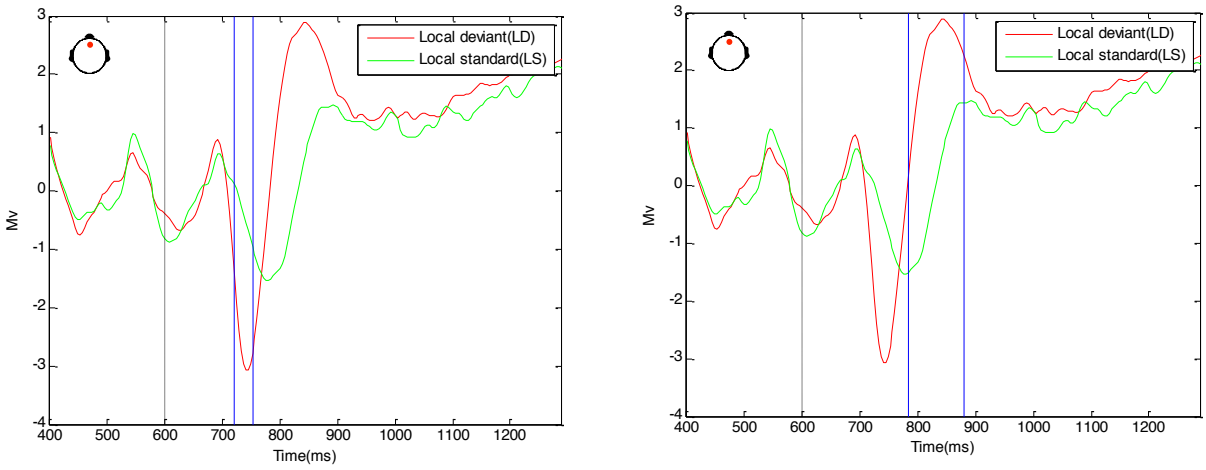

Figure 5.8. Grand average ERPs for the local effect at Fz for the passive condition. Blue lines indicate the regions of significance. Black dashed line (600ms) indicates the onset of the final tone.

Within the initial time window of significance (720-752ms) at electrode Fz, for the passive group local deviance (red line) elicits a mismatch response, whilst locally standard tones (green line) show a reduced response (see left panel on Figure 5.8). In addition to this, the onset of the mismatch response to local deviance is earlier than the onset of the response to local standard, suggesting that participants are quicker to detect local deviance comparing to locally standard tones. Furthermore, the presence of a local effect within the passive group implies that the local effect is robust against changes in attention. What is more, during the second time window of significance, we observe a positive rebound from the mismatch response to local deviance (red line), which is not present for locally standard tones (green line) (see right panel in Figure 5.8); this may be a P3a response which could be linked to the capture of attention by local deviance (Freidman, Cycowicz & Gaeta, 2001).

Passive global effect. The global effect is significant between 876-996ms around frontal electrode Fz (see Figure 5.9).

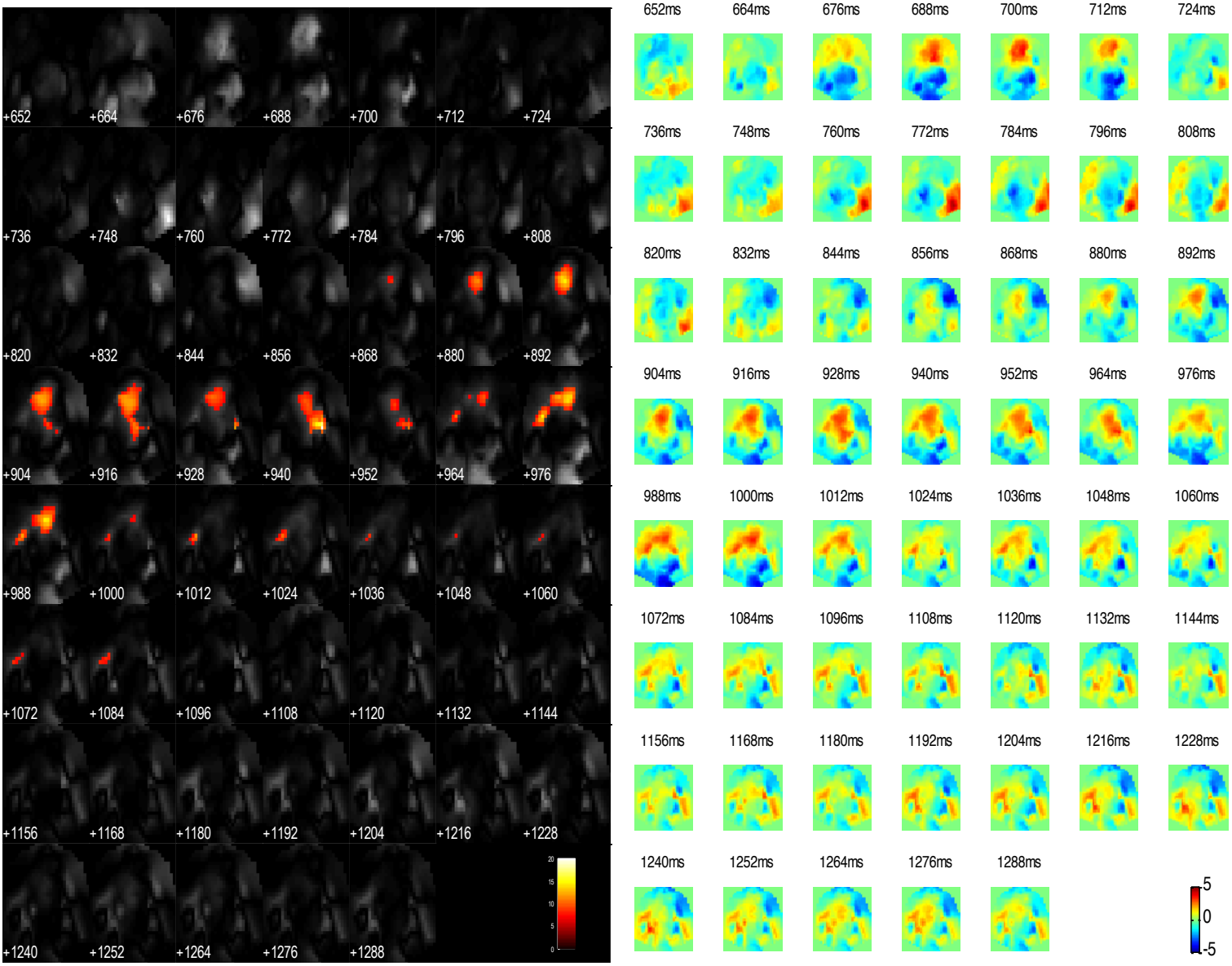

Figure 5.9. Thresholded F-maps ($p < .05$) to show regions of significance for the global effect in the passive condition [PGD-PGS] on the scalp through time (left). Unthresholded T-maps to show the polarity of the effect on the scalp through time (right). Front of the scalp is positioned at the top. Note that time within the left panel is presented below the corresponding row of scalpmaps, whilst time within the right panel is presented above the corresponding row of scalpmaps.

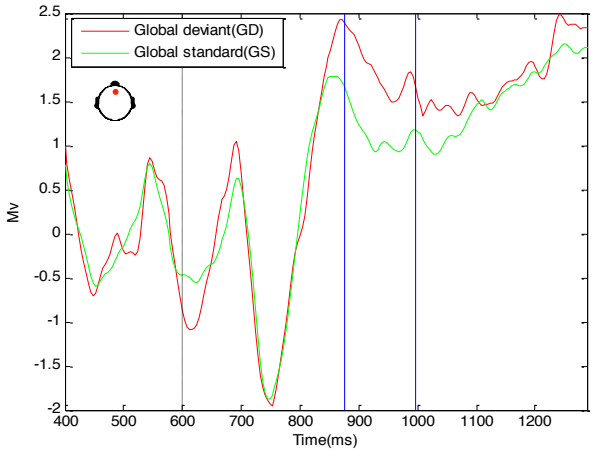

Figure 5.10. Grand average ERP for the global effect at Fz for the passive condition. Blue lines indicate the region of significance. Black dashed line (600ms) indicates the onset of the final tone.

The global effect for the passive condition is located frontally at electrode Fz. The effect, as shown in Figure 5.9, varies a large amount comparing to the global effect observed in the active group (see Figure 5.4). Figure 5.10 reveals that global deviance elicited a larger positive response than globally standard tones, suggesting that there is some evidence of a distinction between globally standard and globally deviant quintuples. What is more, there appears to be no large latency differences between global deviance and global standard, implying that deviance is not accelerating the onset of responses to global violations of auditory regularity. Importantly, the absence of a P3b response (which would be more posterior around 900ms) to globally deviant quintuples suggests that attentional engagement is necessary for the integration of more complex predictive contexts occurring later in the predictive hierarchy (Chennu et al., 2013).

Passive global x local. The global x local interaction is significant between 840-948ms around central electrode Cz and also right laterally at the front of the scalp between 748-820ms (see Figure 5.11).

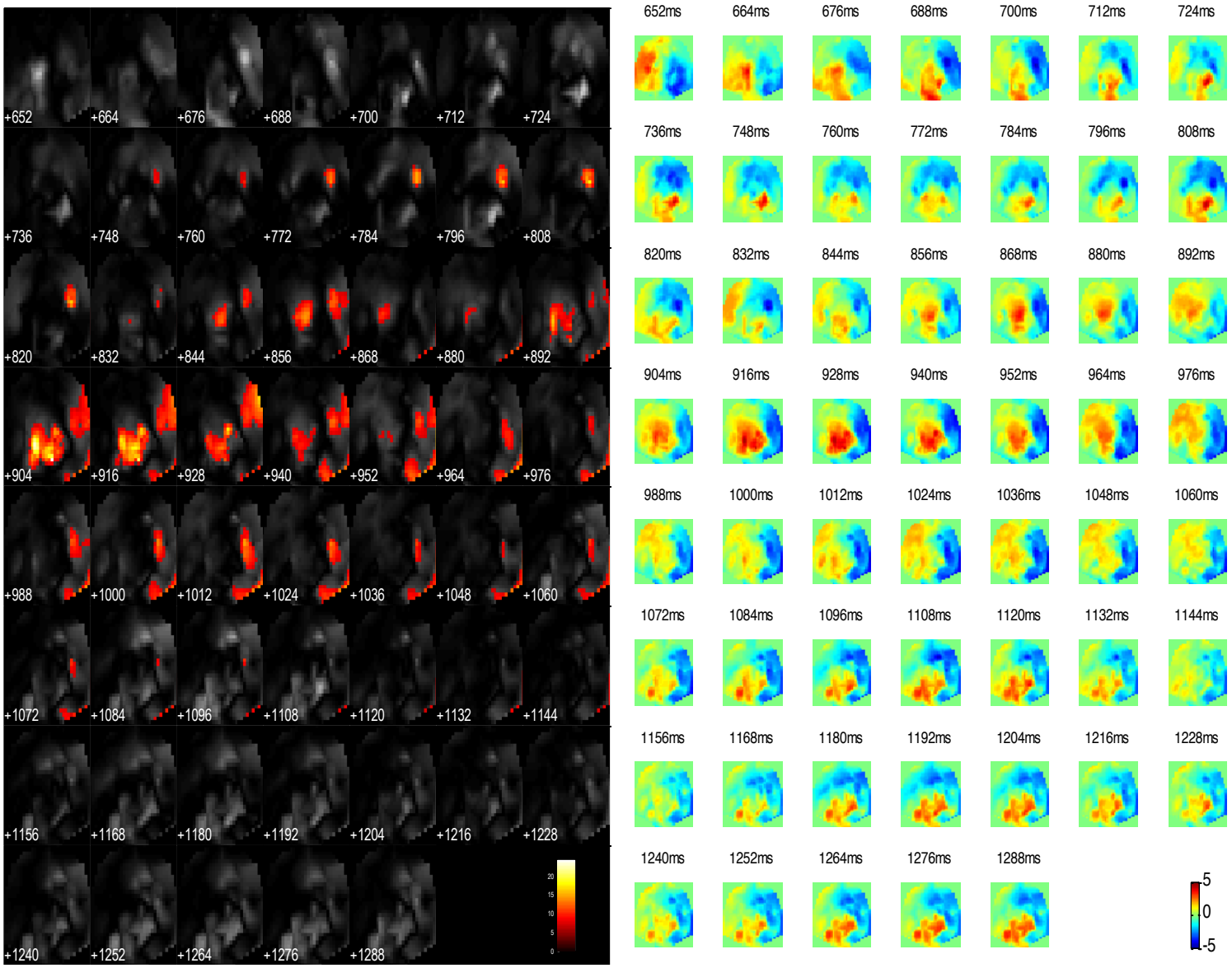

Figure 5.11. Thresholded F-maps ($p < .05$) to show regions of significance for the global x local interaction in the passive condition [(PGDLD-PGSLD)-(PGDLS-PGSLS)] on the scalp through time (left). Unthresholded T-maps to show the polarity of the effect on the scalp through time (right). Front of the scalp is positioned at the top. Note that time within the left panel is presented below the corresponding row of scalpmaps, whilst time within the right panel is presented above the corresponding row of scalpmaps.

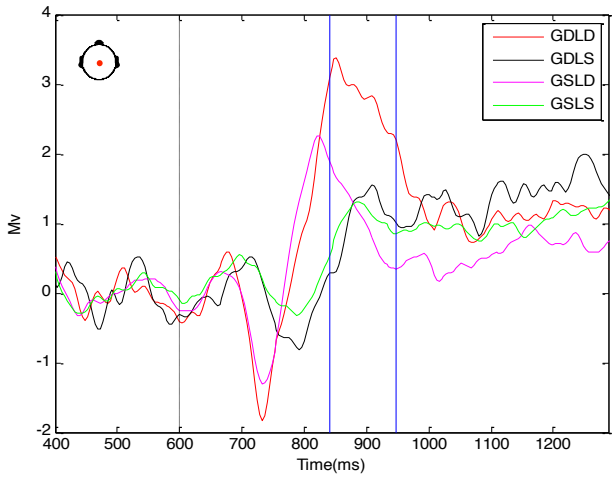

Figure 5.12. Grand average ERPs for the global x local interaction in the passive condition at Cz. Blue lines indicate the region of significance. Black dashed line (600ms) indicates the onset of the final tone.

There is an interaction between global and local effects within the passive group, which reveals that they are not separable in this case (see Figure 5.11). Figure 5.12 shows that GDLD (red line) is eliciting a P3b response, whilst GDLS (black line) is not despite being globally deviant; this may arise because local regularity is impacting upon the detection of global deviance when attention is *not* directed towards the task. In other words, participants are not actively listening for global deviance and therefore only elicit a P3b response when both global and local auditory contexts are violated. It has been argued that the detection of local deviance does not depend upon attentional engagement with the task (Chennu et al., 2013), although it does appear that direct attention is necessary for the detection global deviance, marked by a locally standard quintuple. Therefore, when attention is passive, global deviance can be detected via the additional presence of local deviance, However, global deviance that is marked by a locally standard quintuple does not elicit a P3b response when attention is passive owing to the absence of a local auditory violation.

One may consider these findings within a predictive coding framework whereby prediction error generated at both global and local levels creates multiple violations in expectancy that elicit a P3b response when attention is passive. Whereas, global deviance presented as a locally standard quintuple violates global expectation but not the local expectation of auditory regularity, which has been argued to be robust against wandering attention. Thus, when attention is passive, local regularity appears to mask the detection of global irregularity given that attentional engagement with the task is

necessary for the integration of more complex predictive contexts (Chennu et al., 2013). The presence of a P3b response to GDLD and not GDLS when passive is a finding that can only be explored in the context of an interaction between global and local effects, which consequently reveals an intricate relationship between attention and a hierarchical framework of expectancy. Interestingly, it may be the case that the presence of an interaction between global and local effects within the region of the P3b response may index the absence of directed attention.

The disparity in the size of responses to GDLD and GDLS can explain why no global effect relating to the P3b was found for the passive group. The difference between the presence of a P3b for GDLD (red line) and the absence of a P3b for GDLS (black line) will average to a very small response when overall global deviance is considered. Meanwhile, there is no evident P3b response to either of the globally standard conditions (GSLD [magenta line] and GSLS [green line]), as they do not violate assumptions of global regularity. Therefore, the absence of a P3b response for globally standard conditions matched with the small averaged effect of globally deviant conditions appears to have resulted in a non-significant difference between global deviant and global standard responses.

Summary of results for the passive group

Both global and local effects were observed in the passive group, although the global effect was located frontally. The absence of a typical global effect (ie. centrally around 900ms) may be explained by the presence of an interaction between global and local effects whereby a P3b response exists for GDLD but not for GDLS. When averaged, these responses resulted in a small effect that was not significantly different from responses to globally standard conditions. In addition, it was found that deviance accelerated the onset of responses at the local level, whilst this was not the case at the global level. With regards to the interaction between global and local effects, it appears that the absence of directed attention may result in a failure to detect global deviance that is marked by a locally standard quintuple (GDLS), however participants were still able to detect global deviance that was marked by a locally deviant quintuple (GDLD). We propose that this may be explained in the framework of predictive coding whereby GDLD violates multiple layers of expectancy, evoking prediction error on both local and

global levels, whilst GDLS violates global expectancy but is masked by local regularity given that attention weighted precision is low (ie. attention is not directed towards the task). Critically, it is the presence of a P3b response to GDLD and the absence of a P3b for GDLS which contributes to the disparity of differences that creates the interaction. Given that an interaction arises within the region of the global effect for the passive group, and it is known that direct attention facilitates global responses (Bekinschtein et al., 2009; Chennu et al., 2013), the interaction between global and local effects in this case may provide a marker of passive attention.

Discussion

The work presented within this and the previous Chapter was a full factorial re-analysis of data from the study on varied attention in relation to the global-local task (Bekinschtein et al., 2009). The data was originally collected and published by Bekinschtein et al. (2009), however former analysis has not comprehensively addressed the likelihood of an interaction between global and local effects (Bekinschtein et al., 2009; Wacongne et al., 2011).

Bekinschtein et al. (2009) formally argued that the presence of a global effect signified conscious processing, although manipulations of attention revealed the absence of a global effect when attention was not directed towards the task (Bekinschtein et al., 2009). Our initial analysis (presented within the previous Chapter) showed that global and local effects interact within an early time window, corresponding to the region of the local effect; this suggested that the global context of the block may impact upon the size of local responses to deviance. In other words, increased global expectancy for locally deviant quintuples attenuated the mismatch response by reducing global prediction error (Auksztulewicz & Friston, 2015; Chennu et al., 2013; Wacongne et al., 2011).

Interestingly and furthermore, simple effects analysis (presented within this Chapter) revealed that when attention was not directed towards the task, an interaction between global and local effects occurred within the region of the global effect. In particular, it seems that those in the passive group failed to detect global deviance as a locally standard quintuple (GDLS) (that is elicit a P3b response), whilst they were able to detect

global deviance as a locally deviant quintuple (GDLD). Globally standard patterns (GSLD and GSLS) did not generate a P3b response, as they did not violate assumptions of global regularity and were entirely expected. It may be argued that when attention weighted precision is low, ie. attention is passive, global irregularity becomes masked by local regularity as direct attention is necessary for the integration of more complex predictive contexts (ie. the detection of global violations in auditory regularity) (Chennu et al., 2013). In contrast, global deviance that is marked by a locally deviant tone may be detected (ie. elicit a P3b response) when attention is passive, given that the detection of local deviance is not dependent upon attentional engagement with the task.

Altogether, the presence of an interaction between global and local effects within the region of the global effect appears contingent upon the presence of direct attention, whilst the presence of an interaction between global and local effects within the region of the local effect appears to hinge upon global expectancy. Therefore, contrary to Bekinschtein et al.'s (2009) initial proposals, the global effect should not be considered a functionally isolated marker of conscious processing given the presence of an interaction that renders cognitive subtraction unsuitable. Alternatively, we propose that the presence of an interaction between global and local effects within the region of the global effect, driven by the absence of a P3b response to GDLS, may signify attentional engagement with the task. In addition, the presence of an interaction within the region of the local effect may be indicative of cross-layer modulation within a predictive hierarchy whereby the level of global expectancy (global deviance vs. global standard) is modulating the size of the mismatch response to local deviance. At this level, the presence of a (mismatch) response does not rely upon direct attention, however the presence of direct attention can further enhance the size of the mismatch response by weighting precision. We therefore suggest that examination of the interaction between global and local effects may be an appropriate way to address the possibility of a complex predictive hierarchy within the human brain.

Finally, a reference to consciousness within this and the previous Chapter relates to the cognitive processes that occur when one is awake, namely the transferrable fixation of attention. Within the following Chapter we will expand upon the notion of consciousness as wakefulness to further investigate how manipulating consciousness, as opposed to the fixation of attention, may impact upon responses to the global-local task.

6 Interacting with consciousness III: a full factorial analysis of the effects of sedation on electrophysiological responses to the global-local task

Introduction

Having discussed how manipulations of attention can modulate responses to the global-local auditory task, we will now investigate how manipulating wakefulness using healthy sedation (anaesthesia) may impact upon the ability to process global and local violations of auditory regularity. We explore consciousness within this Chapter as a spectrum of wakefulness, akin to the literature on Disorders of Consciousness (DoC) (Boly et al., 2011; Boly, Moran, Murphy, Boveroux, Bruno, Noirhomme, Ledoux, Bonhomme, Brichant, Tononi, Laureys & Friston, 2012; Loveman, Van Hooff & Smith, 2001). We consider that a spectrum of wakefulness may underlie one's ability to detect patterns of auditory deviance. That is, a reduction in wakefulness may inhibit the availability of cognitive resources necessary to detect hierarchical violations in auditory regularity and therefore impact upon responses to the global-local task. This differs from the previous two Chapters in which we explored consciousness as the cognitive processing underlying attention whilst wakeful (ie. without sedation).

Within this Chapter, we will specifically address how responses to the global-local task may change when attention is always directed towards the task (therefore held constant), while the static state of consciousness (as wakefulness) is reduced via healthy sedation. The findings here may have some relevance to the study of DoC as varying states of wakefulness are examined in the presence of direct attention. Therefore, one is concerned with a variable static state of consciousness, akin to DoC, as opposed to manipulations of attention (ie. active attention vs. passive attention). Consequently, it may be the case that responses to the global-local task when sedated differ from those when attention is passive, implying that it may be possible to distinguish passive

attention from varying states of wakefulness by examining responses to the global-local auditory task. This comparison is addressed in more detail within the subsequent Chapter.

The analysis within this Chapter was performed on data collected by Bekinschtein and colleagues that was shared with us for the purpose of statistical analysis. The task used in this case was identical to that outlined for the study on attention (presented in Chapter 3) and reported in the original work (Bekinschtein et al., 2009). However, participants in this case were tested on two occasions: once when sedated and once when recovered (ie. recovered from sedation) as opposed to being tested only once (as with the attention experiment). Additionally, within the present study, participants had their attention directed towards the task in both conditions (sedation and recovery), that is, the experimenter instructed participants to count the number of globally deviant quintuples they heard (identical to the instructions delivered in the active group of the attention study). In this way, attention is held constant within the current study, whilst wakefulness is reduced via sedation.

Where it has previously been discussed that a lack of direct attention results in the presence of an interaction between global and local effects, we now propose that reducing wakefulness whilst attending to the task may inhibit participant's ability to be conscious *of* global violations in auditory regularity by imposing restriction on the availability of cognitive resources. Therefore, we may expect to find no interaction between global and local effects when sedated, as participants may fail to detect violations in auditory regularity given their reduced state of wakefulness. In contrast, when participants are recovered from sedation (therefore awake and attending to the task), we may expect to find a pattern of results similar to that of the active group within the attention study (presented in the previous Chapter); this is because participants will be attending to the task in the absence of sedation in this case (ie. will be attending in a wakeful state).

Bekinschtein et al. (2009) argued that the presence of a global effect signifies conscious processing, although we have already shown that the global effect may not be functionally isolated as a marker for conscious processing within the previous two Chapters.

At this point, specific emphasis should be placed on the spectral nature of consciousness as wakefulness, that is, we acknowledge that sedation is not an all or none transition. Consequently, encompassing all participants within the same category (or condition) of sedation does not mean that they are all experiencing the same level of sedation in relation to what they consciously experience. What is more, a spectrum implies that individuals may inhabit different positions; therefore conscious experience will be varied across participants within this study.

Design

During the current study, participants were administered the global-local task via headphones on two occasions, as mentioned above. In the first instance, they were sedated and in the second instance they had recovered from sedation. On both occasions they were instructed to count the number of global deviants they heard. Participants were always sedated first and were not administered the task until a set drug level had been administered; this is known as the sedated condition. Subsequently, participants recovered for 20minutes to allow the effects of sedation to alleviate, and were then presented with the global-local task again in what became the recovered condition. All participants were tested in all conditions, which made this a repeated measures design. The current analysis therefore is a three-way repeated-measures ANOVA (sedation x global x local), with three within-subjects factors of sedation (sedated vs. recovered), local (standard vs. deviant) and global (standard vs. deviant) (see Figure 6.1). Statistical analysis was performed using the SPM12 toolbox for EEG within MATLAB 2012b (Friston et al., 1995; Kilner & Friston, 2010).

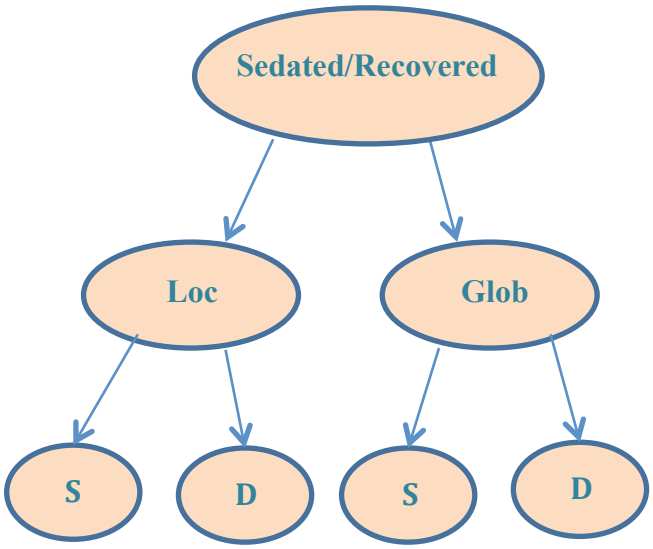

Figure 6.1. Illustration of the three-way mixed ANOVA design. Sedation, global and local are within-subjects factors, each with two levels: Sedation: sedated vs. recovered, local: standard (S) vs. deviant (D) and global (Glob): standard (S) vs. deviant (D).

Methods and Materials

In this section we describe the methods and materials used by Bekinschtein and colleagues to collect the data. This data is currently unpublished but in preparation.

Participants. 18 healthy adults, aged 18-65, with no history of neuropathology, were recruited from the Cambridge Cognitive Neuroscience Research Panel at the MRC Cognition and Brain Sciences Unit, Cambridge. Participants received payment for taking part in the study.

Drug and task administration. Each experimental run began with a baseline period lasting 25-30 minutes, where participants remained awake and aware. Following this, a target-controlled infusion of propofol commenced via a computerized syringe driver (Alaris Asena PK, Carefusion, Berkshire, UK). Using such a system, the anesthesiologist inputs the desired ("target") plasma concentration, and the system then determines the required infusion rates to achieve and maintain the target concentration (using the patient characteristics which are covariates of the pharmacokinetic model). The Marsh model is routinely used in clinical practice to control propofol infusions for general anesthesia (Marsh, White, Morton & Kenny, 1991). Three blood plasma levels

were targeted – 0.6μg/ml (mild sedation), 1.2μg/ml (moderate sedation), and recovery from sedation. A period of 10 minutes was allowed for equilibration of calculated and actual plasma propofol concentrations before behavioural tests were administered.

The state of mild sedation aimed to produce a relaxed but still responsive behavioural state, where awareness could be measured using behavioural tests, ie. subjective visibility ratings. The global-local task was administered at moderate sedation. Participants were instructed to count the number of global deviants they heard and press a button each time.

After the infusion, plasma propofol concentration exponentially declined toward zero. Computer simulations with the *TIVATrainer* pharmacokinetic simulation software revealed that plasma concentration of propofol would approach zero in 15 minutes, which led to behavioural recovery; hence why the experiment was continued 20 minutes after the end of sedation.
The experience of a loss of consciousness will not have been complete for all participants, with some experiencing a greater loss of consciousness (wakefulness) than others given that drug tolerance levels will have varied within the sample.

Data preparation

Pre-processing. Data was collected using an 128-electrode geodesic sensor net (EGI) at a sampling rate of 250 Hz, referenced to vertex (electrode Cz) using the Net Amps 300 amplifier (Electrical Geodesics Inc., Oregon, USA). Participant's eyes were closed in a resting state during data collection. The data was segmented into quintuples from -200ms to 1288ms, relative to the onset of the first and last tone of a quintuple (set of five tones) (see Figure 6.2).

Post artefact rejection, the remaining quintuples were re-referenced to average, band-pass filtered from 0.5 Hz to 20 Hz, and baseline corrected using the 200ms time window occurring before the onset of the final tone in the quintuple (that is from 400ms to 600ms).

Quintuples were then segmented from 650ms (end of the fifth tone) to the end of the time series (1288ms) before converting to image format within SPM (.NIfTI) for statistical analysis in sensor space (see Figure 6.2) (Friston et al., 1995; Kilner & Friston, 2010).

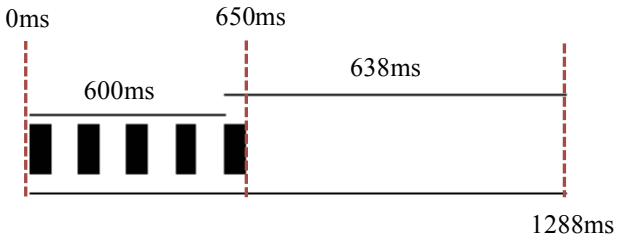

Figure 6.2. Quintuple design illustration and indication of segmentation for statistical analysis.

For statistical analysis, crown electrodes were eliminated (36 channels eliminated, 93 remained) as they were not within our region of interest, and data was statistically analysed from 650ms (the end of the fifth tone) to the end of the time series (1288ms) (for channel locations after elimination see Appendix 2).

ERPs were generated in MATLAB for sedated and recovered groups respectively by averaging across quintuples for all participants in each of the four conditions (GDLD, GDLS, GSLD and GSLS [see Figure 4.5]). An ERP for the main effect of sedation was generated by collapsing across all four conditions separately for the respective sedated and recovered groups (see Figure 6.4). ERPs are presented from 400ms – 1288ms for ease of visual presentation.

Statistical analysis

As discussed in Chapter 4, a first level analysis was conducted within each subject, across the conditions of sedation, global and local. Linear regression was used to estimate beta values for each condition. Each participant acquired 8 beta values, as there were 4 possible conditions for sedation (SGDLD, SGDLS, SGSLD and SGSLS) and 4 possible conditions for recovery (RGDLD, RGDLS, RGSLD and RGSLS).

These betas were taken to a group level analysis (second level analysis) where there were 18 betas in each of the 8 conditions, that is, one beta in each condition, which corresponds to one participant. Therefore, at the group level we have 8 conditions (SGDLD, SGDLS, SGSLD, SGSLS, RGDLD, RGDLS, RGSLD and RGSLS) each with 18 betas (corresponding to the 18 participants). Linear regression was used to estimate new beta values at the group level. The results presented subsequently are those of the group level analysis.

Thresholds. The cluster-forming threshold (first level threshold) was set to $p < .01$ (uncorrected) and the cluster extent threshold (second level threshold) was set to $p < .05$ (Kilner et al., 2005; Kilner & Friston, 2010). Specific P-values and F-values for each significant cluster can be viewed in Appendix 1.4.

Results

Table 6.1 is a summary table to indicate the presence of significant effects within the analysis of this Chapter. It may serve as a good reference as the following is an extensive analysis.

Table 6.1. *Summary of effects for three-way ANOVA (sedation x global x local) and two-way (simple effects) ANOVAs (global x local) for the sedated and recovered conditions. 'Y' indicates there is statistical significance, 'N' indicates there is not statistical significance.*

	Local (L)	Global (G)	GxL	Sedation (S)	SxL	SxG	SxGxL
combined (sedated + recovered)	Y	Y	Y	Y	Y	Y	Y
sedated	Y	Y	Y	-	-	-	-
recovered	Y	Y	Y	-	-	-	-

Y = cluster extent threshold for combined analysis of $p < .05$, cluster extent threshold for sedation and recovered simple effects of $p < .01$, cluster forming threshold for all analyses of $p < .01$

Before presenting the results of statistical analysis we will first address the issue of positive drift within the current dataset.

Positive drift within the data. During data pre-processing we became aware that there was positive drift within the data (see top left panel in Figure 4 and right panel in Figure 14), and so we pay consideration here to how this may impact upon the output of statistical analysis. It is the case that positive drift is occurring within all conditions of the experiment on sedation, eg. whether sedated or recovered (see right panel in Figure 14); therefore differences between conditions will be relative despite the addition of drift. If it were the case that drift were present only in certain conditions but not others then the analysis would be confounded, as differences between conditions may be the result of drift and not the experimental manipulations. We conclude that drift across all conditions will be removed when differences are calculated, as subtracting one condition from another will leave only that which is different between the two (and not that which is the same, ie. the drift).

Three-way ANOVA (sedation x global x local)

Hereafter we present the results of the three-way ANOVA, with consideration of each main effect and subsequently the interaction effects.

Sedation effect. The main effect of sedation is significant around frontal electrode Fz from 688-760ms, and is subsequently significant around left posterior electrode ch.42 from 832-940ms, and right posterior electrode ch.65 from 952-1000ms (see Figure 6.3).

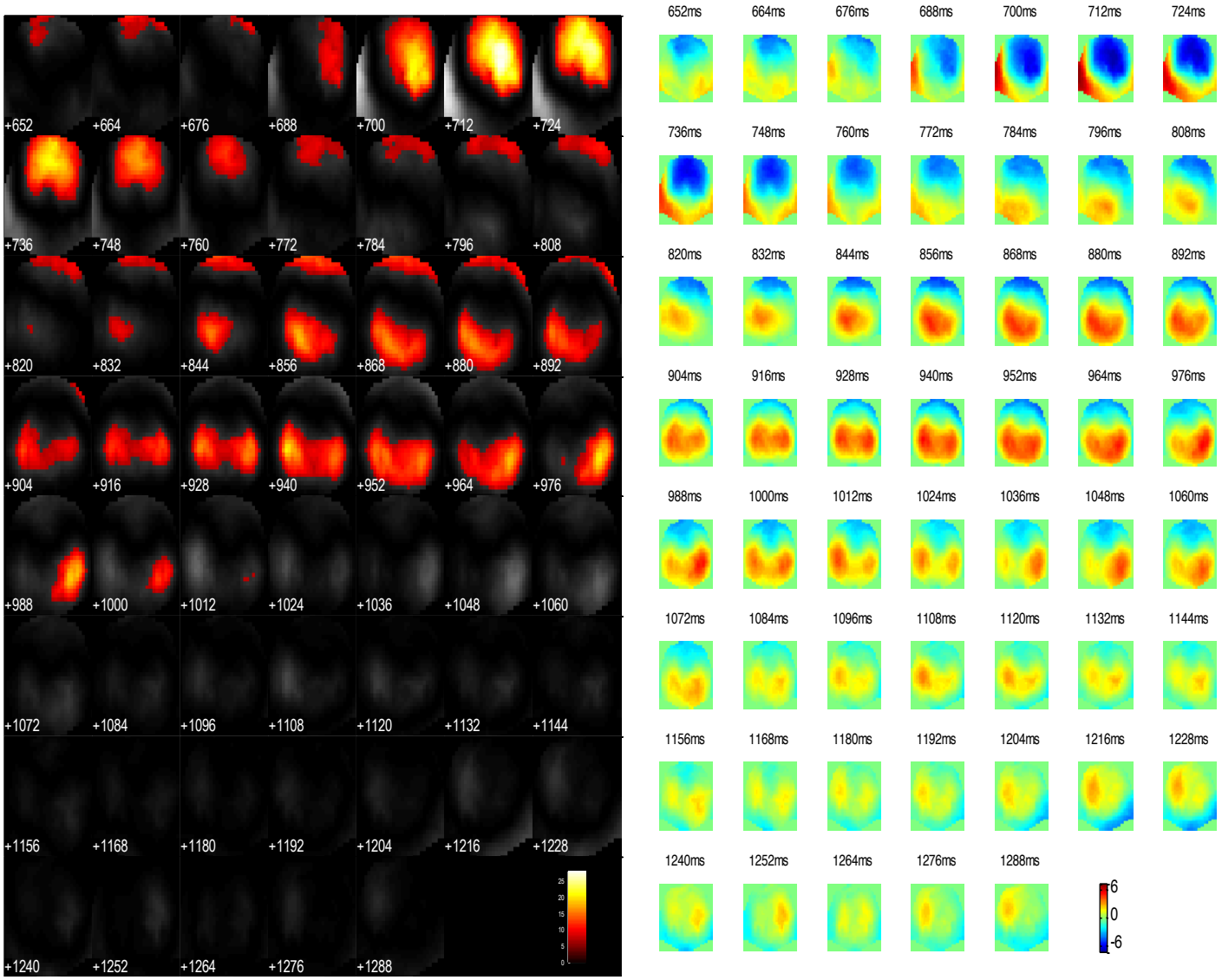

Figure 6.3. Thresholded F-maps ($p < .05$) to show regions of significance for the effect of sedation [recovered-sedated] on the scalp through time (left). Unthresholded T-maps to show the polarity of effect on the scalp through time (right). Front of the scalp is positioned at the top. Note that time within the left panel is presented below the corresponding row of scalpmaps, whilst time within the right panel is presented above the corresponding row of scalpmaps.

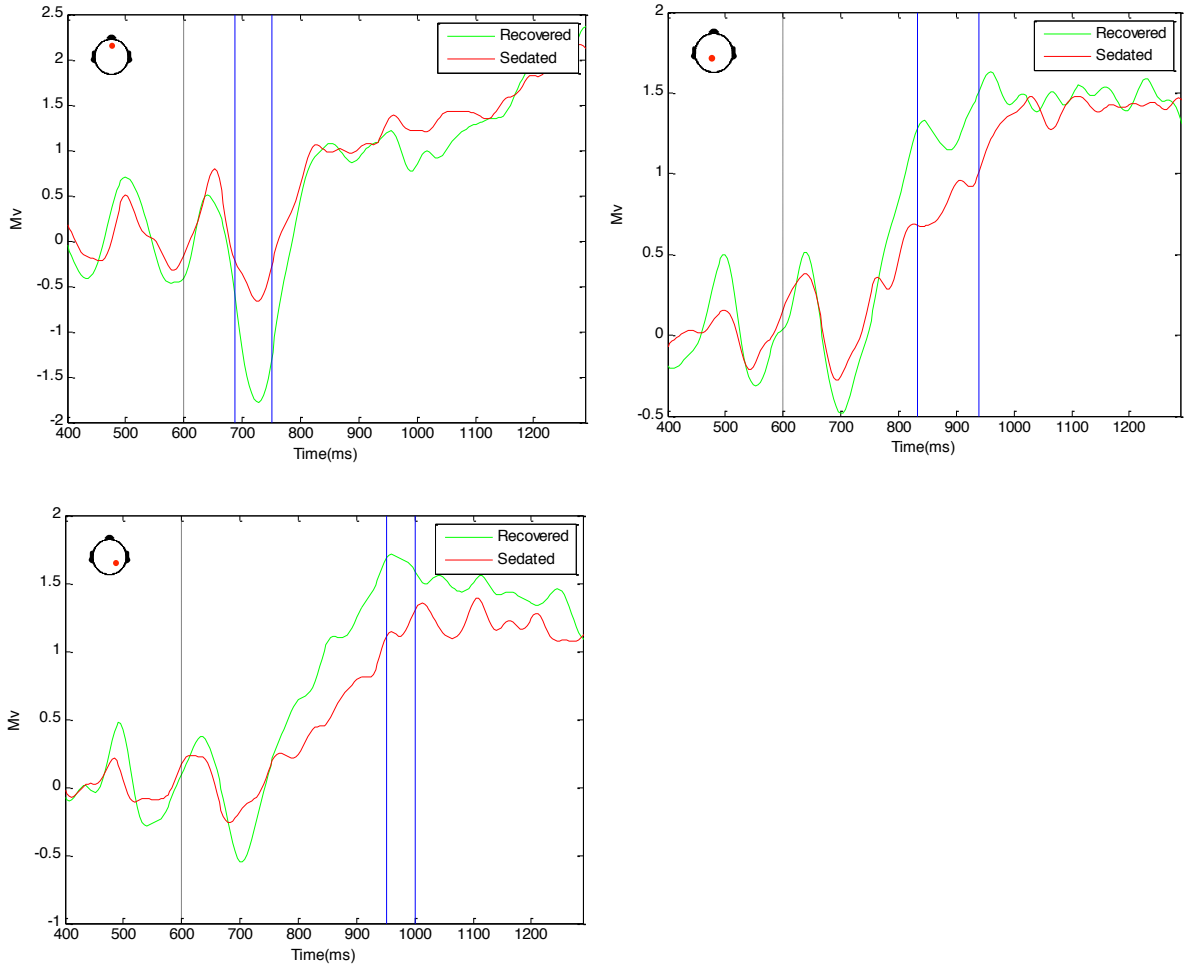

Figure 6.4. Grand average ERPs for the main effect of sedation at Fz (top left), ch.42 (top right) and ch.65 (bottom left). Blue lines indicate the region of significance. Black dashed line (600ms) indicates the onset of the final tone.

The top panels in Figure 6.4 shows that the recovered group elicit a larger negative response at frontal electrode Fz, as well as a larger positive responses posteriorly (ch.42 and ch.65) in comparison to the sedated group (for scalp topography see Figure 6.3). It appears that overall responses when recovered (green lines in Figure 6.4) are larger than responses when sedated (red lines in Figure 6.4). This indicates that sedation may be reducing the size of responses. Notably, there appears to be no marked difference in the latency of early frontal responses (see top left panel in Figure 6.4) between sedation and recovery, indicating possibly that sedation may not reduce the processing speed of early responses (ie. increase response latency).

Local effect. The local effect is significant around frontal electrode Fz from 688-736ms, and then around central electrode Cz from 808-916ms (see Figure 6.5).

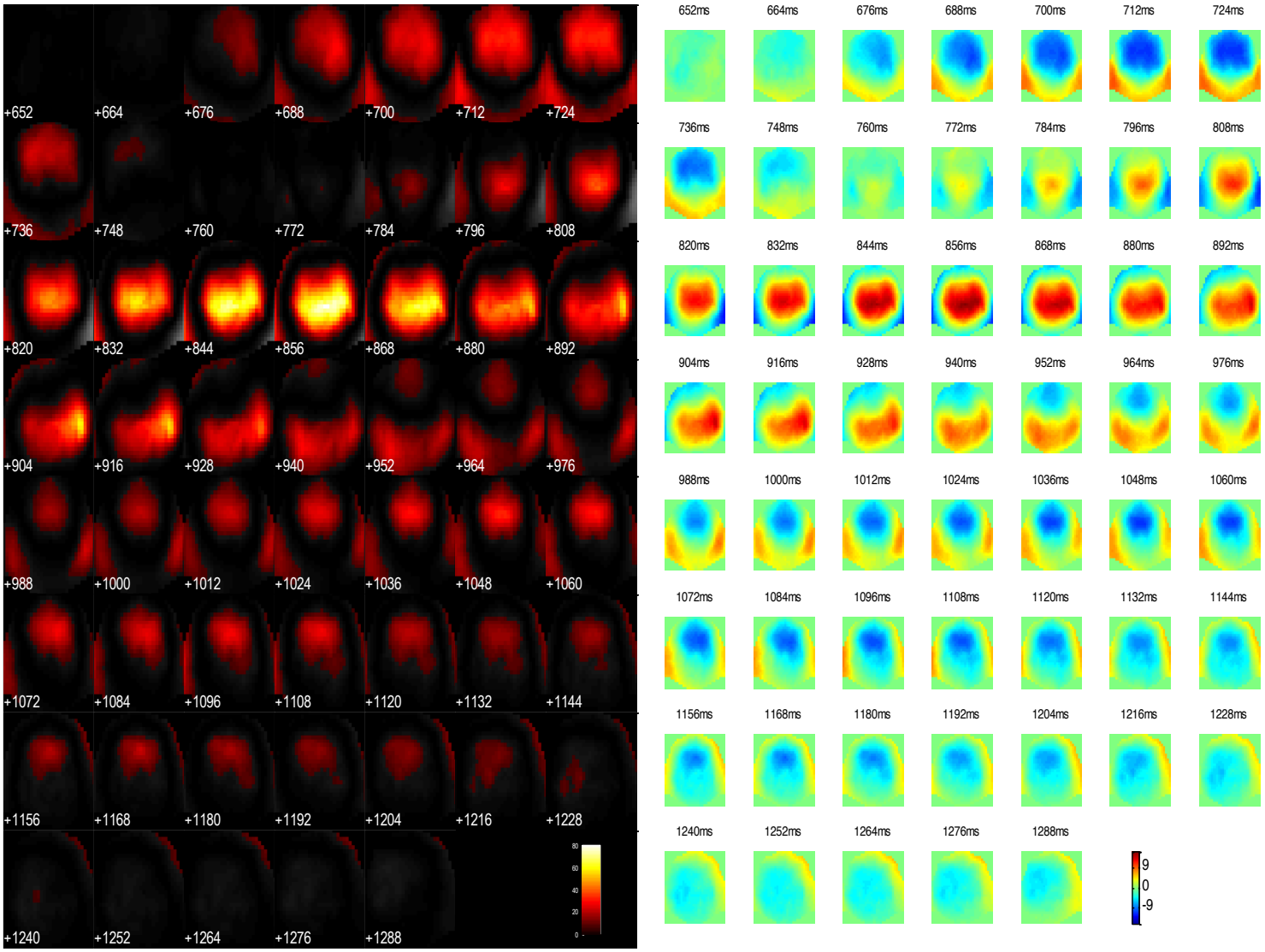

Figure 6.5. Thresholded F-maps ($p < .05$) to show regions of significance for the local effect [LD-LS] on the scalp through time (left). Unthresholded T-maps to show the polarity of effect on the scalp through time (right). Front of the scalp is positioned at the top. Note that time within the left panel is presented below the corresponding row of scalpmaps, whilst time within the right panel is presented above the corresponding row of scalpmaps.

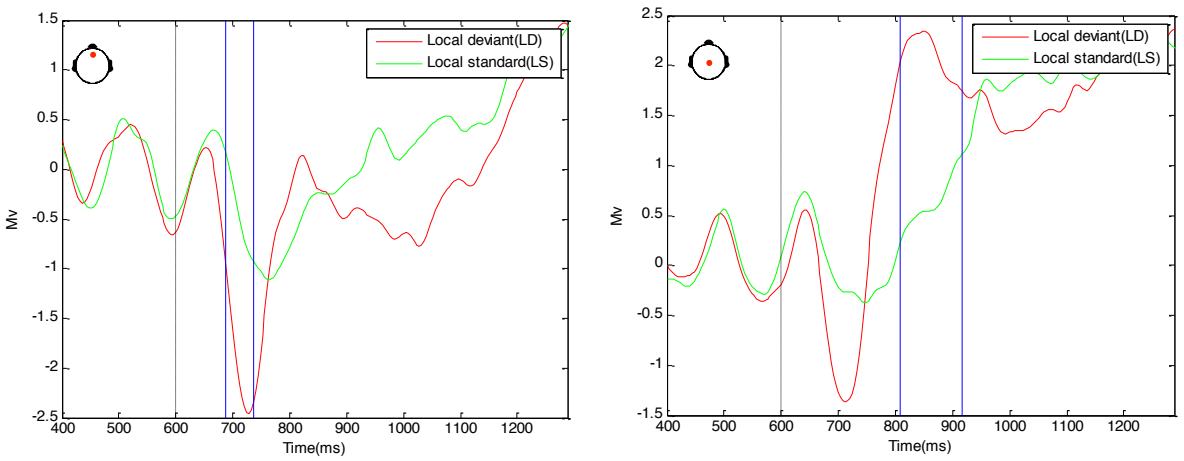

Figure 6.6. Grand average ERPs for the local effect at Fz (left) and Cz (right). Blue lines indicate the region of significance. Black dashed line (600ms) indicates the onset of the final tone.

The local deviance (red lines on Figure 6.6) produces a mismatch response frontally (at Fz), and a subsequent P3a response centrally (at Cz). This is in contrast to the local standard where there is only a very small early response (see left panel in Figure 6.6). Local deviant is eliciting a larger overall response than the local standard, as it is a violation of local auditory regularity, whereas local standard is not (scalp topography can be seen in Figure 6.5). Moreover, the onset of the response to local deviance is earlier than that of local standard, suggesting that deviance may be detected more rapidly than standard stimuli at the local level. These findings are consistent with the local effects observed by Bekinschtein et al. (2009).

Global effect. The global effect is significant between 904-1180ms around central posterior electrode Pz (see Figure 6.7).

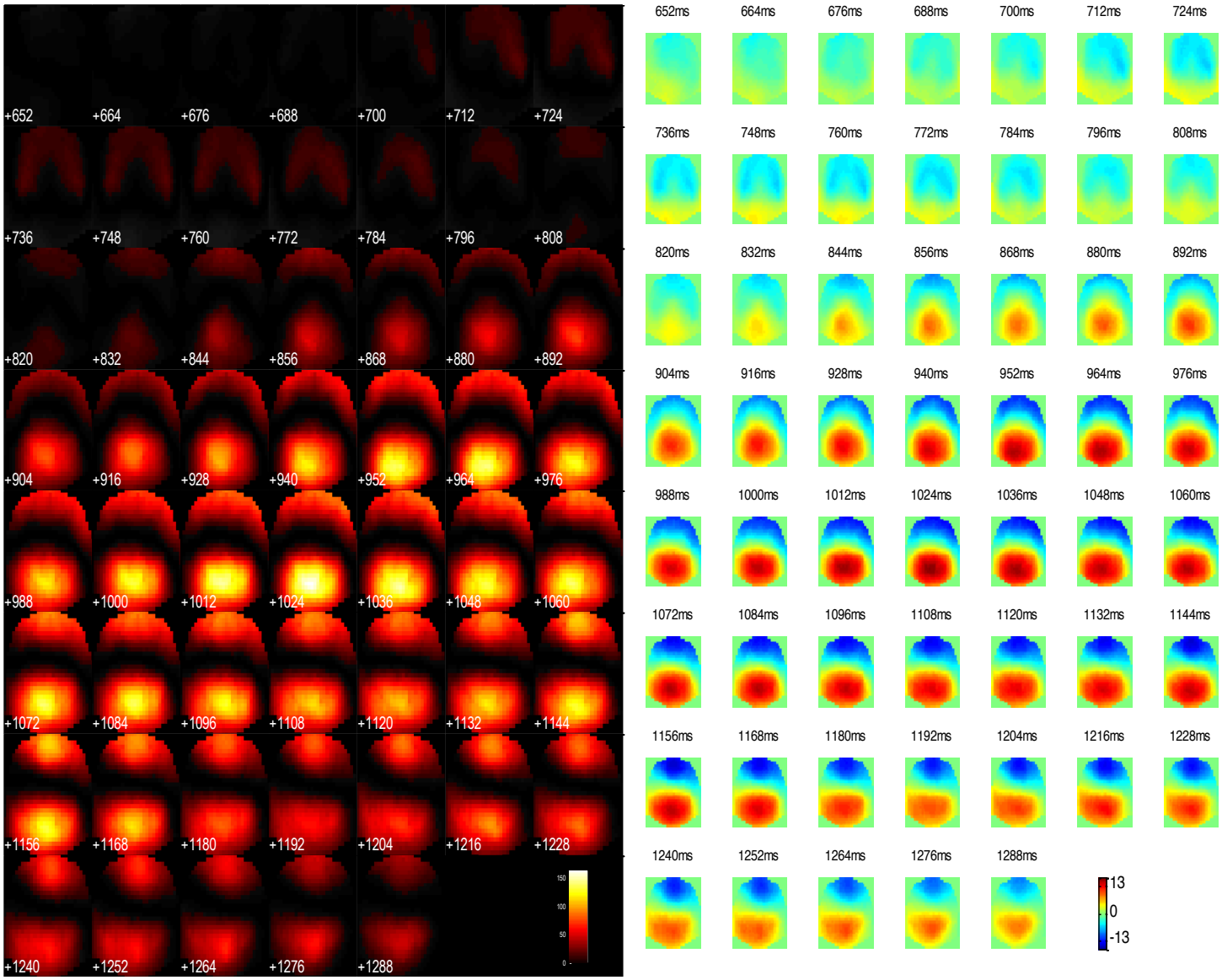

Figure 6.7. Thresholded F-maps ($p < .05$) to show regions of significance for the global effect [GD-GS] on the scalp through time (left). Unthresholded T-maps to show the polarity of effect on the scalp through time (right). Front of the scalp is positioned at the top. Note that time within the left panel is presented below the corresponding row of scalpmaps, whilst time within the right panel is presented above the corresponding row of scalpmaps.

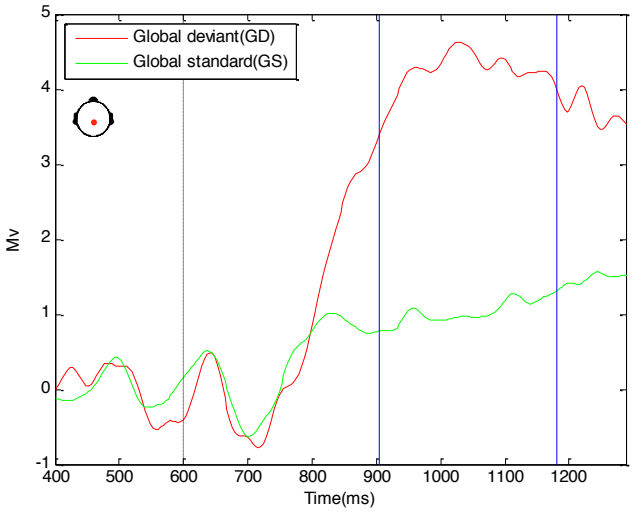

Figure 6.8. Grand average ERPs for the global effect at Pz. Blue lines indicate the region of significance. Black dashed line (600ms) indicates the onset of the final tone.

Figure 6.8 shows that global deviance produces a P3b response (red line), whereas the global standard condition does not (green line). The size of the difference between these two responses is generating a large global effect (scalp topography can be seen in Figure 6.7). This effect is broad posteriorly on the scalp, as can be seen in Figure 6.7 and is consistent through time, which is characteristic of the global effect within the literature (Bekinschtein et al., 2009, Wacongne et al., 2011, Chennu et al., 2013, Pegado et al., 2010).

Interactions

Sedation x local. The sedation x local interaction is significant around central electrode Cz between 796-844ms, and right lateral electrode ch.61 between 820-904ms. Subsequently, there is significance around electrode Pz between 1012-1180ms (see Figure 6.9).

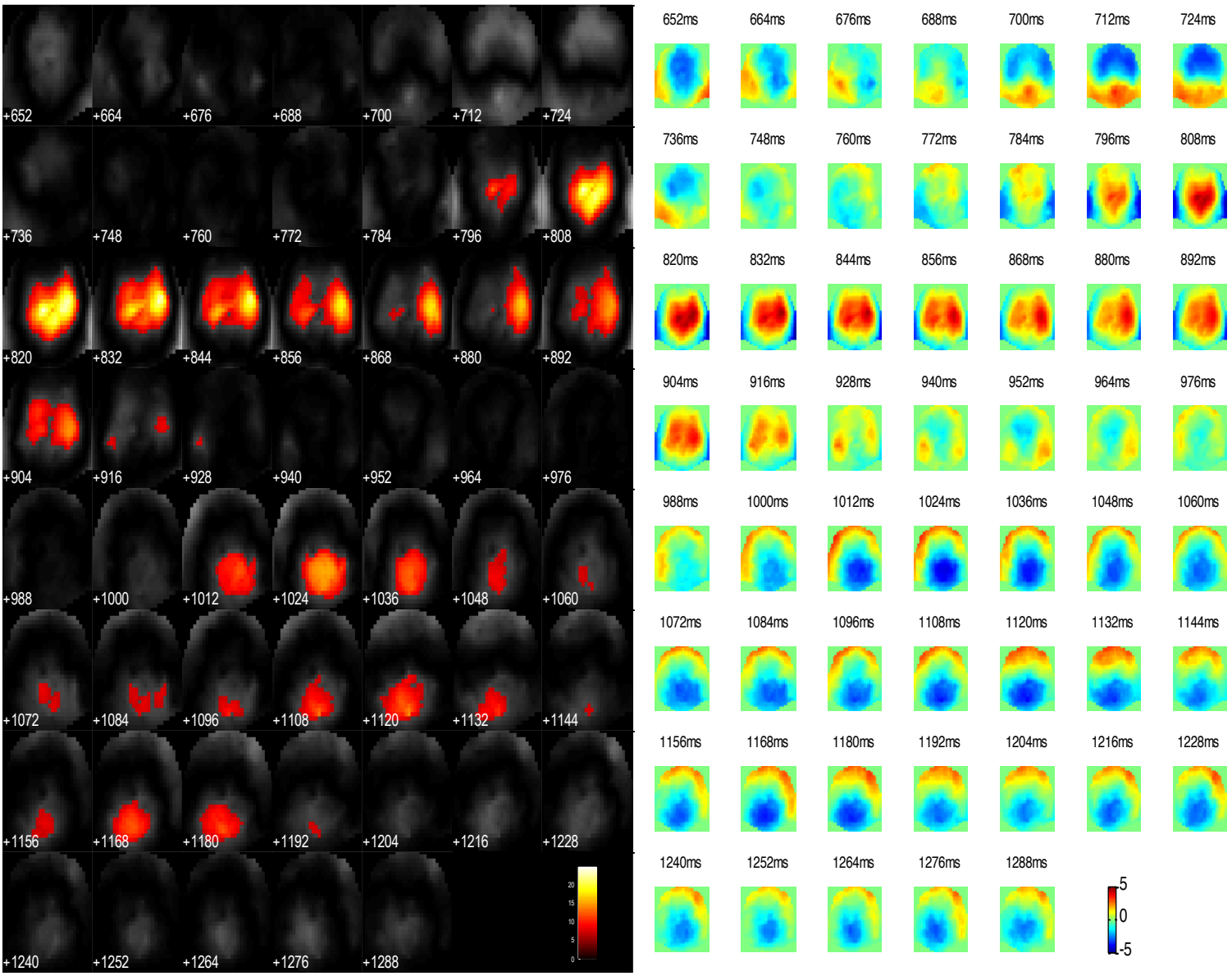

Figure 6.9. Thresholded F-maps ($p < .05$) to show regions of significance for the sedation x local interaction [(RLD-RLS)-(SLD-SLS)] on the scalp through time (left). Unthresholded T-maps to show the polarity of effect on the scalp through time (right). Front of the scalp is positioned at the top. Note that time within the left panel is presented below the corresponding row of scalpmaps, whilst time within the right panel is presented above the corresponding row of scalpmaps.

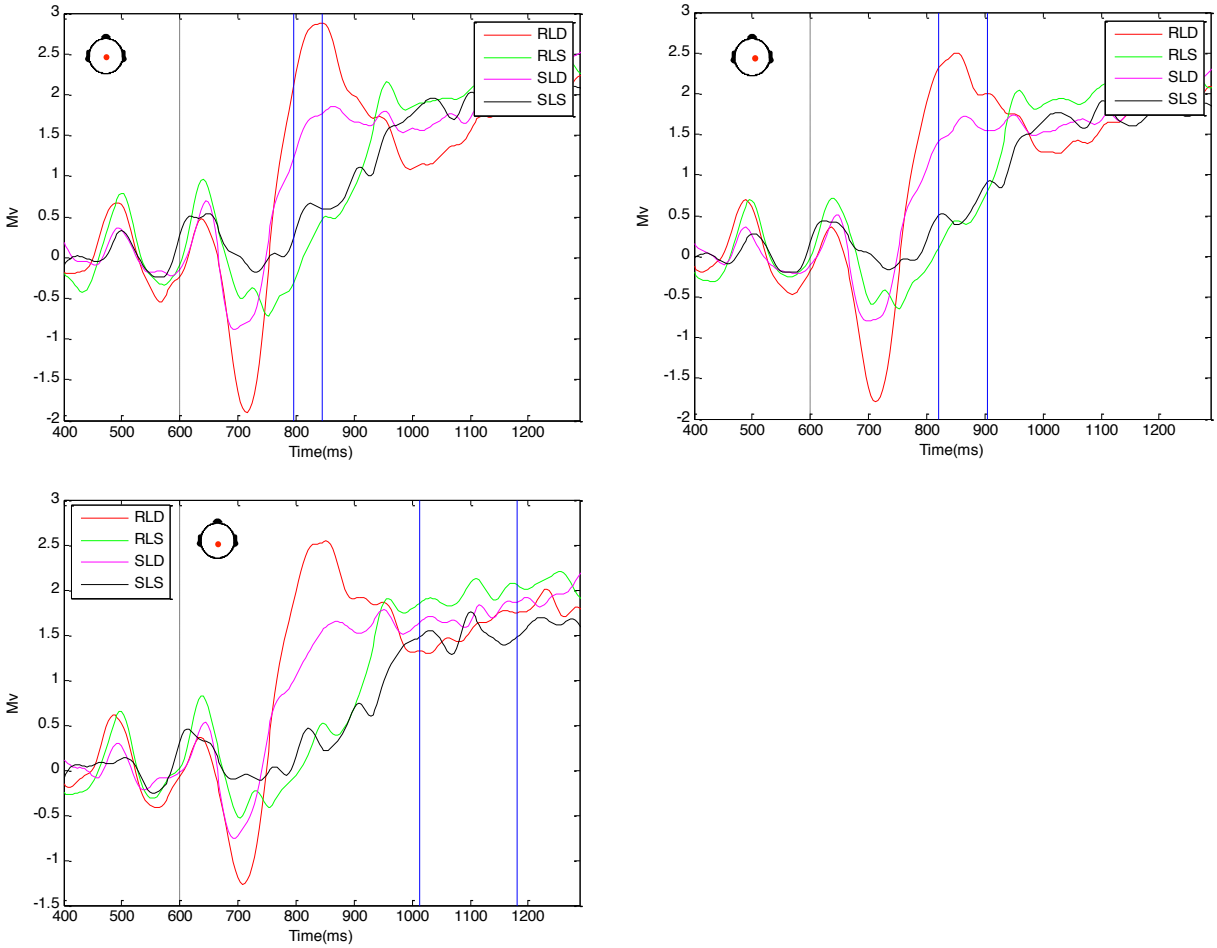

Figure 6.10. Grand average ERPs for the sedation x local interaction at Cz (top left), ch.61 (top right) and Pz (bottom left). Blue lines indicate the region of significance (R: recovered, S: sedated). Black dashed line (600ms) indicates the onset of the final tone.

One can see in Figure 6.10 that during the early regions of significance (796-844ms and 820-904ms), the difference between recovered local deviant (RLD) and recovered local standard (RLS) is bigger than the difference between sedated local deviant (SLD) and sedated local standard (SLS). This indicates that when participants are sedated their response to local deviance may be more similar to that of the local standard condition, comparing to when they are recovered. Put another way, when participants are recovered, they may elicit a larger P3a component than when they are sedated. It is this disparity of differences, which creates an interaction between the level of sedation and the local effect (scalp topography of these effects can be seen on the scalp in Figure 6.9).

Interestingly, there is no marked latency difference between sedated and recovered response; however there is a latency difference between levels of the local effect (deviant and standard). That is, locally deviant responses occur earlier than responses to

locally standard tones; this shows that latency may vary between levels of the local effect, but not between levels of sedation with respect to local effects. Subsequently, there is a central posterior region of significance around 1012-1180ms (see bottom left panel in Figure 6.10), which does not appear to reveal a substantial disparity between responses to local deviance and locally standard tones between sedation and recovery. However, there does appear to be a somewhat larger difference between local deviant and local standard in recovery (red and green lines), comparing to when sedated (magenta and black lines) within this region.

Sedation x global. The sedation x global interaction is significant between 868-1120ms around central posterior electrode Pz. It is also significant between 928-952ms around left mid-line electrode ch.29, and between 964-1060ms around right posterior electrode ch.70 (see Figure 6.11).

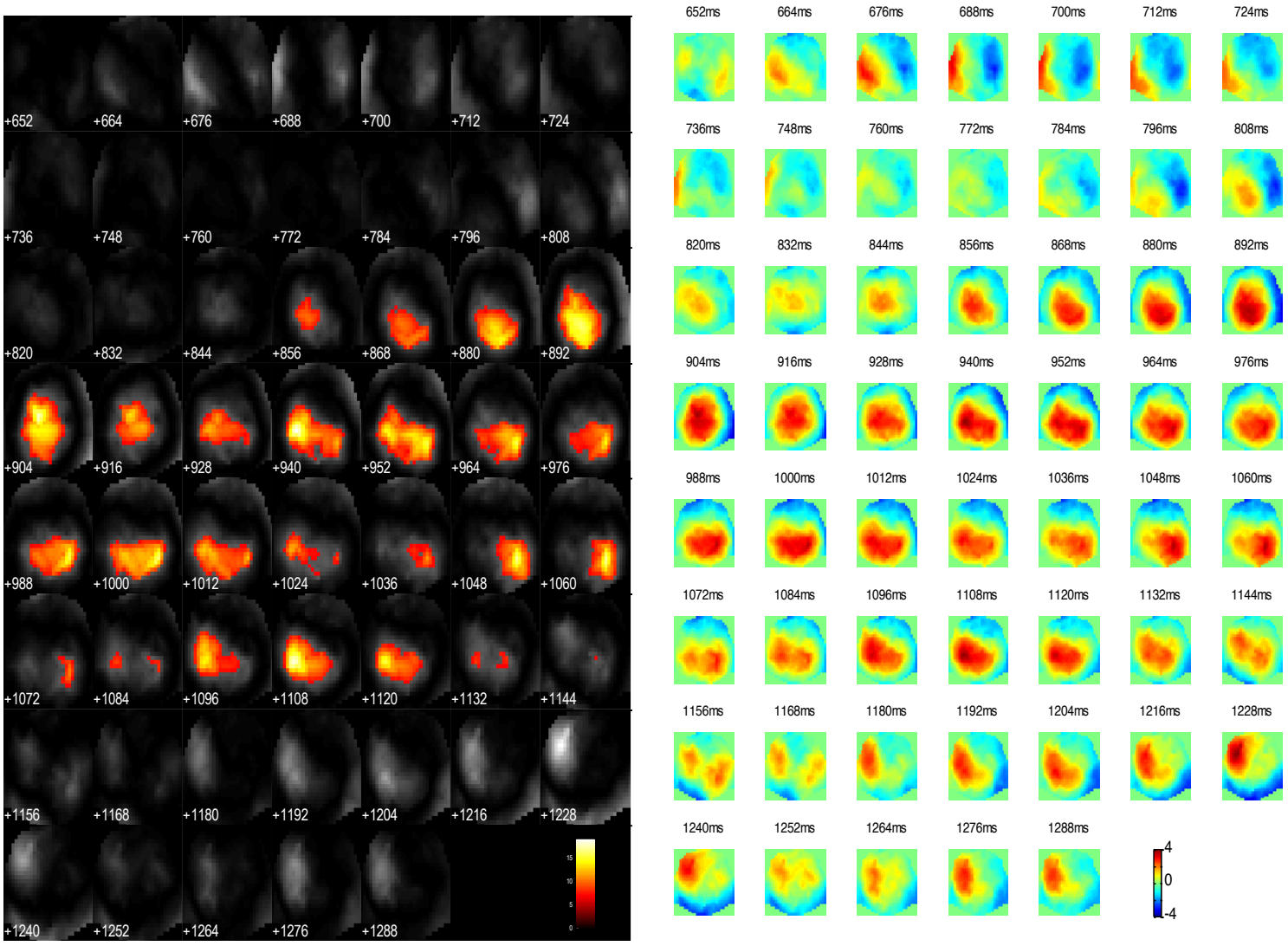

Figure 6.11. Thresholded F-maps ($p < .05$) to show regions of significance for the sedation x global interaction [(RGD-RGS)-(SGD-SGS)] on the scalp through time (left). Unthresholded T-maps to show the polarity of effect on the scalp through time (right). Front of the scalp is positioned at the top. Note that time within the left panel is presented below the corresponding row of scalpmaps, whilst time within the right panel is presented above the corresponding row of scalpmaps.

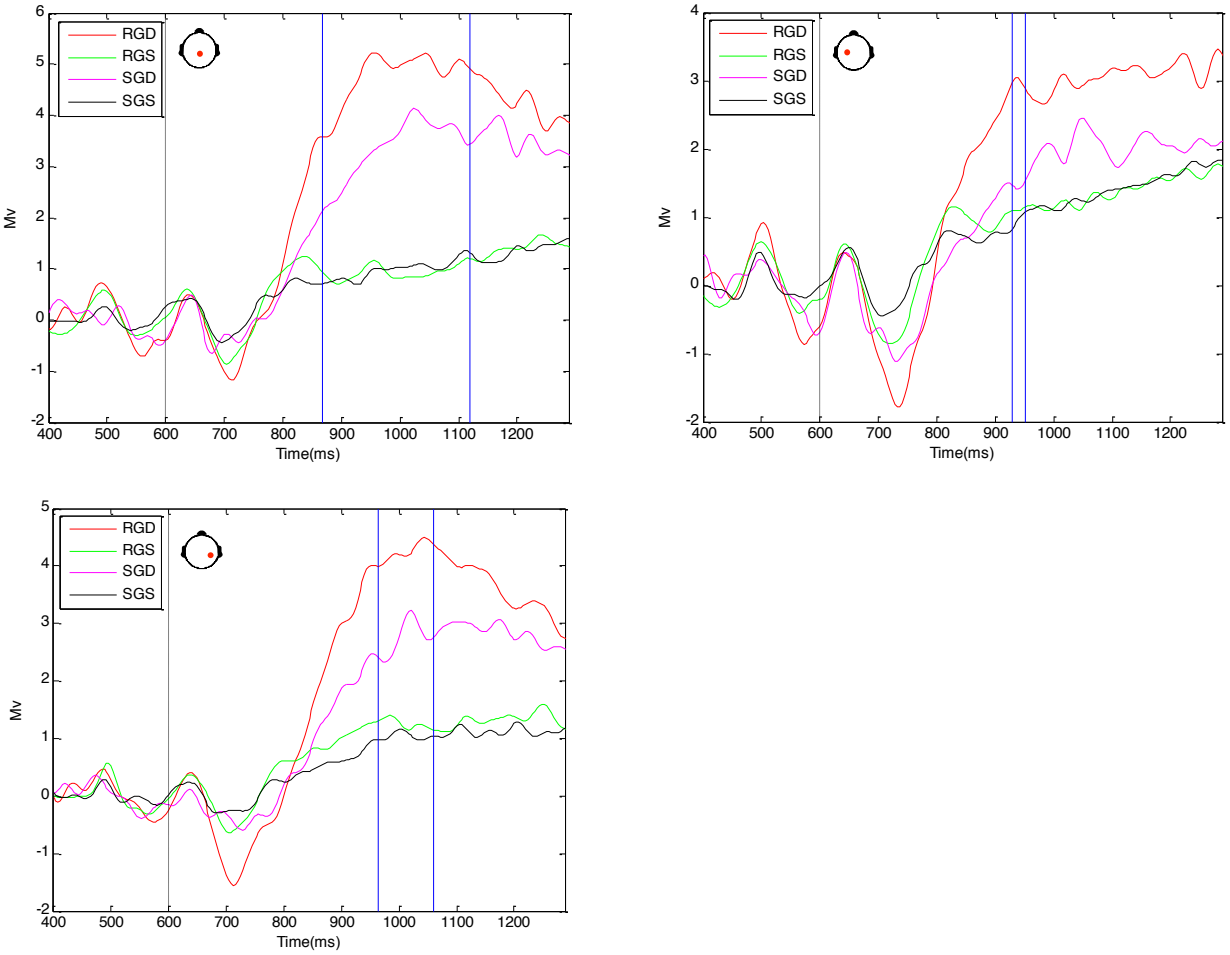

Figure 6.12. Grand average ERPs for the sedation x global interaction at Pz (top left), ch.29 (top right) and ch.70 (bottom left). Blue lines indicate the region of significance (R: recovered, S: sedated). Black dashed line (600ms) indicates the onset of the final tone.

With regards to the sedation x global interaction, Figure 6.12 demonstrates that globally deviant conditions produce P3b responses whilst the globally standard conditions do not. This is because globally standard patterns do not violate global regularity. Moreover, when participants are recovered, they elicit a larger global deviant response than when they are sedated; possibly suggesting that sedation is reducing the size the P3b response (for scalp topography see Figure 6.11). What is more, there appears to be somewhat of a latency difference regarding the onset of the P3b response to global deviance between recovered and sedated conditions. The onset is seemingly later when under sedation. Notably, there is no observable difference between globally standard conditions between sedation to recovery; therefore this difference compared with the difference between globally deviant conditions creates an interaction between level of sedation and the global effect.

Global x local. The global x local interaction is significant around Pz from 832-952ms. Subsequently, the interaction is significant from 1036-1288ms around central electrode Cz (see Figure 6.13).

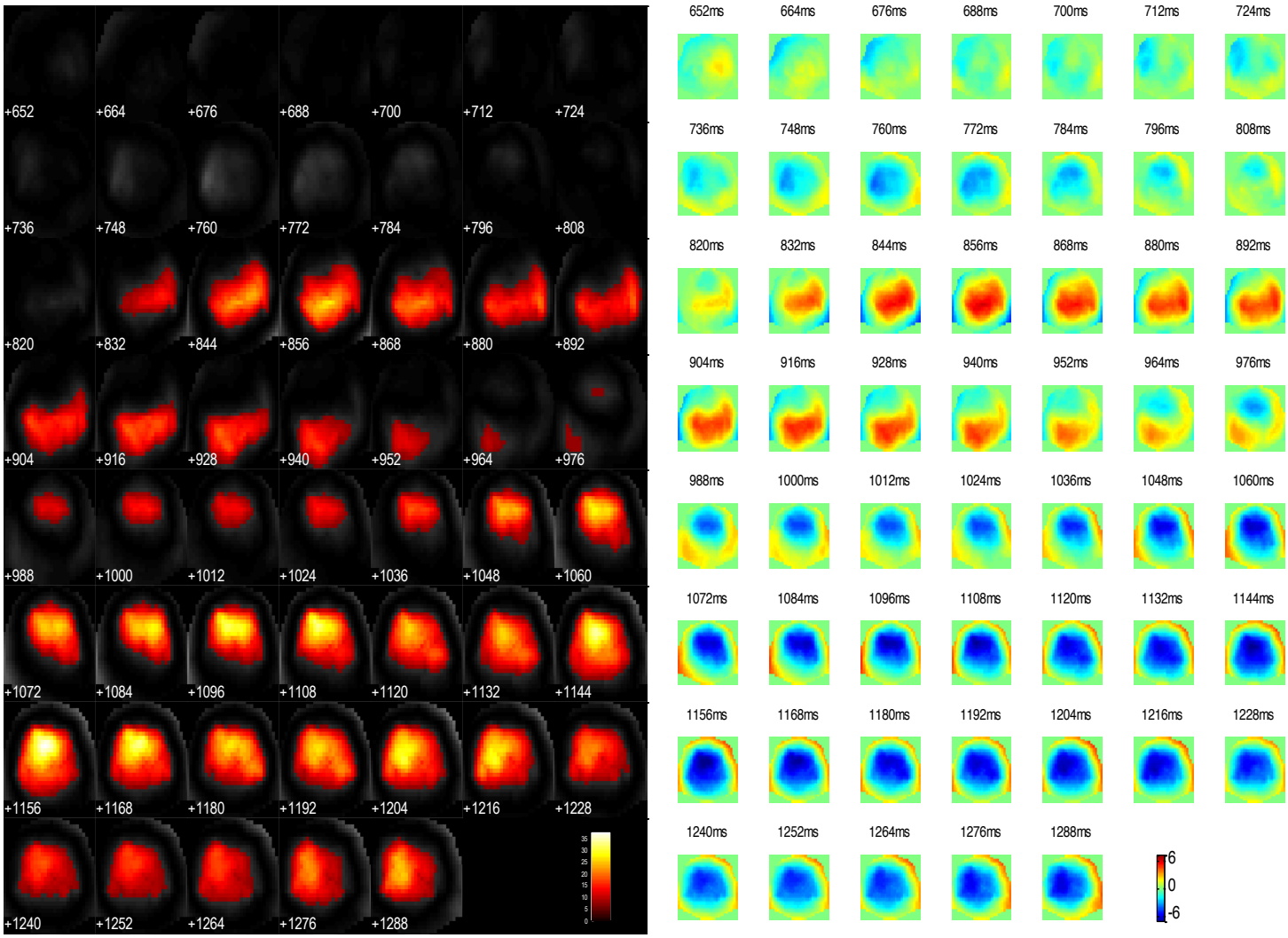

Figure 6.13. Thresholded F-maps ($p < .05$) to show regions of significance for the global x local interaction [(LDGD-LDGS)-(LSGD-LSGS)] on the scalp through time (left). Unthresholded T-maps to show the polarity of effect on the scalp through time (right). Front of the scalp is positioned at the top. Note that time within the left panel is presented below the corresponding row of scalpmaps, whilst time within the right panel is presented above the corresponding row of scalpmaps.

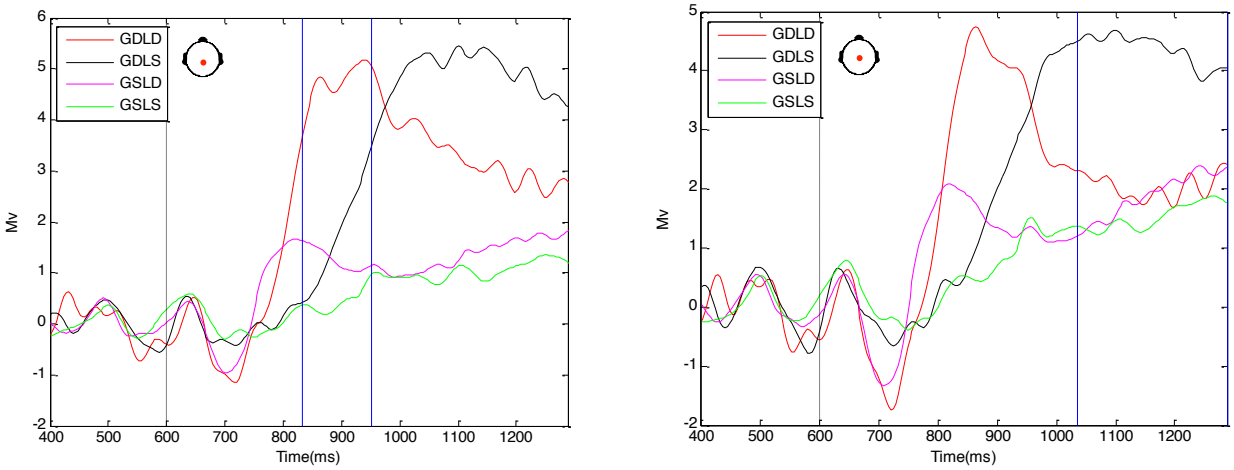

Figure 6.14. Grand average ERPs for the global x local interaction at Pz (left) and Cz (right). Blue lines indicate the region of significance. Black dashed line (600ms) indicates the onset of the final tone.

One can see that during the region of significance (832-952ms) at Pz (left panel in Figure 6.14), there is little difference between globally standard conditions (GSLD, magenta line and GSLS, green line), whereas the globally deviant responses are varying in latency based on the level of the local effect. That is, a global deviant that is also a local deviant (GDLD, red line) elicits a large and relatively short-lived P3b response (see Figure 6.14), whereas a global deviant that is also a local standard (GDLS, black line) elicits a later and longer component that begins almost after the end of the response to GDLD. During the second region of significance (1036-1288ms), shown at Cz (see right panel in Figure 6.14), one can see that the response to GDLD is almost over, however the response to GDLS is ongoing. This difference in response suggests that the brain may be differentiating instances of global deviance based on the presence (or absence) of local deviance (scalp topography can be seen in Figure 6.13). The difference between global deviance conditions (that is, GDLD [red line] and GDLS [black line]), which is large, compared with the difference between global standard conditions (that is, GSLD [magenta line] and GSLS [green line]), which is small, creates the interaction we observe between global and local effects.

Sedation x global x local. The sedation x global x local interaction is significant from 1000-1264ms around Pz (see Figure 6.15).

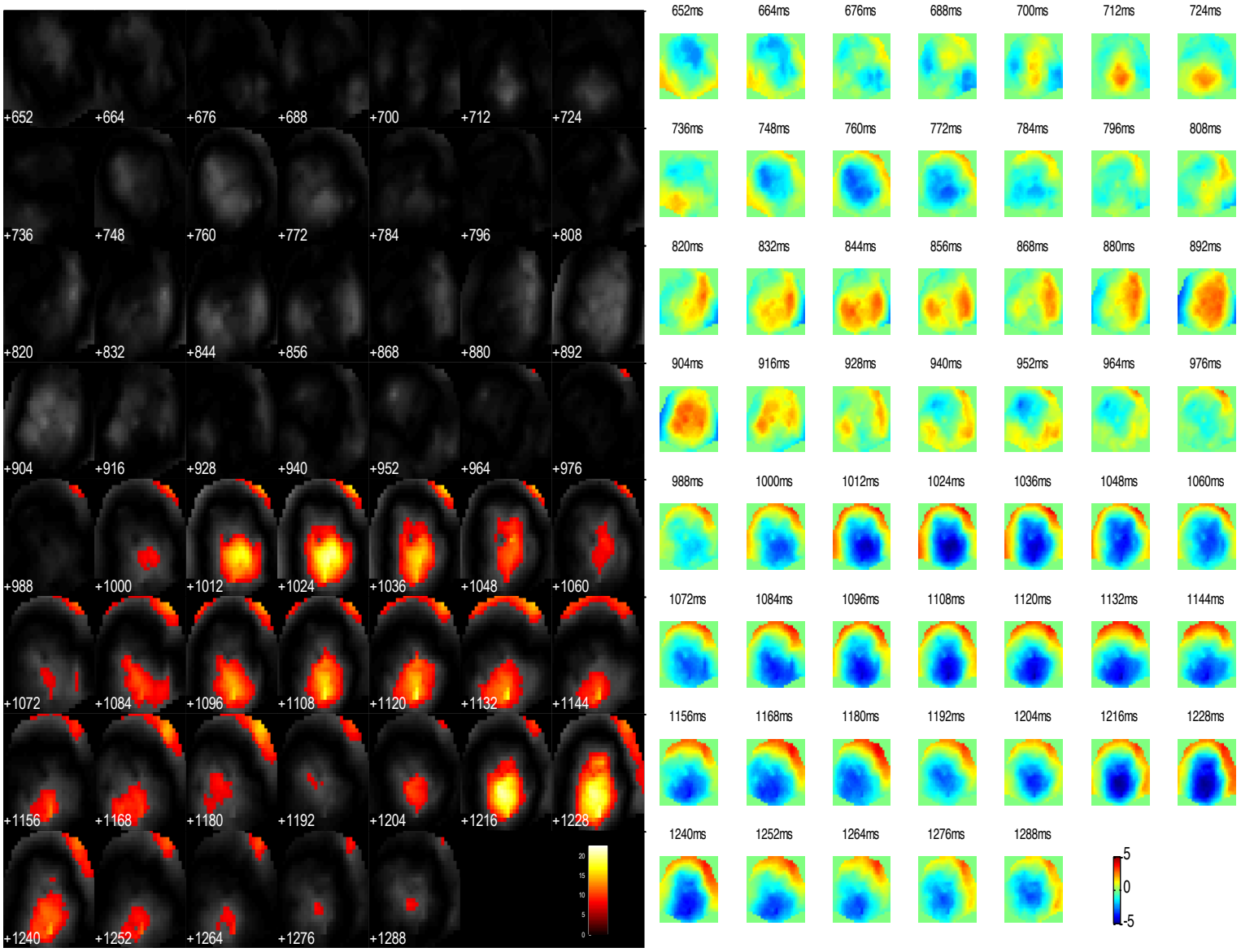

Figure 6.15. Thresholded F-maps ($p < .05$) to show regions of significance for the sedation x global x local interaction [((RLDGD-RLSGD)-(RLDGS-RLSGS))-((SLDGD-SLSGD)-(SLDGS-SLSGS))] on the scalp through time (left). Unthresholded T-maps to show the polarity of effect on the scalp through time (right). Front of the scalp is positioned at the top. Note that time within the left panel is presented below the corresponding row of scalpmaps, whilst time within the right panel is presented above the corresponding row of scalpmaps.

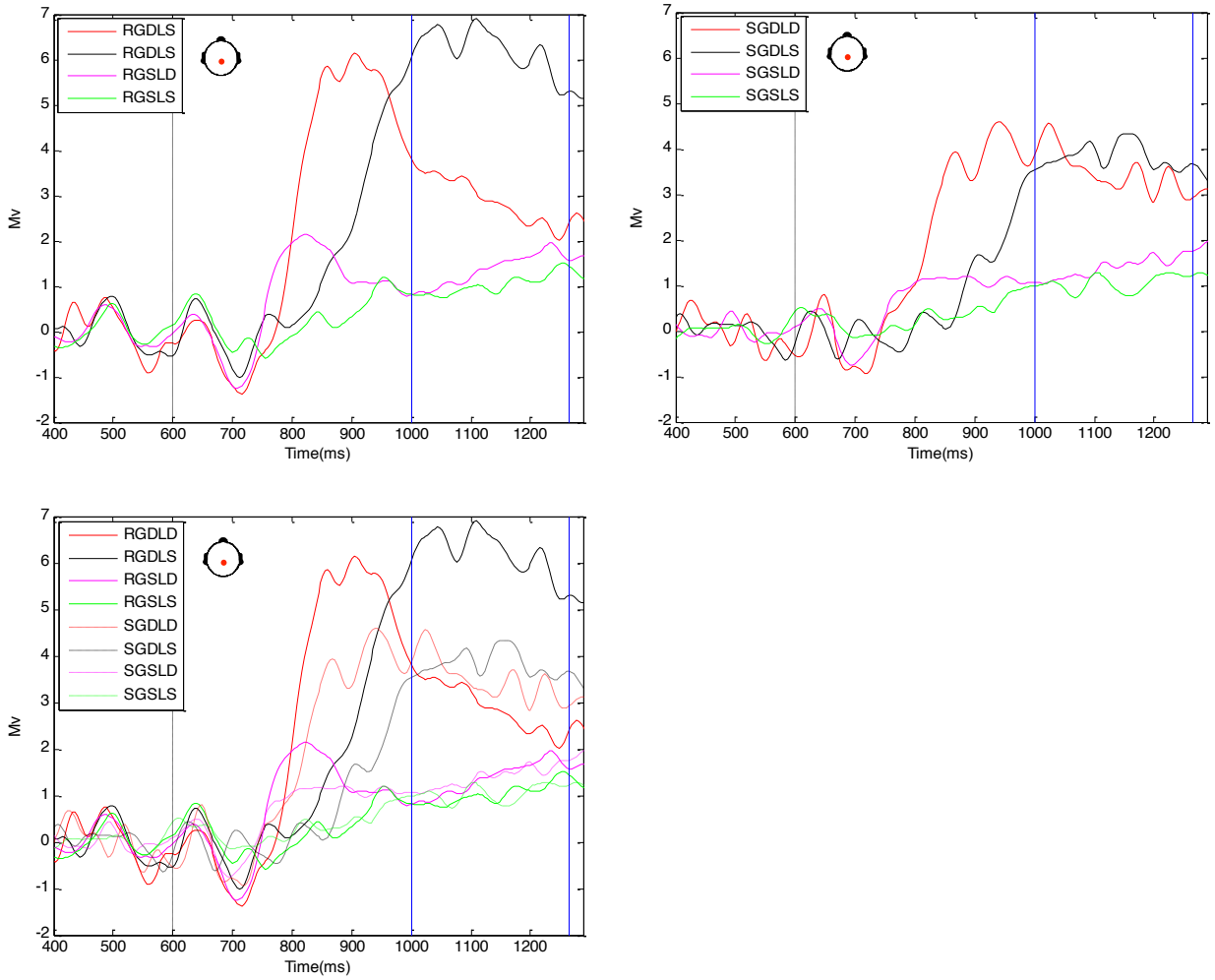

Figure 6.16. Top left panel: Grand average ERPs for the global x local interaction within the recovered condition at Pz. Top right panel: Grand average ERPs for the global x local interaction within the sedated condition at Pz. Bottom left panel: grand average ERPs for the sedation x global x local interaction (including both recovered and sedated conditions) at Pz. Blue lines indicate the region of significance. Black dashed line (600ms) indicates the onset of the final tone.

The sedation x global x local interaction reveals that the global x local interaction is changing between sedated and recovered conditions (see top left and right panels in Figure 6.16). In Figure 6.16, it can be seen that there is little difference between globally standard conditions (magenta and green lines), regardless of whether the participants were sedated or recovered (for scalp topography see Figure 6.15); this is because globally standard conditions do not violate assumptions of global regularity. In contrast, GDLD elicits a much earlier and shorter-lived response than GDLS for the recovered condition (red and black lines in top left panel in Figure 6.16), whilst for the sedated condition both responses continue on even though the onset of GDLD is earlier than that of GDLS (red and black lines in top right panel in Figure 6.16).

There appears to be somewhat of a latency difference between the onset of responses across sedation and recovery (see bottom left panel in Figure 6.16 just after 800ms), suggesting that sedation may somewhat delay response onset. In the bottom left panel in Figure 6.16, the difference between GDLD (red dashed line) and GDLS (black dashed line) in the sedated condition is smaller within the region of significance (1000-1264ms), than the difference between GDLD (red line) and GDLS (black line) in the recovered condition (see also marked regions on significance in top left and right panels in Figure 6.16), seemingly driven by differences in response latency. The disparity of differences when compared against the very small difference amongst globally standard conditions across both sedation and recovery (magenta and green lines within all panels in Figure 6.16) forms the interaction we observe between sedation, global and local effects.

Summary (three-way ANOVA)

Firstly, we were able to replicate the global and local effects observed in the previous Chapter, as well as in the existing literature (Bekinschtein et al., 2009; Wacongne et al., 2011, 2012; Chennu et al., 2013; Pegado et al., 2010). We also found an early effect of sedation, showing that early frontal responses were smaller when sedated compared to when recovered. This may mean that sedation is impacting on the early frontal processing of auditory information (see Figures 6.3 and 6.4). Overall, responses when sedated were smaller than responses in recovery and there appears to be a small increase in response latency under sedation. This may suggest that sedation is dampening responses and possibly slowing down the processing pathway.

With respect to global and local effects, they are varying significantly between sedation and recovery; in particular the local effect is changing significantly within the region of a central P3a response, that is, the central P3a response is larger when recovered comparing to when sedated, generating a larger difference between recovered local deviant (RLD) and recovered local standard (RLS), comparing to the difference between sedated local deviant (SLD) and sedated local standard (SLS), thus forming an interaction that we observe between level of sedation and the local effect (see Figure 6.10). The presence of a larger central P3a response when recovered may be the result of

an increase in wakefulness, whilst on the other hand a smaller P3a response when sedated may be indicative of a reduction in wakefulness.

Moreover, we have argued that a reduction in wakefulness (sedation) may limit the availability of cognitive resources, which could in turn limit the processing of auditory information. At the same time, when recovered, the availability of cognitive resources may be increased so that one may have available to them the necessary resources to facilitate full attentional engagement with the task. This is not to say that when sedated participants were unable to detect violations in auditory regularity, as this was not found to be the case within the current study. It appears that the experience of sedation did indeed vary across participants, as drug level remained consistent across the sample. Therefore, we postulate that it may be more accurate to suggest that attentional engagement with the task was dampened by sedation rather than eliminated altogether based on the fact sedation does not appear to have constituted a complete loss of consciousness (signified by the absence of ERP responses).

In particular, sedation did not eliminate responses to global deviance (see Figure 6.12); that is, despite being sedated participants were still able to detect global violations in auditory regularity, as indexed by a P3b response; this finding appears to be somewhat counterintuitive to what one might expect under sedation. However, one may attribute the presence of global effects within the sedated condition to the varying impact of a standardised drug-level.

Notably, we found that under sedation participants were able to detect global violations in regularity that were marked by both locally deviant and locally standard quintuples (see top right panel in Figure 6.16). That is, sedation did not appear to dramatically disrupt the ability to distinguish global deviance given a varying local context. Thus, the attentional directive of the task does not appear to be disrupted by sedation in this study.

As previously mentioned, there does appear to be some evidence that sedation increases the latency of effects, which may mean that sedation is having some effect on the speed of the processing pathway (see bottom left panel in Figure 6.16). However, the size of the emerging latency differences in this respect are much smaller than those between levels of global and local context (standard vs. deviant) (see Figures 6.10 and 6.12). Therefore, it appears that deviant stimuli have a greater impact on response latency than sedation in this study. Consequently, the onset of responses appears mostly reliant upon

the presence of deviance, whilst the size of responses in this study appears mostly dependent upon whether participants were under sedation or in recovery. Given that attention was directed towards the task in both sedated and recovered conditions, findings are the result of a manipulation in wakefulness and not in attentional directive in this case.

With respect to the global x local interaction, it can be seen that there are latency differences between responses to globally deviant stimuli depending on local regularity (ie. whether the quintuple is locally deviant or locally standard) (see Figure 6.14). More specifically, the response to GDLD begins earlier and is shorter in duration than the response to GDLS (see Figure 6.14). It may therefore be the case that local deviance is accelerating the response to global deviance, given that it is not only a violation of global regularity but also a violation of local regularity. This sits in contrast to global deviance that is marked by a locally standard quintuple (GDLS), which induces a later and longer P3b response given that it is a violation of global regularity but not a violation of local regularity. The presence of a differing P3b response to GDLD and GDLS suggests that participants are not only detecting global deviance marked by both levels of local context (local deviant and local standard), but that responses can be distinguished on this basis, ie. by local regularity.

In sum, whilst it appears that sedation may reduce the size and somewhat impact on the latency of responses, it has not disrupted the attentional directive of the individuals within this study. What is more, response onset appears most dramatically altered by the presence of deviance at both the global and local levels rather than by sedation. That is, the presence of an interaction between global and local effects in this study reveals that GDLD elicits an earlier and shorter-lived P3b response comparing to GDLS, which elicits a later and longer P3b response (see bottom left panel in Figure 6.16). Thus, the shape of the P3b response to global deviance appears to be dependent upon whether or not there is also local deviance. This difference in response is large enough to drive an interaction between global and local effects as the difference between globally standard conditions is small. Further simple effects analysis, presented hereafter, is necessary to ascertain whether there is a significant interaction between global and local effects within each level of sedation respectively (ie. sedation and recovery).

Simple effects analysis

Within the next section, we will present the simple effects analysis conducted to further examine how the interaction between global and local effects may be changing across levels of sedation (ie. sedation and recovery). A two-way ANOVA was applied to both sedated and recovered conditions respectively to assess levels of the local effect (standard vs. deviant) against levels of the global effect (standard vs. deviant).

Post-hoc correction

As we are conducting post-hoc analysis of simple effects, consideration must be paid to adequate correction of the alpha level. Given that the cluster-forming threshold at the first-level defines features of the signal it should not change within the post-hoc analysis. However, the cluster-extent threshold at the second-level can be adjusted to manage the significance of clusters, for example if Bonferroni correction is applied the alpha level of 0.05 should be divided by 2 (as two tests are conducted, one for sedation and one for recovery); therefore 0.05/2 = 0.025. As stated within the previous Chapter, we acknowledge there is some difficulty in accurately correcting for the number of comparisons within time-series data, as one is attempting to correct for post-hoc multiple comparisons made across both time and space simultaneously (Kilner & Friston, 2010). Thus, in order to reduce inflation of the alpha level we implement a cluster-level significance threshold of 0.01 for the following analyses (see Appendix 1.5 and 1.6).

Recovered condition

Two-way ANOVA (global x local)

A two-way ANOVA (global x local) was applied to the recovered condition to examine local (standard vs. deviant) and global (standard vs. deviant) effects.

Recovered local effect. The local effect is significant between 700-736ms around frontal electrode Fz, and subsequently from 808-904ms around central electrode Cz (see Figure 6.17).

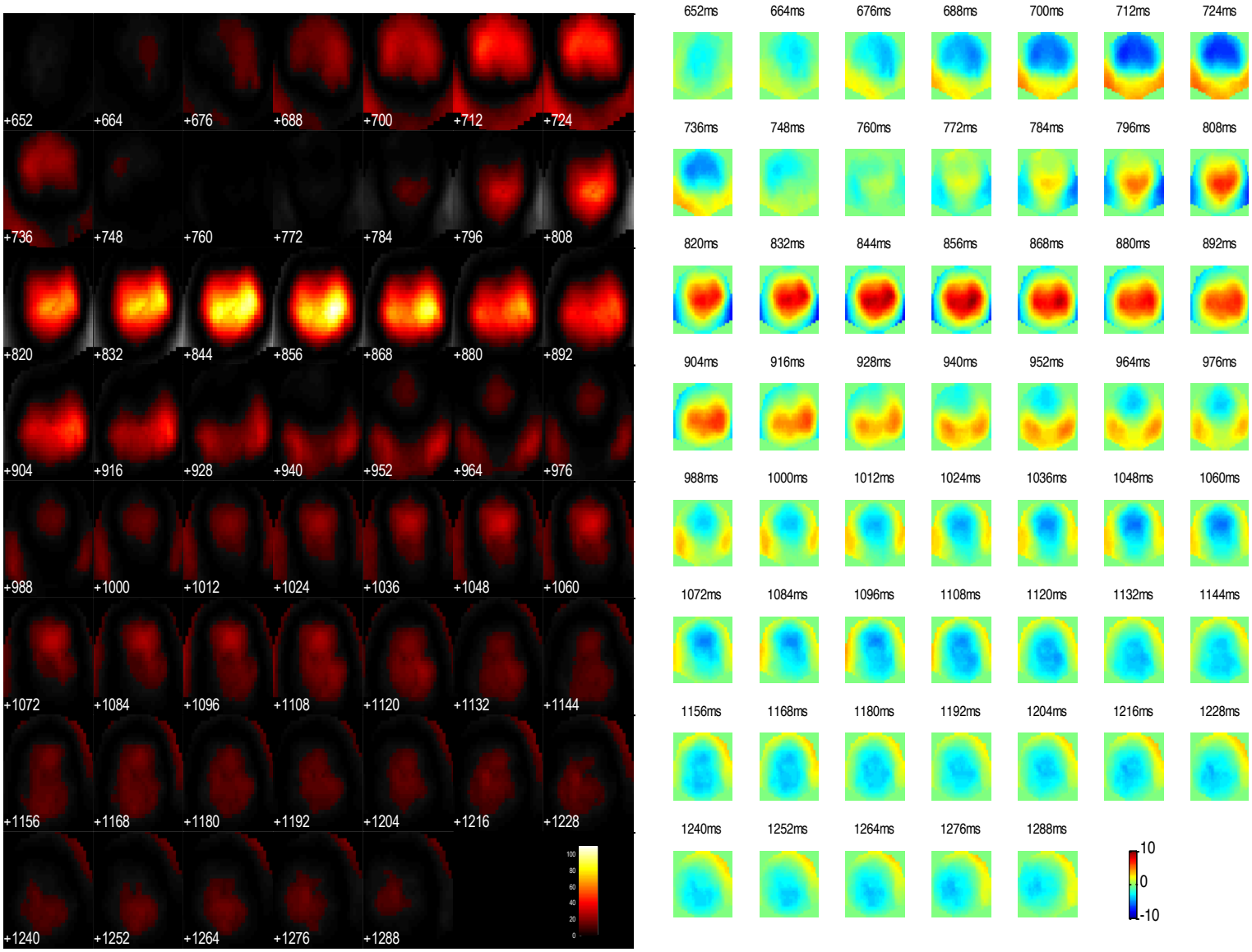

Figure 6.17. Thresholded F-maps ($p < .05$) to show regions of significance for local effect in the recovered condition [RLD-RLS] on the scalp through time (left). Unthresholded T-maps to show the polarity of effect on the scalp through time (right). Note that time within the left panel is presented below the corresponding row of scalpmaps, whilst time within the right panel is presented above the corresponding row of scalpmaps.

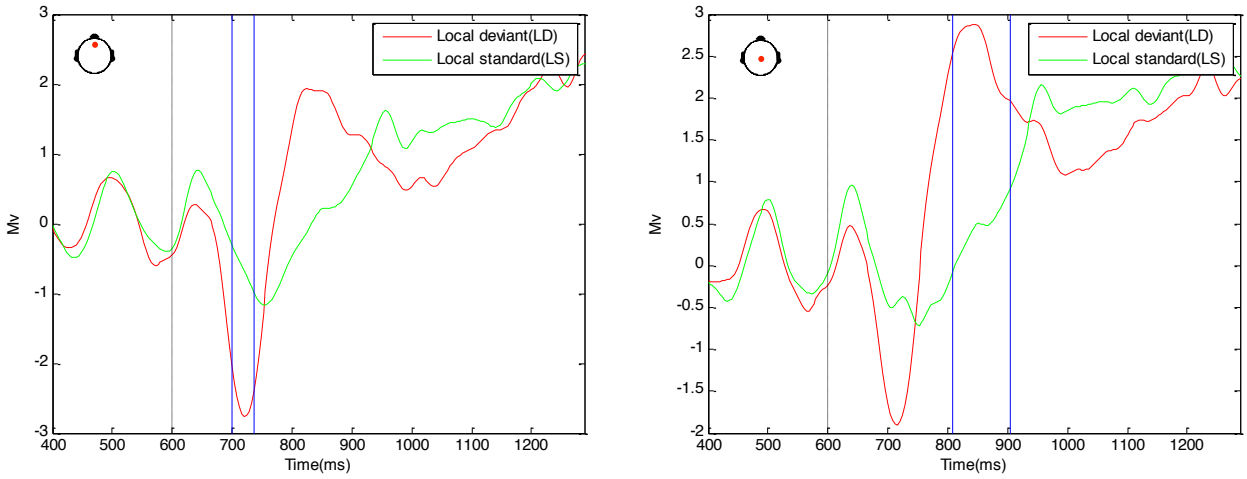

Figure 6.18. Grand average ERPs for the local effect in the recovered condition at Fz (left) and Cz (right). Blue lines indicate the region of significance. Black dashed line (600ms) indicates the onset of the final tone.

Figure 6.18 shows that in an early time window (700-736ms) local deviance produces a MMN at frontal electrode Fz. Subsequently, there is a region of significance at central electrode Cz (between 808-904ms), where local deviance produces a large P3a response that is not present for the locally standard condition. The onset of MMN in the locally deviant condition is earlier than the response to locally standard quintuples; this suggests that the onset of a local response is subject to the presence of deviancy when in recovery. The local effect we observe is consistent with that found in the previous Chapters and elsewhere within the literature (for scalp topography see Figure 6.17) (Bekinschtein et al. 2009; Wacongne et al., 2011, 2012; Chennu et al., 2013; Pegado et al., 2010).

Recovered global effect. The global effect is significant from 892-1216ms around central posterior electrode Pz (see Figure 6.19).

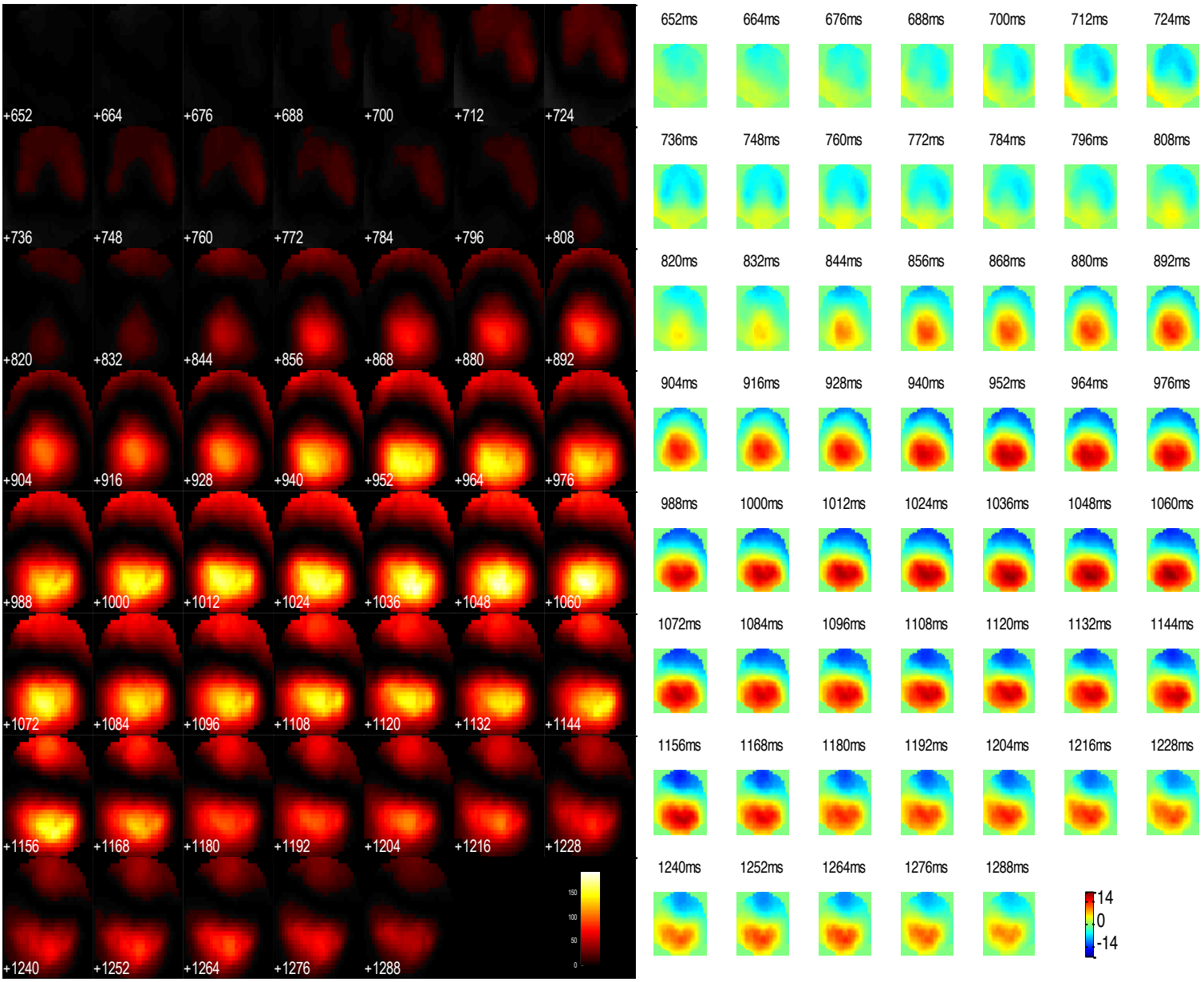

Figure 6.19. Thresholded F-maps ($p < .05$) to show regions of significance for global effect in the recovered condition [RGD-RGS] on the scalp through time (left). Unthresholded T-maps to show the polarity of effect on the scalp through time (right). Front of the scalp is positioned at the top. Note that time within the left panel is presented below the corresponding row of scalpmaps, whilst time within the right panel is presented above the corresponding row of scalpmaps.

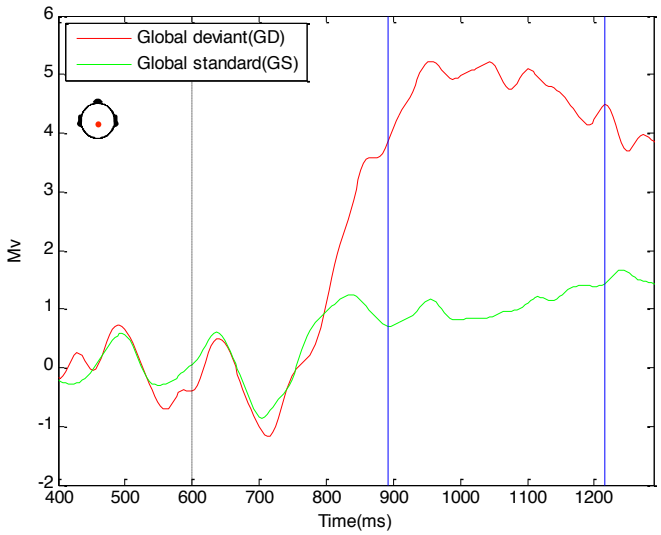

Figure 6.20. Grand average ERPs for the global effect in the recovered condition at Pz. Blue lines indicate the region of significance. Black dashed line (600ms) indicates the onset of the final tone.

Global deviance elicits a large P3b response, whereas globally standard tones do not as they do not violate assumptions of global regularity (see Figure 6.20). This difference in responses creates a global effect (for scalp topography see Figure 6.19). The global effect observed is consistent with previous findings in the literature and also the findings presented in the previous Chapter (Bekinschtein et al. 2009; Wacongne et al., 2011, 2012; Chennu et al., 2013; Pegado et al., 2010).

Recovered global x local. The global x local interaction is significant from 832-952ms around right lateral electrode ch.79 and then between 1012-1288ms around central electrode Cz (see Figure 6.21).

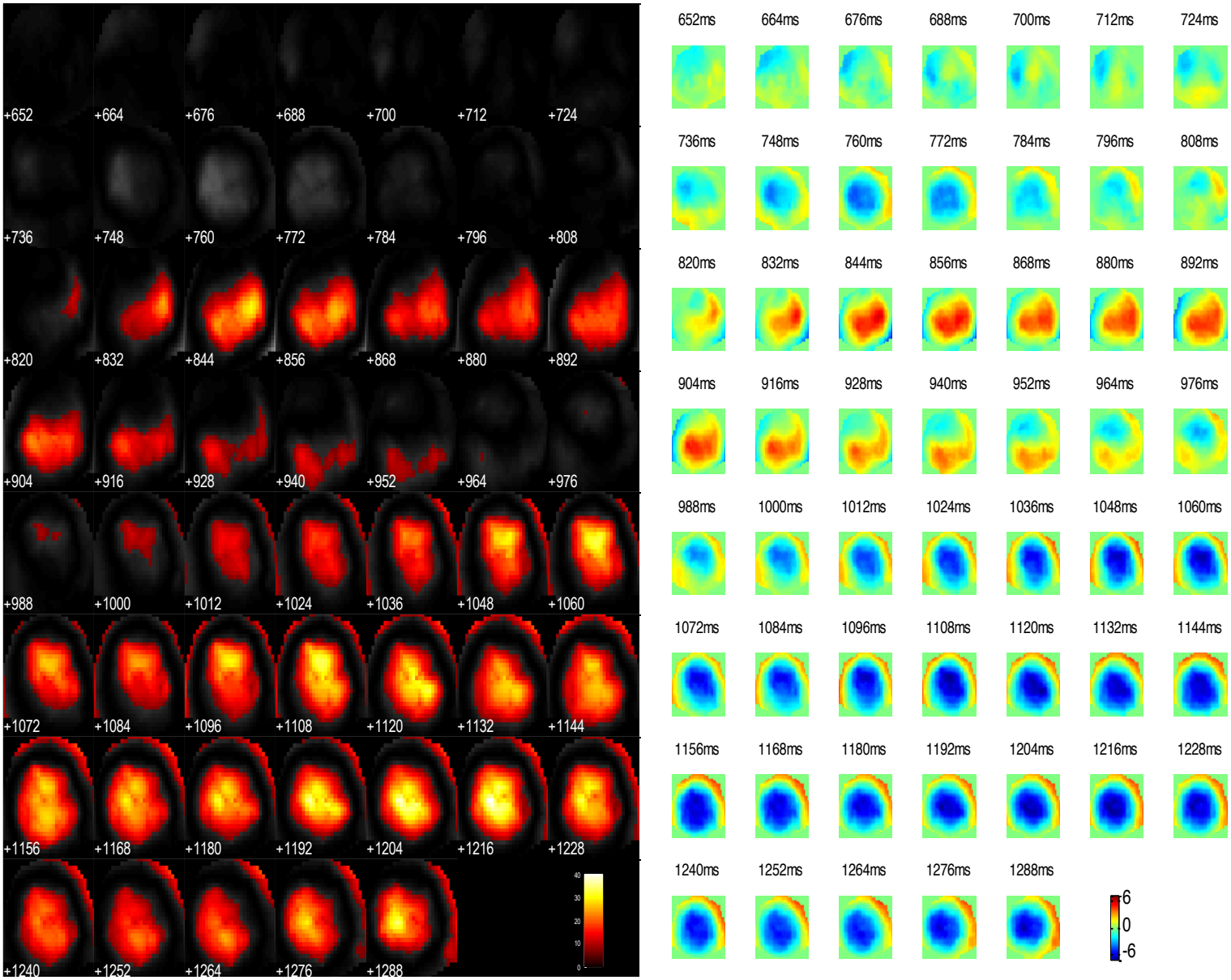

Figure 6.21. Thresholded F-maps ($p < .05$) to show regions of significance for the global x local interaction in the recovered condition [(RLDGD-RLDGS)-(RLSGD-RLSGDS)] on the scalp through time (left). Unthresholded T-maps to show the polarity of effect on the scalp through time (right). Front of the scalp is positioned at the top. Note that time within the left panel is presented below the corresponding row of scalpmaps, whilst time within the right panel is presented above the corresponding row of scalpmaps.

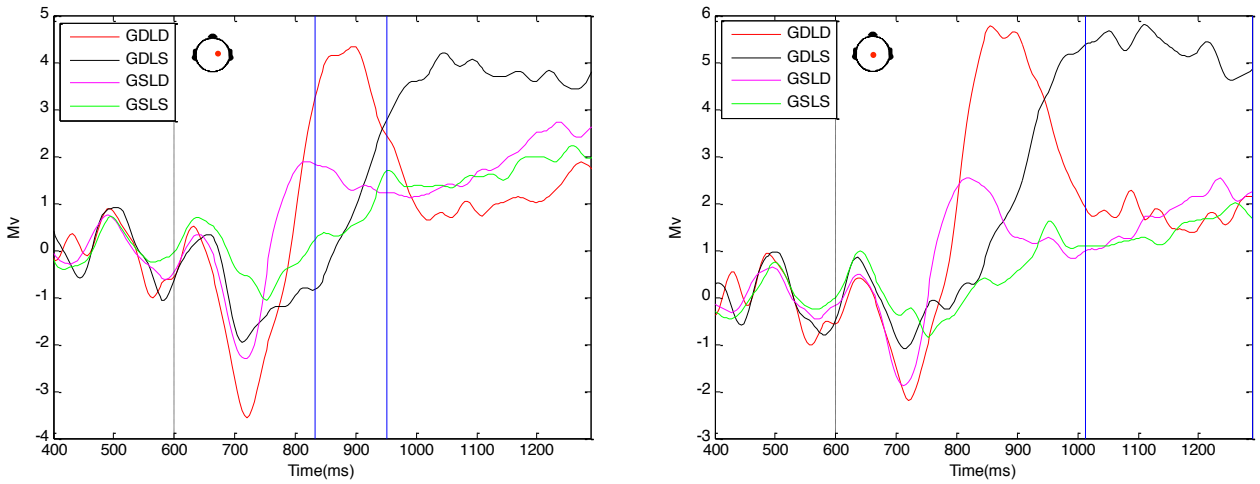

Figure 6.22. Grand average ERPs for the global x local interaction in the recovered condition at ch.79 (left) and Cz (right). Blue lines indicate the region of significance. Black dashed line (600ms) indicates the onset of the final tone.

The global x local interaction is significant in an early time window (832-952ms) at central electrode ch.79 (see Figure 6.21 and left panel in Figure 6.22), where the difference between GDLD (red line) and GDLS (black line) is large, comparing to the difference between GSLD (magenta line) and GSLS (green line), which is small. This disparity of differences creates an interaction between global and local effects. The presence of such an interaction suggests that the shape of the response to global deviance differs depending on whether the quintuple is locally deviant or locally standard. This is only the case in comparison to the small difference that exists between globally standard conditions (that is, GSLD [magenta line] and GSLS [green line]).

Moreover, within the second region of significance (1012-1288ms) at channel Cz, the response to GDLS (black line) is ongoing, however the response to GDLD (red line) is very nearly over (See Figures 6.21 and 6.22). This generates a large difference between the two conditions, which taken in consideration with the difference between GSLD (magenta line) and GSLS (green line), which is close to zero, creates an interaction within this region as well.

Summary (recovered condition)

We find both global and local effects within the recovered condition, which are consistent with the effects found in the previous Chapter and within the existing literature (Bekinschtein et al., 2009; Wacongne et al., 2011, 2012; Chennu et al., 2013; Pegado et al., 2010). What is more we find that both global and local deviant quintuples elicit larger responses than respective global and local standard quintuples (see Figures 6.18 and 6.20). Additionally, we observe an interaction between global and local effects which occurs within the region of the global effect (see Figures 6.21 and 6.22). Specifically, the interaction between global and local effects is taking place in the region of the P3b response, where GDLD is producing an early and short-lived response, which is ending as the response to GDLS begins. The latency difference between responses to GDLD and GDLS is large in comparison to the very small difference between GSLD and GSLS conditions, forming the interaction we observe. The shape of the P3b response to global deviance within the recovered condition appears to depend upon whether the quintuple is locally deviant or locally standard.

Sedated condition

Two-way ANOVA (global x local)

A two-way ANOVA (global x local) was applied to the sedated condition to examine local (standard vs. deviant), global (standard vs. deviant) and interaction effects.

Sedated local effect. The local effect is significant around frontal electrode Fz between 688-736ms and then between 1000-1204ms. Subsequently, there is significance from 892-940ms around right lateral electrode ch.77. What is more, there is significance around central posterior electrode Pz between 844-880ms and 916-952ms (see Figure 6.23).

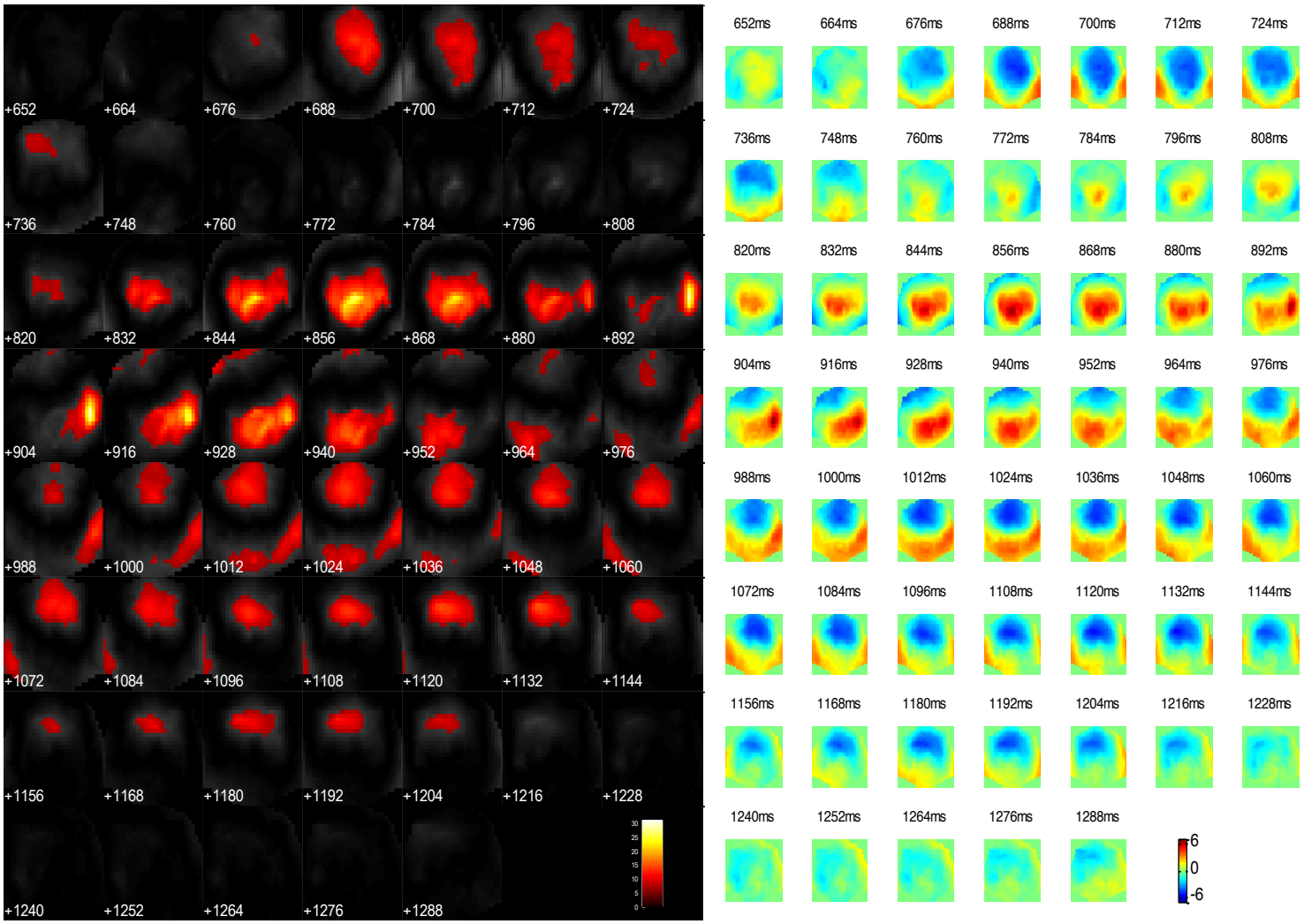

Figure 6.23. Thresholded F-maps ($p < .05$) to show regions of significance for the local effect in the sedated condition [SLD-SLS] on the scalp through time (left). Unthresholded T-maps to show the polarity of effect on the scalp through time (right). Front of the scalp is positioned at the top. Note that time within the left panel is presented below the corresponding row of scalpmaps, whilst time within the right panel is presented above the corresponding row of scalpmaps.

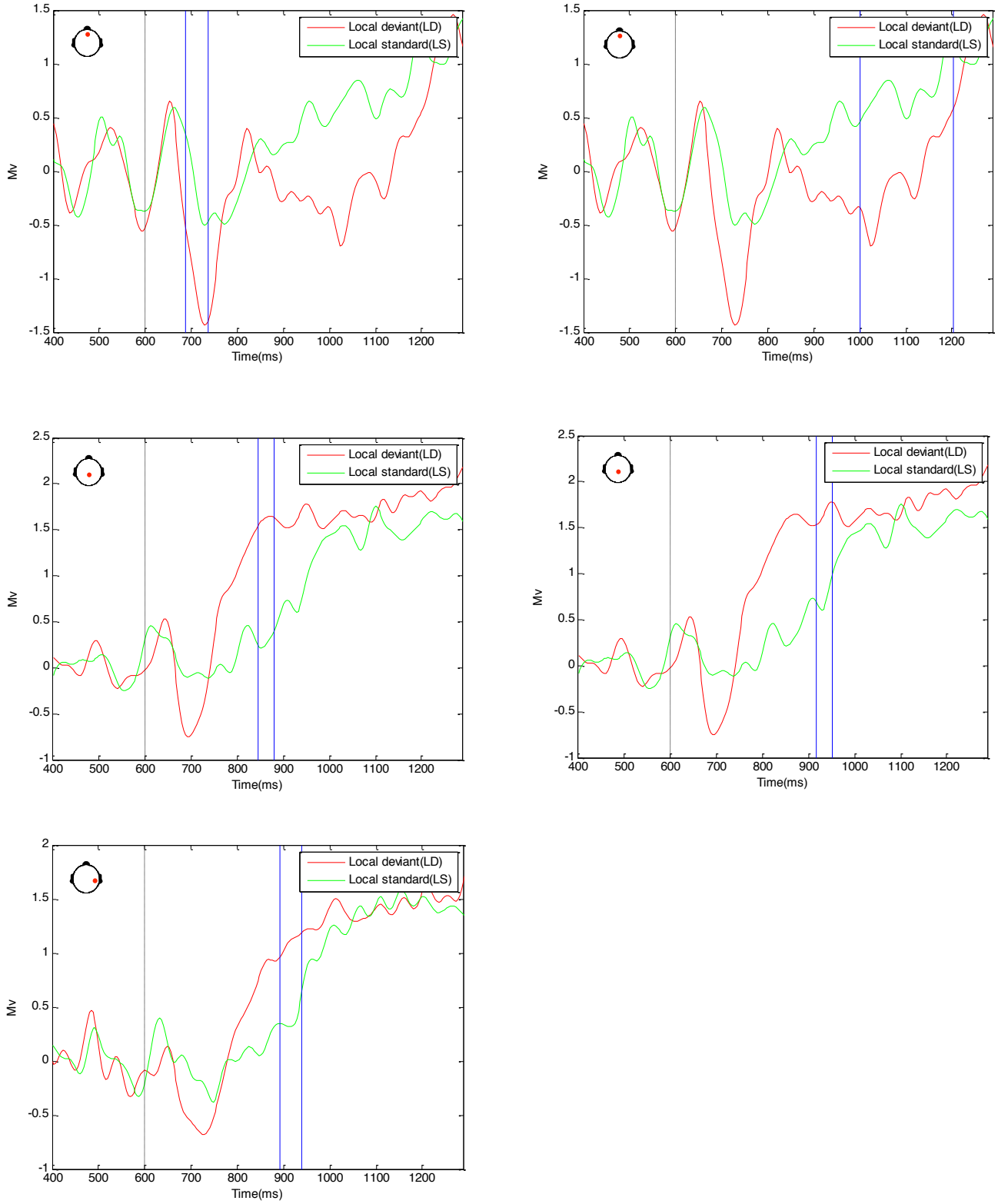

Figure 6.24. Grand average ERPs for the local effect in the sedated condition at Fz (top left and right), Pz (middle left and right) and ch.77 (bottom left). Blue lines indicate the region of significance. Black dashed line (600ms) indicates the onset of the final tone.

Within the sedated condition, one can see that local deviance is generating a large mismatch response that is occurring earlier in time than the response to locally standard quintuples (see top left panel in Figure 6.24). It can also be seen that there is a small but marked P3a response to local deviance at electrode Pz (see middle left and right panels on Figure 6.24). The P3a response is less pronounced than within the recovered condition, as sedation may be attenuating the size of the response (for scalp topography see Figure 6.23). The local effect we observe in sedation is consistent with the local effect observed in the previous Chapter and within the existing literature (Bekinschtein et al., 2009; Wacongne et al., 2011, 2012; Chennu et al., 2013; Pegado et al., 2010).

Sedated global effect. The global effect is significant around posterior electrode Pz between 928-1240ms, in addition to frontal electrode ch.13 between 1012-1252ms (see Figure 6.25).

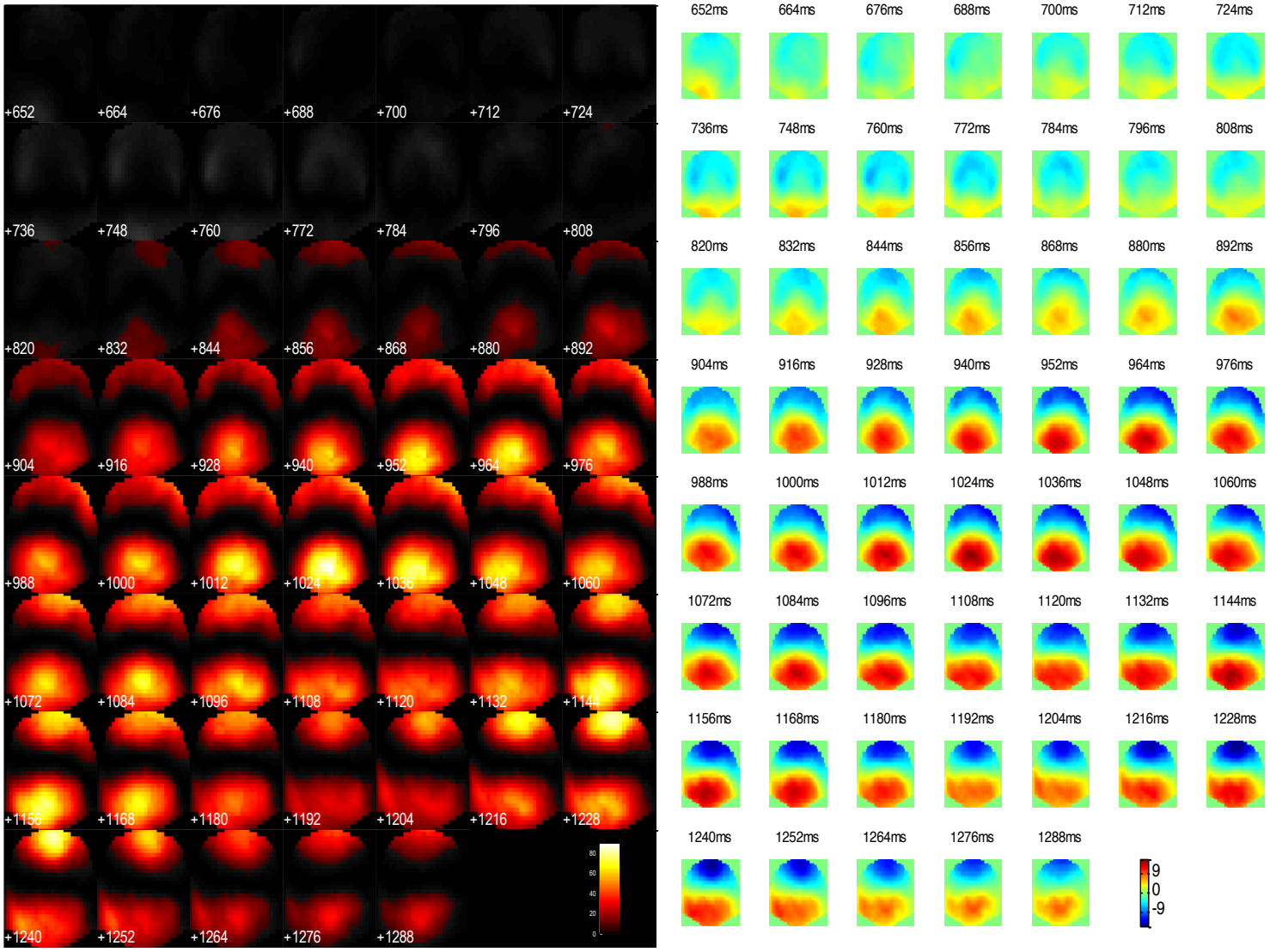

Figure 6.25. Thresholded F-maps ($p < .05$) to show regions of significance for the global effect in the sedated condition [SGD-SGS] on the scalp through time (left). Unthresholded T-maps to show the polarity of effect on the scalp through time (right). Front of the scalp is positioned at the top. Note that time within the left panel is presented below the corresponding row of scalpmaps, whilst time within the right panel is presented above the corresponding row of scalpmaps.

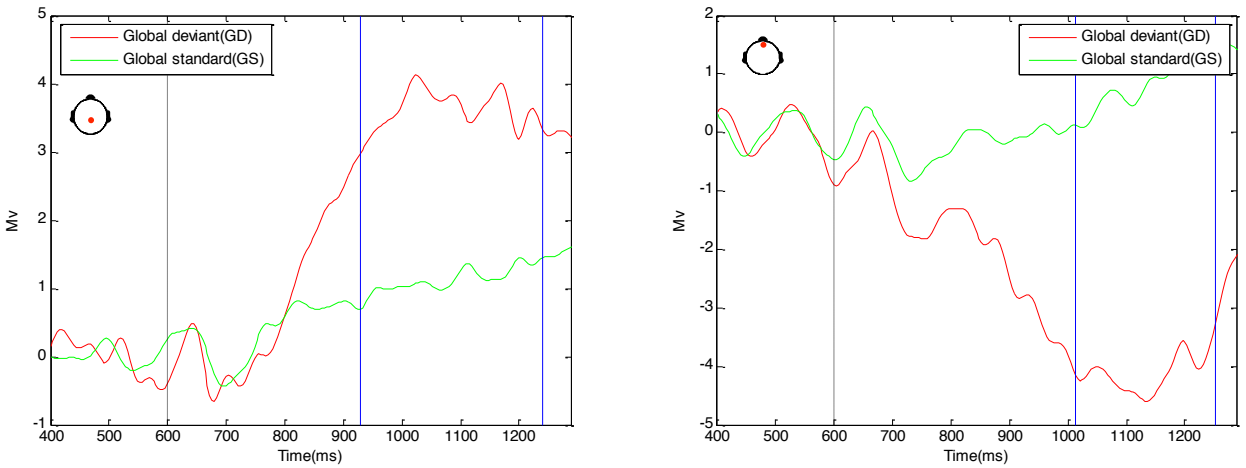

Figure 6.26. Grand average ERPs for the global effect in the sedated condition at Pz (left) and ch.13 (right). Blue lines indicate the region of significance. Black dashed line (600ms) indicates the onset of the final tone.

The global effect for the sedated condition shows that global deviance (red line) produces a P3b response at posterior electrode Pz (see Figure 6.25 and left panel in Figure 6.26), whereas globally standard tones do not (green line). In addition, at frontal electrode ch.13, we can see again a larger response for global deviance, but this time negative as we appear to be observing the other side of the electrical dipole (see right panel in Figure 6.26). The global effect in the sedated condition manifests in much the same way (although with reduced amplitude) as it does within the recovered condition, suggesting that the presence of a global effect is robust against sedation within this experiment (for scalp topography see Figure 6.25).

Sedated global x local. The global x local interaction is significant around frontal electrode Fz from 1060-1204ms (see Figure 6.27).

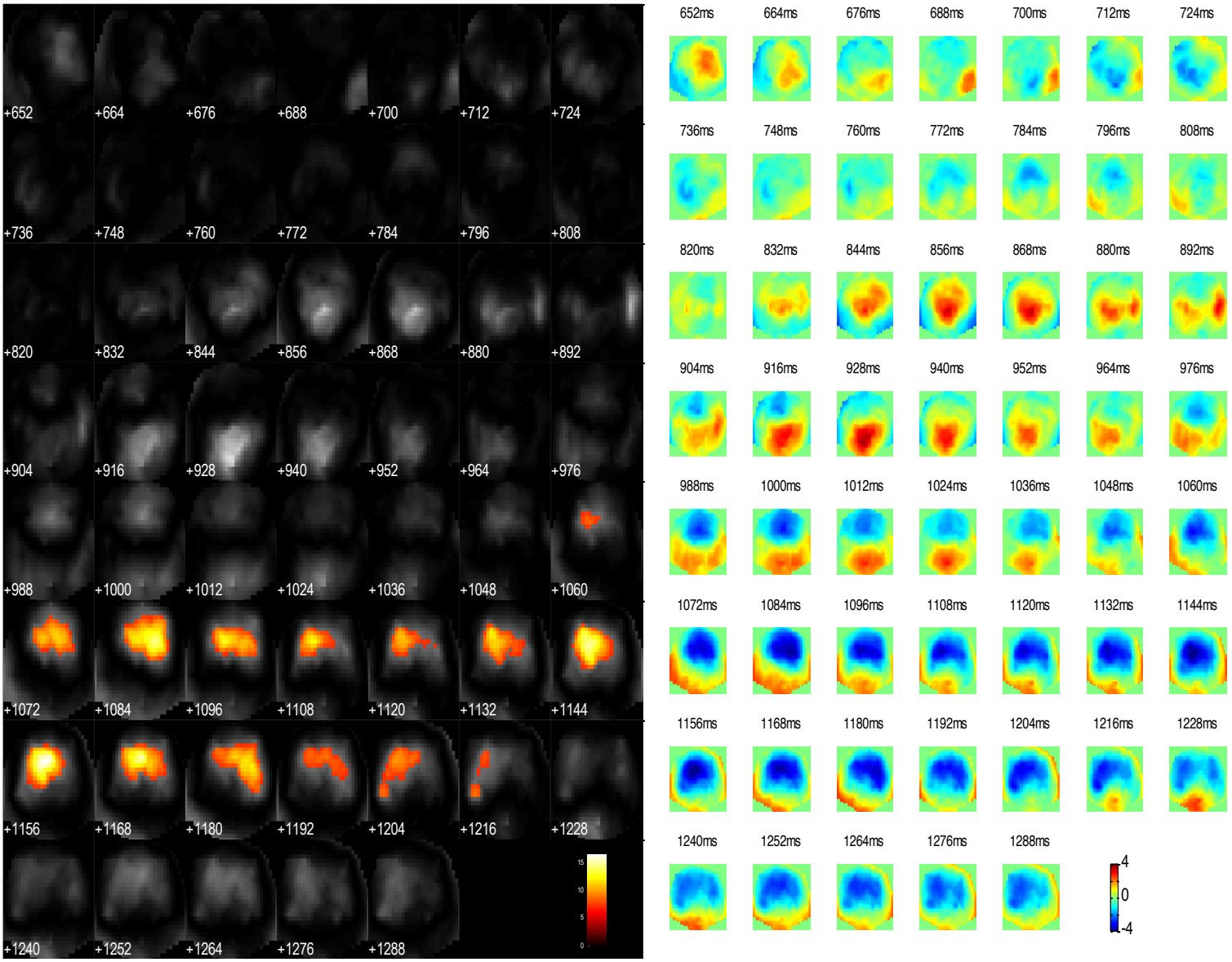

Figure 6.27. Thresholded F-maps ($p < .05$) to show regions of significance for the global x local interaction in the sedated condition [(SLDGD-SLDGS)-(SLSGD-SLSGS)] on the scalp through time (left). Unthresholded T-maps to show the polarity of effect on the scalp through time (right). Front of the scalp is positioned at the top. Note that time within the left panel is presented below the corresponding row of scalpmaps, whilst time within the right panel is presented above the corresponding row of scalpmaps.

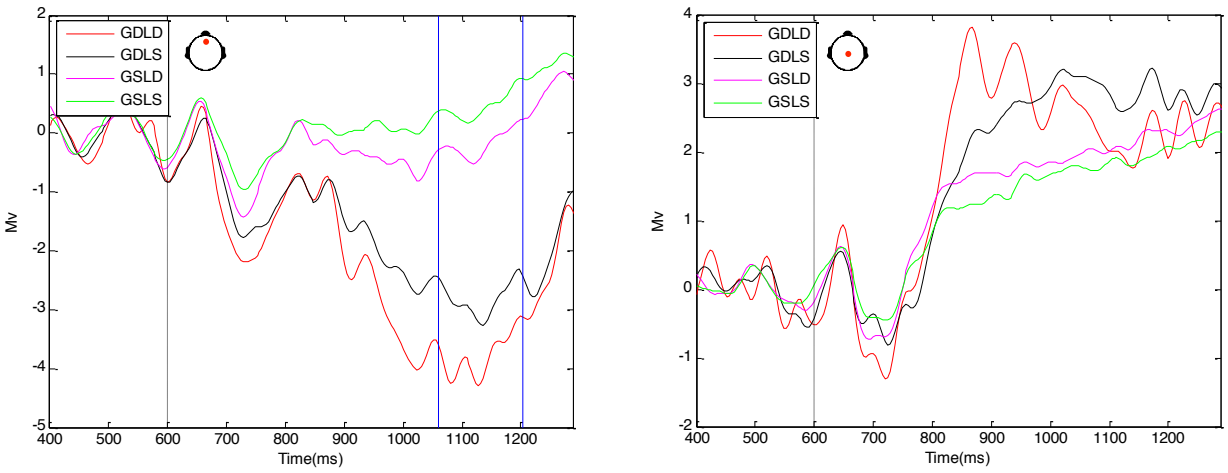

Figure 6.28. Grand average ERPs for the global x local interaction in the sedated condition at Fz (left) and Cz (right). Blue lines indicate the region of significance. Black dashed line (600ms) indicates the onset of the final tone.

It can be seen in Figure 6.28 that within the region of significance (1060-1204ms), GDLD (red line) and GDLS (black line) elicit a larger negative response compared with GSLD (magenta line) and GSLS (green line) (scalp topography can be seen in Figure 6.27). The interaction is occurring frontally and beginning 460ms after stimulus onset (1060ms). The interaction between global and local effects at sedation is different to the interaction generated when recovered as it is occurring frontally whilst when recovered we observe the interaction within the region of the global effect. Looking at electrode Cz in Figure 6.28 (right panel), one can see that the difference between GDLD (red line) and GDLS (black line) is far less pronounced than within the recovered condition. The difference between these two conditions, compared to the difference between globally standard conditions (magenta and green lines) is not sufficient to constitute an interaction within this region. Therefore, when sedated we find that the interaction appears frontally, whilst in recovery it appears centrally.

The T-maps in Figure 6.27 show that around the time region of the significant interaction (1072-1096ms) there is also a positive effect occurring in a posterior region on the scalp; this may indicate that the interaction we observe around Fz is an effect at one side of the dipole, with a positive effect occurring at the opposite side of the dipole across posterior electrodes.

Summary (sedated condition)

We find both global and local effects within the sedated condition, which are consistent with the effects found in the previous Chapter and within the existing literature (Bekinschtein et al., 2009; Wacongne et al., 2011, 2012; Chennu et al., 2013; Pegado et al., 2010). Global and local deviants generate larger responses than respective standard stimuli (see Figures 6.24 and 6.26). The presence of a global effect under sedation is counterintuitive, although is likely to reflect the varying experience of sedation across participants within this study. That is, sedation does not appear to have constituted a complete loss of consciousness within this study. Therefore, the presence of a global effect under sedation is likely to indicate that participants were indeed conscious (awake) albeit drowsy.

Moreover, we observe an interaction between global and local effects that is taking place in a late time window (1060-1204ms) around frontal electrode Fz (see Figures 6.27 and 6.28). This appears to be an effect at one side of the dipole, with a positive effect also occurring across posterior electrodes within the same time region (but not reaching significance). Nevertheless, a significant interaction between global and local effects around frontal electrodes in a late time window sits in contrast to the interaction between global and local effects observed at recovery. We find that there is some evidence of an emerging interaction centrally around 850ms, although this does not reach statistical significance in the current dataset.

Discussion

Within this Chapter, we presented the results of a full factorial analysis of the global-local task with sedation, whereby participants were administered the task on two occasions: once under sedation and once when recovered (20 minutes later). At both points, participants were instructed to count the number of globally deviant quintuples they heard, which meant that attention was directed towards the task in both conditions. Therefore, attention was held constant within this study whilst consciousness as a spectrum of wakefulness was manipulated via sedation.

Importantly, the experience and level of sedation will have varied across participants within the study, so one should be mindful that sedation in this case did not constitute a complete loss of consciousness necessarily (wakefulness). Accordingly, we found altogether that response size was smaller within the sedated condition comparing to when recovered, whilst differences in the shape of responses between deviant and standard stimuli were preserved across both conditions (sedation and recovery), which is likely to reflect the level of conscious processing maintained under sedation.

Interestingly, the mismatch response (MMN) is smaller when under sedation comparing to when recovered, which could suggest that a reduction in wakefulness inhibits the level of precision afforded by direct attention that has typically been found to enhance the size of the mismatch response (Chennu et al., 2013; Auksztulewicz & Friston, 2015). Moreover, sedation also dampens the subsequent central P3a response, which could be associated with a lack of attentional engagement with the task (Freidman, Cycowicz & Gaeta, 2001). In respect of global deviance, the P3b response elicited under sedation peaks later (around 1000ms) than that of recovery (around 950ms), which may mean that sedation increases response latency somewhat at the level of global violations; however this does not appear to be the case with regard to local deviancy (where sedation seemingly does not impact upon response latency).

Nevertheless, the presence of a global x local interaction when recovered reveals that global deviance, which is also locally deviant, elicits an earlier and shorter-lived P3b response in comparison to global deviance that is locally standard. The size of the difference between these responses is large when considered against the difference between globally standard conditions (GSLS and GSLD), which do not violate global regularity and therefore do not elicit a P3b response.

One might consider the finding within a framework of predictive coding whereby the violation of both local and global expectancy (GDLD) quickens the onset of the P3b response in comparison to when there is only a global predictive violation (in the absence of a local violation) (Friston, 2010; Chennu et al., 2013). The hastened response may reflect prediction error at both global and local levels of the hierarchy, which fully violates expectation. Interestingly, when global deviance is marked by a locally standard quintuple (GDLS), this is again a violation of global expectancy although local

regularity is preserved. Thus, the later onset and longer duration of a P3b response to GDLS may reflect the time it takes for prediction error to reach the global level (when there is no predictive violation at the local level) and the adjustment of global expectation to integrate a new patterns of sound.

Critically, under sedation, the interaction appears frontally although there is a trend towards significance within the region of the global effect (ie. centrally around Cz), where local deviance is still accelerating the P3b response. Therefore, it seems that whilst the presence of direct attention predominantly impacts upon the shape of responses, by facilitating the detection of deviant stimuli at the global level (in particular the presence of GDLS), sedation predominantly appears to dampen the size of effects in this study.

In the previous two Chapters, we have considered that the global effect may not be a functionally isolated marker of conscious processing as suggested by Bekinschtein et al. (2009). Within this Chapter, we have found that the manipulation of wakefulness via healthy sedation did not appear to disrupt the attentional directive of the individual with respect to detecting instances of global deviance and this may be attributed to sedation constituting a reduction in wakefulness as opposed to a complete loss of consciousness. Moreover, we observed an interaction between global and local effects within the region of the global effect, in the presence of direct attention and without sedation (ie. within the recovered condition). An interaction in this case suggests that the shape of the P3b response to global deviance may mark the level of local regularity (whether the quintuple is locally deviant or locally standard).

These findings sit somewhat in contrast to the interaction observed within the previous Chapters on attention, as when attention was passive, participants altogether failed to detect instances of global deviance that were marked by a locally standard quintuple. Consequently, within the subsequent Chapter we will directly compare the findings on attention with the findings on sedation in relation to the global-local auditory task. We will conduct an exploratory analysis to further examine the presence of an interaction between global and local effects, whilst also discussing in more detail how and why the interaction may be changing between levels of attention vs. levels of sedation (ie. a reduction in wakefulness).

7 Interacting with consciousness IV: a full factorial comparison between attention and sedation on electrophysiological responses to the global-local task

Introduction

We have previously explored how manipulating attention may impact on the detection of global violations of auditory regularity. Furthermore, we have also explored how manipulating the fundamental static state of consciousness as wakefulness (via healthy sedation) may impact on the way in which auditory information is processed. In this Chapter, we seek to expand upon previous findings by directly comparing manipulations of attention to manipulations of wakefulness; in doing so we may further explore the manifestations of the interaction between global and local effects across variations in attention and wakefulness. It must be said that within this Chapter, we are predominantly conducting an exploratory analysis to better understand how varying attention may compare to varying wakefulness with respect to the global-local task. Throughout this Chapter, we explicitly highlight the possible limitations of combining the data from two studies in order to perform a statistical comparison. Within the results section, we specifically address two confounds, which were identified when data was combined, that may have an influence on resulting F-values of the analysis. Consideration will be paid to each confound in relation to each effect from the analysis and justification is provided for the results we present and discuss within this Chapter.

Additionally, we chose to address in more detail how the relationship between global and local effects may provide a possible index of attentional state and/or level of wakefulness, which could have important implications for clinical explorations into states of low awareness, such as Minimally Conscious and Vegetative State (MCS and VS). Whilst it is known that those in MCS are transiently awake and aware of their surroundings, there is space for discussion around the capability of such individuals to

attend and perceive auditory information (Giacino et al., 2002; Boly et al., 2005). If indeed the global-local task can highlight an interaction between global and local effects, which is changing in nature based on varied states of attention, then it may be possible to deduce whether those in states of low awareness can direct their attention towards the task by examining the relationship between global and local responses (ie. the interaction).

Whilst we are optimistic about the applicability of the global-local task to such clinical settings, we very much accept the limitations of the current work. The global-local task was designed as a research tool to examine the cognitive processing of hierarchical violations in auditory regularity, and although the findings in this thesis are from studies of healthy individuals we propose that the presence of an interaction between global and local effects signifies a much more complex processing pathway than was initially hypothesised by Bekinschtein et al. (2009). It is the presence of such complex processing in healthy individuals, which could be taken forward as a marker of higher-level cognitive ability in those within low awareness states (such as MCS), that is the detection of more complex processing than one might have expected. With this in mind, we attempt to address how direct attention (or lack thereof) may impact on the interaction in comparison to how reducing wakefulness (via sedation) may impact on the interaction.

In order to directly compare the findings of the previous three Chapters we combined the data into a factorial analysis, considering both manipulations of attention and wakefulness. To clarify, within the study on attention, attention was either engaged in the task (active group) or allowed to wander (passive group); whilst within the study of sedation, participants were first sedated and then tested again when recovered, where attention was always directed towards the task. Given that those in the active group and those at recovered are both actively engaging with the task, we suggest that findings in both these cases may be comparable.

By way of contrast, the passive group differ from those at sedation given the fact they do not have their attention directed towards the task, consequently sedation is providing a pure manipulation of wakefulness (as opposed to attention); thus, direct comparison of the passive group and the sedated condition may reveal how attention can manipulate the shape of responses in comparison to how sedation can manipulate the shape of

responses. Moreover, given that those who were sedated were then subsequently tested as recovered (within-subjects design), it may be the case that the after effects of sedation impact on subsequent responses when recovered, that is the initial impact of sedation carries into recovery. We therefore consider that there may be some variation in responses at recovery and responses in the active group (who were never sedated and only tested on one occasion). Furthermore, as expressed within the previous Chapter in regards to sedation, it is highly likely that the experience of sedation will have varied between participants, considering that drug tolerance and the response to sedation will have varied from person to person.

Additionally, we have explored consciousness within this thesis as the cognitive process of conscious perception involving attention, but also we have explored consciousness as a spectrum of wakefulness upon which one inhabits a fundamental static state of consciousness that sub-serves the ability to consciously perceive and may also impact upon the depth with which one is able to process information. Within the current Chapter, we attempt to draw together the previous explorations to provide a basis for future work. Exploring a comparison between manipulations of attention and manipulations of wakefulness (via healthy sedation) may highlight regions of interest, which could be validated through further research. Consequently, we present the subsequent analysis as an informative comparison, which should be viewed with a mind to future testing.

Design

In order to conduct our analysis, as mentioned, we combined the data from both attention and sedation experiments to create a structure that included four levels of task context. As attention was a between-subjects factor, whilst sedation was a within-subjects factor, we created one factor of task context which encompassed all four levels (active, passive, sedated and recovered) as a between-subjects factor. Thus, sedation and recovery were treated as two separate groups within the analysis as opposed to one group tested on two occasions.

We chose to adopt a between-subjects design in this case as we sought to compare levels of attention with levels of sedation and creating a between-subjects factor of sedation provided the most appropriate statistical analysis (ie. was necessarily conservative) given the nature of the datasets. Considering sedation as a between-subjects factor reduces the statistical power of the test rather than inflates the false positive rate (Type I error rate); this is because the test does not take advantage of the correlation between the data points in the sedated and recovered conditions, which is how within-subject designs gain statistical power. Significant effects therefore, are highly likely to be reliable, providing the noted confounds (discussed later in this Chapter) are not having an influence. Conversely, the likelihood of false negatives (Type II error rate) increases in this case, that is, null findings (or non-significance) may be the result of an overly conservative statistical test. Thus, once again, we emphasise the exploratory nature of the following analysis, where statistical significance should be viewed as a marker of regions of potential interest that should be investigated with further research.

Accordingly, a 4 x 2 x 2 mixed ANOVA was constructed with a between-subjects factor of task context, where participants were active, passive, recovered or sedated. Within-subjects factors were local (deviant vs. standard) and global (deviant vs. standard) as all participants experienced all levels of these factors (see Figure 7.1).

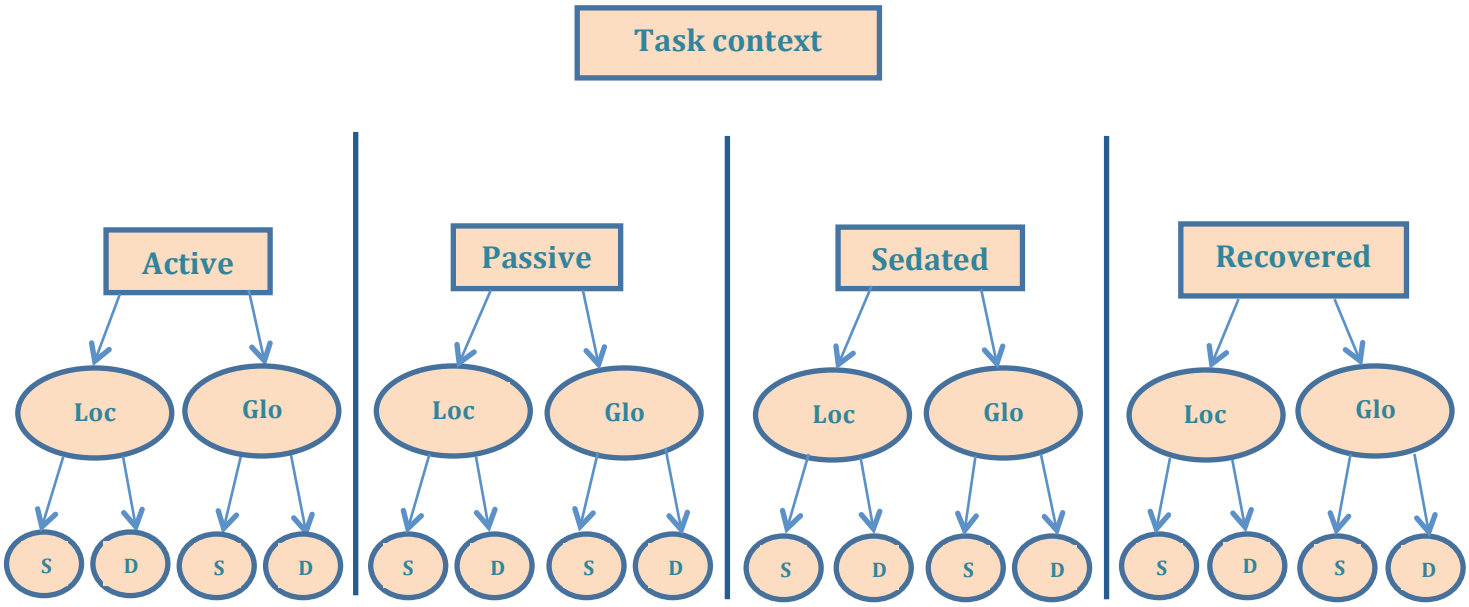

Figure 7.1. Illustration of the 4x2x2 mixed model ANOVA design. Task context (between-subjects), global and local (within-subjects) are factors, one with four levels and two with two levels; task context: active vs. passive vs. sedated vs. recovered, local (Loc): standard (S) vs. deviant (D) and global (Glob): standard (S) vs. deviant (D).

One issue that arises from combining the attention and sedation datasets is that there are different sample sizes between experiments (11 participants for active attention, 11 participants for passive attention & 18 participants for sedation/recovery). Thus, we selected 11 participants at random from the sedation study to combine with the 11 within the attention study (11 active & 11 passive). Selecting 11 participants at random reduces the likelihood of biasing effects given that effects are equally likely to exist across all participants within that group. What is more, having an equal number of participants across active, passive, sedated & recovered reduces the likelihood that differences in noise levels confound the comparison. In total, 33 participants were included in the following analysis (11 from active attention, 11 from passive attention and 11 from sedation/recovery). Additional exploratory analysis, including all participants from the sedation study (18 participants from sedation study and 22 from attention study) found that F-values changed, whilst the pattern of significant effects remained the same (see Appendix 4 for F-values).

As participants within the study of sedation were tested on two occasions (sedation and recovery), each of the 11 participants have one set of data for sedation and one set of data for recovery. Given that task context is a between-subjects factor, attention groups remain as either active or passive whilst sedation and recovery are now treated as though they were gathered from two different samples rather than from the same person twice. Thus, variability between groups in the following analysis is assumed to be unequal, when in reality it is likely to be equal (in a statistical sense) for sedation and recovery. This means that the statistical test may be over estimating the amount of variance that exists between groups for sedation and recovery and therefore inflating the likelihood of Type II errors (or false negatives) as opposed to Type I errors within this analysis.

For this reason, we reiterate the exploratory nature of the following analysis and suggest that significance be viewed within the context of the proposed limitations. Our emphasis remains firmly on drawing a comparison between manipulations of attention and manipulations of wakefulness, for the purpose of informing how these processes may be distinguished with future research.

Data Preparation

Pre-processing. Data was converted to SPM, baseline corrected using a 200ms window before the onset of the fifth tone (ie. 400-600ms), segmented from 650ms (end of the fifth tone) to 1288ms and then converted to image format (.NIfTI) for statistical analysis in sensory space (see Figure 2) (Friston et al., 1995; Kilner & Friston, 2010).

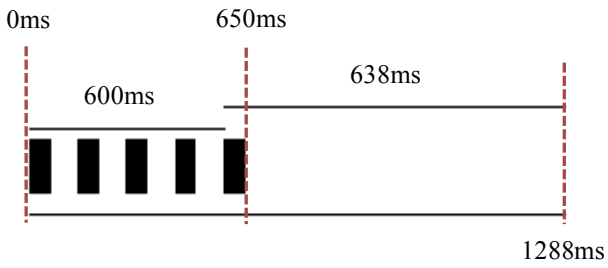

Figure 7.2. Quintuple design illustration and indication of segmentation for statistical analysis.

Data from both studies was gathered using a 128-electrode geodesic sensor net (EGI) referenced to vertex and then re-referenced to mastoid. For statistical analysis, crown electrodes were eliminated (36 channels eliminated, 93 remained) as they were not within our region of interest (for channel locations after elimination see Appendix 2), and data was statistically analysed from 650ms (the end of the fifth tone) to the end of the time series (1288ms).

ERPs were generated in MATLAB 2012b by averaging across quintuples for all participants in each of the four conditions (GDLD, GDLS, GSLD and GSLS [see Figure 4.5]). An ERP for the main effect of conscious state was generated by collapsing across each of the four conditions (GDLD, GDLS, GSLD and GSLS) separately for the respective states of consciousness (active, passive, sedated and recovered) (see left panel in Figure 7.4). ERPs are presented from 400-1288ms for ease of visual presentation.

Statistical analysis

First level analysis was conducted within each participant, across the levels of global and local. That is, all participants were tested in both levels of local (standard vs. deviant) and both levels of global (standard vs. deviant). This meant that there were four possible conditions for each participant: GDLD, GDLS, GSLD and GSLS.

Linear regression was used to estimate beta values and each participant provided four beta values (one per condition). Data from the sedation experiment is now accommodated in a between-subjects design, so that where previously each participant had eight possible conditions, four within sedation (SGDLD, SGDLS, SGSLD, SGSLS) and four within recovery (RGDLD, RGDLS, RGSLD, RGSLS), they now contribute four conditions to sedation and four conditions to recovery as though from two separate participants. For example, Participant 1 has a value for SGDLD and a value for RGDLD, they now become Participant 1 in sedation and Participant 1 in recovery respectively.

Betas from the first level analysis were taken to a group level analysis (second level analysis), where there were 16 possible conditions, that is, four for active, four for passive, four for sedation and four for recovery (the four in each case being GDLD, GDLS, GSLD and GSLS). Participants fell into only one of the four task contexts, that is, active, passive, sedated or recovered.

As there are 11 participants for each of the task contexts, the 16 possible conditions are each comprised of 11 beta values obtained at the first level. Linear regression was again used to estimate new group level beta values. The following findings are the results of the group level analysis.

Thresholds. The cluster-forming threshold (first level threshold) for this analysis was set to $p < .01$ (uncorrected). The cluster extent threshold (second level threshold) for this analysis was set at $p < .01$, which is more stringent than previous mixed ANOVA analyses, but in line with the significance threshold of previous simple effects analyses (Kilner, Kiebel & Friston, 2004; Kilner & Friston, 2010). Specific P-values and F-values for each cluster can be viewed in Appendix 1.7.

Results

Table 7.1 is a summary table to indicate significant effects within the subsequent analysis; this may serve as a good overview with respect to the pattern of effects that have been found within this Chapter.

Table 7.1. *Summary of effects for three-way ANOVA (task context x global x local). 'Y' indicates there is statistical significance 'N' indicates there is not statistical significance.*

	Local (L)	**Global (G)**	**GxL**	**Task context (TC)**	**TCxL**	**TCxG**	**TCxGxL**
Task context (active, passive, sedated or recovered)	Y	Y	Y	Y	Y	Y	Y

Y = cluster extent threshold of $p < .01$, cluster forming threshold of $p < .01$

Before presenting the results of statistical analysis, we will first highlight the two confounds, previously mentioned, that influence the statistical test when comparing datasets from the studies of attention and sedation. Both confounds will subsequently be addressed in relation to each effect presented.

Confound 1. We observe a de-synchronisation between the steady state auditory evoked potentials (SSAEPs) leading up to the onset of the fifth tone (ie. 600ms) between the study of attention and the study of sedation (see left panel in Figure 7.3), although this was not found to be consistent across all electrodes (see right panel in Figure 7.3). De-synchronisation between SSAEPs can contribute to statistical analysis given that it creates a disparity in the latency of effects between the two experiments. Therefore, any effect that considers the difference between responses from the attention study and responses from the sedation study could include what appears to be an artificial disparity in the latency of evoked responses (see dotted circle in left panel of Figure 7.3). Disparity of responses in this way may give rise to short windows (in time) of spurious statistical significance like that which we observe for the main effect of task context (see

left panel in Figure 7.3); this is because de-synchronisation appears to be short in time (around 50ms) and localised in space (around electrode Fz).

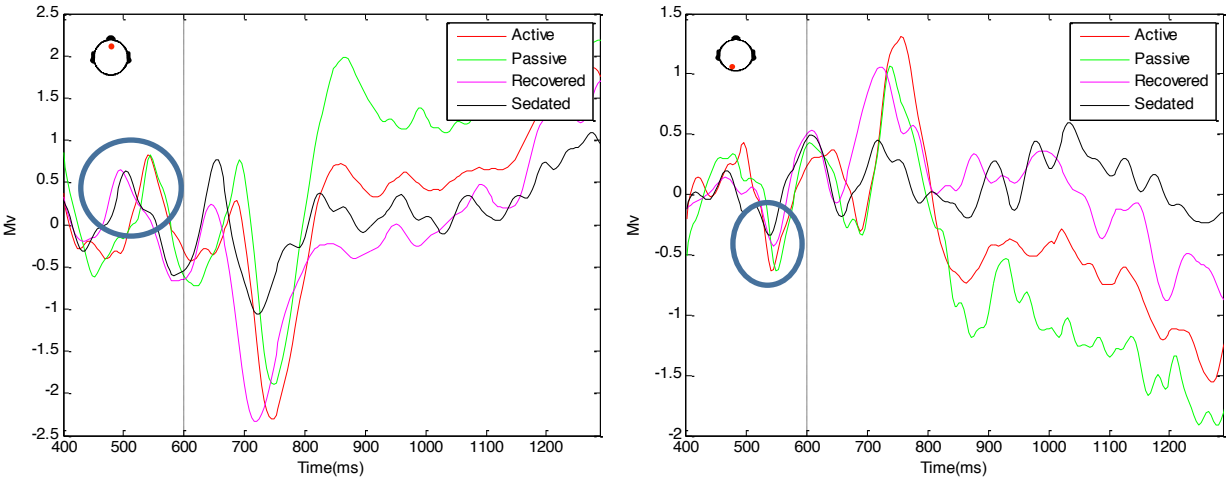

Figure 7.3. Grand average ERP for the main effect of task context at Fz. (left) and posterior electrode ch.46 (right). Black dashed line (600ms) indicates the onset of the final tone. The left panel illustrates the de-synchronisation of SSAEPs between attention and sedation studies (circled in blue), whilst the right panel illustrates the synchronisation of SSAEPs before the onset of the final tone (600ms).

Thus, the de-synchronisation may present a problem for statistical analysis when we consider effects that compare across the four levels of task context (active, passive, sedated and recovered), these are the main effect of task context, the task context x local interaction, the task context x global interaction and the task context x global x local interaction. The de-synchronisation of SSAEPs should not dramatically confound the statistical analysis with regard to the local, global and global x local interaction effects, as in this case it is the difference between standard and deviant conditions that is tested.

In particular, given that one is collapsing across the four levels of task context (active, passive, sedation and recovery) in this case, the de-synchronisation will impact equally upon the latency of responses for all conditions. This means that the onset of responses for local, global and global x local interaction effects may be somewhat compromised. Nevertheless, any impact on latency will exist for all conditions (deviant and standard) meaning that whilst latency may be compromised, differences in responses are still present. Therefore, broadly speaking, regions of statistical significance are still representing regions of significant difference between responses although there may be inaccuracies in the estimated latencies of these effects.

Critically, it is the case that confound 1 may confound statistical analysis when effects across the four levels of task context (active, passive, sedated and recovered) are

considered (ie. the main effect of task context, the task context x local interaction, the task context x global interaction and the task context x global x local interaction), given that there appears to be a difference in response latency between the two experiments (attention vs. sedation). Moreover, a de-synchronisation of around only 50ms suggests that broad regions of significance that are observed, such as the P300 which has a duration of approximately 200ms, are unlikely to be exclusively the result of confound 1.

Confound 2. The second confound we observe is positive drift within the ERPs from the study of sedation (see Figure 7.4). The drift is occurring around 900ms and will contribute to statistical analysis when effects are again considered across the four levels of task context; for example, the main effect of task context; this is because drift is impacting on responses within the sedation study but not responses from the attention study, therefore again an artificial difference may be created whereby responses from the sedation experiment appear to be bigger (in amplitude) than those of the attention experiment. A difference occurring in this way may confound the analysis by generating regions of statistical significance, which fall within areas of positive drift for the sedation experiment.

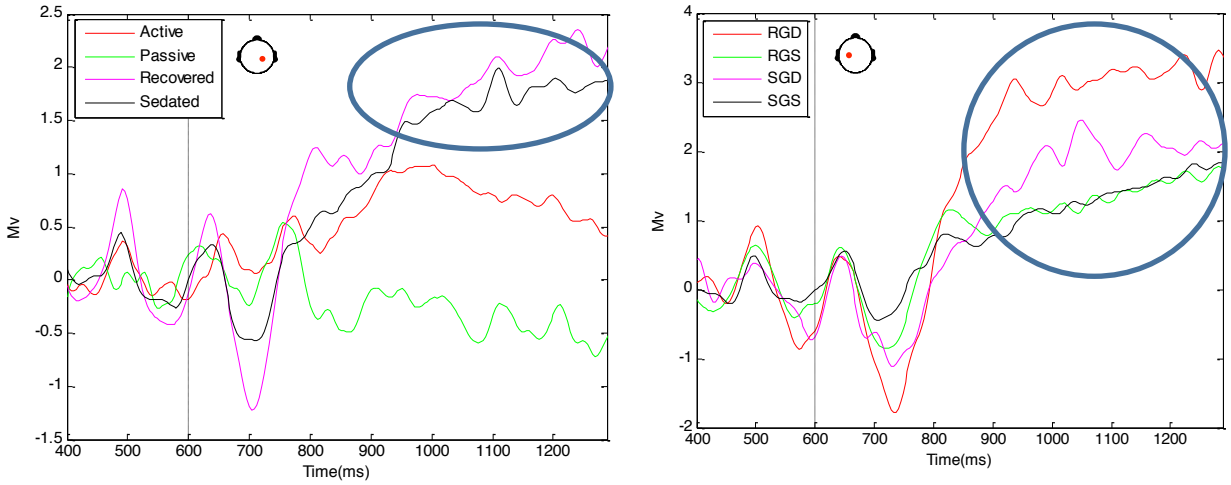

Figure 7.4. Grand average ERP for the main effect of task context at central electrode ch.66 (left) and the sedation x global interaction at left lateral electrode ch.29 (right); R: recovered, S: sedated. Black dashed line (600ms) indicates the onset of the final tone. These panels illustrate the positive drift occurring within the sedation experiment (circled in blue).

However, interaction effects which compare across the two experiments (ie. the task context x local, the task context x global and the task context x global x local interaction) should not be dramatically confounded by the presence of drift within the

sedation experiment. This is because the difference between levels of the global and local effects (deviant vs. standard) will be calculated for each experiment separately so that an interaction term can be generated; this means that it is *the difference* between standard and deviant responses respectively for the separate experiments that contributes to the statistical analysis and not a direct comparison across the four levels of task context (where responses with drift are compared to responses without drift). Therefore, given that drift is impacting on all conditions within the sedation experiment, differences between standard and deviant responses that are relative remain meaningful, providing an accurate comparison of responses between the attention and sedation experiments.

Furthermore, the presence of drift within the data for the sedation experiment (sedation and recovery) should not confound the analysis with regard to the local, global and global x local interaction effects, as once again it is the difference between standard and deviant conditions that is considered. In this case however, one collapses across the two experiments, meaning that drift is contributing to all conditions (levels of factors) equally[1]. The result of this is that when difference between standard and deviant responses is considered for local, global and global x local interaction effects, the impact of drift is subtracted out (as it is the same for all) when standard is taken from deviant, leaving only the difference between the two conditions.

Altogether, confound 2 may confound analysis when effects are considered across the four levels of task context (ie. the main effect of task context), because one is considering responses that include drift (sedation data) against responses that do not (attention data). However, confound 2 should not dramatically confound significant findings regarding local, global and interaction (task context x local, task context x global, global x local and task context x global x local) effects.

Equality of quintuples. Another issue to consider when conducting this analysis was the ratio of quintuple information contributed by each experiment. Specifically, the proportion of trials from each experiment is not different in deviant and in standard. If this were the case then the analysis would be confounded given that the size of contribution from each experiment (one of which, for example, contains drift) is changing between standard and deviant conditions. Below is an illustration of the aforementioned ratio:

[1] It should be noted that drift within the time-series may impact non-linearity, specifically the proximity to saturation. However, this issue is endemic to all EEG research and therefore is acknowledged here but not discussed in specific detail.

$$\frac{Quin(D_{S/R})}{Quin(D_{A/P})} = \frac{Quin(S_{S/R})}{Quin(S_{A/P})}$$

Where capital D denotes deviant trials, capital S denotes standard trials. S/R denotes sedated/recovered, and A/P denotes active/passive. As one can see, the ratio of quintuple information allows for greater overall contribution (across standard and deviant effects) from either the sedation or attention experiments. This would not confound statistical analysis as it would mean that a greater overall contribution is made to both standard and deviant conditions, maintaining the ratio of S/R – A/P quintuples. However, a disparity across experiments relating to the number of quintuples which contribute to standard and deviant conditions would confound statistical analysis given that one experiment would then contribute to one condition more than the other. The number of contributing quintuples was assessed across all participants included in the current analysis and no disparity across conditions was found, although the sedation experiment did have a higher overall contribution of quintuples than the attention experiment (across both deviant and standard conditions) (see Appendix 5 for exact values).

Three-way ANOVA (task context x global x local)

Hereafter we present the results of the three-way ANOVA, with consideration of each main effect and subsequently the interaction effects.

Task context. The effect of task context was considered to be a confounded effect given that both confound 1 and confound 2 are influencing the statistical test across the four levels of task context (active, passive, sedated and recovered). Consequently, we do not present the results here but within Appendix 6, and we draw no conclusions from this analysis.

Local effect. The local effect is observed as significant from 712-748ms around frontal electrode Fz. Subsequently, we observe significance from 796-892ms around central electrode Cz (see Figure 7.5).

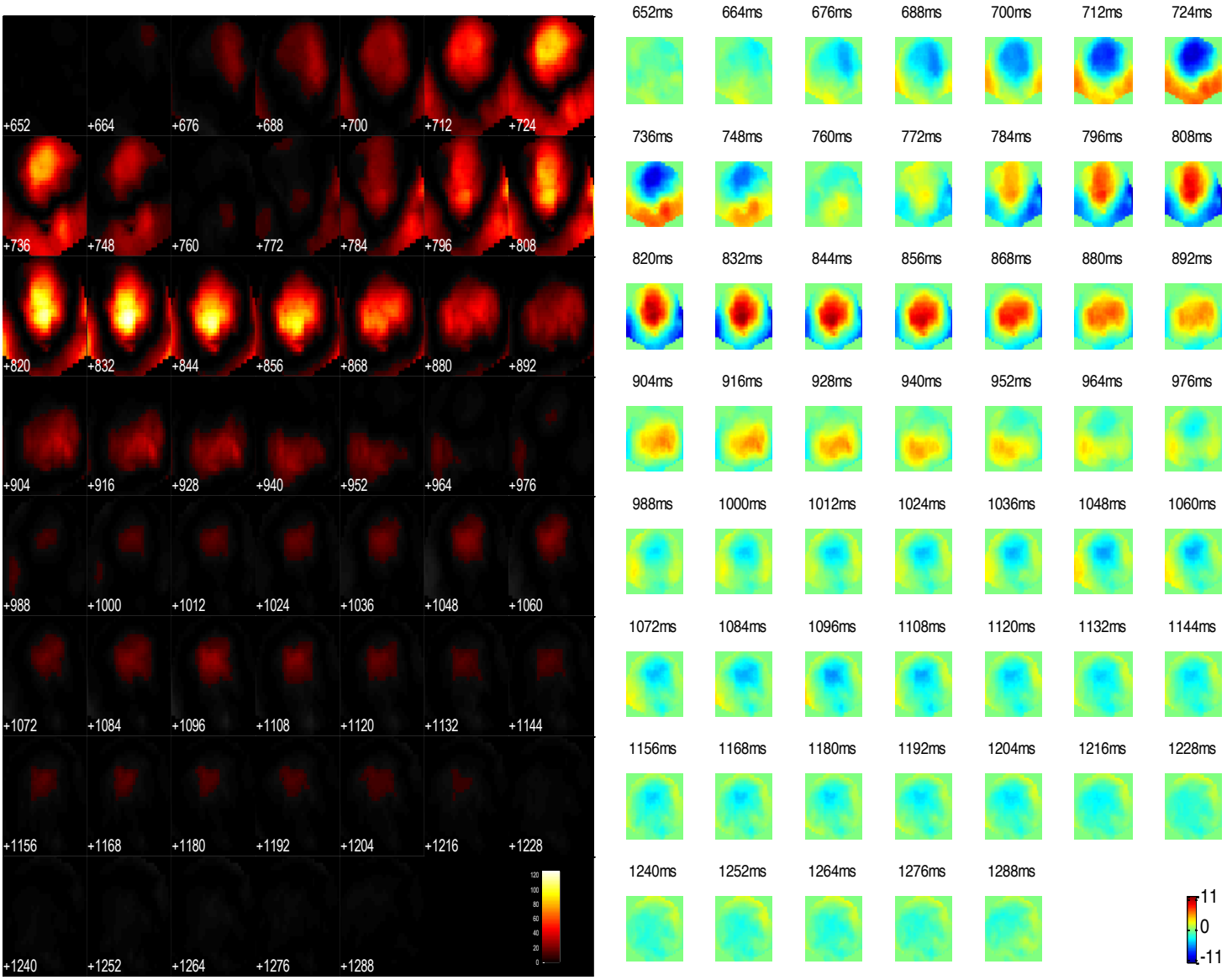

Figure 7.5. Thresholded F-maps ($p < .01$) to show regions of significance for the local effect on the scalp through time (left). Unthresholded T-maps to show the polarity of effect on the scalp through time (right). Front of the scalp is positioned at the top. Note that time within the left panel is presented below the corresponding row of scalpmaps, whilst time within the right panel is presented above the corresponding row of scalpmaps.

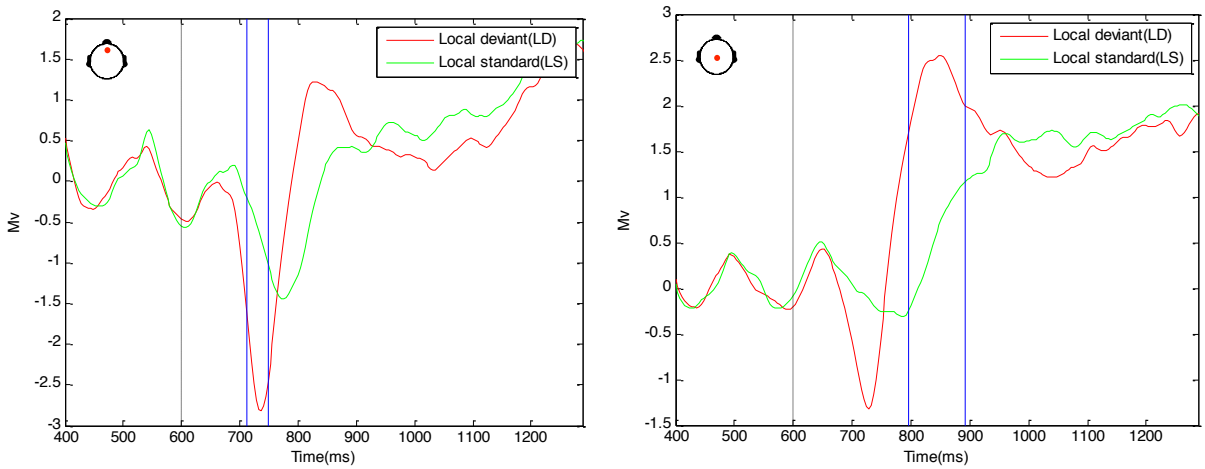

Figure 7.6. Grand average ERPs for the local effect at Fz (left) and Cz (right). Blue lines indicate the region of significance. Black dashed line (600ms) indicates the onset of the final tone.

The early region of significance in which we observe the local effect (712-748ms, left panel in Figure 7.6), is consistent with the existing literature and also previous Chapters, where it was found that local deviance elicits a faster response than locally standard quintuples for both attention and sedation studies (Bekinschtein et al., 2009; Wacongne et al., 2011, 2012; Chennu et al., 2013). Therefore, it is unlikely that confounds 1 and 2 are confounding statistical significance in this case. Local deviance appears to elicit a large mismatch response frontally whilst local standards elicit a slightly later negative response.

A second region of significance (796-892ms, right panel in Figure 7.6) shows a P3a response centrally (red line), which is not observed in the locally standard condition (green line) (for scalp topography see Figure 7.5). This finding is consistent with the previous findings of the active group, sedation and recovered, where we observed a central P3a response to local deviance when attention is directed towards the task. However, within the passive group a frontal (as opposed to central) P3a response was observed, which could be linked to the capture of attention (Freidman, Cycowicz & Gaeta, 2001). Thus, in this case it appears that the second region of significance is driven by responses from the active group, sedation and recovery and not by confounds 1 or 2.

Global effect. The global effect is significant from 892-1240ms around central posterior electrode Pz (see Figure 7.7).

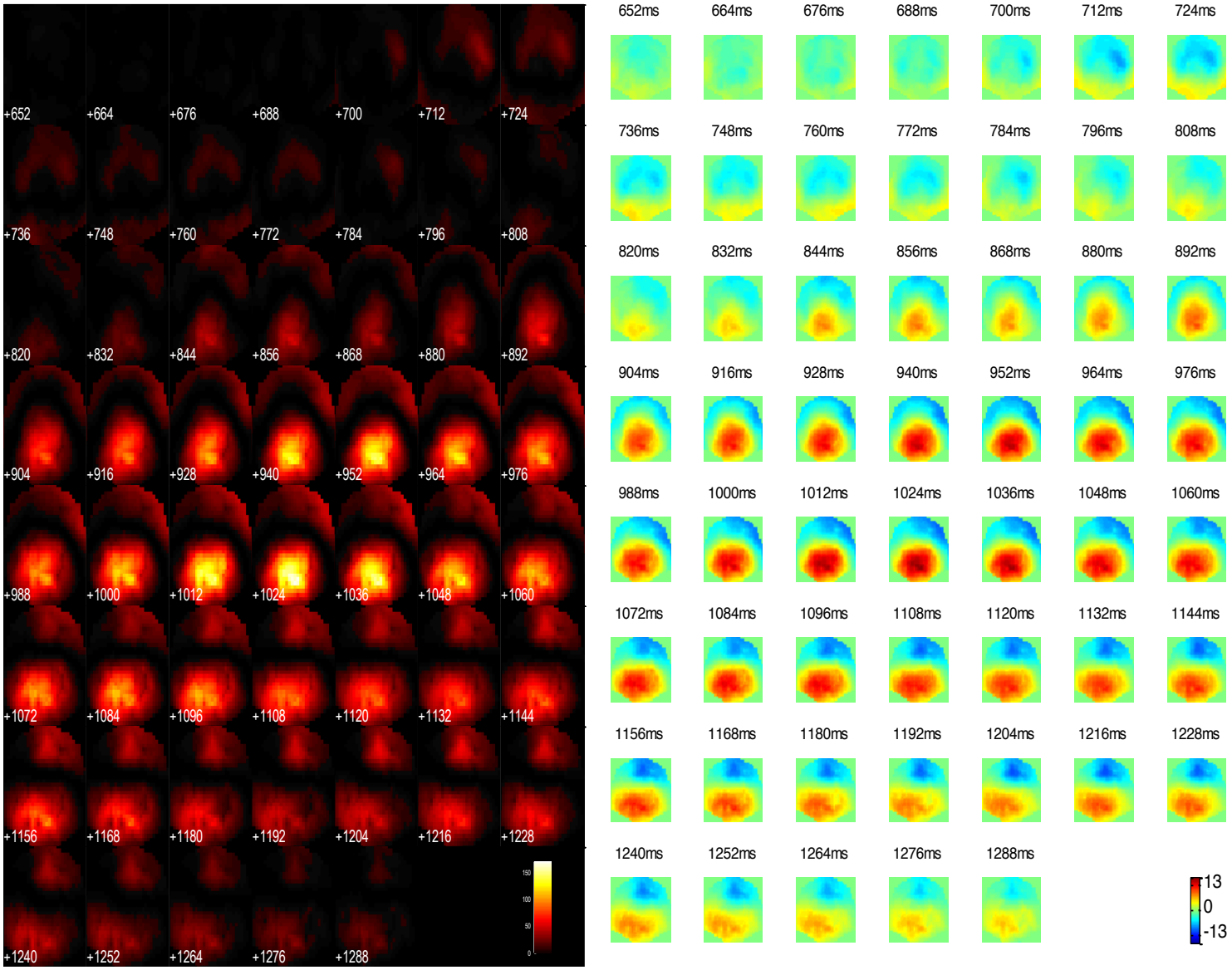

Figure 7.7. Thresholded F-maps ($p < .01$) to show regions of significance for the global effect [GD-GS] on the scalp through time (left). Unthresholded T-maps to show the polarity of effect on the scalp through time (right). Front of the scalp is positioned at the top. Note that time within the left panel is presented below the corresponding row of scalpmaps, whilst time within the right panel is presented above the corresponding row of scalpmaps.

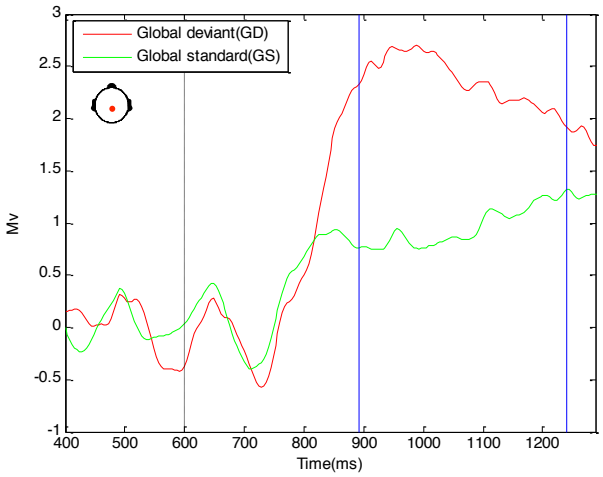

Figure 7.8. Grand average ERPs for the global effect at Pz. Blue lines indicate the region of significance. Black dashed line (600ms) indicates the onset of the final tone.

The observed global effect is consistent with that found in previous Chapters on attention and sedation. It is also consistent with the global effect reported in the existing literature (Bekinschtein et al., 2009; Wacongne et al., 2011; Chennu et al., 2013). As can be seen in Figure 7.8, global deviance is producing a P3b response (red line), whilst globally standard tones do not (green line) (for scalp topography see Figure 7.7). It appears that this effect is driven by global deviance consistently generating a P3b response centrally around 900ms across both attention and sedation studies, as opposed to being driven by confounds 1 or 2. It may be the case that confound 1 (de-synchronisation between studies) is increasing the latency of the difference somewhat, however if this were the case then both global deviance and globally standard conditions would be effected, rendering no impact on the size of the difference between responses (global deviant and global standard), only the latency of response onset. Nevertheless, we observe that the latency of the effect in this case is consistent with that reported in the existing literature (Bekinschtein et al., 2009; Wacongne et al., 2011; Chennu et al., 2013). Moreover, the duration of the region of significance in this case, being greater than 300ms, further supports the likelihood that the effect is not driven solely by the presence of confound 1.

Interactions

Task context x local. The task context x local interaction is significant from 688-760ms around Fz. Subsequently, the interaction is significant between 796-952ms around central electrode Cz (see Figure 7.9).

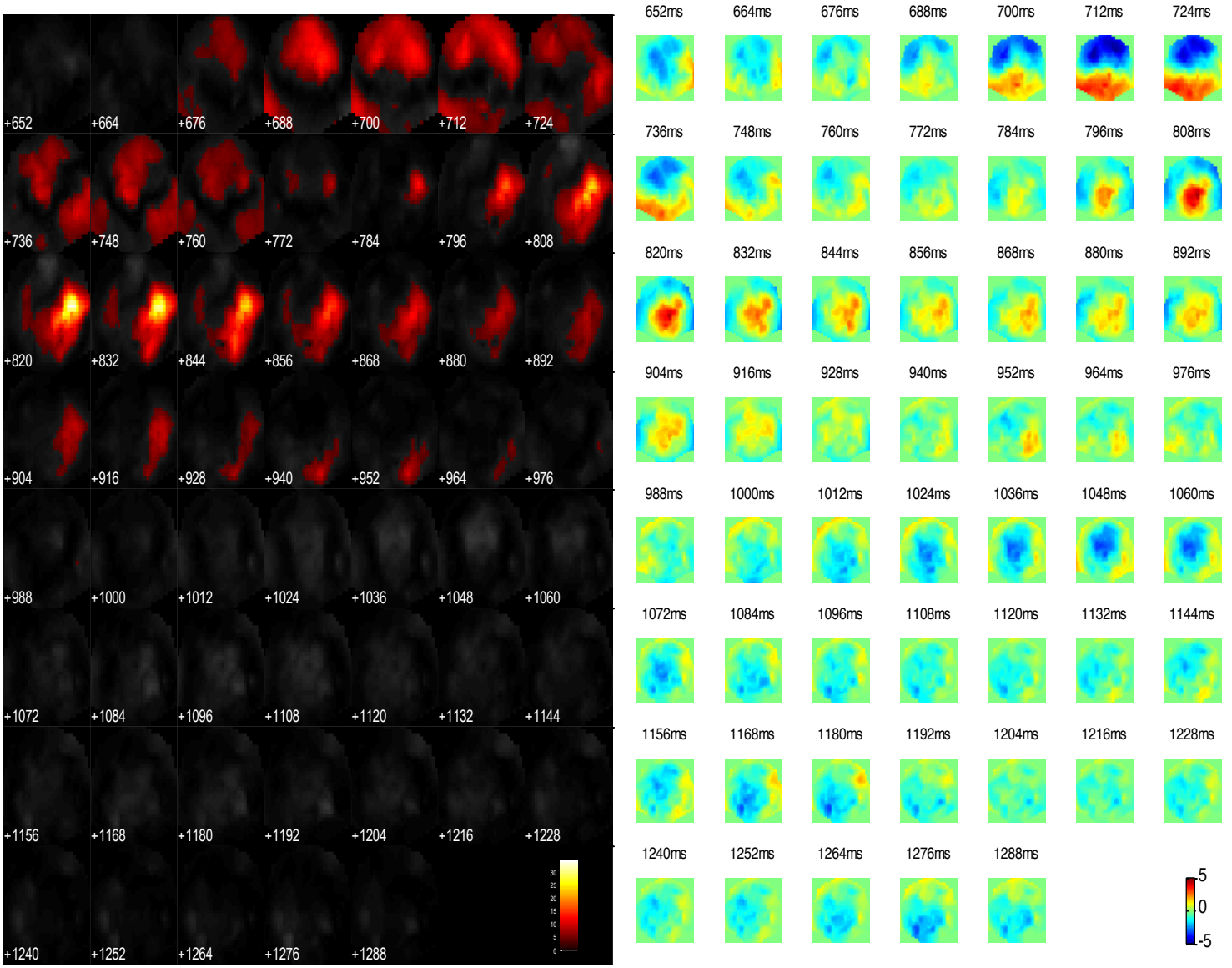

Figure 7.9. Thresholded F-maps ($p < .01$) to show regions of significance for the task context x local interaction on the scalp through time (left). Unthresholded T-maps to show the polarity of effect on the scalp through time (right). Front of the scalp is positioned at the top. Note that time within the left panel is presented below the corresponding row of scalpmaps, whilst time within the right panel is presented above the corresponding row of scalpmaps.

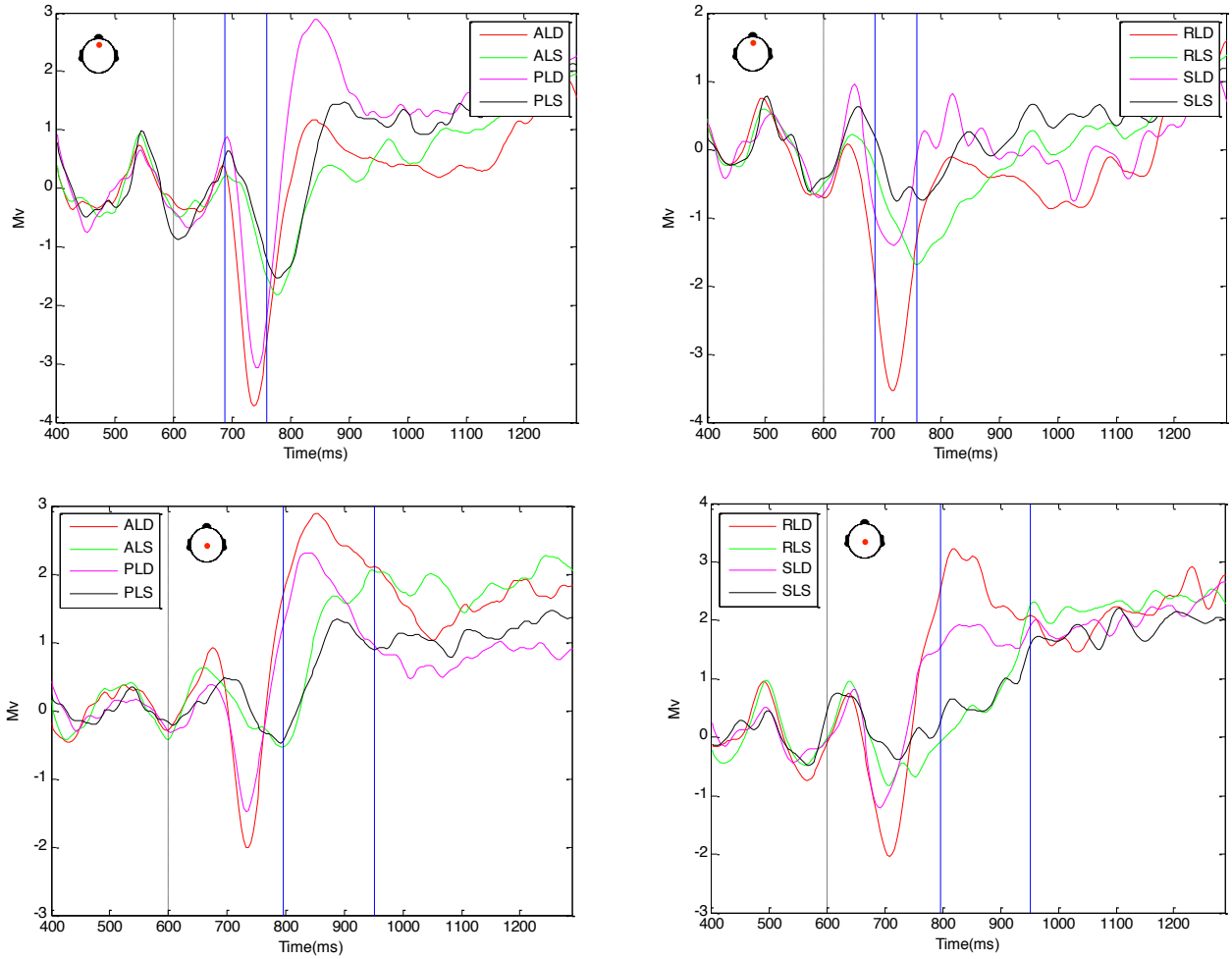

Figure 7.10. Grand average ERPs for the task context x local interaction at Fz (top left and top right) and Cz (bottom left and bottom right). Blue lines indicate the region of significance. Active and passive groups are presented on the left, whilst sedated and recovered groups are presented on the right (A: active, P: passive, R: recovered, S: sedated). Top row shows early window of significance (between 688-760ms) and bottom row shows later time region of significance (between 796-592ms). Black dashed line (600ms) indicates the onset of the final tone.

The presence of a task context x local interaction suggests that local responses are changing significantly across the four levels of task context (that is active, passive, sedated and recovered) (for scalp topography see Figure 7.9). Within an early window of significance (688-760ms), we observe that active, passive and recovered groups, all elicit a mismatch response to local deviance, whilst under sedation the response is attenuated (see top left and right panels in Figure 7.10). However, given that confound 1 is increasing the latency of effects for the active and passive groups, and the time region of significance is narrow in this case (approximately 100ms), it is possible that the significance we observe here is driven by disparity in response latency between attention and sedation studies (ie. confound 1), rather than a pure difference between the size of

responses. Although, the fact that the window of significance just about straddles the entire MMN for all four levels of task context (ie. active, passive, sedated and recovered) suggests that confound 1 may not be solely responsible for the effect.

Interestingly, sedation appears to not only reduce the size of the locally deviant responses but also locally standard responses (just after 700ms in the top right panel in Figure 7.10), possibly indicating that sedation induces smaller responses overall at the local level compared to when recovered. Comparatively, the difference between responses to local standard between active and passive groups is far less pronounced (see just before 800ms in top left panel in Figure 7.10), supporting the possibility that a reduction in the static state of consciousness (ie. sedation) leads to a global reduction in response size at the local level.

Moreover, responses to local deviance are occurring earlier than responses to locally standard tones (see top panels in Figure 7.10), presumably owing to the unexpected nature of the deviant stimuli, and this is consistent across both attention and sedation studies, whilst also being consistent with the findings within the existing literature (Chennu et al., 2013; Wacongne et al. 2011; Bekinschtein et al., 2009).

Furthermore, a second region of significance appears centrally (see bottom left and right panels in Figure 7.10) around 796-952ms, where there is a positive peak for active, passive and recovered local deviance, whilst the response is again attenuated under sedation (see red and magenta lines in bottom panels of Figure 7.10). It does appear however, that confound 1 (de-synchronisation between experiments) may be increasing the latency of this peak for active and passive groups in comparison to sedation and recovery. However, the fact that the region of significance in this instance is fairly broad (ie. greater than 100ms), speaks against the likelihood of confound 1 being entirely responsible for the effect.

What is more, confound 2 (drift within the sedation study data) appears to be influencing locally standard conditions for sedation and recovery (see green and black lines on bottom right panel in Figure 7.10). However, because confound 2 is impacting on both sedation and recovery alike, the impact of drift is subtracted out when one takes the difference between locally deviant and locally standard responses. It is the size of this difference that one can view as being compared across the four levels of task context.

Findings here highlight how sedation appears to attenuate responses to local deviance and local standard despite attention being directed towards the task. In contrast, the absence of active attention attenuates the local effect to a much smaller degree, and enhances a frontal positive rebound to local deviance (see top left panel in Figure 7.10). Once again, it appears that locally deviant stimuli provoke a faster response than locally standard stimuli, and this is consistent across the four levels of task context (active, passive, sedation and recovery). It should be noted that ERPs from sedation and recovery presented here may appear somewhat different to the same effects presented within the previous Chapter, as 7 participants of the original 18 were discarded for the present analysis (as discussed at the beginning of this Chapter).

Task context x global. The task context x global interaction is significant between 856-1288ms around posterior electrode Pz (see Figure 7.11).

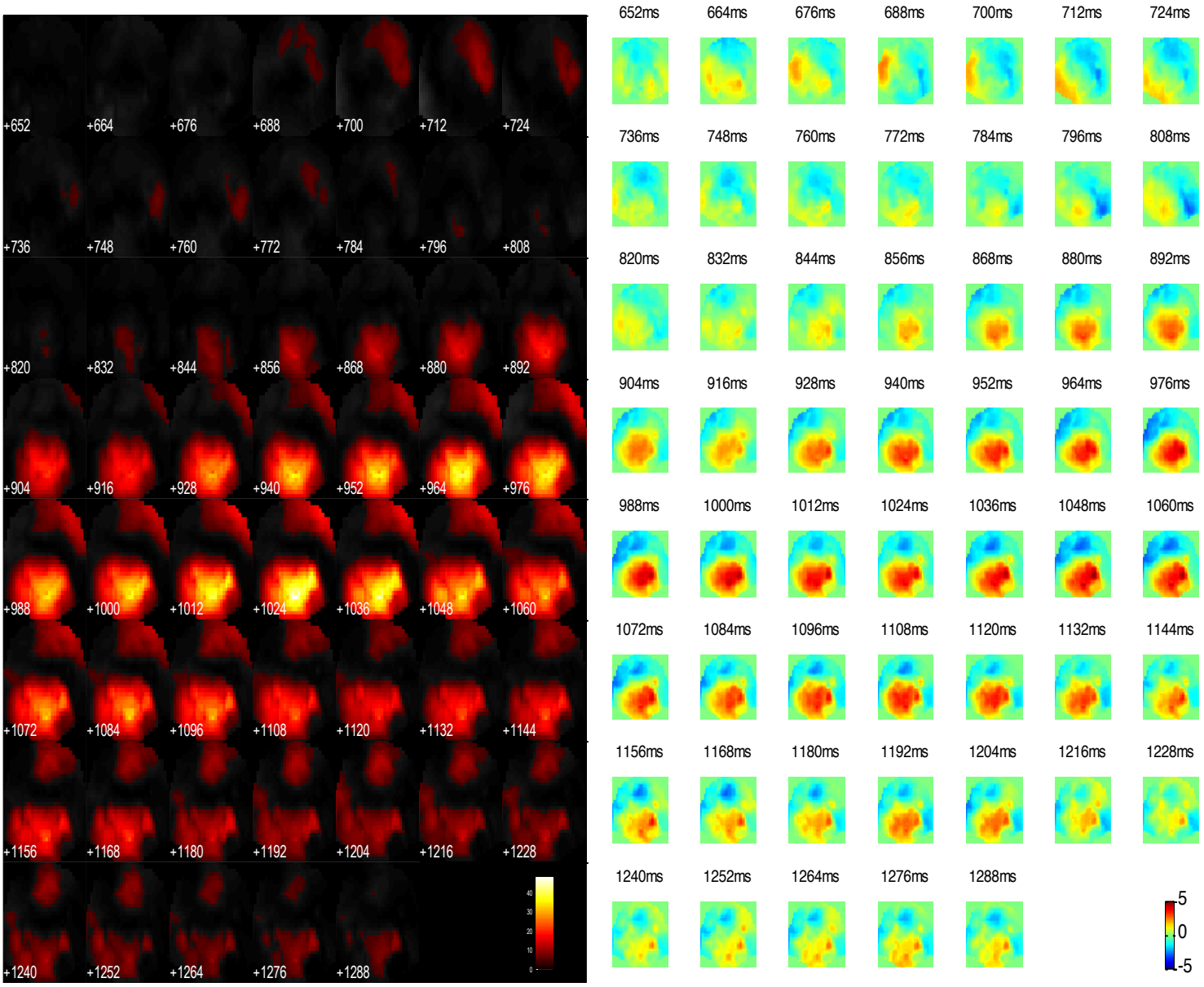

Figure 7.11. Thresholded F-maps ($p < .01$) to show regions of significance for the task context x global interaction on the scalp through time (left). Unthresholded T-maps to show the polarity of effect on the scalp through time (right). Front of the scalp is positioned at the top. Note that time within the left panel is presented below the corresponding row of scalpmaps, whilst time within the right panel is presented above the corresponding row of scalpmaps.

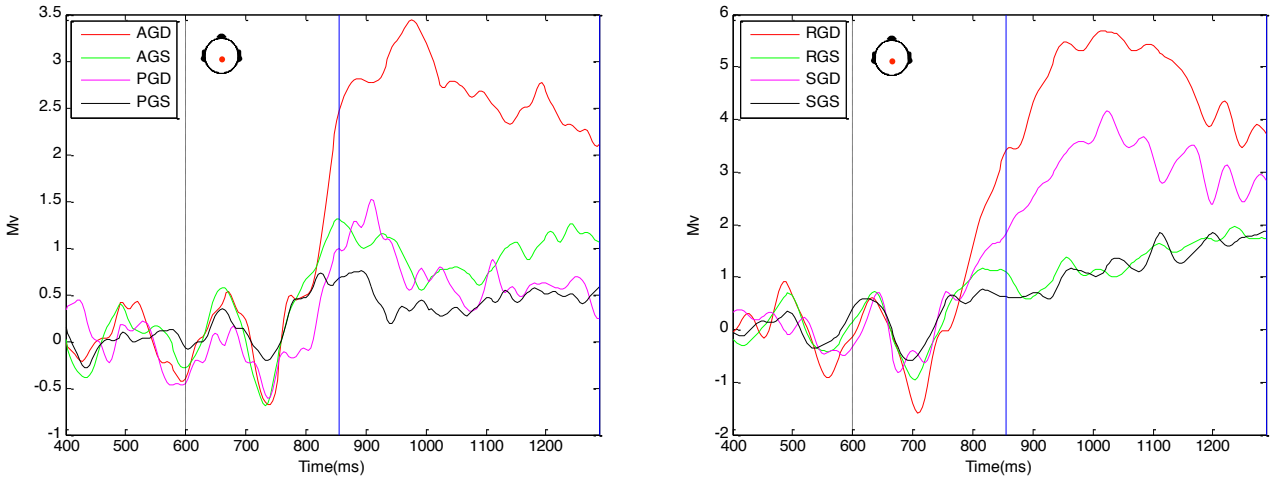

Figure 7.12. Grand average ERPs for the task context x global interaction at Pz (left and right). Blue lines indicate the region of significance (A: active, P: passive, R: recovered, S: sedated). Black dashed line (600ms) indicates the onset of the final tone.

An interaction between task context and the global effect suggests that the global effect is changing across the four levels of task context (active, passive, sedated and recovered). A P3b response to global deviance appears to only be present when attention is directed towards the task (ie. for the active group, sedation and recovery) (see both panels in Figure 7.12). Interestingly, there is no apparent P3b response to global deviance for the passive group (see left panel in Figure 7.12) (for scalp topography see Figure 7.11). It may be that confound 1 is increasing the latency of the P3b response for the active group, however the region of significance in this case is broad in time (856-1288ms) indicating that the effect is robust across time and space (the scalp) and therefore not accounted for solely by confound 1.

Furthermore, there does appear to be some drift within globally standard responses of sedation and recovery (see green and black lines on right panel in Figure 7.12). Thus, confound 2 may be impacting on the size of globally deviant and globally standard responses. However, as confound 2 is impacting on both sedation and recovery alike, the impact of drift is subtracted out when one takes the difference between globally deviant and globally standard responses. One can interpret that it is the size of this difference which is compared across the four levels of task context.

Global x local. The global x local interaction is significant from 832-952ms around central posterior electrode Pz. The global x local interaction is again significant from 1048-1288ms around Cz (see Figure 7.13).

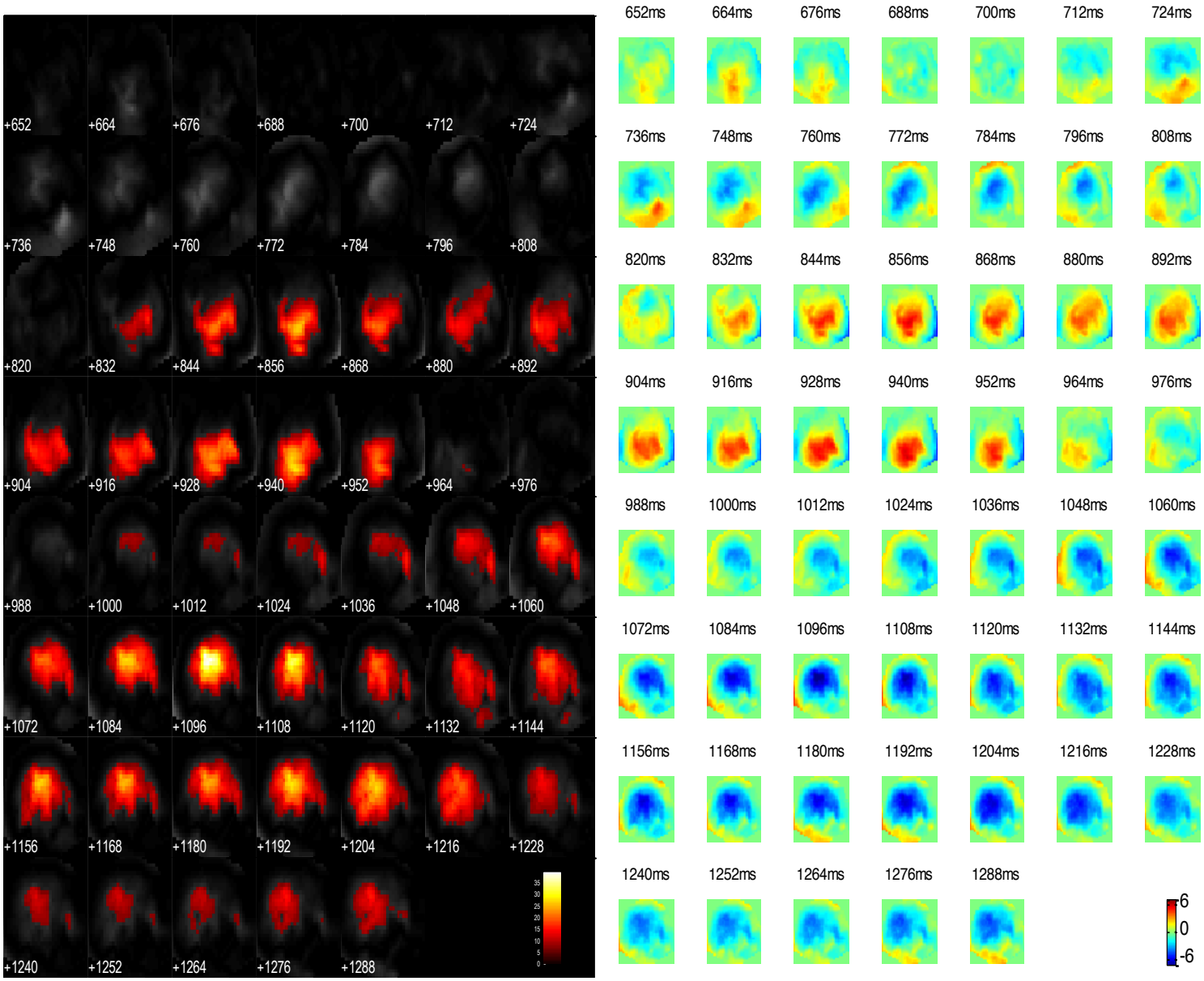

Figure 7.13. . Thresholded F-maps ($p < .01$) to show regions of significance for the global x local interaction on the scalp through time (left). Unthresholded T-maps to show the polarity of effect on the scalp through time (right). Front of the scalp is positioned at the top. Note that time within the left panel is presented below the corresponding row of scalpmaps, whilst time within the right panel is presented above the corresponding row of scalpmaps.

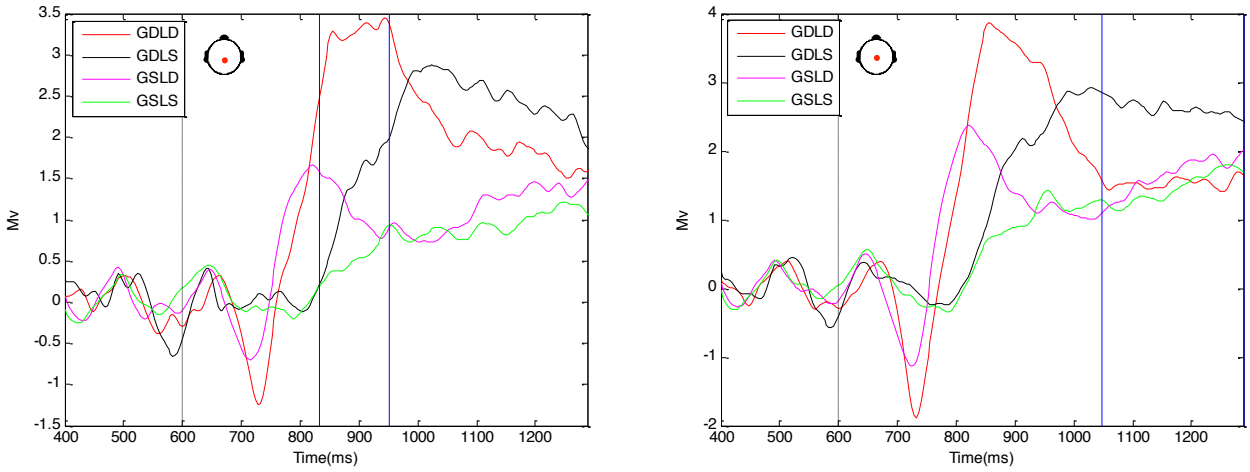

Figure 7.14. Grand average ERPs for the global x local interaction at Pz (left) and Cz (right).Blue lines indicate the region of significance. Black dashed line (600ms) indicates the onset of the final tone.

The presence of a global x local interaction indicates that the global and local effects are not independent of one another and that the levels of one effect may depend upon the levels of the other. The early region of significance (between 832-952ms) shows that a global deviant which is also a local deviant (GDLD) (see red line in left panel of Figure 7.14) is producing a larger and earlier P3b response than that of a global deviant which is locally standard (GDLS) (black line); this difference is unlike the difference between global standard that is locally deviant (GSLD - magenta line) and global standard that is locally standard (GSLS - green line), resulting in an interaction located centro-posteriorly on the scalp.

Furthermore, within the second region of significance (between 1048-1288ms) the response to GDLD (red line) is coming to an end, whilst the response to GDLS is ongoing (see right panel in Figure 7.14). Meanwhile, the difference in responses to GSLD (magenta line) and GSLS (green line) becomes even smaller, therefore it is this disparity of differences between globally deviant conditions (GDLD and GDLS) and globally standard conditions (GSLD and GSLS) that generates an interaction within this region (for scalp topography see Figure 7.13).

With respect to arising confounds, despite the possibility that confound 1 may impact on the latency of response onset, it will be impacting upon all four conditions (GDLD, GDLS, GSLD and GSLS) in this case given that one has collapsed across the four levels of task context (active, passive, sedation and recovery). Therefore, the latency of all

effects here may be somewhat compromised by the presence of confound 1; however responses do remain relative to one another thus, significant findings should be reliable relative to confound 1. In addition, the duration of significance within both early and late time windows is suggestive that de-synchronisation is unlikely to be the sole reason for this effect. Moreover, there does appear to be a small amount of positive drift around 1000ms, thus confound 2 may be impacting on response size. However, given that one is collapsing across the four levels of task context, confound 2 will again be influencing all four conditions (GDLD, GDLS, GSLD, GSLS), because the sedation experiment (within which the drift exists) is present within each. Thus, it is the case that drift within responses will be subtracted out when the interaction term is calculated as follows:

$$I = (GDLD - GDLS) - (GSLD - GSLS)$$

Where the four conditions (GDLD, GDLS, GSLD and GSLS) contain trials from all four levels of task context (active, passive, sedation and recover). Therefore, with respect to the interaction between global and local effects, confound 1 may impact upon the latency of response onset, yet confound 2 is subtracted out within the statistical analysis, meaning that differences between conditions (GDLD, GDLS, GSLD and GSLS) are preserved.

Task context x global x local. The task context x global x local interaction is initially significant from 820-928ms around right lateral electrode ch.78 (see Appendix 7). There is also subsequent significance from 1012-1288ms around central electrode Cz (see Figure 7.15).

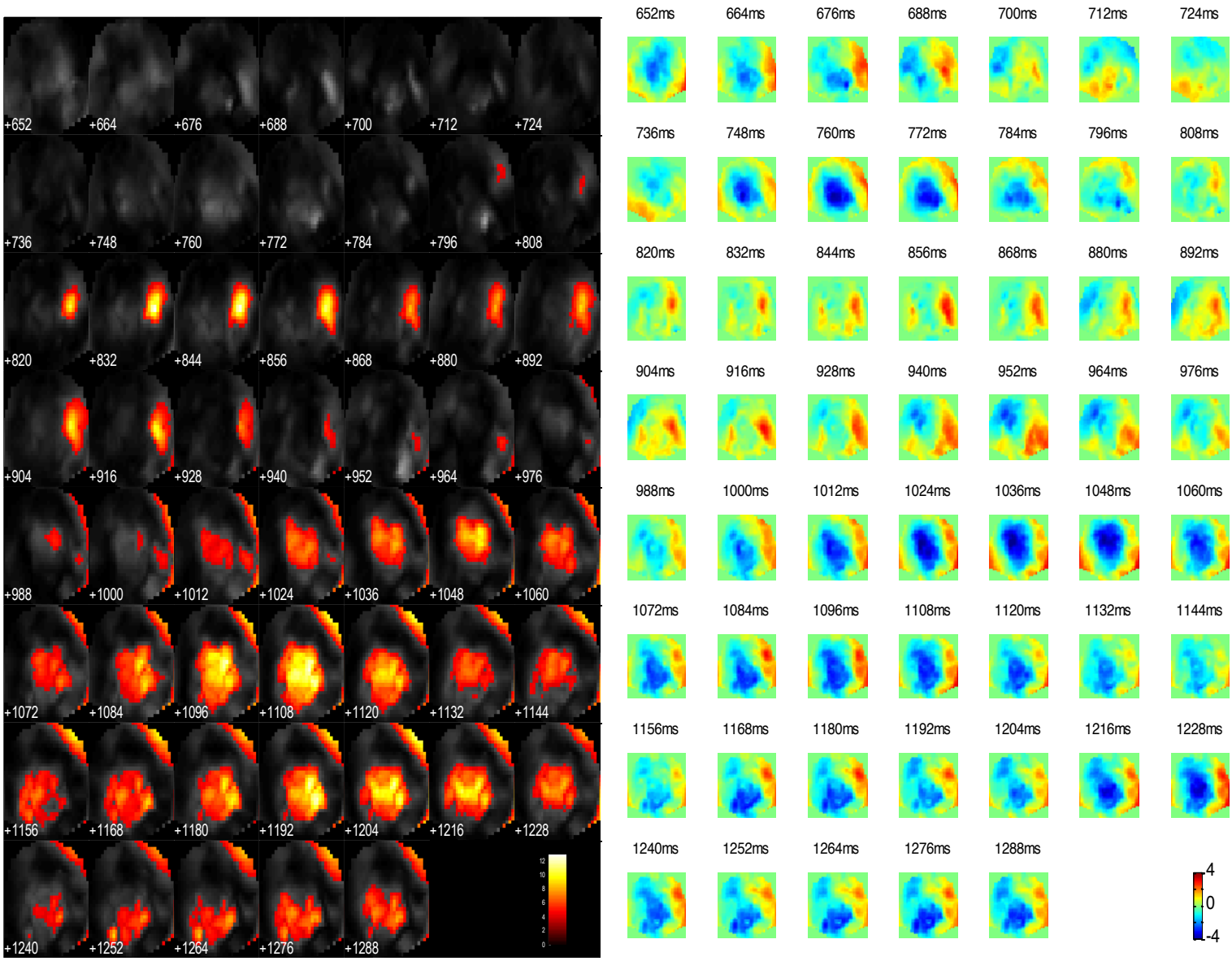

Figure 7.15. Thresholded F-maps ($p < .01$) to show regions of significance for the task context x global x local interaction on the scalp through time (left). Unthresholded T-maps to show the polarity of effect on the scalp through time (right). Front of the scalp is positioned at the top. Note that time within the left panel is presented below the corresponding row of scalpmaps, whilst time within the right panel is presented above the corresponding row of scalpmaps.

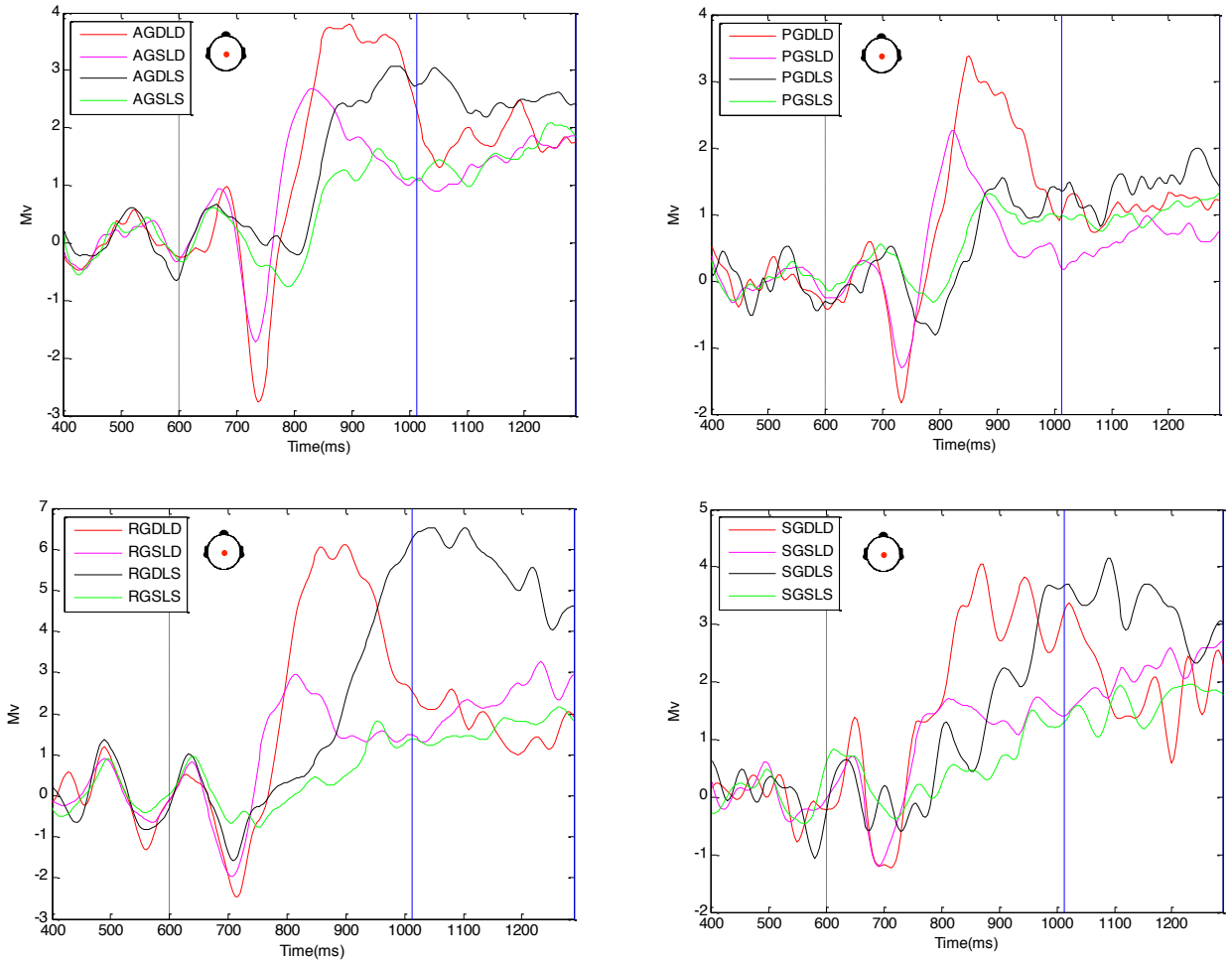

Figure 7.16. Grand average ERPs for the task context x global x local interaction at Cz for all four conditions of task context (active: A, passive: B, recovered: R, sedated: S). Blue lines indicate the region of significance. Black dashed line (600ms) indicates the onset of the final tone. Do note that above different panels have different scales.

The presence of an interaction between task context x global x local suggests that the global x local interaction is changing across the four levels of task context (active, passive, sedation and recovery). Within an early time region of significance (820-928ms around electrode ch.78) there appears to be a positive (right) lateralised effect, which we mention here but report within Appendix 7 as it appears to be a fringe effect. Within a later time region of significance (between 1012-1288ms), it can be seen that the response to GDLD (red lines) is ending for recovery and sedation, whilst the response to GDLS (black lines) is increasing and then ongoing (see bottom panels in Figure 7.16). For the active group, both GDLD (red line) and GDLS (black line) are producing bigger responses compared to GSLD (magenta line) and GSLS (green line) (see top left panel in Figure 7.16). For the passive group it appears that GDLS (black line) does not elicit a P3b response, yet the response to GDLD (red line) is over within the window of

significance, therefore, there is no tangible difference between responses to GDLD, GDLS, GSLD and GSLS within this region for the passive group (see top right panel in Figure 7.16). Altogether, there appears to be a trend towards similar effects within the active, recovered and sedated groups, whilst the absence of a P3b response to GDLS reveals a marked difference in response for the passive group within this region (see top right panel in Figure 7.16) (for scalp topography see Figure 7.15).

The time window of significance for the task context x global x local is greater than 200ms, which suggests that it is unlikely to be driven by confound 1. This is because the effect is sustained through time (and space) for a considerably longer period than the total magnitude of de-synchronisation (which is around 50ms), therefore it is highly unlikely that confound 1 is producing a region of statistical significance through a disparity in latency across the two experiments. Furthermore, the interaction between global and local effects is being examined across the four levels of task context in this case, therefore a question is raised regarding the impact of confound 2 on the presence of statistical significance. With consideration we deduce that confound 2 (positive drift within the responses of the sedation experiment) should not impact upon the presence of statistical significance within the task context x global x local interaction because existing drift is once again subtracted out when the interaction term is calculated as we discuss now.

Firstly, the interaction is calculated for each level of task context (active, passive, sedated and recovered) respectively; where confound 2 will be subtracted out for sedation and recovery as it is present within all four conditions (GDLD, GDLS, GSLD and GSLS):

$$I_a = (LDGD - LSGD) - (LSGD - LSGS)$$

$$I_p = (LDGD - LSGD) - (LSGD - LSGS)$$

$$I_s = (LDGD - LSGD) - (LSGD - LSGS)$$

$$I_r = (LDGD - LSGD) - (LSGD - LSGS)$$

Secondly, the average interaction for the four levels of task context is calculated as follows:

$$\bar{I} = \frac{(I_a + I_p + I_s + I_r)}{4}$$

Finally, the interaction term for the task context x global x local interaction is calculated by substracting the interaction term for each level of task context (active, passive, sedated and recovered) from the value of the mean interaction across the four ($\bar{I}$):

$$I = (I_a - \bar{I})^2 + (I_p - \bar{I})^2 + (I_s - \bar{I})^2 + (I_r - \bar{I})^2$$

Thus, with respect to the interaction between task context x global x local, confound 1 is not substantially confounding results given that the region of signficance is broad and consistent across time and space (on the scalp). What is more, confound 2 is subtracted out within the calculation of the interaction term, which means that differences between conditions (GDLD, GDLS, GSLD and GSLS) should be preserved without the influence of positive drift (ie. confound 2).

Summary (three-way ANOVA)

The main effect of task context was considered to be a confounded effect given that there appears to be de-synchronisation between the SSAEPs for the attention and sedation experiments and because the sedation experiment contains drift (see Figure 7.3 and Appendix 6).

Both global and local effects were observed in accordance with those presented in previous Chapters. Moreover, global and local effects are consistent with findings within the existing literature, suggesting that confounds 1 and 2 were not significantly confounding analysis in this case (Bekinschtein et al., 2009; Chennu et al., 2013; Wacongne et al., 2011; Pegado et al., 2010). Instances of global and local deviance evoked larger responses than instances of global and local standard stimuli (see Figures 7.6 and 7.8). Furthermore, global and local effects are changing significantly across the four levels of task context (active, passive, sedation and recovery). With respect to variations in the local effect, active, passive and recovered groups elicit a large mismatch response (active being the largest), around 700ms to local deviance, whilst the same response for the sedated group is greatly reduced (see top panels in Figure 7.10). This region was found to be significant although confound 1 may be contributing to latency differences between attention and sedation studies.

Within a later central region of significance (between 796-952ms), a central P3a response is observed for local deviance across all four levels of task context, whilst there is a much smaller or non-existent response to locally standard quintuples (see bottom panels in Figure 7.10).

With respect to variations in the global effect, a P3b response to global deviance is present for the active, recovered and sedated groups; meanwhile there is no P3b response to global deviance within the passive group (see Figure 7.12). Globally standard quintuples did not generate a P3b response, as they do not violate assumptions of global regularity.

The global x local interaction in this case falls within the region of the global effect (832-952ms); that is, global deviance that is also locally deviant (GDLD) elicits a P3b response occurring earlier in time, with shorter duration (approximately 100ms) than the P3b response to global deviance which is locally standard (GDLS) (see left panel in

Figure 7.14); appearing to peak later in time (around 1000ms) and continuing for a longer duration (approximately 300ms). The early and short P3b response to GDLD considered against the later and longer P3b response to GDLS creates a difference that when compared against the difference between responses to globally standard conditions (GSLD and GSLS), generates a significant interaction between global and local effects (see Figure 7.13).

Within a late time region (1048-1288ms) one can see that the P3b response to GDLD is over whilst the P3b response to GDLS continues, which generates a disparity of differences that once again when compared against the (effectively zero) difference between globally standard conditions (GSLD and GSLS), evokes an interaction between global and local effects (see right panel in Figure 7.14).

Finally, the interaction between global and local effects is changing across the four levels of task context (active, passive, sedation and recovery). Within a late time region (1012-1288ms), where the P3b response to GDLD for sedation and recovery is ending, the response to GDLS is increasing and on-going (see bottom left and right panels in Figure 7.16). Concurrently, there is a trend towards a similar difference for the active group, however we have not found this to be significant within the current dataset (see top left panel in Figure 7.16 and also Figures 5.5 and 5.6). Importantly, there appears to be no marked difference in responses between GDLD and GDLS for the passive group at this point (see top right panel in Figure 7.16).

Discussion

Within this Chapter, we have presented an exploratory analysis directly comparing manipulations of attention (active vs. passive) with manipulations of wakefulness (sedation vs. recovery) in respect of responses towards the global-local auditory task. In order to directly compare the findings of the previous three Chapters, we combined the datasets of attention and sedation into a comprehensive factorial analysis providing four levels of task context (active, passive, sedated and recovered).

Crucially, we are aware of a number of limitations associated with the analysis presented in this Chapter, particularly issues surrounding inflation of the Type II error rate and the

selection of participants at random from the sedation experiment. In addition, we highlight two confounds within the data (de-synchronisation of SSAEPs and positive drift) which compromise the accuracy of the statistical analysis. However, we have discussed each confound within the context of each effect and presented justification for the results that we discuss within this Chapter. Moreover, we emphasise once again the necessity to view the current analysis as an exploratory investigation, revealing patterns of interest that may inform future research on the global-local task. We certainly acknowledge the statistical limitations of the current work but are optimistic that comparative trends within the data are valuable and so focus our discussion predominantly upon these.

Initially, it was proposed that the active group and recovery may be comparable, as in both cases attention is directed towards the task in the absence of sedation. Moreover, those in the sedated group also had their attention directed towards the task but were subject to reduced wakefulness (induced by sedation); this may suggest that findings under sedation reflect a reduction in wakefulness rather than a lack of attentional directive. By way of contrast, those within the passive group did not have their attention directed towards the task, meaning that findings in this case are likely to reflect the absence of directed attention as opposed to reduced wakefulness.

Interestingly, it was found that responses to global and local violations in auditory regularity change across the four levels of task context (active, passive, recovered and sedated), that is the mismatch response to local deviance is enhanced by direct attention whilst reduced when attention is passive. It may be the case that direct attention enhances precision to increase the size of the mismatch response when local deviance is present (Auksztulewicz & Friston, 2015). Furthermore, the level of precision afforded by direct attention appears to be attenuated under sedation, as those within the sedated group elicit the smallest mismatch response despite having their attention directed towards the task; this may suggest that those who occupy low states of awareness have a limited capacity for attentional engagement. Furthermore and interestingly, early negative responses to locally standard quintuples were also reduced under sedation, suggesting that a reduction in wakefulness may lead to an overall reduction in response size at the local level.

Moreover, a subsequent P3a response manifests centrally for those whose attention is directed towards the task, whilst the P3a response manifests frontally for those who are mind wandering (passive); this implies that local deviance may be engaging cognitive processes, which have been associated with the distribution of attentional resources (Freidman, Cycowicz & Gaeta, 2001). Thus, the presence of local deviance may capture attention from a wandering state when one is passively listening to the task.

With regard to the global effect, no apparent response to global deviance is observed when attention is wandering (ie. passive), as there is a P3b response to GDLD but no apparent P3b response for GDLS within the passive group. This appears to be the result of averaging the two responses (GDLD and GDLS), creating a small response, which does not differ significantly from responses to globally standard quintuples (which do not violate assumptions of global regularity). The absence of a response to global deviance when attention is passive suggests that direct attention is necessary for the detection of global deviance as a locally standard quintuple (GDLS). In contrast, when attention is directed towards the task (as in active, recovered and sedated groups), the response to global deviance is large, whatever the local regularity, and is only reduced (although it remains present) when under sedation (ie. wakefulness is reduced); this suggests that reducing wakefulness may also disrupt the level of precision afforded by direct attention at a global level of auditory regularity (ie. the auditory context of the block).

Interestingly, the interaction between global and local effects is occurring within the region of the global effect, which suggests that the local auditory context of a quintuple may shape responses in relation to the global expectancy of the block. One can interpret this as indicative of cross-layer modulation with respect to expectancy within a hierarchical predictive framework whereby the local context in which global deviance is presented (GDLD vs. GDLS) impacts upon the shape of the P3b response (Friston, 2010; Haenschel et al., 2005; Chennu et al. 2013). In other words, high prediction error at multiple levels of the hierarchy may evoke quicker and shorter global responses compared with violation at only one level. Specifically, global deviance that is also locally deviant (GDLD) appears to accelerate the P3b response in time and shorten it in duration, given that it is both a violation of global and local auditory regularity. On the other hand, the P3b response to global deviance that is locally standard (GDLS) is later in time and longer in duration, given that there is a violation of global context but not

local regularity. As suggested in the previous Chapter, the delayed onset of a P3b response to GDLS may represent the time it takes for prediction error to reach the global level and for global predictions to be updated. Importantly, the disparity in responses to global deviance sits in contrast to the difference in responses between globally standard conditions (GSLD and GSLS) and thus global and local effects cannot be considered as independent.

Importantly, when direct attention is absent (ie. passive), global deviance marked by a locally standard quintuple (GDLS) does not elicit a P3b response, which suggests that participants may miss instances of global deviance that are marked by locally standard quintuples. Alternatively, it may be the case that participants within the passive group are engaging in spontaneous activity that distracts them from processing the task. Equally, it may be the case that global deviance is masked by local regularity because attention is not directed towards the task. In accordance with existing findings, it appears that the maintenance and integration of global predictive contexts is contingent upon attentional engagement with the task (Chennu et al., 2013). Accordingly, the absence of a P3b response to GDLS contributes to an interaction between global and local effects that could be consider a marker of passive attention.

Alternatively, when attention is directed towards the task, a P3b response is present for both GDLD and GDLS, however the shape and latency of this response differs. The size of the difference in responses is large compared to the difference between GSLD and GSLS, forming an interaction between global and local effects in this case as well as for the passive group, but for a different reason. The structure of the interaction between global and local effects when attention is directed towards the task (in fact specifically within recovery, but also seen as a trend within the active group and sedation), indicates that the level of the local effect (standard vs. deviant) is impacting upon the shape and latency of responses to global deviance but seemingly not responses to global standard. Therefore, the presence of an interaction between global and local effects, composed of differing P3b responses to global deviance, based on local context, could be considered a marker of attentional engagement with the task.

Furthermore, sedation does not appear to have the same impact on responses as a lack of directed attention; that is, reducing wakefulness did not appear to disrupt the attentional directive of the individual with respect to the task in the current dataset. We

acknowledge that it may seem counterintuitive to consider that participants could be processing more of the task when under sedation compared to when awake but passive. However, we would reiterate an important point, that is, sedation did not constitute a complete lack of consciousness for all participants within the study. Therefore, what we observe may be the result of reduced wakefulness, ie. a drowsy state, as opposed to a complete loss on consciousness. Additionally, it is also important to hold in mind the two-fold consideration of consciousness within this thesis, that is consciousness as wakefulness but also consciousness as conscious perception facilitated by attention. Here we are speaking to the notion that a reduced wakefulness did not appear to disrupt individual's ability to consciously perceive global deviance marked by both locally standard and locally deviant quintuples (GDLD & GDLS), possibly because their attention had been directed towards the task throughout the experiment (in both sedated and recovered conditions). However, a lack of direct attention (ie. in the passive group) did appear to result in a failure to detect global deviance that was marked by a locally standard quintuple (GDLS). One may consider the findings from the standpoint that despite being sedated participants still appear to have been somewhat wakeful (conscious), but one may also consider the findings as highlighting the importance of direct attention in facilitating conscious perception.

Thus, whilst the shape of responses under sedation are similar to those at recovery and within the active group, it is the case that a reduction in wakefulness attenuates the size of responses at both global and local levels, as well as somewhat impacting upon the latency of response onset at the global level. Altogether, while sedation does not appear to disrupt the attentional directive of the individual, it may limit the level of precision afforded by direct attention with respect to the size of responses at the local level, and the shape and latency of responses at the global level.

In sum, it appears that the presence of an interaction between global and local effects in isolation is not sufficient to determine variations in attention or wakefulness. It is in fact the presence and composition of an interaction between global and local effects, within the region of the global effect, which may be informative. We have found that responses to global deviance are sensitive to changes in attention and wakefulness. More specifically, direct attention is necessary for the presence of a P3b response to global deviance that is marked by a locally standard quintuple (GDLS), whilst the shape and latency of P3b responses to global deviance differ depending on the local context in

which they are presented (GDLD or GDLS) when attention is directed towards the task. Moreover and interestingly, this difference is present but reduced when under sedation, suggesting that the presence of a P3b response to GDLS may be a marker of direct attention, whilst a reduction in the differing shape of P3b responses to GDLD and GDLS may relate to a reduction in wakefulness.

Our findings suggest that it may be possible to distinguish active attention from passive mind wandering within states of low awareness, by considering the composition of the interaction between global and local effects (see top left and right panels in Figure 7.16). What is more, it may be possible to highlight states of low awareness in the presence of direct attention by considering the presence of an interaction between global and local effects within the region of the global effect (see bottom right panel in Figure 7.16).

In conclusion, we once again suggest that the global effect may not be functionally isolated as a marker of conscious processing because global and local effects were found to interact. Critically, it is also the case that the presence of an interaction between global and local effects within the region of the global effect is not, in and of itself, sufficient to imply the absence of direct attention, as we not only observe an interaction when attention is active (in recovery), but also when attention is wandering (passive). Therefore, we propose that an interaction between global and local effects is necessary but not sufficient to constitute a marker of direct attention. It is in fact the absence of a P3b response to GDLS that may signify a lack of attentional engagement with the task. With respect to sedation, it is the case that an interaction between global and local effects within the region of the global effect may signify higher levels of wakefulness, as this may point to greater attentional engagement with the task (where there is a largely differing P3b response to GDLD vs. GDLS). Moreover, this may be supported by the fact we do not observe an interaction between global and local effects within the region of the global effect in the sedation simple effects analysis (see Figures 6.27 & 6.28).

8 Re-aligning EEG data: A method for extracting discontinuities from time-series data

Within this Chapter we address an issue of discontinuity in the EEG time-series, which arose during the initial stages of the formally presented analysis. In response to the issue we devised a method for correcting the data, which prevents the rejection of trials and/or participants resulting in a loss of statistical power in subsequent analyses. We present and discuss the method here for the purpose of clarity, but also because it may serve as a useful tool in other channels of research.

Initially, the problem of discontinuity will be outlined, along with how it may be characterised. We present the explorative analysis conducted in order to address the definition of discontinuity (including pre-processing methods) and we then present three versions of the method as we continued to refine the process by which the method tends to the data. The data presented in this Chapter is data from the attention study conducted by Bekinschtein et al. (2009) and data from the sedation study, also conducted by Bekinschtein and colleagues. All data presented in previous Chapters relating to the study on attention by Bekinschtein et al. (2009) (not the study of sedation) is data that has been corrected using the following method. The body of this Chapter addresses exactly how discontinuity in the data is defined, by considering differences between time-points within Event-Related Potential (ERP) time-series, along with how this can be rectified by adjusting extreme differences in-line with the surrounding context of differences. Lastly, we will discuss how the method was tested on data without discontinuity, to ensure that the original integrity of the time-series was preserved. Conclusions are drawn regarding how the method is a viable alternative to discarding data.

The discontinuity problem

After running initial analyses on the data obtained by Bekinschtein et al. (2009), it was observed that discontinuity existed within the ERP time-series around 1000ms (see Figures 8.1, 8.2 and 8.3); this was observed for both active and passive groups. Discontinuity in the time-series manifested as a 'jump' up or down to a different voltage (Mv) between and across sequential time-points. The word discontinuity is used in this context to describe voltage jumps in the data, across sequential time-points that exceed the amount of change one would expect to observe between time-points within an EEG time-series. The most likely explanation for discontinuity in the data is problems with the digitisation process during recording, that is, the transformation of the signal from analogue to digital. The presence of such discontinuity may raise concerns for subsequent statistical analysis, particularly in Statistical Parametric Mapping (SPM), as it may lead to the misrepresentation of data to statistical analysis, moreover incorrect instances of statistical significance. This is of particular relevance to the SPM approach because of the implementation of Random Field Theory (RFT). RFT considers clusters of activity on the scalp through both space and time in order to deduce whether there is statistical significance. In some cases, discontinuity in the EEG time-series increases the amplitude of EEG components (as in Figure 8.2), which misrepresents the actual size of the response. Given that RFT assesses the size of effects, this presents the opportunity for erroneous findings of statistical significance; Figures 8.1, 8.2 and 8.3 contain examples of discontinuity that were found.

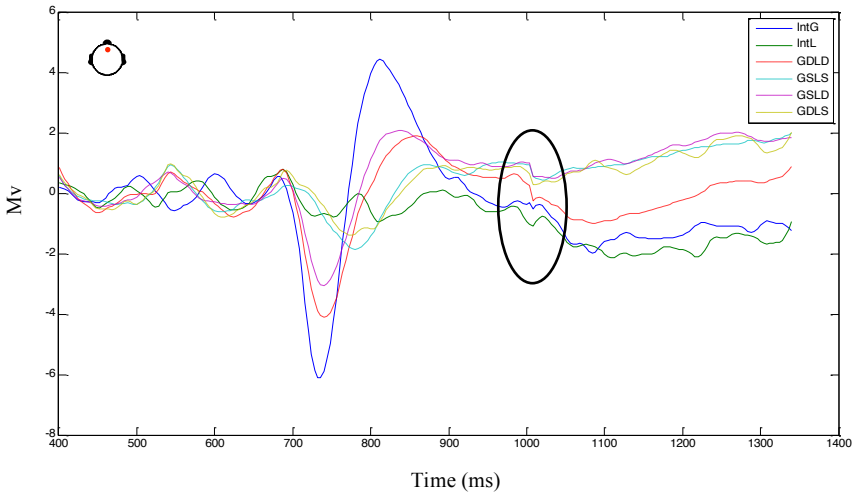

Figure 8.1. ERPs for all conditions and the interaction at Fz (11). Includes both active and passive groups..

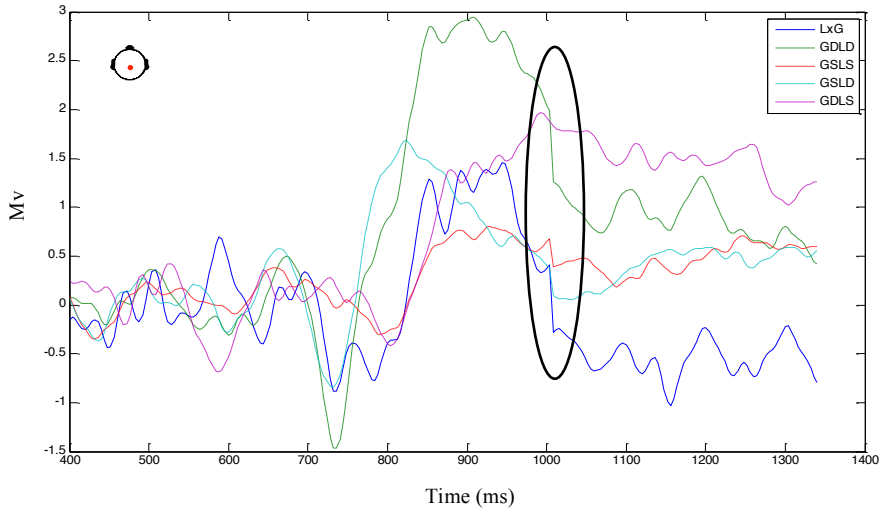

Figure 8.2. ERPs for all conditions and the interaction at Pz (55). Includes both active and passive groups.

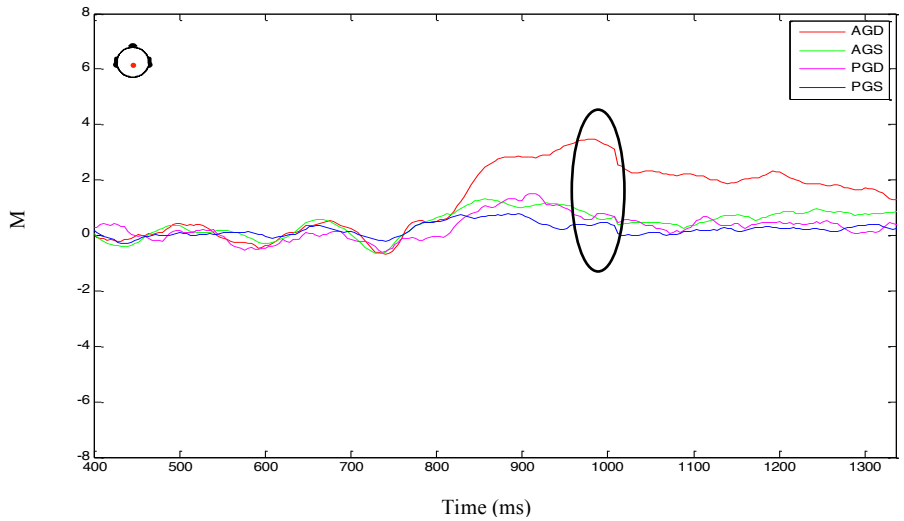

Figure 8.3. ERPs for active (A) and passive (P) groups: global deviant (GD) vs. global standard (GS) at Pz (55).

The statistical analysis of EEG data is an important part of the research presented within this thesis, therefore we present and discuss the method we devised in order to re-align the time-series. Re-aligning the time-series meant that the problem of discontinuity was eliminated without the need to discard any of the data; What is more, rectifying the problem of discontinuity ultimately prevented the misrepresentation of data to subsequent statistical analysis.

Characterising discontinuity

We characterised discontinuity as an abnormally large jump in the time-series from one voltage (Mv) to another between 2-4 consecutive time-points. No discontinuity was found to exceed four time-points. An abnormally large jump was considered to be more than seven standard deviations away from the mean time-point difference value for the time-series. A jump between 2-4 consecutive time-points constituted a jump between 4ms-16ms as each time-point was sampled at 4ms (sampling frequency of 250Hz); this was considered to be adequate criteria for the characterisation of discontinuity as variation at this level (>7 standard deviations) greatly exceeds that which one would expect to find within a typically occurring ERP time-series.

In order illustrate that discontinuity does exceed the typically occurring variation within the time-series, we plotted a distribution of time-point difference Z-scores at the ERP level (ie. the grand average or group level average). Differences between time-points were calculated along the ERP for each condition (global deviant local deviant [GDLD], global deviant local standard [GDLS], global standard local deviant [GSLD] and global standard local standard [GSLS]) at a specific electrode. A Z-score can then be calculated for each time-point difference based on a local context of six surrounding time-point differences (three before and three after the current time-point difference). Figures 8.4 and 8.5 plot the distribution of Z-scores for differences at electrodes Fz and Pz, which are the focus of the global and local effects.

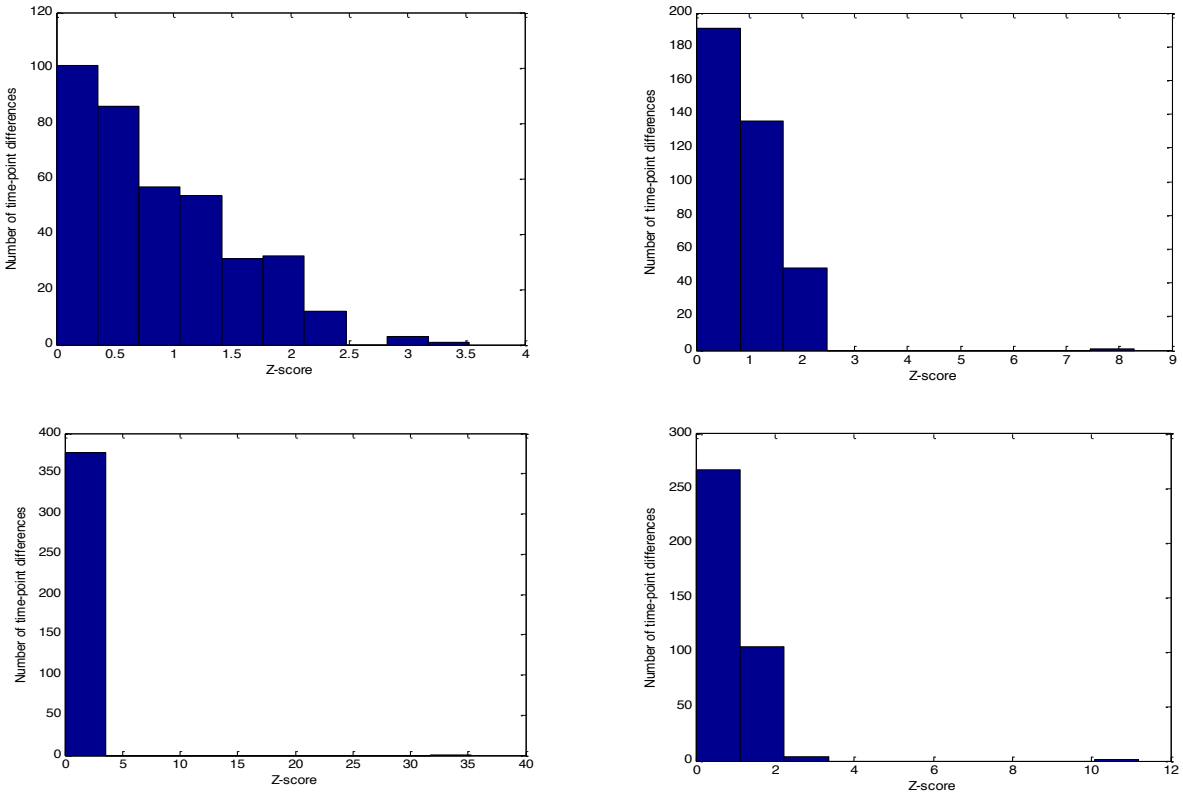

Figure 8.4. Distribution of time-point differences using Z-scores. Conducted at the ERP level for each condition: GDLD (top left), GDLS (top right), GSLD (bottom left) and GSLS (bottom right), at electrode Fz (11).

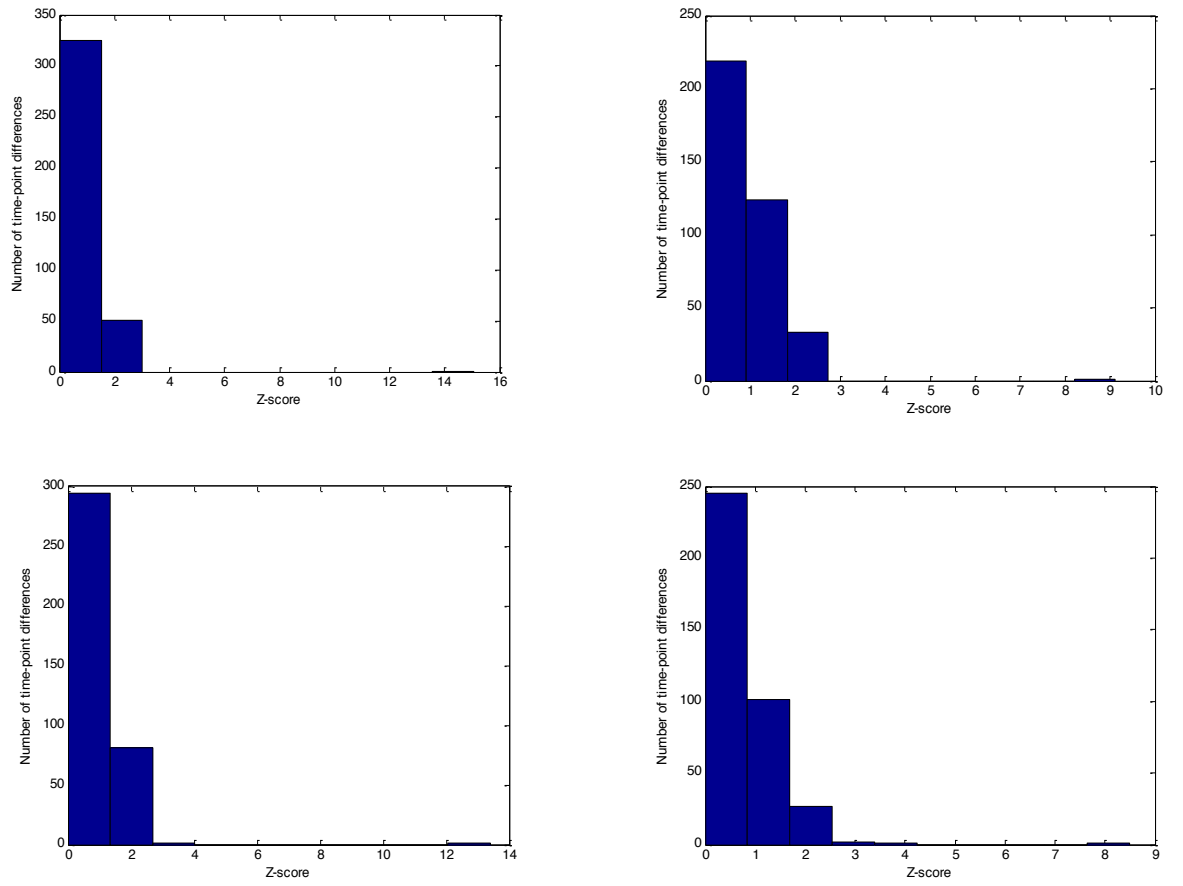

Figure 8.5. Distribution of time-point differences using Z-scores. Conducted at the ERP level for each condition: GDLD (top left), GDLS (top right), GSLD (bottom left) & GSLS (bottom right), at electrode Pz(55).

The distribution of Z-scores provides information about how far away from the average time-point difference (ie. the average difference between time-points within the time-series), each time-point difference is. From Figures 8.4 and 8.5 one can see that most time-point difference Z-scores fall within three standard deviations of the mean time-point difference value. Therefore, a threshold of more than seven standard deviations for the classification of discontinuity is necessarily sufficient to capture abnormally large jumps within the time-series without removing typically occurring variation. Put another way, discontinuity in the data is substantially larger than the otherwise occurring variability within the time-series, making it easy to characterise and subsequently remove.

Importantly, the presence of such discontinuity in the data distorts the shape of the time-series (see Figures 8.1, 8.2 and 8.3), which can make peaks appear larger in amplitude. As previously mentioned, this distortion could influence subsequent statistical analysis given that the smoothness and size of responses in space and through time contribute to the estimate of significance within SPM. What is more, the discovery of discontinuity in the group level average (ERP) suggests that jumps are occurring in a large number of trials across all participants. However, on further inspection it was observed that discontinuity differed in time, direction, space (by electrode), size and also by participant and condition (GDLD, GDLS, GSLD and GSLS). To begin with, the impact of typical EEG pre-processing methods, such as smoothing and trial elimination, were considered in relation to rectifying the discontinuity problem.

Pre-processing methods

Smoothing the data (band-pass filtering). Data was filtered in SPM using a band-pass filter (0.5-20Hz), in accordance with Bekinschtein et al. (2009).

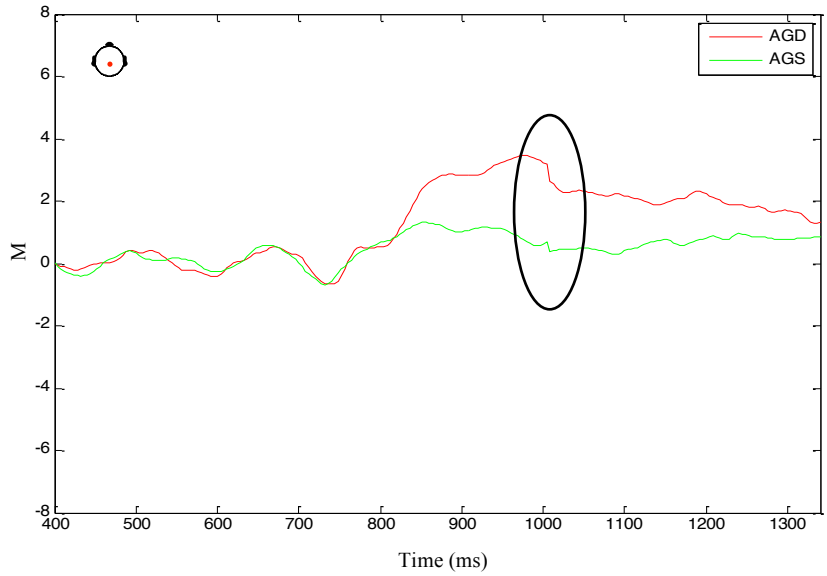

Figure 8.6. Global deviant (GD) and global standard (GS) for the active group (A) before filtering at Pz (55).

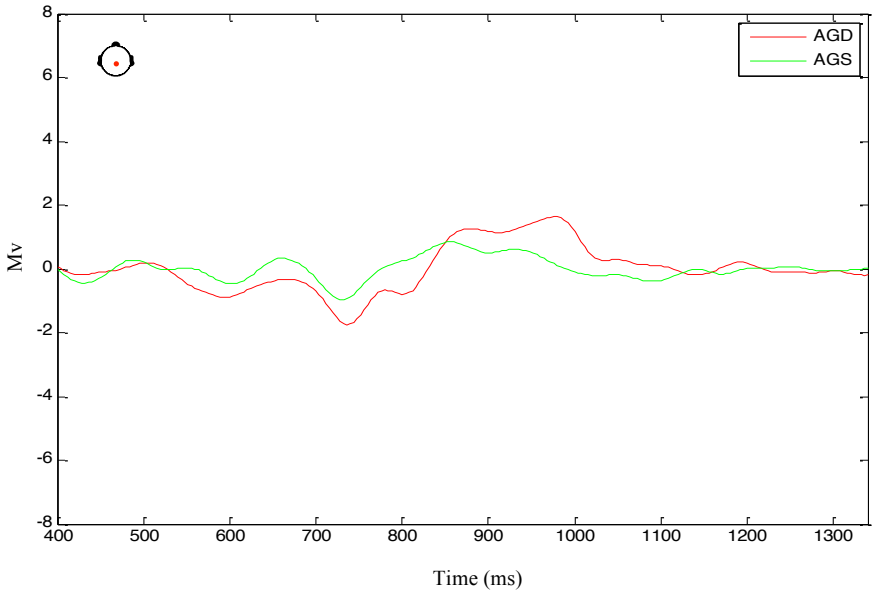

Figure 8.7. Global deviant (GD) and global standard (GS) for active group (A) after filtering at Pz (55).

As one can see from Figures 8.6 and 8.7, filtering changed the shape of the data. Discontinuity is not removed but smoothed resulting in the shape of the time-series being distorted. Whilst it is known that filtering may change the shape of the data, the preservation of discontinuity in this case meant that the data would be misrepresented to subsequent statistical analysis. In particular, the difference between global standard

(green line) and global deviant (red line) in Figure 8.7 was distorted to the extent that the difference between conditions is misleading, therefore the result of subsequent statistical analysis on this difference will not be accurate. In conclusion, the pre-processing method of filtering does not adequately address discontinuity in the time-series and so other pre-processing methods were considered.

Eliminating bad trials and/or participants. For some participants the majority of trials contained discontinuity therefore eliminating such participants from the analysis would have been the only option. Although, with a sample size of only 11, eliminating participants from the analysis would impact on statistical power. As with filtering, it was concluded that trial/ participant elimination was not an adequate resolution for discontinuity given that it would reduce the statistical power of subsequent analyses. Consequently, given that filtering distorted the data and elimination reduces statistical power, the implementation of such methods was abandoned in favour of developing a new method to preserve power, along with the original integrity of the time-series.

The Method – Version I (difference threshold of 1)

To our knowledge there are no existing methods which specifically remove discontinuity whilst maintaining the typically occurring variation of the EEG time-series. Therefore, we followed no specific convention when developing the following method. All versions of the method were written in MATLAB 2012b to work on raw matrix files (.mat files). We also expanded the method to incorporate EEGlab files (.set files) by firstly reverting them to MATLAB 2012b files (.mat files) and then applying the method. Preserving the integrity of the time-series (including artefacts) was of paramount importance and as such the new method needed only to target discontinuity and not existing artefacts in the data.

The initial method calculated the difference between consecutive time-points along the time-series and compared the difference values against an externally set threshold of 1. An externally set threshold of 1 was chosen as an initial starting point to assess the amount of variability between time-points that was captured with this threshold. In specific, for every participant (11 in total) in every condition (global and local) the

method searches within every trial and observes all time-points (385 in total). The method begins at the first time-point of a trial (tp0) and saves the value into a new matrix (with the same dimensions as the raw data). There are three dimensions to the data given that we have each time-point of each trial at every electrode on the scalp (electrode x time-point x trial). Subsequently, the second time-point in the time-series (tp1) was then compared against the first to attain the difference. Specifically, a subtraction was performed between the two consecutive time-points (tp1 – tp0); the difference observed was then compared against an arbitrary value of 1. If the difference value was lower than 1 then the second time-point value (tp1) is saved to the new matrix and the method continues to the next time-point. If the difference value is greater than 1, the difference value is then subtracted from the second time-point (tp1) and all subsequent time-points until the end of the time-series; the new value of the second time-point is then saved into the new matrix and the method continues to the next time-point (tp1 now becomes tp0).

In principle, the method is consistently working on the time-point following the current time-point (that is tp1), as it is detecting discontinuity between the current time-point (tp0) and the consecutive time-point (tp1). Therefore, correcting discontinuity is achieved by subtracting the jumping distance from the following time-point (tp1 and all proceeding time-points) in order to re-align the following time-point with the current time-point value. All discontinuity within the time-series that exceeded a value of 1, was corrected with the current method, as the jumping distance was not only subtracted from the following time-point (tp1) but also all subsequent time-points until the end of the time-series. The last time-point in the time-series was not subjected to the method, as there was no proceeding time-point (tp1) from which to subtract it; in addition, any large jump between the penultimate and ultimate time-points would already have been corrected by the method during the previous step.

It was found that imposing a difference threshold of 1 actually distorted the time-series further, as there were a number of differences between time-points that exceeded 1 but were not the result of discontinuity. Thus, the method was correcting differences throughout the time-series that should have been preserved; Figures 8.8 and 8.9 illustrate how the method was correcting typically occurring variance within the time-series.

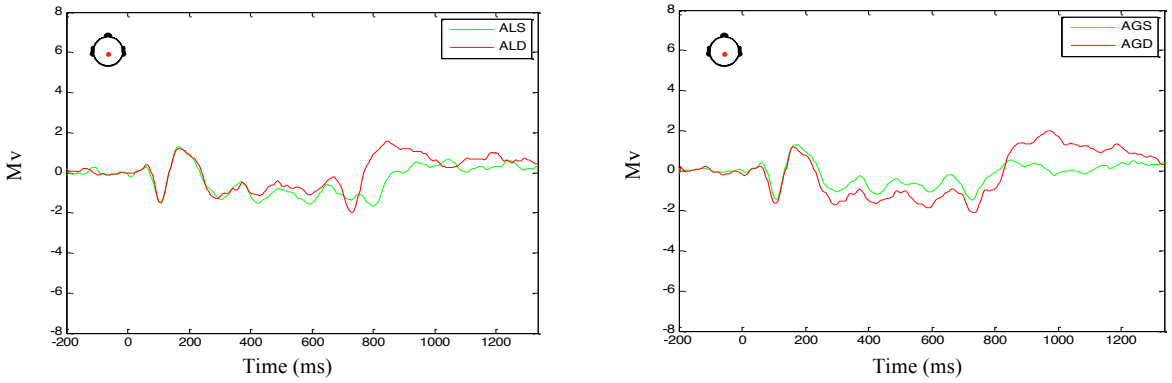

Figure 8.8. Local standard (LS) and local deviant (LD) ERPs for the active group (A) at Pz (55) before re-alignment (left panel). Global deviant (GD) and global standard (GS) ERPs for the active group at Pz (55) before re-alignment (right panel).

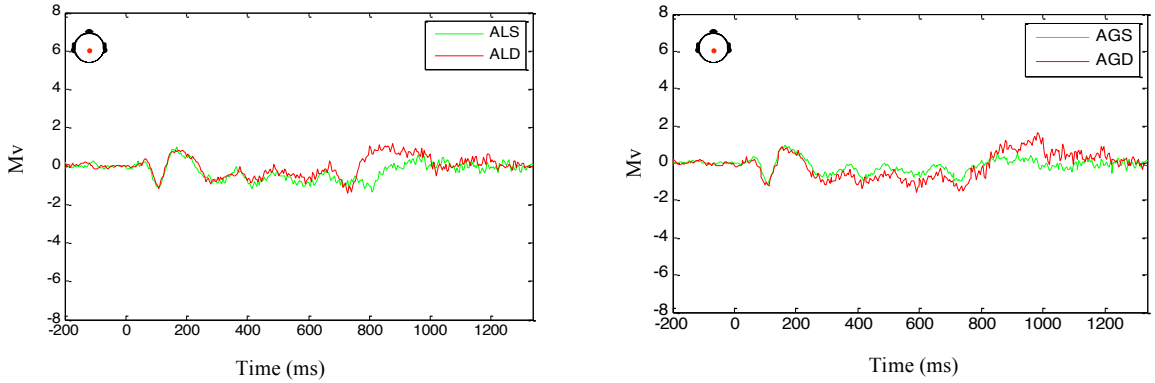

Figure 8.9. Local standard (LS) and local deviant (LD) for the active group (A) at Pz (55) after Method I re-alignment (left panel). Global standard (GS) and global deviant (GD) for active group at Pz (55) after Method I re-alignment (right panel).

In sum, setting a difference threshold of 1 disrupted the original integrity of the time-series by misclassifying typically occurring variance as discontinuity. What is more, further investigation revealed the impact of a number of difference thresholds (see Appendix 8), however it was concluded that the most accurate characterisation of discontinuity would come from setting a threshold based on the average time-point difference of a given trial, that is, a threshold that is set on a trial specific basis as opposed to arbitrarily. Moreover, within the current method, time-point differences are only considered in comparison to the subsequent time-point, thus a broader local context of time-point differences would provide a more accurate classification of discontinuity as it occurs within a given trial. Consequently, Version II of the method replaces the

externally set threshold with a local context of time-point differences and the introduction of Z-scores.

The Method – Version II (four-point difference Z-score)

The second iteration of the method included a window of context, which compared the current time-point difference against a local context of time-point differences. The context window included three time-point differences before (tpdiffm1, tpdiffm2, tpdiffm3) and three time-point differences after (tpdiff1, tpdiff2, tpdiff3) the current time-point *difference* (tpdiff), which is tp1-tp0. That is, four time-points before (tpm1, tpm2, tpm3, tpm4) and four time-points after (tp1, tp2, tp3, tp4) the current time-point (tp0) were noted and subtractions were performed (as under Version I) to generate a vector of six differences (three before and three after the current time-point *difference*). The current time-point difference (tpdiff) itself was not included in this vector as it was to be compared against the local context of differences.

Under Version II of the method a Z-score for the current time-point difference is calculated, using the local context of the six surrounding differences. Z-scores were introduced to the method because they are a normalised measure, thus converting the difference value to a Z-score means that one can assess how far away from the average difference of the context window the current difference stands. In this way, one can classify discontinuity based on the surrounding levels of variation. In other words, the method assesses whether the current time-point difference is abnormally larger than the variation surrounding it.

To be exact, Version II of the method subtracts the mean of the vector of differences from the current difference, and then divides the product by the standard deviation of the vector of differences. The resulting Z-score is then compared against a value of two, which represents two standard deviations away from the mean. For a normal distribution it is always the case that 95.44% of values fall within two standard deviations of the mean, and hence the application of two standard deviations here (Altman & Bland, 2005). So, if a value falls outside two standard deviations of the mean it may be considered an outlier, or in this case discontinuity. If this is the case then the value of the

current difference (tp1 – tp0) is subtracted from the next time-point (tp1) and all subsequent time-points up to the end of the time-series. The data is then saved into a new matrix (with the same dimensions as the raw data) exactly as was outlined under Version I. The method then continues to the next time-point. Once again, the difference is not subtracted from the current time-point as the jump is occurring between the current time-point and the subsequent time-point. Therefore, it is the succeeding time-points (tp1 onwards) that are re-aligned and not the current time-point (tp0) itself. If the resulting Z-score for the current time-point difference is below two, that is, it is not more than two standard deviations away from the mean difference of the local context window, then the current value of the following time-point (tp1) will be saved to the new matrix and the method will continue to the next time-point.

Version II of the method, as before, observes all participants in all conditions at every electrode on the scalp, whilst within each trial the method works along each time-point up to the end. To achieve a context of three time-point differences before and after the current time-point difference, the first four time-points and the last four time-points of a trial are saved to the new matrix (which has the same dimensions as the raw data) without alteration. As there are 385 time-points in a trial, this means that the first analysed time-point difference is between the 4^{th} and 5^{th} time-points. Equally, the last analysed time-point difference in a trial is between the 381^{st} and 382^{nd} time-points.

It was observed that whilst Version II did capture some of the discontinuity with the time-series, it did not capture all occurrences. Specifically, discontinuity that was occurring over a number of consecutive time-points (between two and four) was not being captured by this method (see Appendix 9). Version II of the method failed to capture these jumps because discontinuity between surrounding time-points was contributing to the Z-score calculation. In other words, a jump occurring within the local context window increases the size of the mean for that given context window; thus, when the mean is subsequently subtracted from the current time-point difference (tpdiff), the resulting value is low. A low value is unlikely to reach the threshold of two standard deviations away from the mean, and so the current difference is not identified as discontinuity within the local context of time-point differences. Ultimately, the method required expansion to include a wider context window against which local

discontinuity could be assessed; this had to include discontinuity that was occurring across more than two time-points.

The Method – Version III (two-step Z-score re-alignment)

In order to address the issue of discontinuity occurring across more than two time-points, a wider contextual window of comparison was introduced to the method. Firstly, the method remained as previously described for detecting successive discontinuity in the data (ie. a jump between two successive time-points), but within Version III of the method a second pass was introduced whereby an additional Z-score is calculated based on a larger contextual window of over three times as many time-points as under Version II. For clarity, we subsequently reiterate Version II of the method, which became the first pass under Version III. Thereafter we introduce the second pass Z-score calculation, which was added under Version III and resolves the issue of gradual discontinuity in the time-series.

First pass Z-score calculation. Version II of the method became the first pass Z-score calculation under Version III of the method, that is, the local contextual Z-score calculation occurs at the first pass under Version III and subsequently there is the addition of a wider contextual Z-score calculation (a second pass), which addresses the issue of gradual discontinuity in the data. Once again, the method is applied to time-points within each trial of every condition at each electrode for all subjects. The first pass of Version III begins at the first time-point of a trial and saves the initial four time-points (this is also the case for the last four time-points which are saved at the end of the process); this allows for a context window of four time-points before and four time-points after the current time-point, meaning that the first time-point inspected by the method is the 5th time-point in the trial, respectively, the last time-point inspected by the method is the 381st time-point. The time-point difference is calculated by subtracting the current time-point (tp1) from the subsequent time-point (tp0), (ie. tp1–tp0), and then the method notes the four time-points before the current time-point value (tpm1-4), and four time-points after the current time-point value (tp1-4) in order to create a vector of six differences. There are six difference values because we perform six subtractions: tpm3 –

tpm4, tpm2 – tpm3, tpm1 – tpm2 / tp2 – tp1, tp3 – tp2, tp4 – tp3; this vector of differences provides the local context (see Figure 8.10).

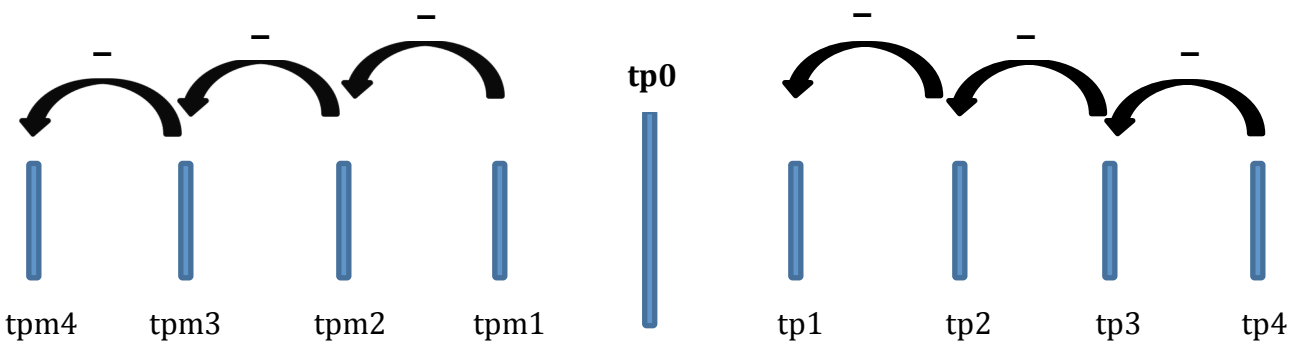

Figure 8.10. Visual representation of how the difference vector (local context window) is calculated.

The difference between the current time-point (tp0) and the previous time-point (tpm1) is not included in the vector along with the difference between the current time-point (tp0) and the following time-point (tp1), this is because a comparison is to be made against the surrounding local context in the absence of the current time-point, so that the presence of discontinuity between the current time-point difference (tp1-tp0) and the local context can be established. To make such a comparison, the mean of the difference vector is subtracted from the current time-point difference (tpdiffmmean) and the result is then divided by the standard deviation of the difference vector to provide a Z-score for the current time-point difference (tpdiffzab).

The resulting Z-score is compared against a threshold value of seven, which represents seven standard deviations away from the mean of the difference vector. Additional analyses revealed that the difference threshold of seven standard deviations away from the mean was effective for removing discontinuity between subsequent time-points whilst preserving the integrity of the raw time-series (see Appendix 10). Thus, if the Z-score of the current time-point difference exceeds seven then the method will subtract the current time-point difference (tpdiff [note: the actual difference not the Z-score value]) from the proceeding time-point (tp1), and all other subsequent time-points until the end of the time-series, this is then saved to a new matrix (with the same dimensions as the raw data) and the method continues. Crucially, the current time-point difference is not subtracted from the current time-point itself because if present, discontinuity is

occurring between the current time-point and the proceeding time-point, therefore the method re-aligns the subsequent time-point to be consistent with the current time-point along with all time-points thereafter until the end of the time-series.

With regard to the difference threshold of seven, lowering the Z-score threshold would mean that high levels of variation in the data may be characterised as discontinuity and subsequently removed, even if it were typically occurring variation within the time-series; in this way, the data is smoothed by removing (subtracting out) the large time-point differences (incorrectly) from trials resulting in a distorted representation of the time-series that has lost the majority of its original integrity. By way of contrast, increasing the Z-score threshold means that the method is less likely to inaccurately characterise typically occurring variation as discontinuity and remove it. In fact, discontinuity in the data is by definition an abnormally large shift in voltage and thus setting the Z-score threshold to a high value will still capture discontinuity whilst preserving the typically occurring variation of the time-series. If the Z-score threshold is too high then indeed there is a failure to capture genuine instances of discontinuity, and so a number of threshold values were examined in order to find an effective threshold, which balanced the capture of discontinuity with the maintenance of original integrity (see Appendix 10).

Second pass Z-score calculation. For the novel part of Version III, a second pass Z-score calculation is introduced to the method, which enables the characterisation and removal of gradual discontinuities in the data (across more than two time-points). Within the second pass of the method, the first ten time-points of the time-series are noted, along with the last ten time-points of the time-series; from these, nine difference values are created (in the same way as previously presented at the first pass) for the initial ten time-points, and another nine are created for the last ten time-points. In total, a vector of eighteen differences is created, which provides a substantially larger contextual window with which to compare time-point differences.

The method begins at the first time-point and moves through the time-series calculating the current time-point difference (tpdiff) by subtracting the current time-point value (tp0) from the subsequent time-point value (tp1) (as before). The mean of the difference vector created is then subtracted from the current time-point difference value and the

product is divided by the standard deviation of the difference vector to generate the Z-score. The Z-score is compared against a threshold value of eight, that is, eight standard deviations away from the mean of the difference vector. If the current Z-score is more than eight standard deviations away from the mean of the difference vector then the value of current time-point difference (actual value not Z-score value) is subtracted from the next time-point (tp1) and all subsequent time-points until the end of the time series. As previously, the current time-point difference value is not subtracted from the current time-point itself (tp0) because the method is seeking to remedy discontinuity by re-aligning the proceeding time-points (tp1 onwards) with the current time-point (tp0).

Setting the difference threshold to eight standard deviations away from the mean was also investigated within additional analyses where it was found that a difference threshold of eight standard deviations away from the mean captured gradual discontinuity within the time-series (see Appendix 10). In other words, we did explore the best combination of Z-score thresholds, at first and second passes, to remove all types of discontinuity from the data whilst preserving the typically occurring variation of the time-series. Importantly, maintaining the shape of the original time-series included maintaining any artefacts that may exist within the data, such as eye blinks and other muscle artefacts, therefore pre-processing could be applied after re-alignment, which may improve the accuracy of subsequent statistical analysis.

For clarity, the second pass of Z-score calculation identifies and removes gradual discontinuity from the time-series by comparing the current time-point difference to a broader contextual window of time-point differences than implemented at the first pass. By widening the contextual window, a more accurate measure of variability between time-points within a trial is gathered, this means that discontinuity which occurs over a number of time-points can be identified and removed successfully; this differs from the first pass Z-score calculation as the first pass relies on only a local context of surrounding time-points, therefore if the surrounding time-points include discontinuity, then consequently this will contribute to the calculation of the Z-score for the current time-point difference. To be specific, surrounding discontinuity will increase the mean and standard deviation of the difference vector at the first pass (consisting of six time-point differences, three before and three after the current time-point difference), and so when the mean is subtracted from the current time-point difference and the result is

divided by the standard deviation, what remains is a very small number that does not reach above the externally set Z-score threshold. Therefore, the method fails to identify discontinuity. Consequently, first and second pass Z-score calculations detect local and gradual discontinuities within the time-series, without disrupting the typically occurring variation of the data.

In sum, both a first and second pass Z-score calculations are implemented in Version III of the method, with the first pass eliminating consecutive time-point discontinuity and the second pass addressing gradual instances of discontinuity (across more than two time-points). The resultant time-series is one that has all discontinuity removed and the highest degree of typically occurring variation preserved.

Testing the Method (Version III)

In order to confirm that the method was removing discontinuity without removing typically occurring variation from the time-series, we applied the method to a dataset that did not contain discontinuity. In principle, the method is only targeting discontinuity within the data therefore it should have no impact on a time-series void of discontinuity. In other words, the difference between a time-series before and after the method should be zero when the dataset contains no discontinuity. Thus, we applied the method to the sedation dataset, which was collected by Bekinschtein and colleagues. The dataset was selected because it contained a high level of variation (as participants were under sedation) but no discontinuity. The principle aim was to ensure that the method would not misclassify a large amount of variation in the time-series as discontinuity.

To measure the effectiveness of the method we observed the error difference between the time-series before and after application of the method. In other words, we observed the difference between the same time-point values before and after the method; this assessment was conducted at the ERP level (that is, the level of the grand average).

Firstly, the ERP (consisting of 18 participants) before re-alignment was generated and the same ERP was generated after re-alignment (see Figure 8.11). Secondly, a vector of time-point differences was created for both the ERP before and the ERP after applying

the method. The result was two vectors, one containing time-point difference values for the pre-method time-series, and one containing time-point difference values for the post-method time-series. Each trial contains 375 time-points (as this is now the sedation dataset and not the attention dataset), therefore both of the two vectors contain 374 time-point difference values. Every time-point difference value for the pre-method ERP was compared against the relative time-point difference value for the post-method ERP in order to create a new vector that contained the difference of differences; this vector again contained 374 values. Every value within the new vector was squared individually, and the resulting values were summed to give the Sum Squared Error (SSE); this is an absolute quantification of the difference between the data before and after running the re-alignment method.

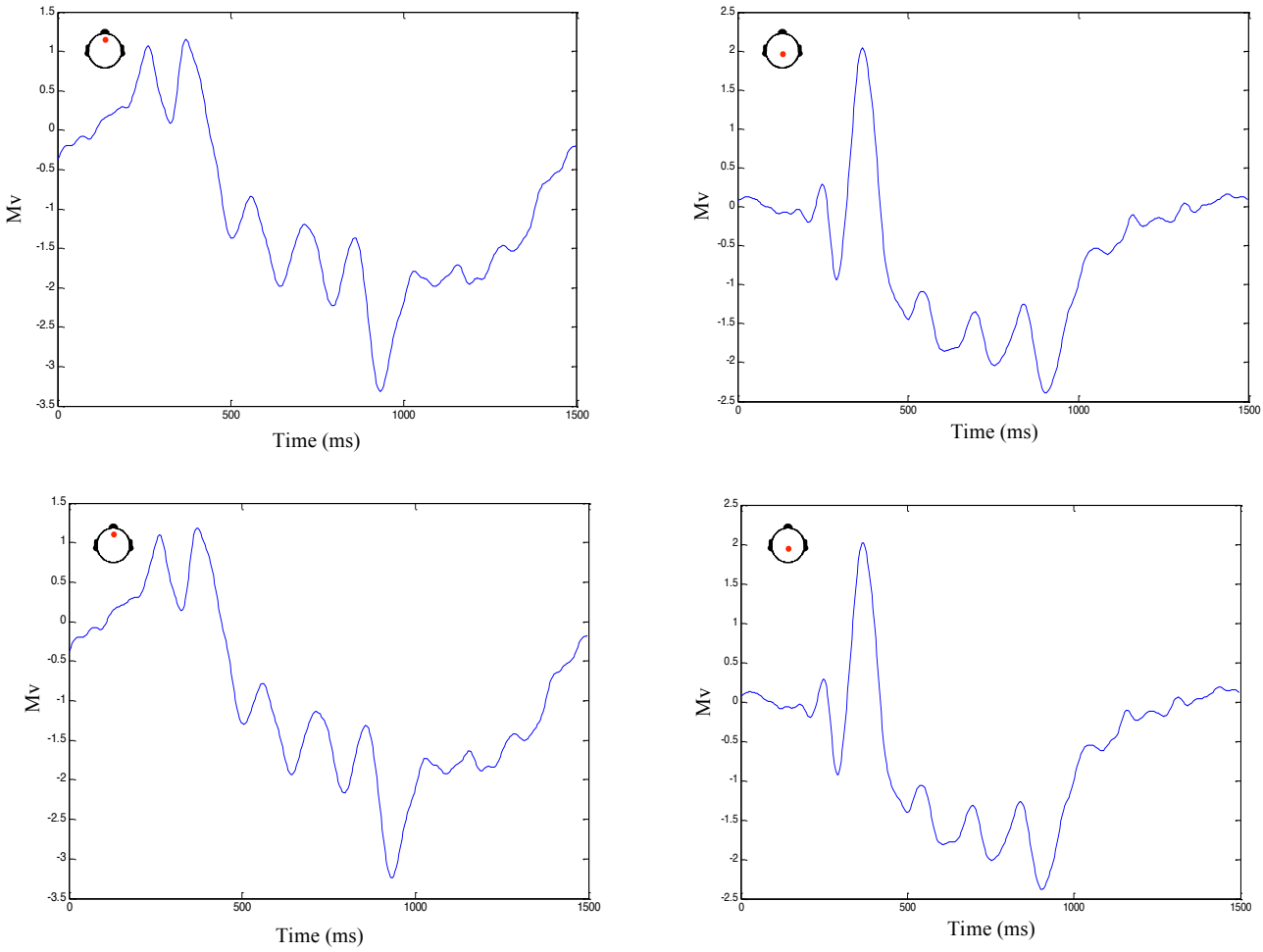

Figure 8.11. ERPs for sedation data at Fz (11) (top left panel) and Pz (55) (top right panel) before re-alignment. ERPs for sedation data at Fz (11) (bottom left panel) and Pz (55) (bottom right panel) after re-alignment.

The SSE for electrodes Fz and Pz was found to be zero, indicating that there was no difference between time-points before and after applying the method; this suggests that the method is not dramatically changing the time-series unless discontinuity is present. Furthermore, to consider how the method is applied on a trial-by-trial basis (as opposed to at the ERP level), all the trials for every condition at a specific electrode were considered, in this case, by participant (individually) as opposed to across all participants. Each corresponding trial was compared against itself before and after application of the method; for example, the first time-point in a trial before applying the method, and the first time-point in a trial after applying the method were compared. The value of the difference was then placed into a new vector, and the process was repeated for all the remaining time-points within the trial (of which there were 374). Each value within the new vector is subsequently squared individually and the values are summed to give the SSE; a histogram of all trials by error was plotted for every participant (see Appendix 11). If the method is changing nothing about the data when discontinuity is absent then the SSE of trials should be zero, given that there is no difference between time-series before and after the method has been applied. SSE was found to be zero for all trials, illustrating that the time-point values within the time-series are not being changed by the method.

Altogether, Version III of the re-alignment method captures all types of discontinuity in the data without disrupting the typically occurring variation within the time-series; this is achieved by using first pass local contextual comparison and subsequently a second pass wider contextual comparison window. In order to confirm that Version II of the method was removing only discontinuity from the data and not large amounts of typically occurring variation, we tested the method by applying it to data that had a large amount of variation throughout the time-series. It was found that the method did not dramatically change the data when discontinuity was not present, despite there being large amounts of variation within the time-series. Thus, we argue that Version III of the method appears to be successful at capturing both local and gradual forms of discontinuity, whilst preserving existing variation within the time-series. As a result, the time-series (post application of the method) can be pre-processed and subjected to statistical analysis without any loss of data.

Conclusion

Within this Chapter we discuss and present a re-alignment method that was devised in order to remove discontinuity from EEG time-series without the need to discard data. Discontinuity was defined as a large shift in amplitude between consecutive time-points (between two and four), as the result of problems during the digitisation process, that clearly exceeds the typically occurring variation of EEG data. Three Versions of the method were presented to illustrate how the process was refined to ensure that all instances of discontinuity were removed without disrupting the typically occurring variation. In order to ensure that the method was only capturing discontinuity, we applied it to a dataset with a large amount of variance but no discontinuity. It was observed that the method did not alter the time-series despite a large amount of variance between time-points and therefore it is proposed that the method is a viable way of eliminating instances of discontinuity whilst maintaining the integrity of the raw data. Furthermore, application of the method prevents the necessity to discard data, which subsequently presents the issue of reduced statistical power at the analysis stage. Altogether, as the method is only targeting discontinuity within the time-series and not artefacts, it is possible to subsequently subject the time-series to pre-processing methods without disturbing its integrity. Therefore, the method is ultimately maximising the efficiency of the data so that statistical analysis may be applied.

9 Discussion

Within this thesis we have explored both manipulations of attention and wakefulness in relation to expectancy using electrophysiological (EEG) responses towards the global-local auditory task. We have re-analysed the data of Bekinschtein et al. (2009) using a factorial design analysis so that we were able to address the possibility of an interaction between global and local effects that cannot be captured using cognitive subtraction. What is more, we went on to analyse (using a factorial analysis) the data of a study on healthy sedation to investigate a possible interaction between global and local effects when attention was always directed towards the task. Finally, we conducted an exploratory analysis comparing manipulations of attention to healthy sedation, opening a discussion around the nature of conscious processing in relation to the direction of attention and the level of wakefulness one possesses.

Additionally, within the final research Chapter, we presented a method for re-aligning time-series data (specifically EEG data), when discontinuity between time-points is occurring. The method we present corrects discontinuity to allow for the application of subsequent statistical analysis and therefore can eliminate the need to discard EEG data at the pre-processing stage. Hereafter, we will outline the main findings of this thesis in relation to local, global and interaction (global x local) effects, whilst considering differences between attention and sedation studies. Furthermore, we will discuss what possible relevance our findings may have to DoC. Thereafter, we will review the development of our method for re-aligning time-series data and summarise the key findings from this thesis. We will directly address each of the central hypotheses that were outlined within Chapter 2, before lastly discussing possible future directions for the research.

Local effect (MMN)

Mismatch negativity (MMN) is known to be sensitive to changes in expectancy and attention (Auksztulewicz & Friston, 2015; Chennu et al., 2013). We found that direct attention (active attention) enhanced the size of the mismatch response, whilst increased global expectancy in the form of a local deviant that was a globally regular pattern (GSLD), attenuated the size of the mismatch response; this is congruent with the findings of Wacongne et al. (2011). Interestingly, sensitivity to expectancy was also present when attention was passive; however, the overall size of the mismatch response is smaller, arguably through a lack of direct attention. It has previously been argued that attentional engagement affords a level precision, which enhances the size of early responses (local responses) to local auditory deviancy (Auksztulewicz & Friston, 2015). Sensitivity to global expectancy also attenuated local responses to auditory deviance for those in recovery (following sedation), possibly because sedation was not inhibiting the availability of cognitive resources at this point.

In contrast, when sedated, the size of the mismatch response was reduced, despite the presence of direct attention. This may suggest that sedation is somewhat dampening the level of precision afforded by direct attention, possibly because sedation imposes restriction on the availability of cognitive resources, as mentioned above. Furthermore, the presence of local deviance appears to impact on the latency of effects. More specifically, early negative responses to local deviance appear earlier than those of local standard across variations of attention and sedation, suggesting that incongruent stimuli are detected more rapidly by the brain than congruent stimuli at the local level. It could be argued that the latency of local responses is subject to the presence of local deviancy.

Notably, following the initial frontal negative response (N1 response), a P3a response is present across variations of attention and sedation. Although, when attention is not directed towards the task (ie. attention is passive), we observe the P3a response more frontally, which could suggest it may reflect a wandering attentional state, as previous work has shown that a frontal presentation P3a response is linked to the capture of attention by an unanticipated stimulus (Freidman, Cycowicz & Gaeta, 2001).

Altogether, at the local level, the latency of effects appears to depend upon the presence of locally deviant stimuli, whilst the size of the mismatch response is subject to changes in global expectancy and also attentional engagement with the task. Interestingly, we find that despite the presence of direct attention, reducing wakefulness can attenuate the size of the mismatch response, which may speak to the limited availability of cognitive resources, such as attention, in low levels of awareness.

Global effect (P3b)

Bekinschtein at el. (2009) originally proposed that the presence of a global effect, within the region of the P3b, might signify conscious processing. Interestingly however, we found that a global effect existed both at sedation and recovery, when attention was directed towards the task in both cases, suggesting that a reduction in wakefulness did not disrupt the attentional directive of the individual to detect instances of global deviance. One should note that sedation did not constitute a complete loss of consciousness and therefore is more likely to reflect a state of reduced wakefulness (drowsiness).

Moreover, we found that when attention was passive, there was a failure to detect global deviance that was marked by a locally standard quintuple (GDLS); this is possibly because one is not actively listening for instances of global deviance and therefore may miss occurrences where global deviance is marked by five identical tones. Alternatively, it may have been the case that those in the passive group were engaging in other cognitive processes that led to the pattern of results we observed. However, one may interpret these findings as global prediction error failing to reach the level of global expectation within the predictive hierarchy due to a lack of attentional engagement with the ongoing auditory task (ie. not counting the number of global deviants heard). That is, local regularity masks instances of global deviance when attention is passive, implying that attentional engagement with the task is necessary for the detection of global deviance as marked by a locally standard quintuple (GDLS). This finding speaks to Chennu et al.'s (2013) suggestion that the focus of top-down attention modulates responses to hierarchical violations in auditory regularity, which involve complex processing and the maintenance of auditory information across time.

Furthermore, the size of the global effect appears to be dependent upon both attention and sedation, that is, direct attention facilitates the presence of a P3b response, whilst sedation (a reduction in wakefulness) appears to reduce the amplitude and somewhat increase the latency of the P3b response. It is seemingly the case that global deviance elicits a P3b response because there is a violation of global regularity; meanwhile, globally standard conditions do not elicit a P3b response, as there is no violation in global regularity. Whilst the presence of a global effect within the region of the P3b may signify attentional engagement with the task, it cannot be considered a functionally isolated marker of conscious processing as we have found that the size and shape of P3b responses to global deviance are dependent upon the level of the local effect (ie. whether the quintuple is locally standard or locally deviant), and this is explained in more detail below.

Global x local

Bekinschtein et al. (2009) initially proposed that global and local effects were independent of one another and therefore one effect may be subtracted from another to view each in isolation. We have comprehensively addressed the matter of an interaction between global and local effects by re-analysing the data of Bekinschtein et al. (2009) using a factorial analysis, and further analysing the data of a study involving healthy sedation. Moreover, an interaction has previously been reported within the region of the local effect (Wacongne et al., 2011), although we have expanded upon this to report an interaction between global and local effects that is occurring within the region of the global effect (see Chapters 5 & 6).

We found that direct attention appears to be necessary for the detection of global deviance as a locally standard quintuple (GDLS), meaning that when attention is passive, responses to global deviance are dependent upon local regularity. What is more, when attention is directed towards the task, the shape and the latency of P3b responses to global deviance changes based again upon local regularity, that is, global deviance marked by a locally deviant quintuple (GDLD) elicits an earlier and shorter-lived P3b response comparing to global deviance that is marked by a locally standard quintuple (GDLS). Therefore, when the difference between responses to globally deviant stimuli

(GDLD & GDLS) are compared against the close to zero difference between responses to globally standard stimuli (GSLD & GSLS), an interaction between global and local effects appears within the region of the global effect. One may consider that when attention is directed towards the task, individuals are better able to detect instances of global deviance as they are actively listening for them. Seemingly, the brain not only detects both compositions of global deviance when attention is directed towards the task, but also elicits a different shape of P3b response based on local context; this difference was large enough within the recovered condition of the sedation study that it constituted a statistically significant interaction (when considered against responses to global standard).

In relation to a framework of predictive coding, it may be the case that a faster and shorter-lived P3b response to GDLD signifies prediction error at both local and global levels of the predictive hierarchy eliciting a sharp response to what is seemingly a complete violation of prediction (at both local and global levels). Conversely, a later and longer lasting P3b response to GDLS may reflect the time it takes for prediction error to reach the global level of the hierarchy, given that local regularity is preserved in this case (ie. there is no prediction error at the local level). Moreover, the increased duration of this response (compared with P3b responses to GDLD) may speak to the process of maintaining old and integrating new predictive contexts in working memory. Akin to Bekinschtein et al.'s (2009) original suggestion that conscious processing allows for the maintenance of perceptual representations across time.

Crucially, both when attention is directed towards the task and when attention is passive, an interaction is formed within the region of the global effect, but for different reasons. When attention is directed towards the task, the latency and shape of the P3b response to global deviancy changes dependent on the level of local regularity (ie. whether the quintuple is locally standard or locally deviant), this creates a disparity in the responses that compared with the close to zero difference in responses between globally standard conditions (GSLD & GSLS) creates an interaction within the region of the global effect. In the case of passive attention, there appears to be no marked P3b response to global deviancy that is presented as a locally standard quintuple (GDLS), therefore a disparity between responses to global deviance is created (as there *is* a marked P3b response to GDLD), which compared to the close to zero difference between globally standard

conditions (GSLD & GSLS) also creates an interaction within the region of the global effect.

In sum, the presence of local deviancy appears to accelerate responses to global deviance when attention is directed towards the task. Meanwhile, instances of local deviance appear to determine the presence of a response to global deviance when attention is passive. When wakefulness is reduced, the size of the difference between P3b responses to global deviance (dependent on local regularity) is reduced, which suggests that reduced wakefulness may dampen the ability to distinguish global deviance by local context. However, the presence of a P3b response to global deviance that is marked by a locally standard quintuple suggests that although a reduction in wakefulness may have dampened the size of effects within the study, it did not disrupt the attentional directive of the individual to attend to instances of global deviance. In this way, passive attention can be distinguished from reduced wakefulness (awareness) using ERP responses to the global-local task.

Relevance to DoC

Within this thesis, we have explored the possibility that an interaction exists between global and local effects within the region of the global effect, which suggests the global effect may not be a functionally isolated marker of conscious processing, as originally proposed by Bekinschtein et al. (2009). Our findings suggest that direct attention may be indexed by the presence of a P3b response to global deviance that is marked by a locally standard quintuple (GDLS). Furthermore, there is the possibility that a level of healthy sedation inhibits the availability of cognitive resources, which reduces the size of responses without disrupting the attentional directive of the individual. These findings may bare relevance to those in DoC, given that responses to the global-local task may reveal an interaction between effects (global and local), which can be dissected and understood with a mind to attentional focus and the availability of cognitive resources. In other words, the composition of an interaction between global and local effects may help to indicate a level of cognitive processing that can be associated with conscious perception (ie. conscious processing). Crucially, it is the composition of an interaction between global and local effects, which reveals the brain's predictive nature and thus

may inform a judgement about whether or not one possesses the cognitive ability to consciously process the task (the global-local task). With this in mind, we present the ideas within this section as only possible considerations for thought following the findings of this thesis. We firmly acknowledge the neural complexity underlying human consciousness and would like to emphasise the need for further research to determine a reliable marker of conscious processing.

Re-alignment method for time-series data

Within this thesis, we presented a method for handling discontinuity within time-series data, specifically EEG data. The method corrects discontinuity occurring between and across time-points that may contribute to the estimation of subsequent statistical analysis. Discontinuity was defined as a large shift in amplitude between consecutive time-points (two-four) resulting from problems during the digitisation process. In order to ensure the method was capturing discontinuity and not just noise within the data, we applied the method to the sedation dataset, which included high amounts of noise but no discontinuity. We found that the method did not alter the sedation time-series, despite the large amount of noise it contained. Thus, we propose that the method is a viable way of eliminating artificial discontinuity whilst maintaining the integrity of the raw data (including artefacts) for subsequent pre-processing and statistical analysis.

Key findings

The key findings within this thesis are summarised below:

- A level of sedation (reduced wakefulness) counteracts the enhanced MMN afforded by direct attention.
- The P3a response occurs frontally when attention is passive, but centrally when attention is directed towards the task.
- Direct attention may be necessary for the detection of global deviance as marked by a locally standard quintuple (GDLS).
- An interaction between global and local effects occurs within a late time window (820-1288ms), that is, the region of the global effect, seemingly because P3b

responses to global deviance vary in latency and shape subject to levels of the local effect when attention is directed towards the task.

Central hypotheses (revisited)

1. ***We proposed that an interaction between global and local effects within the region of the global effect might exist***.

2. ***We proposed that the interaction between global and local effects within the region of the global effect would be subject to changes in attention and wakefulness.***

An interaction between global and local effects within the region of the global effect was found to occur when attention was passive, due in part to the possible failure to detect (elicit a marked P3b response to) global deviance that was marked by a locally standard quintuple (GDLS). Alternatively, we also found that an interaction between global and local effects within the region of the global effect exists when attention is directed towards the task, but for a different reason. When attention is directed towards the task, P3b responses to global deviance vary in shape and latency dependent on the level of local regularity, which creates a disparity in responses at the global level that is reliant upon local context (LD vs. LS). Altogether, this suggests that an interaction between global and local effects can manifest whether or not attention is directed towards the task. However, the composition of the interaction in relation to responses to global deviance (not globally standard stimuli, as differences between responses were always close to zero) may indicate whether an individual is actively attending to the task.

3. ***We proposed that the interaction between global and local effects within the region of the global effect would also be subject to changes in expectancy.***

Our findings suggest that the local context of global irregularity is crucial to the manifestation of the global response (P3b response), particularly as responses to globally standard stimuli do not elicit a P3b response. One may argue that direct attention is critical for the maintenance of global expectancy, as local regularity may mask global deviance when attention is not directed towards the task (ie. attention is passive). More specifically, when attention is passive, higher levels of the predictive hierarchy are more difficult to access, resulting in reliance upon lower-level predictive contexts (ie. the local tonal features of the task) to determine global patterns of irregularity; this may be why we observe a P3b response to GDLD but not GDLS when attention is passive.

Moreover, when attention is directed towards the task, the shape and latency of the P3b response is dependent upon the level of the local effect, which suggests that not only is global expectancy impacting upon early responses to local deviance (as found by Wacongne et al., 2011), but also that local expectancy is impacting upon the manifestation of global responses to deviancy when attention is directed toward the task. One may argue that the level of precision afforded by direct engagement with the task allows not only for the detection of global deviancy as both a locally standard and locally deviant quintuple (GDLD & GDLS), but also for the distinction of global deviancy by local context (as the shape of P3b response changes between GDLD & GDLS with active attention).

Conclusion

The work within this thesis expands upon the existing literature on responses to the global-local task by no longer considering the global and local effects in isolation, but investigating an interaction between them. What is more, we have explored the composition of an interaction between global and local effects to reveal differences in responses to global deviancy that are subject to the direction of attention and the level of wakefulness. Our findings can be interpreted within a predictive coding framework,

whereby an interaction between global and local effects is indicative of a complex hierarchy of auditory predictions that consider both global and local predictive contexts subject to the availability (and direction) of cognitive resources.

Future work

Whilst we acknowledge that some of the work within this thesis should be viewed in light of a number of limitations, we are optimistic that future work would alleviate a number of concerns that have arisen.

Firstly, one may want to directly compare, within one study, manipulations of attention and manipulations of sedation in relation to the global-local task. This would address the issue of comparing two separate studies within one analysis. What is more, one may be inclined to implement a more absolute level of sedation, whereby participants are gradually sedated and administered the global-local task at varying levels of sedation. This may reveal how sedation is impacting upon response to the global-local task as an individual gradually loses consciousness (ie. as wakefulness is reduced). In addition, to examine in more detail how the interaction between global and local effects may be changing across levels of attention, one may introduce another interference condition and observe how responses compare to those within passive and active attention conditions.

Furthermore, one could attempt to construct a neural network model, which accounts for responses to both global and local violations in auditory regularity. Particularly, one would like to account for global violations in auditory regularity based on the presence of an interaction between global and local effects, therefore expanding on the findings of this thesis. Moreover, one would also consider how manipulations of attention and wakefulness impact upon such a network, with a mind to the clinical relevance of such work to DoC.

Lastly, one would hope to explore the presence of an interaction between global and local effects (within the region of the global effect) with patients in low awareness states specifically (DoC); this would address a greater level of complexity with respect to marking conscious processing. Those with DoC can in some cases be transiently aware;

therefore one may plausibly expect to find an interaction when an individual is able to direct their attention towards the global-local task. As mentioned previously, this may indicate a level of cognitive processing that could be associated with conscious perception (conscious processing) and therefore serve as a marker of cognitive ability in these individuals.

Whilst we are optimistic about the applicability of the research within this thesis, we acknowledge the complexity of studying human consciousness as a concept, as well as the complexity around attempting to measure conscious processing. We would therefore like to close this thesis by stating that the detection of neural markers of human consciousness, by observing the activity expressed through EEG, is not an attempt to reduce human consciousness into an objective measurement, but is in fact an exploration into the cognitive components which underlie one of the most highly debated concepts in neuroscience. Consequently, the work presented within this thesis has been an extension of an existing body of research, which is focussed on exploring the neural activity associated with conscious processing; this lends to the enhancement of a collective understanding around the cognition behind human consciousness.

Appendix

Appendix 1: Statistical results of cluster–level analyses

Below are tables containing the statistical results of the cluster-level analyses conducted in Chapters 4-7. Each analysis is presented within its own section and tables within sections 1.1, 1.4 and 1.7 are split between main effects and interactions for ease of presentation.

1.1. Three-way ANOVA (attention x global x local) summary tables of main effects and interactions (Chapter 4):

Table A1.1.1.1. Cluster-level analysis summary table for main effects: Attention (A – active vs. passive), Local (L – deviant vs. standard), and Global (G – deviant vs. standard). Cluster forming threshold of 0.01 and FWE_{corr} = 0.05. The significant clusters ($P_{FWE\text{-}corr}$) and their corresponding cluster size (K_E) are presented for each main effect. Degrees of freedom = [1,80]. The peaks (local maxima) of each active cluster (F-value) and their location in time and space are also shown. With regard to spatial position of peaks of clusters, the origin (0,0) is at the electrode Cz and (x,y) shows the coordinates of the peaks; i.e. +x shows a position on right hemisphere and +y a position at the front of the scalp. The highest peak in a significant cluster is presented in bold. The peaks that are not significant after the peak-level FWE correction are presented in italic. We have presented up to three peaks in each significant cluster. The height threshold for cluster forming threshold is F = 6.96. Voxel level refers to uncorrected statistics, i.e. after a cluster forming threshold is set (here at 0.01), every single voxel in a cluster can be significant at an uncorrected level.

Effect	Cluster-level statistics		Peak-level statistics	F-value	Local maxima			Voxel level
	$P_{FWE\text{-}corr}$	K_E	$P_{FWE\text{-}corr}$		x	y	ms	
A	0.000	2713	*0.369*	*17.92*	*26*	*-19*	*976*	*0.000*
			0.505	*16.71*	*30*	*-25*	*936*	*0.000*
			0.721	*15.03*	*17*	*-14*	*968*	*0.000*
L	0.000	18051	**0.000**	**196.29**	**-13**	**18**	**732**	**0.000**
			0.000	193.25	4	40	732	0.000
			0.000	188.19	9	24	732	0.000
	0.000	5938	**0.000**	**115.81**	**-13**	**18**	**816**	**0.000**
			0.000	114.01	0	13	828	0.000
			0.000	96.14	4	34	812	0.000
G	0.000	4628	**0.001**	**36.24**	**17**	**-9**	**944**	**0.000**
			0.025	26.39	26	-9	976	0.000
			0.130	*21.35*	*17*	*-3*	*980*	*0.000*

Table A1.1.1.2. Cluster-level analysis summary table for interactions: Attention x Local (AxL), Attention x Global (AxG), Global x local (GxL) and Attention x Global x local (AxGxL). Cluster forming threshold of 0.01 and FWE_{corr} = 0.05. The significant clusters ($P_{FWE-corr}$) and their corresponding cluster size (K_E) are presented for each main effect. Degrees of freedom = [1,80]. The peaks (local maxima) of each active cluster (F-value) and their location in time and space are also shown. With regard to spatial position of peaks of clusters, the origin (0,0) is at the electrode Cz and (x,y) shows the coordinates of the peaks; i.e. +x shows a position on right hemisphere and +y a position at the front of the scalp. The highest peak in a significant cluster is presented in bold. The peaks that are not significant after the peak-level FWE correction are presented in italic. We have presented up to three peaks in each significant cluster. The height threshold for cluster forming threshold is F = 6.96. Voxel level refers to uncorrected statistics, i.e. after a cluster forming threshold is set (here at 0.01), every single voxel in a cluster can be significant at an uncorrected level.

Effect	Cluster-level statistics		Peak-level statistics	F-value	Local maxima			Voxel level
	$P_{FWE-corr}$	K_E	$P_{FWE-corr}$		x	y	ms	
AxL	0.008	1633	**0.035**	**25.34**	**-21**	**24**	**712**	**0.000**
			0.039	25.00	-21	34	716	0.000
			0.538	*16.45*	*4*	*61*	*712*	*0.000*
AxG	0.000	4841	**0.010**	**29.19**	**26**	**-41**	**976**	**0.000**
			0.028	26.03	9	-57	972	0.000
			0.139	*21.15*	*30*	*-36*	*1052*	*0.000*
	0.007	1677	*0.118*	*21.66*	*-55*	*-3*	*976*	*0.000*
			0.125	*21.48*	*-34*	*2*	*976*	*0.000*
			0.565	*16.24*	*-51*	*-9*	*1080*	*0.000*
	0.010	1556	*0.736*	*14.90*	*-9*	*29*	*1060*	*0.000*
			0.783	*14.51*	*-9*	*29*	*1088*	*0.000*
			0.825	*14.14*	*-4*	*29*	*1152*	*0.000*
GxL	0.003	1951	**0.041**	**24.88**	**-13**	**2**	**772**	**0.000**
			0.285	*18.83*	*21*	*29*	*716*	*0.000*
			0.314	*18.49*	*-13*	*8*	*732*	*0.000*
	0.010	1577	*0.166*	*20.59*	*64*	*13*	*900*	*0.000*
			0.183	*20.29*	*64*	*13*	*924*	*0.000*
			0.258	*19.17*	*68*	*2*	*900*	*0.000*
AxGxL	0.418	515	0.192	20.14	43	-9	684	0.000
			0.943	12.73	30	8	660	0.001
			0.999	10.27	60	-57	680	0.002

1.2. Two-way ANOVA (global x local) for active attention group simple effects analyses (Chapter 5):

Table A1.1.2.1. Cluster-level analysis summary table for effects: Local (L), Global (G) and Global x local (GxL) for the simple effects analysis of the active attention group. Cluster forming threshold of 0.01 and FWE_{corr} = 0.01. The significant clusters ($P_{FWE\text{-}corr}$) and their corresponding cluster size (K_E) are presented for each main effect. Degrees of freedom = [1,40]. The peaks (local maxima) of each active cluster (F-value) and their location in time and space are also shown. With regard to spatial position of peaks of clusters, the origin (0,0) is at the electrode Cz and (x,y) shows the coordinates of the peaks; i.e. +x shows a position on right hemisphere and +y a position at the front of the scalp. The highest peak in a significant cluster is presented in bold. The peaks that are not significant after the peak-level FWE correction are presented in italic. We have presented up to three peaks in each significant cluster. The height threshold for cluster forming threshold is F = 7.31. Voxel level refers to uncorrected statistics, i.e. after a cluster forming threshold is set (here at 0.01), every single voxel in a cluster can be significant at an uncorrected level.

Effect	Cluster-level statistics		Peak-level statistics	F-value	Local maxima			Voxel level
	$P_{FWE\text{-}corr}$	K_E	$P_{FWE\text{-}corr}$		x	y	ms	
L	0.000	3711	**0.000**	**108.17**	**-13**	**18**	**738**	**0.000**
			0.000	103.81	13	24	732	0.000
	0.000	4288	**0.000**	**65.33**	**26**	**-68**	**728**	**0.000**
			0.000	61.42	51	-36	720	0.000
			0.000	59.70	-9	-95	732	0.000
	0.000	3144	**0.001**	**47.54**	**68**	**-25**	**828**	**0.000**
			0.004	38.71	60	-3	820	0.000
			0.006	36.77	26	-9	796	0.000
	0.001	2907	**0.001**	**45.82**	**0**	**8**	**828**	**0.000**
			0.001	44.19	0	-3	828	0.000
			0.006	36.94	-13	18	828	0.000
	0.003	2232	**0.022**	**31.49**	**-60**	**-46**	**828**	**0.000**
			0.035	29.53	-51	-19	824	0.000
			0.061	*27.36*	*-47*	*-19*	*808*	*0.000*
G	0.000	5118	*0.114*	*24.82*	*26*	*-14*	*976*	*0.000*
			0.197	*22.57*	*4*	*-57*	*952*	*0.000*
			0.201	*22.48*	*17*	*-9*	*972*	*0.000*
GxL	0.077	1094	0.228	21.96	-9	-3	772	0.000
			0.828	15.18	-13	-8	736	0.000
			0.983	12.30	-21	-9	768	0.001

1.3. Two-way ANOVA (global x local) for passive attention group simple effects analyses (Chapter 5):

Table A1.1.3.1. Cluster-level analysis summary table of effects: Local (L), Global (G) and Global x local (GxL) for the simple effects analysis of the passive attention group. Cluster forming threshold of 0.01 and FWE_{corr} = 0.01. The significant clusters ($P_{FWE\text{-}corr}$) and their corresponding cluster size (K_E) are presented for each main effect. Degrees of freedom = [1,40]. The peaks (local maxima) of each active cluster (F-value) and their location in time and space are also shown. With regard to spatial position of peaks of clusters, the origin (0,0) is at the electrode Cz and (x,y) shows the coordinates of the peaks; i.e. +x shows a position on right hemisphere and +y a position at the front of the scalp. The highest peak in a significant cluster is presented in bold. The peaks that are not significant after the peak-level FWE correction are presented in italic. We have presented up to three peaks in each significant cluster. The height threshold for cluster forming threshold is F = 7.31. Voxel level refers to uncorrected statistics, i.e. after a cluster forming threshold is set (here at 0.01), every single voxel in a cluster can be significant at an uncorrected level.

Effect	Cluster-level statistics		Peak-level statistics	F-value	Local maxima			Voxel level
	$P_{FWE\text{-}corr}$	K_E	$P_{FWE\text{-}corr}$		x	y	ms	
L	0.000	10435	**0.000**	**126.04**	**9**	**45**	**732**	**0.000**
			0.000	100.69	9	18	728	0.000
			0.000	94.55	0	18	728	0.000
	0.000	6191	**0.000**	**124.46**	**-13**	**18**	**728**	**0.000**
			0.000	118.49	0	56	804	0.000
			0.000	116.15	4	40	812	0.000
	0.000	4074	**0.000**	**106.40**	**30**	**-52**	**728**	**0.000**
			0.000	72.79	55	-52	724	0.000
			0.000	68.82	51	-62	724	0.000
G	0.022	1357	*0.380*	*20.18*	*26*	*-14*	*940*	*0.000*
			0.838	*15.48*	*0*	*24*	*984*	*0.000*
			0.888	*14.84*	*-34*	*2*	*976*	*0.000*
GxL	0.021	1367	*0.146*	*24.28*	*9*	*-57*	*904*	*0.000*
			0.197	*23.03*	*-17*	*-36*	*904*	*0.000*
			0.514	*18.71*	*13*	*-14*	*924*	*0.000*
	0.000	3693	*0.536*	*18.49*	*38*	*-3*	*812*	*0.000*
			0.728	*16.64*	*60*	*29*	*924*	*0.000*
			0.752	*16.40*	*68*	*-41*	*1016*	*0.000*

1.4. Three-way ANOVA (sedation x global x local) summary tables of main effects and interactions (Chapter 6):

Table A1.1.4.1. Cluster-level analysis summary table for main effects: Sedation (S – sedated vs. recovered), Local (L – deviant vs. standard), and Global (G – deviant vs. standard). Cluster forming threshold of 0.01 and $FWE_{corr} = 0.05$. The significant clusters ($P_{FWE\text{-}corr}$) and their corresponding cluster size (K_E) are presented for each main effect. Degrees of freedom = [1,136]. The peaks (local maxima) of each active cluster (F-value) and their location in time and space are also shown. With regard to spatial position of peaks of clusters, the origin (0,0) is at the electrode Cz and (x,y) shows the coordinates of the peaks; i.e. +x shows a position on right hemisphere and +y a position at the front of the scalp. The highest peak in a significant cluster is presented in bold. The peaks that are not significant after the peak-level FWE correction are presented in italic. We have presented up to three peaks in each significant cluster. The height threshold for cluster forming threshold is F = 6.82. Voxel level refers to uncorrected statistics, i.e. after a cluster forming threshold is set (here at 0.01), every single voxel in a cluster can be significant at an uncorrected level.

Effect	Cluster-level statistics		Peak-level statistics	F-value	Local maxima			Voxel level
	$P_{FWE\text{-}corr}$	K_E	$P_{FWE\text{-}corr}$		x	y	ms	
S	0.069	1506	0.000	34.59	-65	-25	708	0.000
	0.000	6594	0.003	28.06	23	26	716	0.000
			0.003	27.80	23	9	712	0.000
			0.020	23.05	36	-8	708	0.000
	0.000	6531	*0.053*	*20.52*	*36*	*-43*	*980*	*0.000*
			0.056	*20.36*	*-36*	*-31*	*940*	*0.000*
			0.085	*19.23*	*45*	*-37*	*984*	*0.000*
L	0.000	18262	**0.000**	**80.87**	**9**	**-20**	**856**	**0.000**
			0.000	77.76	-0	-20	852	0.000
			0.000	75.84	23	-14	856	0.000
	0.000	10834	**0.000**	**36.86**	**-63**	**-60**	**844**	**0.000**
			0.000	33.76	5	20	1048	0.000
			0.002	29.10	-0	15	1100	0.000
	0.000	4921	**0.000**	**35.72**	**5**	**26**	**720**	**0.000**
			0.000	35.64	18	26	720	0.000
			0.000	34.83	-18	26	720	0.000
	0.013	2338	**0.001**	**30.20**	**-59**	**-48**	**716**	**0.000**
			0.016	23.71	63	-43	716	0.000
			0.203	*16.81*	*-0*	*-94*	*724*	*0.000*
G	0.000	38436	**0.000**	**162.43**	**-5**	**-54**	**1024**	**0.000**
			0.000	142.42	-0	-60	960	0.000
			0.000	140.24	-9	-54	1064	0.000
	0.000	29022	**0.000**	**113.74**	**5**	**61**	**1152**	**0.000**
			0.000	95.76	5	72	1054	0.000
			0.000	94.03	-0	66	1104	0.000
	0.067	1523	0.404	14.69	-9	-83	752	0.000
			0.706	12.46	-59	-66	720	0.001
			0.716	12.38	-50	-71	724	0.001

Table A1.1.4.2. Cluster-level analysis summary table for interactions: Sedation x Local (SxL), Sedation x Global (SxG), Global x local (GxL) and Sedation x Global x local (SxGxL). Cluster forming threshold of 0.01 and FWE_{corr} = 0.05. The significant clusters ($P_{FWE-corr}$) and their corresponding cluster size (K_E) are presented for each main effect. Degrees of freedom = [1,136]. The peaks (local maxima) of each active cluster (F-value) and their location in time and space are also shown. With regard to spatial position of peaks of clusters, the origin (0,0) is at the electrode Cz and (x,y) shows the coordinates of the peaks; i.e. +x shows a position on right hemisphere and +y a position at the front of the scalp. The highest peak in a significant cluster is presented in bold. The peaks that are not significant after the peak-level FWE correction are presented in italic. We have presented up to three peaks in each significant cluster. The height threshold for cluster forming threshold is F = 6.82. Voxel level refers to uncorrected statistics, i.e. after a cluster forming threshold is set (here at 0.01), every single voxel in a cluster can be significant at an uncorrected level.

Effect	Cluster-level statistics		Peak-level statistics	F-value	Local maxima			Voxel level
	$P_{FWE-corr}$	K_E	$P_{FWE-corr}$		x	y	ms	
SxL	0.001	4271	**0.011**	**24.67**	**-5**	**-14**	**816**	**0.000**
			0.015	23.87	32	-3	824	0.000
			0.019	23.20	14	-25	812	0.000
	0.005	2899	*0.320*	*15.45*	*18*	*-37*	*1024*	*0.000*
			0.345	*15.21*	*9*	*-43*	*1024*	*0.000*
			0.476	*14.12*	*5*	*-71*	*1116*	*0.000*
SxG	0.000	6954	*0.097*	*18.89*	*-27*	*-25*	*940*	*0.000*
			0.123	*18.23*	*-32*	*-25*	*1108*	*0.000*
			0.143	*17.81*	*32*	*-43*	*1056*	*0.000*
GxL	0.000	15175	**0.000**	**37.45**	**-5**	**9**	**1152**	**0.000**
			0.000	34.03	-9	15	1104	0.000
			0.001	31.10	-18	-14	1208	0.000
	0.000	6214	**0.004**	**27.16**	**9**	**-20**	**856**	**0.000**
			0.014	23.97	23	-14	848	0.000
			0.019	23.18	27	-8	844	0.000
SxGxL	0.000	6218	**0.026**	**22.36**	**-5**	**-37**	**1220**	**0.000**
			0.054	*20.43*	*18*	*-31*	*1020*	*0.000*
			0.055	*20.38*	*5*	*-60*	*1224*	*0.000*
	0.014	2306	*0.259*	*16.10*	*41*	*49*	*1176*	*0.000*
			0.266	*16.02*	*41*	*61*	*1028*	*0.000*
			0.320	*15.45*	*41*	*61*	*1128*	*0.000*

1.5. Two-way ANOVA (global x local) for recovered condition simple effects analyses (Chapter 6):

Table A1.1.5.1. Cluster-level analysis summary table of effects: Local (L), Global (G) and Global x local (GxL) for the simple effects analysis of the recovered condition. Cluster forming threshold of 0.01 and FWE_{corr} = 0.01. The significant clusters ($P_{FWE\text{-}corr}$) and their corresponding cluster size (K_E) are presented for each main effect. Degrees of freedom = [1,68]. The peaks (local maxima) of each active cluster (F-value) and their location in time and space are also shown. With regard to spatial position of peaks of clusters, the origin (0,0) is at the electrode Cz and (x,y) shows the coordinates of the peaks; i.e. +x shows a position on right hemisphere and +y a position at the front of the scalp. The highest peak in a significant cluster is presented in bold. The peaks that are not significant after the peak-level FWE correction are presented in italic. We have presented up to three peaks in each significant cluster. The height threshold for cluster forming threshold is F = 7.02. Voxel level refers to uncorrected statistics, i.e. after a cluster forming threshold is set (here at 0.01), every single voxel in a cluster can be significant at an uncorrected level.

Effect	Cluster-level statistics		Peak-level statistics	F-value	Local maxima			Voxel level
	$P_{FWE\text{-}corr}$	K_E	$P_{FWE\text{-}corr}$		x	y	ms	
L	0.000	18244	**0.000**	**110.06**	**23**	**-14**	**852**	**0.000**
			0.000	93.06	-9	-20	844	0.000
			0.000	88.08	9	-8	844	0.000
	0.000	5020	**0.000**	**54.47**	**-18**	**26**	**716**	**0.000**
			0.000	48.21	18	32	720	0.000
	0.074	1602	0.000	43.84	-63	-66	844	0.000
			0.197	17.84	-59	15	852	0.000
			0.244	17.13	-53	-37	896	0.000
	0.012	2606	**0.000**	**37.22**	**-54**	**-66**	**716**	**0.000**
			0.009	27.43	53	-54	716	0.000
			0.011	26.95	53	-66	712	0.000
	0.000	12825	**0.001**	**33.59**	**9**	**9**	**1056**	**0.000**
			0.010	27.29	5	15	1100	0.000
			0.041	22.81	23	-31	1116	0.000
G	0.000	39221	**0.000**	**191.81**	**-5**	**-54**	**1056**	**0.000**
			0.000	187.64	9	-60	1040	0.000
			0.000	182.64	-0	-60	1040	0.000
	0.000	28446	**0.000**	**96.45**	**-0**	**61**	**1152**	**0.000**
			0.000	85.83	-5	66	1056	0.000
			0.000	85.78	-9	61	1108	0.000
	0.064	1678	0.031	23.68	-59	-66	716	0.000
			0.515	14.36	-14	-94	720	0.000
			0.776	12.25	-14	-94	768	0.001
GxL	0.000	17391	**0.000**	**40.31**	**-18**	**-14**	**1216**	**0.000**
			0.001	36.10	-0	-25	1212	0.000
			0.001	34.91	9	-20	1204	0.000
	0.000	6499	**0.004**	**29.85**	**32**	**-8**	**844**	**0.000**
			0.016	25.80	-18	-31	848	0.000
			0.039	22.98	-23	-25	904	0.000
	0.002	3697	*0.121*	*19.40*	*45*	*55*	*1260*	*0.000*
			0.123	*19.36*	*45*	*55*	*1132*	*0.000*
			0.145	*18.84*	*45*	*55*	*1160*	*0.000*

1.6. Two-way ANOVA (global x local) for sedated condition simple effects analyses (Chapter 6):

Table A1.1.6.1. Cluster-level analysis summary table of effects: Local (L), Global (G) and Global x local (GxL) for the simple effects analysis of the sedated condition. Cluster forming threshold of 0.01 and FWE_{corr} = 0.01. The significant clusters ($P_{FWE-corr}$) and their corresponding cluster size (K_E) are presented for each main effect. Degrees of freedom = [1,68]. The peaks (local maxima) of each active cluster (F-value) and their location in time and space are also shown. With regard to spatial position of peaks of clusters, the origin (0,0) is at the electrode Cz and (x,y) shows the coordinates of the peaks; i.e. +x shows a position on right hemisphere and +y a position at the front of the scalp. The highest peak in a significant cluster is presented in bold. The peaks that are not significant after the peak-level FWE correction are presented in italic. We have presented up to three peaks in each significant cluster. The height threshold for cluster forming threshold is F = 7.02. Voxel level refers to uncorrected statistics, i.e. after a cluster forming threshold is set (here at 0.01), every single voxel in a cluster can be significant at an uncorrected level.

Effect	Cluster-level statistics		Peak-level statistics	F-value	Local maxima			Voxel level
	$P_{FWE-corr}$	K_E	$P_{FWE-corr}$		x	y	ms	
L	0.000	4967	**0.003**	**31.45**	**50**	**-20**	**900**	**0.000**
			0.010	27.11	5	-20	856	0.000
			0.140	18.99	18	-43	928	0.000
	0.001	4611	*0.363*	*15.78*	*-18*	*32*	*1128*	*0.000*
			0.539	*14.21*	*-9*	*38*	*1020*	*0.000*
			0.581	*13.88*	*-5*	*20*	*1104*	*0.000*
	0.045	1858	*0.474*	*14.76*	*54*	*-31*	*984*	*0.000*
			0.668	*13.19*	*59*	*-31*	*1020*	*0.001*
			0.828	*11.83*	*5*	*-71*	*1020*	*0.001*
	0.058	1723	0.573	13.94	5	20	688	0.000
			0.631	13.48	18	3	688	0.000
			0.961	10.06	18	-31	708	0.002
G	0.000	32420	**0.000**	**88.40**	**-0**	**-54**	**1024**	**0.000**
			0.000	81.00	-5	-54	1148	0.000
			0.000	78.47	-18	-66	1148	0.000
	0.000	20607	**0.000**	**84.41**	**9**	**61**	**1232**	**0.000**
			0.000	55.79	9	61	1148	0.000
			0.000	60.49	45	55	1028	0.000
GxL	0.005	3101	*0.299*	*16.48*	*-5*	*15*	*1156*	*0.000*
			0.514	*14.41*	*23*	*15*	*1084*	*0.000*
			0.663	*13.23*	*-9*	*15*	*1100*	*0.001*

1.7. Three-way ANOVA (task context x global x local) summary tables of main effects and interactions (Chapter 7):

Table A1.1.7.1. Cluster-level analysis summary table for main effects: Task Context (TC – active, passive sedated or recovered), Local (L – deviant vs. standard), and Global (G – deviant vs. standard). Cluster forming threshold of 0.01 and FWE_{corr} = 0.01. The significant clusters ($P_{FWE\text{-}corr}$) and their corresponding cluster size (K_E) are presented for each main effect. Degrees of freedom = [3,160]. The peaks (local maxima) of each active cluster (F-value) and their location in time and space are also shown. With regard to spatial position of peaks of clusters, the origin (0,0) is at the electrode Cz and (x,y) shows the coordinates of the peaks; i.e. +x shows a position on right hemisphere and +y a position at the front of the scalp. The highest peak in a significant cluster is presented in bold. The peaks that are not significant after the peak-level FWE correction are presented in italic. We have presented up to three peaks in each significant cluster. The height threshold for cluster forming threshold is F = 3.91. Voxel level refers to uncorrected statistics, i.e. after a cluster forming threshold is set (here at 0.01), every single voxel in a cluster can be significant at an uncorrected level.

Effect	Cluster-level statistics		Peak-level statistics	F-value	Local maxima			Voxel level
	$P_{FWE\text{-}corr}$	K_E	$P_{FWE\text{-}corr}$		x	y	ms	
TC	0.000	41320	**0.000**	**53.17**	**30**	**-36**	**1012**	**0.000**
			0.000	44.05	34	-30	1096	0.000
			0.000	41.97	30	-36	980	0.000
	0.000	6277	**0.000**	**32.41**	**26**	**24**	**708**	**0.000**
			0.000	23.10	-17	18	7000	0.000
			0.000	19.90	43	-9	724	0.000
	0.000	11111	**0.000**	**15.71**	**43**	**56**	**1020**	**0.000**
			0.000	14.51	43	56	972	0.000
			0.000	13.84	9	72	1020	0.000
L	0.000	17345	**0.000**	**125.70**	**0**	**-14**	**828**	**0.000**
			0.000	107.93	-4	8	824	0.000
			0.000	86.05	-21	-19	856	0.000
	0.000	6186	**0.000**	**115.50**	**68**	**-25**	**820**	**0.000**
			0.000	112.59	68	-19	804	0.000
			0.000	86.20	-64	-52	824	0.000
	0.000	5614	**0.000**	**93.39**	**-13**	**24**	**728**	**0.000**
			0.000	91.60	0	18	728	0.000
			0.000	89.16	4	40	728	0.000
	0.000	4878	**0.000**	**26.50**	**0**	**13**	**1096**	**0.000**
			0.000	24.10	0	13	1056	0.000
			0.000	16.57	17	24	1080	0.000
G	0.000	40771	**0.000**	**170.66**	**4**	**-62**	**1028**	**0.000**
			0.000	151.53	-13	-52	1024	0.000
			0.000	146.80	0	-57	948	0.000
	0.000	26589	**0.000**	**59.08**	**4**	**40**	**1216**	**0.000**
			0.000	53.59	4	45	1148	0.000
			0.000	53.07	47	51	1028	0.000

Table A1.1.7.2. Cluster-level analysis summary table for interactions: Task Context x Local (TCxL), Task Context x Global (TCxG), Global x local (GxL) and Task Context x Global x local (TCxGxL). Cluster forming threshold of 0.01 and FWE_{corr} = 0.01. The significant clusters ($P_{FWE-corr}$) and their corresponding cluster size (K_E) are presented for each main effect. Degrees of freedom = [3,160]. The peaks (local maxima) of each active cluster (F-value) and their location in time and space are also shown. With regard to spatial position of peaks of clusters, the origin (0,0) is at the electrode Cz and (x,y) shows the coordinates of the peaks; i.e. +x shows a position on right hemisphere and +y a position at the front of the scalp. The highest peak in a significant cluster is presented in bold. The peaks that are not significant after the peak-level FWE correction are presented in italic. We have presented up to three peaks in each significant cluster. The height threshold for cluster forming threshold is F = 3.91. Voxel level refers to uncorrected statistics, i.e. after a cluster forming threshold is set (here at 0.01), every single voxel in a cluster can be significant at an uncorrected level.

Effect	Cluster-level statistics		Peak-level statistics	F-value	Local maxima			Voxel level
	$P_{FWE-corr}$	K_E	$P_{FWE-corr}$		x	y	ms	
TCxL	0.000	16697	**0.000**	**34.56**	**38**	**-3**	**824**	**0.000**
			0.000	27.28	26	-14	820	0.000
			0.000	20.10	17	-25	816	0.000
TCxG	0.000	32484	**0.000**	**47.78**	**4**	**-62**	**1028**	**0.000**
			0.000	41.19	26	-41	1024	0.000
			0.000	40.74	17	-52	1028	0.000
	0.000	11705	**0.000**	**19.29**	**47**	**51**	**1020**	**0.000**
			0.000	16.64	47	51	972	0.000
			0.000	15.43	55	29	972	0.000
GxL	0.000	10768	**0.000**	**39.35**	**-4**	**13**	**1100**	**0.000**
			0.000	38.98	-13	18	1096	0.000
			0.003	28.35	-9	2	1196	0.000
	0.000	5107	**0.003**	**28.04**	**-4**	**-57**	**940**	**0.000**
			0.005	26.71	-9	-41	940	0.000
			0.005	26.53	0	-30	856	0.000
TCxGxL	0.000	6855	**0.002**	**12.75**	**38**	**-9**	**832**	**0.000**
			0.010	10.99	47	51	1204	0.000
			0.014	10.64	43	56	1116	0.000
	0.000	10801	**0.002**	**12.41**	**13**	**-14**	**1196**	**0.000**
			0.002	12.30	13	-19	1108	0.000
			0.003	12.25	21	-41	1112	0.000

Appendix 2: Channel labels after elimination of crown electrodes

Below is a map of the channel locations (electrode positions on the scalp) that corresponds to all analyses presented within this thesis. Channel map presented in Chapter 2 (Figure 2.1) represents standard EGI sensor net channel locations, however after channel elimination for statistical analysis locations were re-labelled by SPM as below. All channel labels for ERPs presented within this thesis correspond to labels as below. Channel FidNz represents the nasion. Fid T9 and Fid T10 represent the respective mastoid electrodes, which contribute to the re-referencing that takes place in the pre-processing stage of data analysis (see 'pre-processing' in Chapter 4). Midline electrodes Fz, Cz and Pz are presented in blue.

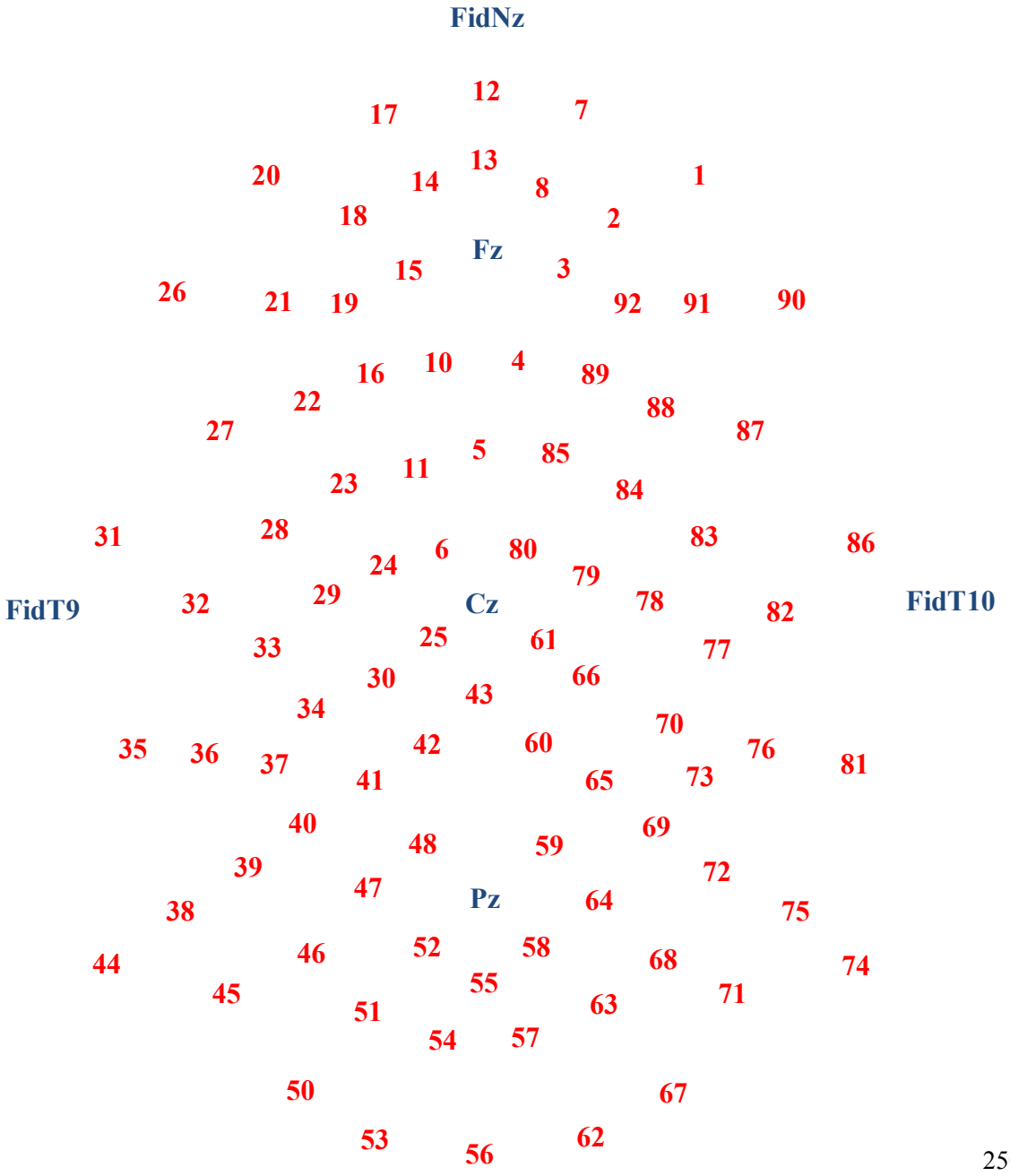

Appendix 3: Left lateralised cluster observed within the attention x global interaction (Chapter 4)

Here we present the ERP for the left lateralised significant cluster observed within the Attention (active vs. passive) x Global (deviant vs. standard) interaction in Chapter 4 (Figure 4.15). The cluster appears around 976ms in the region of frontal electrode ch.22 and appears to be the opposite side of the dipole observed at this time.

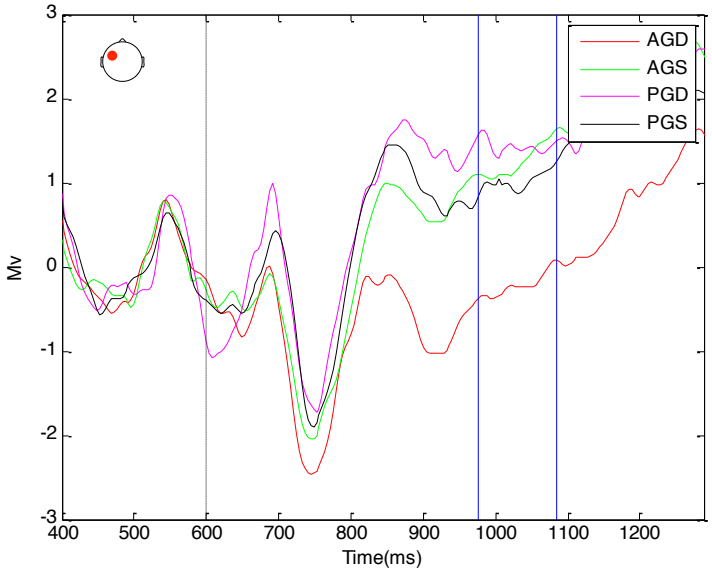

Figure A3.1. Grand average ERPs for the attention x global interaction at ch. 15. Blue lines indicate the region of significance. Black dashed line (600ms) indicates the onset of the final tone. (A: active condition, P: passive condition).

Appendix 4: Statistical results of the exploratory analysis discussed within Chapter 7

Below are tables containing the statistical results of the exploratory cluster-level analysis containing 22 participants from the attention study (11 active and 11 passive) and 18 participants from the sedation study (discussed in Chapter 7). The results reveal that including all 18 participants from the sedation study to the analysis changes the F-value of effects but does not change the pattern that we observe.

Table A4. 1 Cluster-level analysis summary table for main effects: Task Context (TC – active, passive sedated or recovered), Local (L – deviant vs. standard), and Global (G – deviant vs. standard). Cluster forming threshold of 0.01 and FWE_{corr} = 0.01. The significant clusters ($P_{FWE-corr}$) and their corresponding cluster size (K_E) are presented for each main effect. Degrees of freedom = [3,216]. The peaks (local maxima) of each active cluster (F-value) and their location in time and space are also shown. With regard to spatial position of peaks of clusters, the origin (0,0) is at the electrode Cz and (x,y) shows the coordinates of the peaks; i.e. +x shows a position on right hemisphere and +y a position at the front of the scalp. The highest peak in a significant cluster is presented in bold. The peaks that are not significant after the peak-level FWE correction are presented in italic. We have presented up to three peaks in each significant cluster. The height threshold for cluster forming threshold is F = 3.87. Voxel level refers to uncorrected statistics, i.e. after a cluster forming threshold is set (here at 0.01), every single voxel in a cluster can be significant at an uncorrected level.

Effect	Cluster-level statistics		Peak-level statistics	F-value	Local maxima			Voxel level
	$P_{FWE-corr}$	K_E	$P_{FWE-corr}$		x	y	ms	
TC	0.000	44455	**0.000**	**55.68**	**30**	**-36**	**1012**	**0.000**
			0.000	50.57	34	-30	1096	0.000
			0.000	48.60	30	-36	980	0.000
	0.000	8388	**0.000**	**22.98**	**26**	**24**	**708**	**0.000**
			0.000	20.53	-17	18	7000	0.000
			0.000	19.57	43	-9	724	0.000
	0.000	16269	**0.000**	**20.50**	**43**	**56**	**1020**	**0.000**
			0.000	19.78	43	56	972	0.000
			0.000	19.42	9	72	1020	0.000
L	0.000	20221	**0.000**	**145.28**	**0**	**-14**	**828**	**0.000**
			0.000	122.67	-4	8	824	0.000
			0.000	96.25	-21	-19	856	0.000
	0.000	12516	**0.000**	**139.92**	**68**	**-25**	**820**	**0.000**
			0.000	138.93	68	-19	804	0.000
			0.000	131.74	-64	-52	824	0.000
	0.000	7511	**0.000**	**38.40**	**-13**	**24**	**728**	**0.000**
			0.000	32.69	0	18	728	0.000
			0.000	28.02	4	40	728	0.000
G	0.000	47750	**0.000**	**188.48**	**4**	**-62**	**1028**	**0.000**
			0.000	180.64	-13	-52	1024	0.000
			0.000	173.21	0	-57	948	0.000
	0.000	34636	**0.000**	**96.56**	**4**	**40**	**1216**	**0.000**
			0.000	87.40	4	45	1148	0.000
			0.000	81.76	47	51	1028	0.000

Table A4. 2. Cluster-level analysis summary table for interactions: Task Context x Local (TCxL), Task Context x Global (TCxG), Global x local (GxL) and Task Context x Global x local (TCxGxL). Cluster forming threshold of 0.01 and FWE_{corr} = 0.01. The significant clusters ($P_{FWE-corr}$) and their corresponding cluster size (K_E) are presented for each main effect. Degrees of freedom = [3,216]. The peaks (local maxima) of each active cluster (F-value) and their location in time and space are also shown. With regard to spatial position of peaks of clusters, the origin (0,0) is at the electrode Cz and (x,y) shows the coordinates of the peaks; i.e. +x shows a position on right hemisphere and +y a position at the front of the scalp. The highest peak in a significant cluster is presented in bold. The peaks that are not significant after the peak-level FWE correction are presented in italic. We have presented up to three peaks in each significant cluster. The height threshold for cluster forming threshold is F = 3.87. Voxel level refers to uncorrected statistics, i.e. after a cluster forming threshold is set (here at 0.01), every single voxel in a cluster can be significant at an uncorrected level.

Effect	Cluster-level statistics		Peak-level statistics	F-value	Local maxima			Voxel level
	$P_{FWE-corr}$	K_E	$P_{FWE-corr}$		x	y	ms	
TCxL	0.000	15159	**0.000**	**34.33**	**38**	**-3**	**824**	**0.000**
			0.000	33.67	26	-14	820	0.000
			0.000	24.54	17	-25	816	0.000
	0.000	7537	0.000	14.91	-30	13	56	0.000
			0.000	13.57	30	-41	88	0.000
			0.000	13.08	34	24	56	0.000
	0.001	2561	*0.192*	*8.11*	*30*	*-41*	*436*	*0.000*
			0.258	*7.80*	*13*	*13*	*416*	*0.000*
			0.323	*7.55*	*-17*	*8*	*396*	*0.000*
TCxG	0.000	56501	**0.000**	**50.73**	**4**	**-62**	**1028**	**0.000**
			0.000	49.47	26	-41	1024	0.000
			0.000	43.24	17	-52	1028	0.000
	0.005	2096	**0.006**	**11.36**	**47**	**51**	**1020**	**0.000**
			0.287	*7.68*	*47*	*51*	*972*	*0.000*
			0.684	*6.54*	*26*	*34*	*56*	*0.000*
GxL	0.000	12894	**0.000**	**39.98**	**-4**	**13**	**1100**	**0.000**
			0.000	38.95	-13	18	1096	0.000
			0.003	37.86	-9	2	1196	0.000
	0.000	5107	**0.003**	**35.03**	**-4**	**-57**	**940**	**0.000**
			0.005	28.91	-9	-41	940	0.000
			0.005	28.34	0	-30	856	0.000
	0.013	2040	0.016	23.50	-13	2	124	0.000
			0.026	22.27	-9	13	132	0.000
			0.121	18.43	-30	-14	108	0.000
TCxGxL	0.000	21940	**0.002**	**14.712**	**38**	**-9**	**832**	**0.000**
			0.010	13.17	47	51	1204	0.000
			0.014	13.01	43	56	1116	0.000

Appendix 5: Table containing number of trials contributed to each condition across the four levels of task context

Below is a table containing the number of trials for each condition (standard vs. deviant) across the four levels of task context (active, passive, sedated and recovered). In Chapter 7, we highlighted the importance of maintaining the ratio between standard and deviant quintuple contributions. If, for example, the sedation study contributed more deviant quintuples to the analysis than the attention study contributed standard quintuples to the analysis, then this would be a confound. We found this not to be the case in our datasets, as globally standard trial numbers consistently out number globally deviant trial numbers:

Table A5.1. The number of quintuples in each condition (GDLD, GSLD, GDLS & GSLS) for the four levels of task context contributing to statistical analysis in Chapter 7. One can see that across the four levels of task context (active, passive, recovered and sedated), the number of globally deviant quintuples do not succeed the number of globally standard quintuples, ensuring that global regularity is maintained within the analysis.

	GDLD	**GSLD**	**GDLS**	**GSLS**
Active	960	2121	1083	1932
Passive	1035	1932	970	1953
Recovered	362	1686	362	1720
Sedated	364	1674	367	1701

Appendix 6: The main effect of task context (F-maps, T-maps and ERPs)

Here we present the F-maps, T-maps and ERPs for the main effect of task context (TC), as discussed in Chapter 7. The main effect of TC was considered to be a confounded effect as both confounds 1 and 2 were influencing what we observed during time windows of statistical significance (689-730ms and 892-1288ms) (see Figure A6.2).

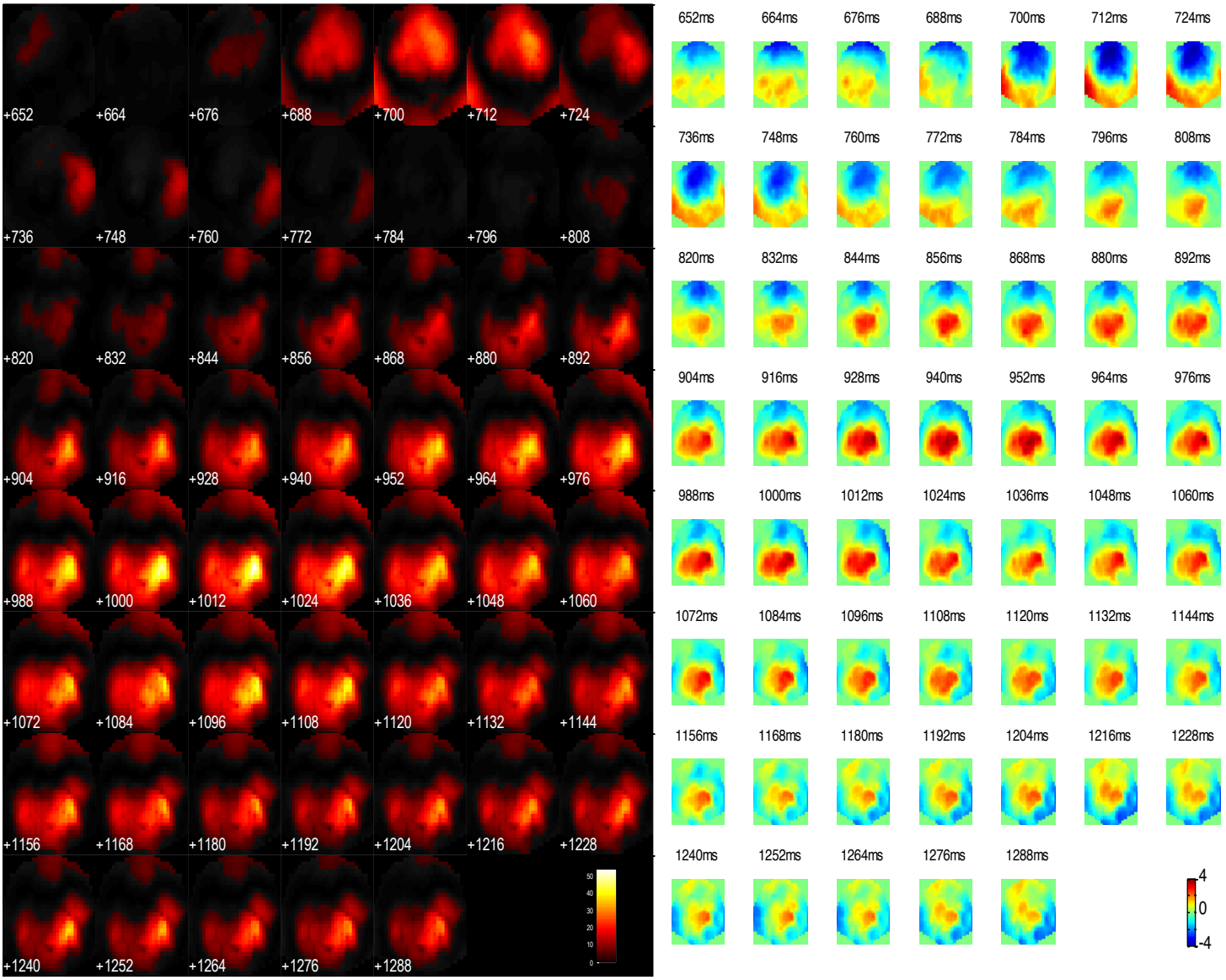

Figure A6.1. Thresholded F-maps ($p < .01$) to show regions of significance for the effect of task context on the scalp through time (left). Unthresholded T-maps to show the polarity of effect on the scalp through time (right). Front of the scalp is positioned at the top. Note that time within the left panel is presented below the corresponding row of scalpmaps, whilst time within the right panel is presented above the corresponding row of scalpmaps.

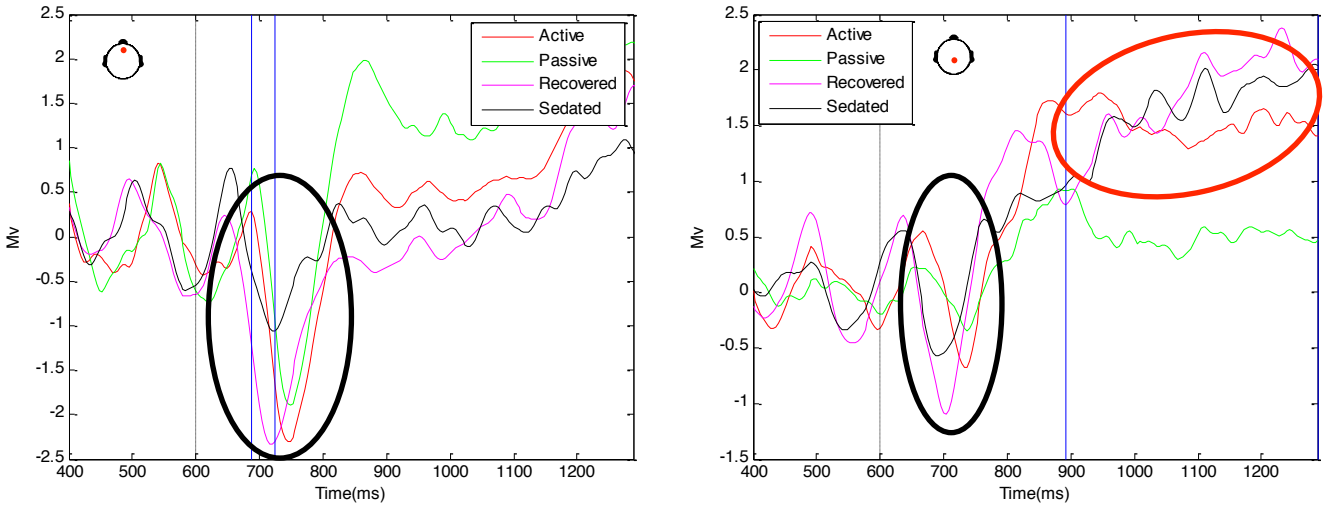

Figure A6.2. Grand average ERPs for the main effect of task context at Fz (left) and Pz (right). Blue lines indicate the region of significance (689-730ms and 892-1288ms). Black dashed line (600ms) indicates the onset of the final tone. Presence of Confound 1 (de-synchronisation of SSAEP) is circled in black. Presence of Confound 2 (drift within sedation dataset) is circled in red.

Appendix 7: ERPs for fringe effect observed within the task context x global x local interaction (Chapter 7)

Here we present the ERPs for the right lateralised fringe effect observed within the task context x global x local interaction (Figure 7.15). The effect is significant from 820-928ms around right lateral electrode ch. 78.

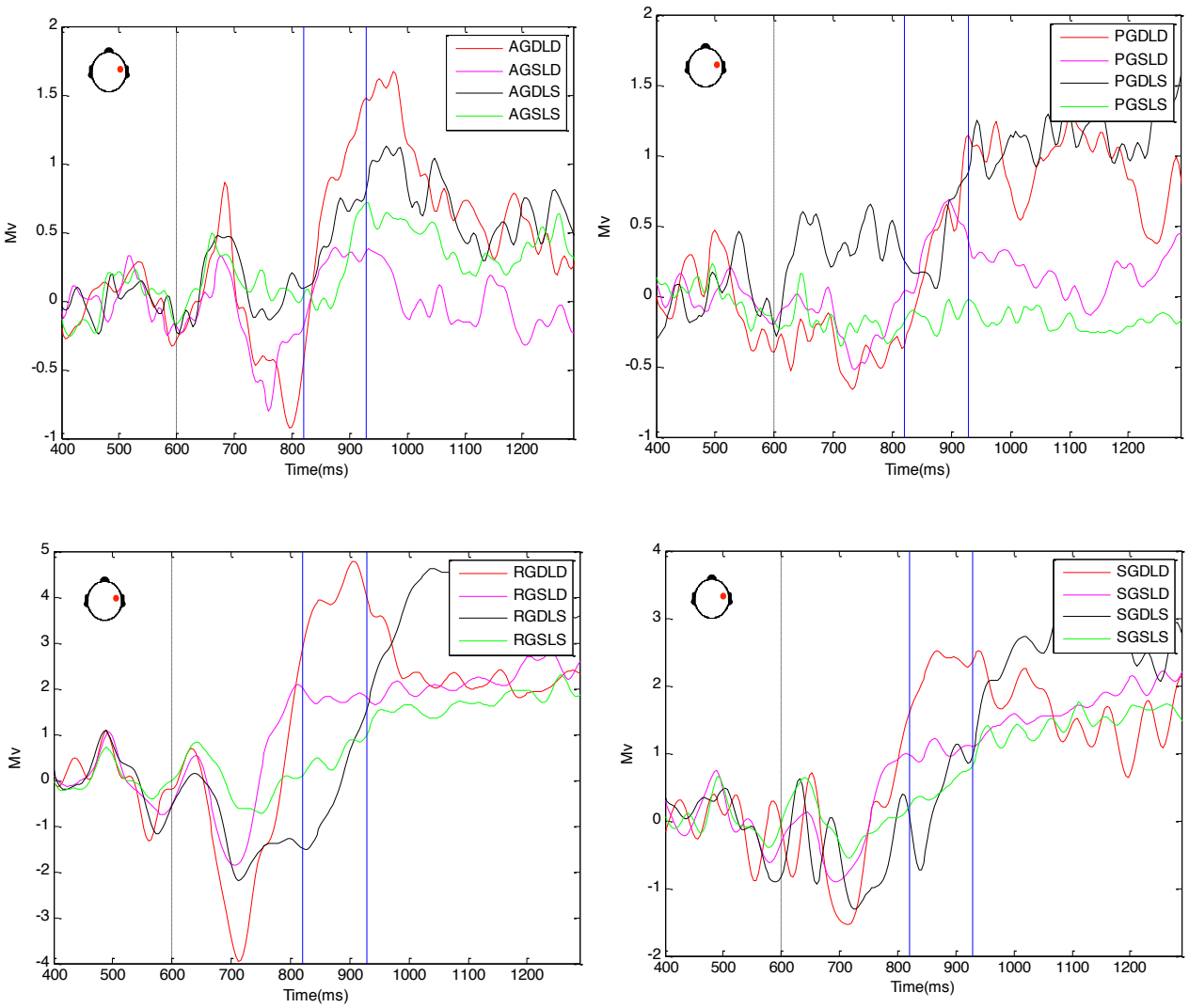

Figure A7.1. Grand average ERPs for the task context x global x local interaction at ch. 78 for all four conditions of task context (active: A, passive: P, recovered: R, sedated: S). Blue lines indicate the region of significance. Black dashed line (600ms) indicates the onset of the final tone.

Appendix 8: Preliminary investigations of difference thresholds in Version I of the method for re-alignment

Here we present the results of preliminary investigations we conducted using a number of difference thresholds in Version I of our method for re-aligning time-series data containing discontinuity (as discussed within Chapter 8).

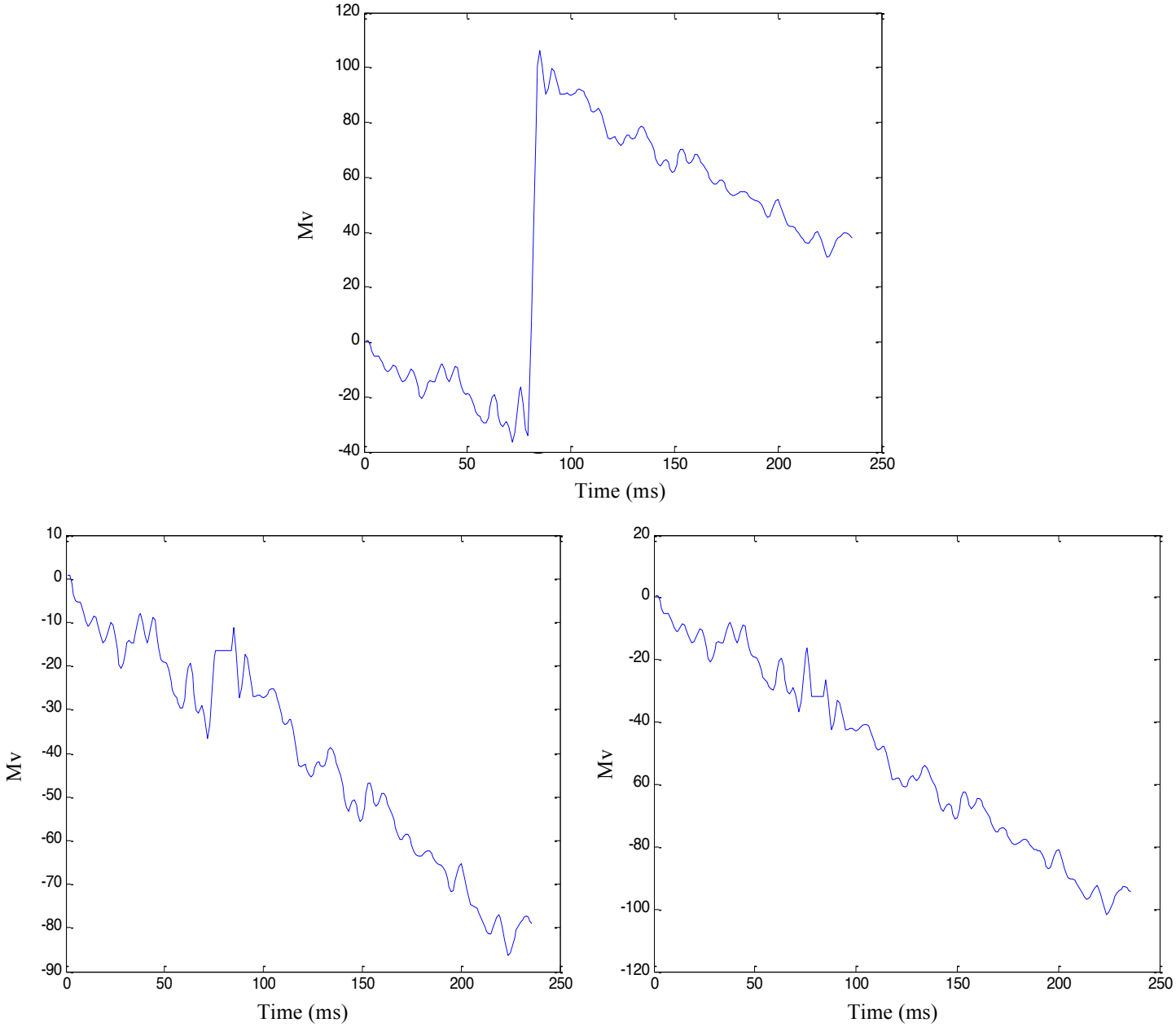

Figure A8.1. Top panel shows the raw time-series data from active participant 10 in the GDLD condition, trial 71at ch. 100. Top panel includes discontinuity between time-points 73-86 (circled in black). Bottom left panel shows the time-series after application of version I of our method with an arbitrary difference threshold of >2 across three consecutive time-points; one can see that this has not addressed the problem (circled in black). The bottom right panel shows the time-series after application of version I of our method with an arbitrary difference threshold of >0.5 between only two consecutive time-points; one can see that this does not address the problem (circled in black).

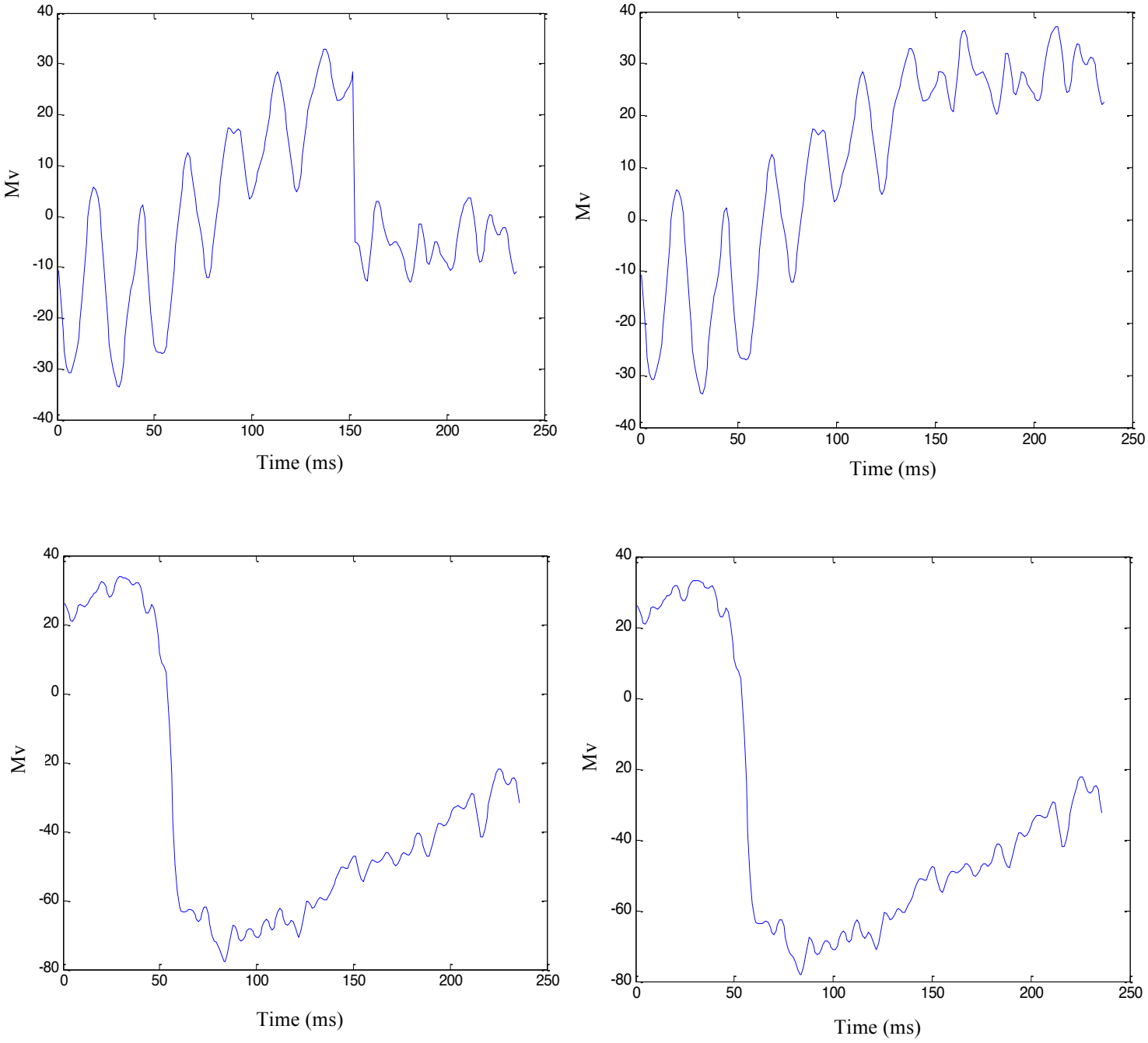

Figure A8.2. Top panels show the time-series data from active participant 5 in the GDLD condition, trial 29 at ch. 43. Top left shows the raw time-series data with discontinuity occurring between time-points 152-153 (circled in black). Top right shows the time-series after version I of our method was applied, with an arbitrary difference threshold of >15 between two consecutive time-points; one can see that this threshold appears to address the problem in this case. Bottom panels show the time-series data from active participant 8 in the GDLS condition, trial 144 at ch. 53. Bottom left shows the raw time-series data with what appears to be sequential discontinuity between time-points 16-21 (circled in black). Bottom right shows the time-series after version I of our method was applied, with an arbitrary difference threshold of >20 between two consecutive time-points. Version I of the method did not correct discontinuity within in the bottom right panel, suggesting that variation within the data may be noise as opposed to discontinuity. However, it may be the case that a number of sequential jumps in the data exist, which do not exceed a value of 20. Setting an arbitrary difference threshold may not capture all instances of discontinuity across trials.

Appendix 9: Preliminary investigations (using a Z-score threshold of 2) in Version II of the method for re-alignment

Below we present the results of preliminary investigations we conducted using a Z-score threshold of 2 from Version II of our method for re-aligning time-series data containing discontinuity (discussed within Chapter 8).

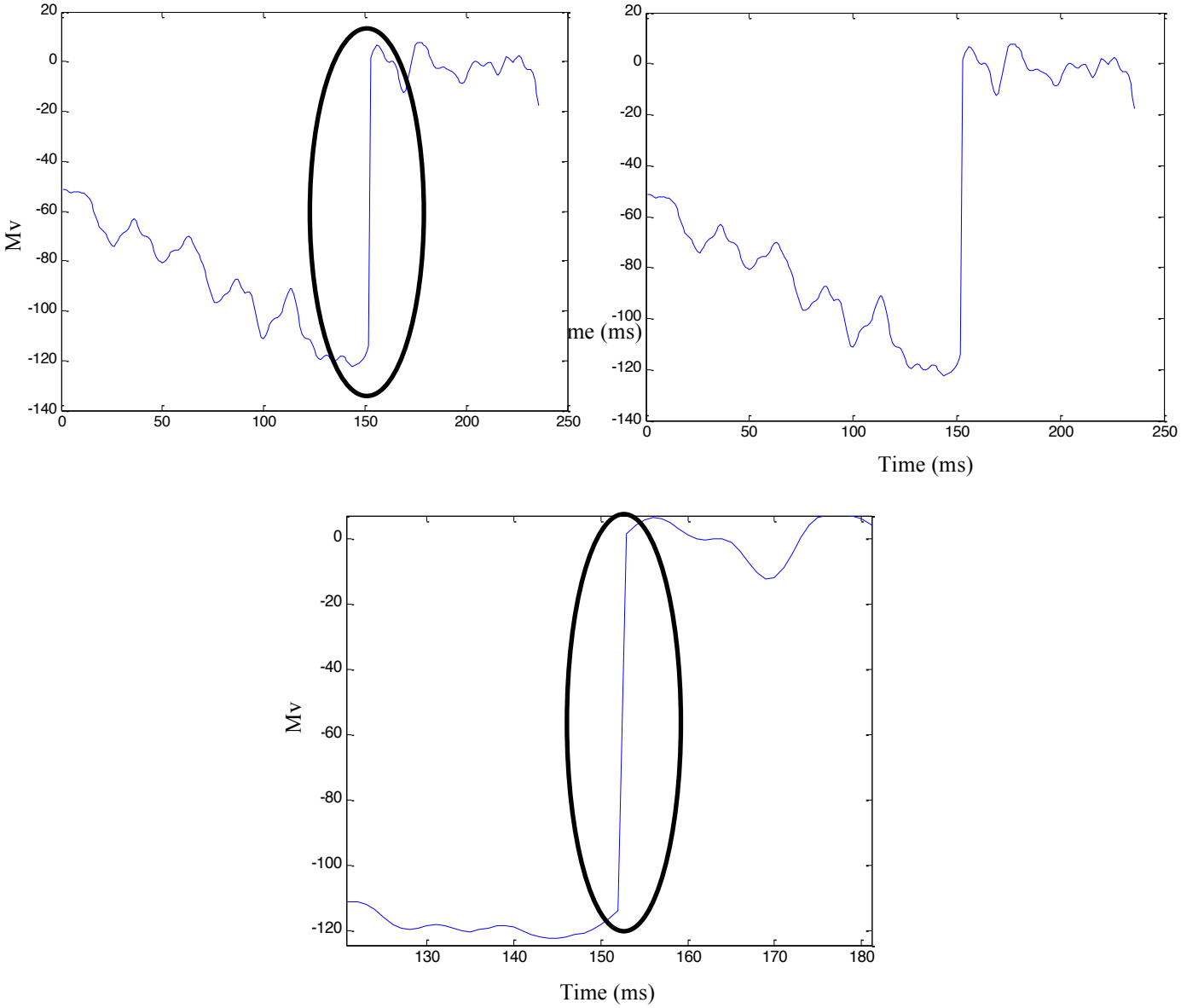

Figure A9.1. All panels show raw data from active participant 5 in the GDLD condition, trial 25 at ch. 49. Top left shows raw time-series with sequential jumps between time-points 152-156 (circled in black). Top right shows time-series after version II of our method was applied (Z-score = 2); one can see that discontinuity has not been remedied by the method as a Z-score threshold of 2 was not large enough to capture all instances of discontinuity when a series of jumps are increasing the amount of variance within the time-series. Bottom panel reveals that there are four sequential jumps within the raw time-series (circled in black).

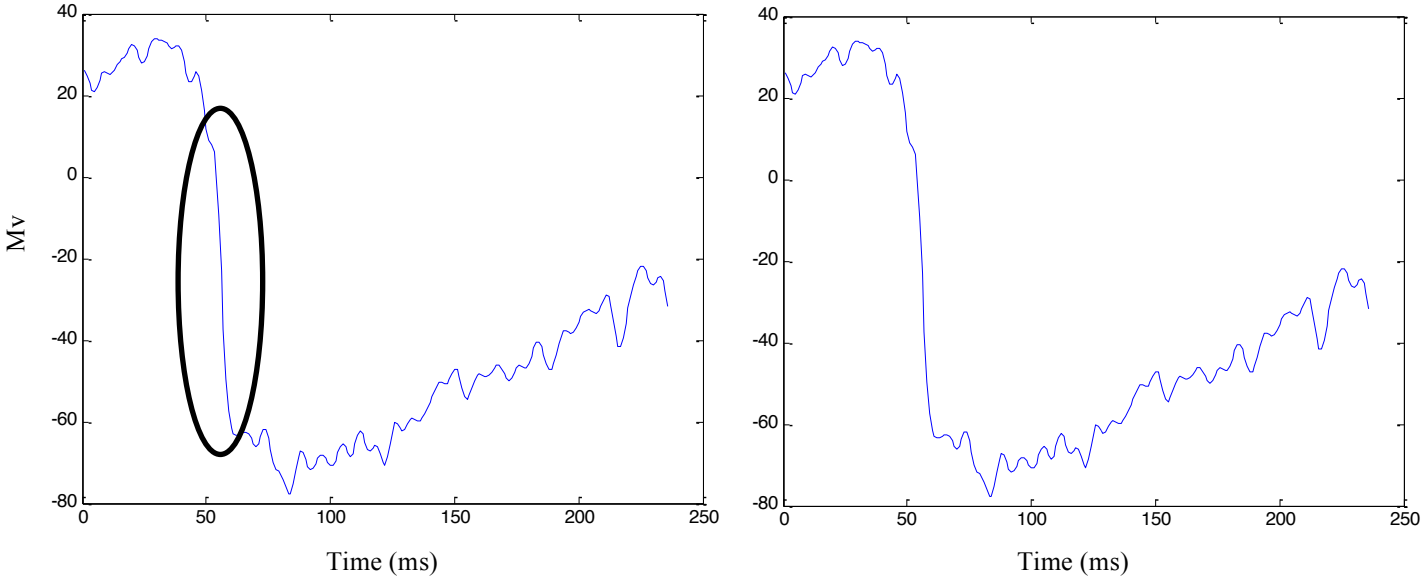

Figure A9.2. Both panels show raw time-series data from active participant 8 in the GDLS condition, trial 144 at ch. 53. Left panel shows raw time-series with discontinuity between time-points 16-21 (circled in black). Right right panel shows time-series after version II of our method was applied (Z-score = 2); one can see that discontinuity has not been remedied by the method as a Z-score threshold of 2 was not large enough to capture all instances of discontinuity when a series of jumps are increasing the amount of variance within the time-series.

Appendix 10: Preliminary investigations examining differing two-step Z-score thresholds within Version III of the method for re-alignment

Below are the results of preliminary investigations we conducted to examine the impact of differing two-step Z-score thresholds within Version III of our method to re-align time-series data containing discontinuity (discussed within Chapter 8). Differing combinations of Z-score thresholds impacted on the time-series depending on the amount of variation in the data (sometimes increased by a series of jumps between time-points).

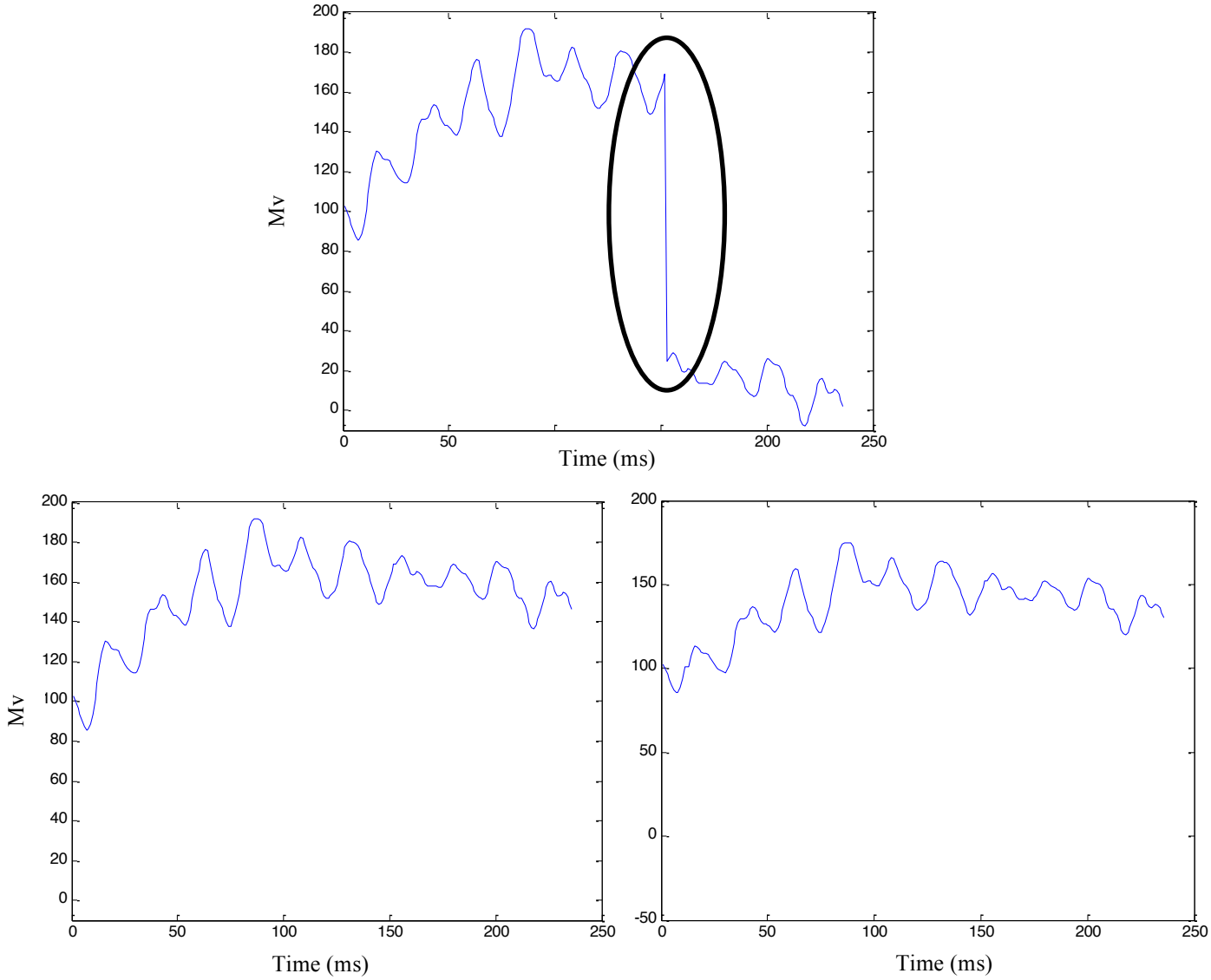

Figure A10.1. All panels show raw time-series data from active participant 5 in the GDLD condition, trial 25 at ch. 67. Top panel shows raw time-series with discontinuity between time-points 152-153 (circled in black). Bottom right panel shows time-series after version III of our method was applied with first-pass Z-score threshold = 3 and second pass Z-score threshold = 4. Bottom left panel shows time–series after version III of our method was applied with first pass Z-score threshold = 7 and second pass Z-score threshold = 8. One can see that the higher Z-score thresholds preserve more of the variance within the data comparing to lower Z-score thresholds, whilst also removing discontinuity.

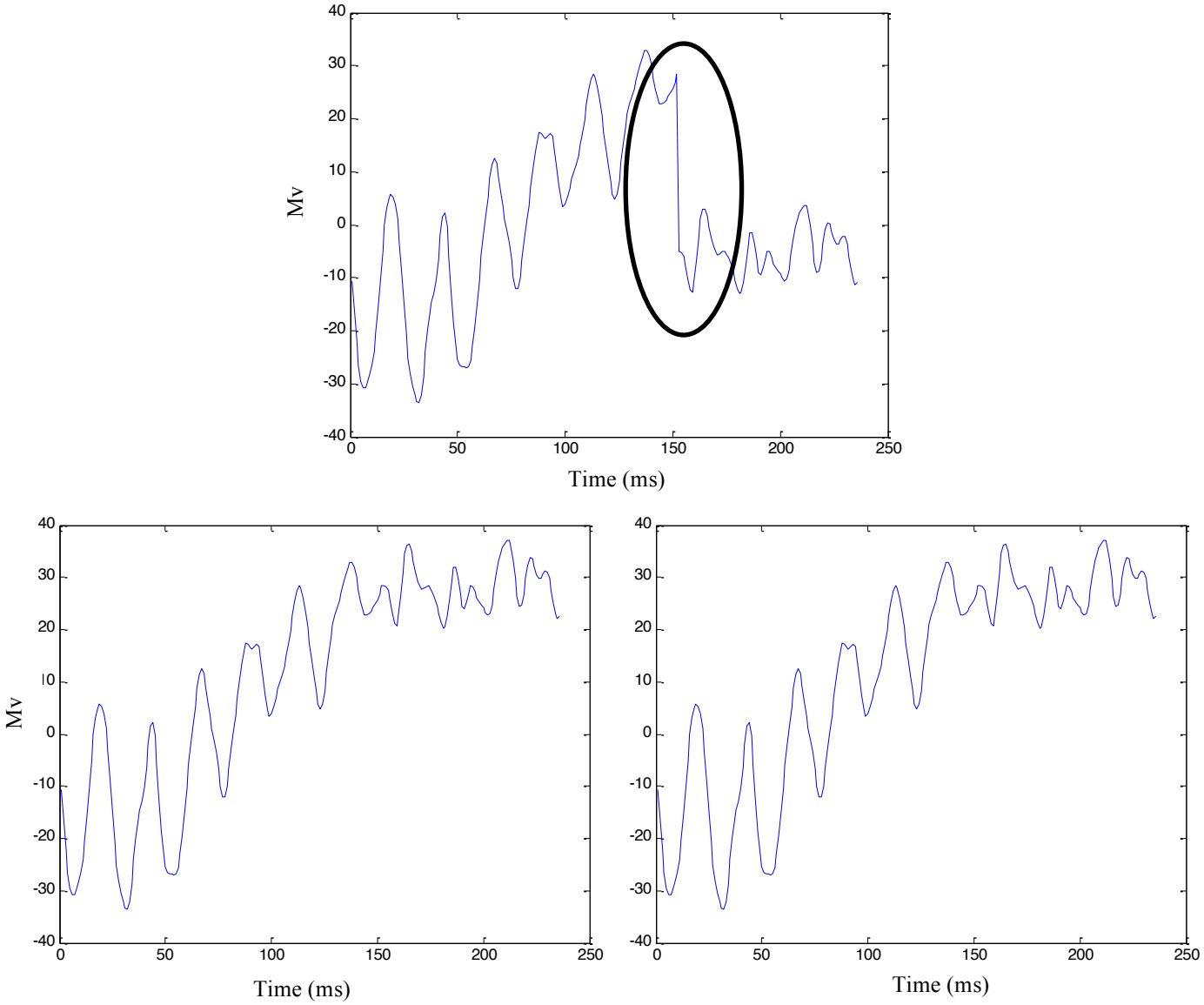

Figure A10.2. All panels show raw time-series data from active participant 5 in the GDLD condition, trial 29 at ch. 43. Top panel shows raw time-series with discontinuity between time-points 152-153 (circled in black). Bottom right panel shows time-series after version III of our method was applied with first-pass Z-score threshold = 9 and second pass Z-score threshold = 10. Bottom left panel shows time–series after version III of our method was applied with first pass Z-score threshold = 7 and second pass Z-score threshold = 8. One can see that in both instances (bottom panels) the two-pass Z-score thresholds have captured discontinuity and maintained variance within the time-series.

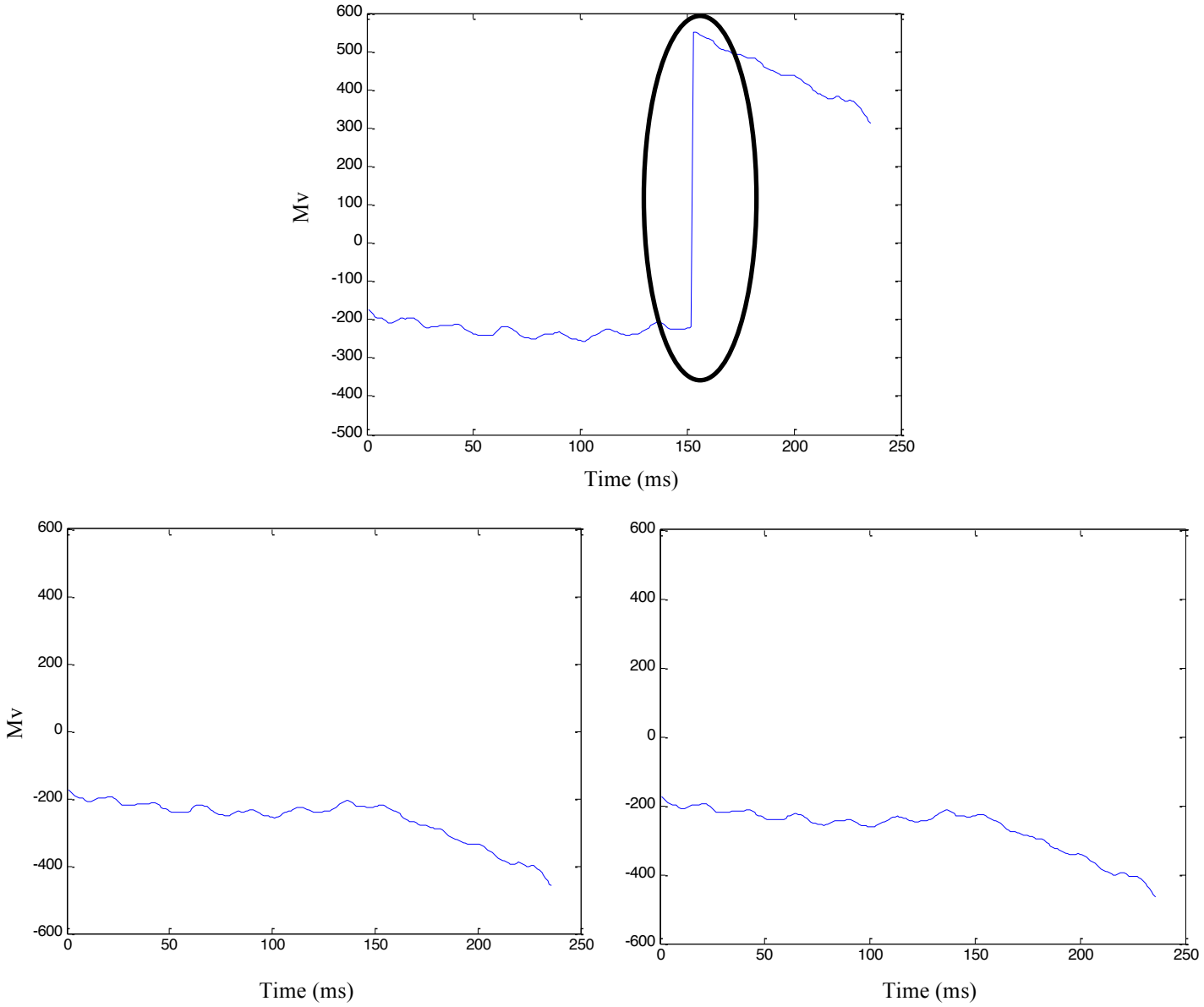

Figure A10.3. All panels show raw time-series data from active participant 5 in the GDLD condition, trial 45 at ch. 22. Top panel shows raw time-series with discontinuity between time-points 152-153 (circled in black). Bottom right panel shows time-series after version III of our method was applied with first-pass Z-score threshold = 11 and second pass Z-score threshold = 12. Bottom left panel shows time–series after version III of our method was applied with first pass Z-score threshold = 7 and second pass Z-score threshold = 8. One can see that in both instances (bottom panels) the two-pass Z-score thresholds have captured discontinuity and maintained variance within the time-series.

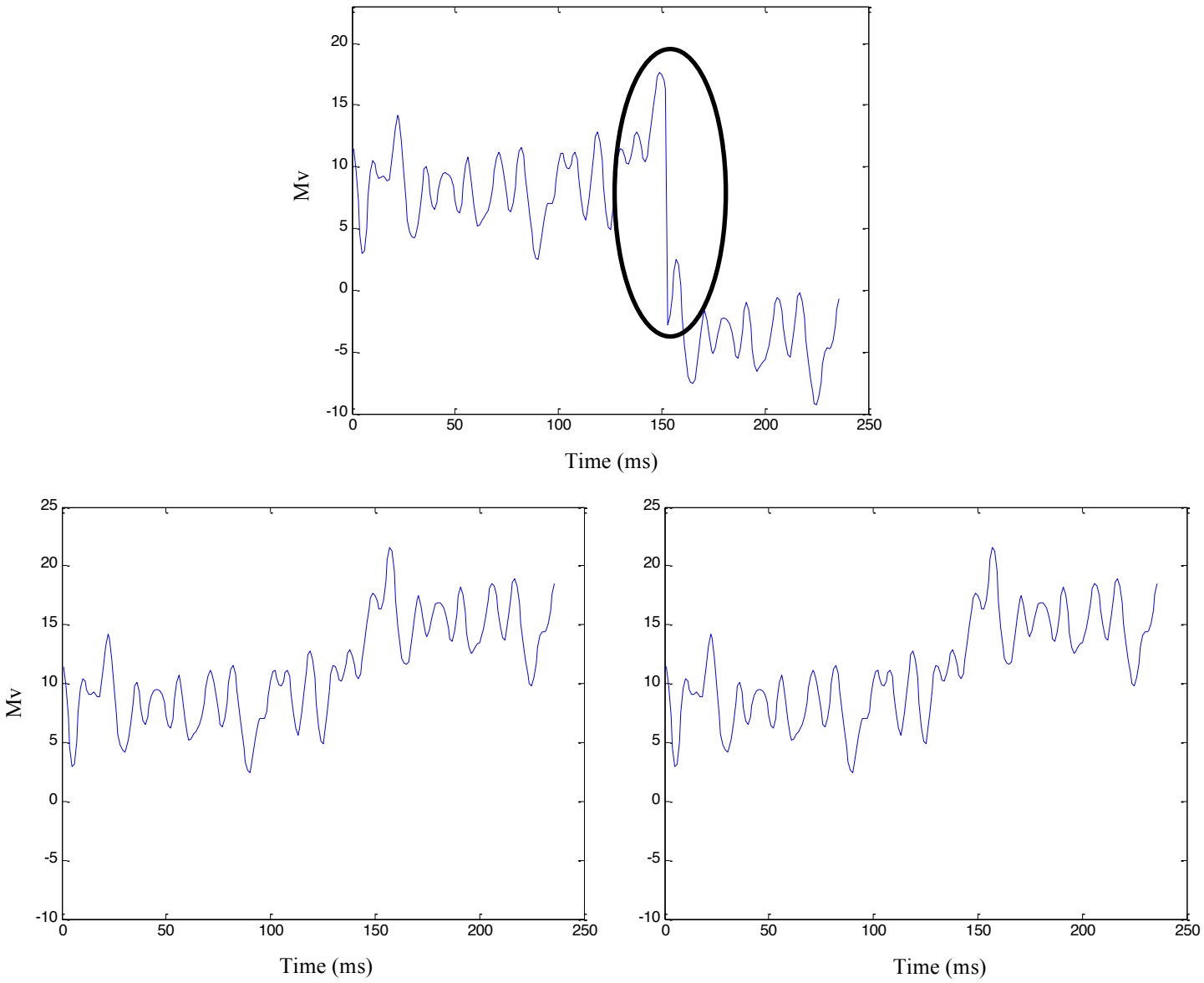

Figure A10.4. All panels show raw time-series data from passive participant 8 in the GSLS condition, trial 61 at ch. 43. Top panel shows raw time-series with discontinuity between time-points 152-153 (circled in black). Bottom right panel shows time-series after version III of our method was applied with first-pass Z-score threshold = 3 and second pass Z-score threshold = 4. Bottom left panel shows time–series after version III of our method was applied with first pass Z-score threshold = 7 and second pass Z-score threshold = 8. One can see that in both instances (bottom panels) the two-pass Z-score thresholds have captured discontinuity and maintained variance within the time-series.

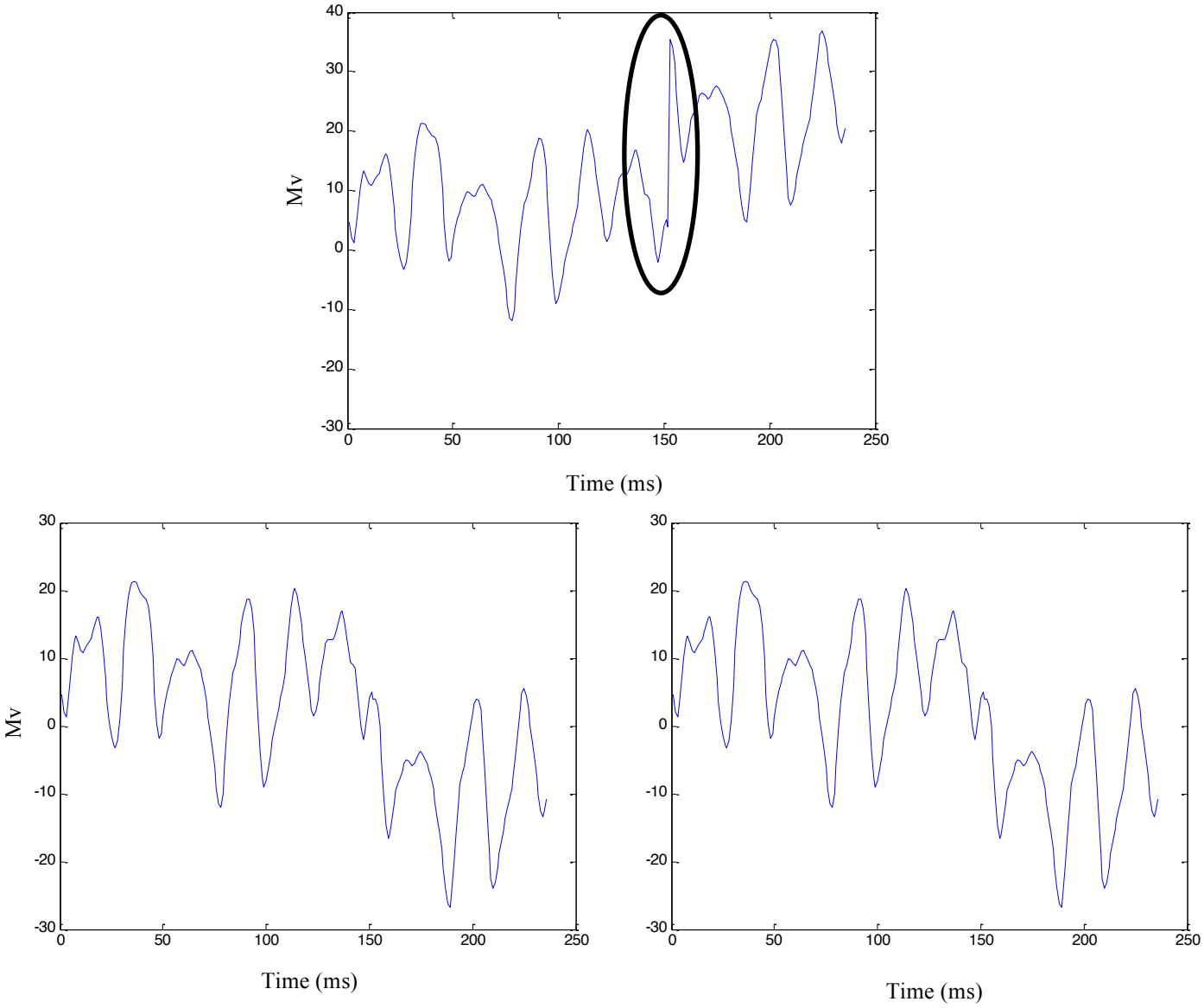

Figure A10.5. All panels show raw time-series data from passive participant 8 in the GSLS condition, trial 68 at ch. 60. Top panel shows raw time-series with discontinuity between time-points 152-153 (circled in black). Bottom right panel shows time-series after version III of our method was applied with first-pass Z-score threshold = 5 and second pass Z-score threshold = 6. Bottom left panel shows time–series after version III of our method was applied with first pass Z-score threshold = 7 and second pass Z-score threshold = 8. One can see that in both instances (bottom panels) the two-pass Z-score thresholds have captured discontinuity and maintained variance within the time-series.

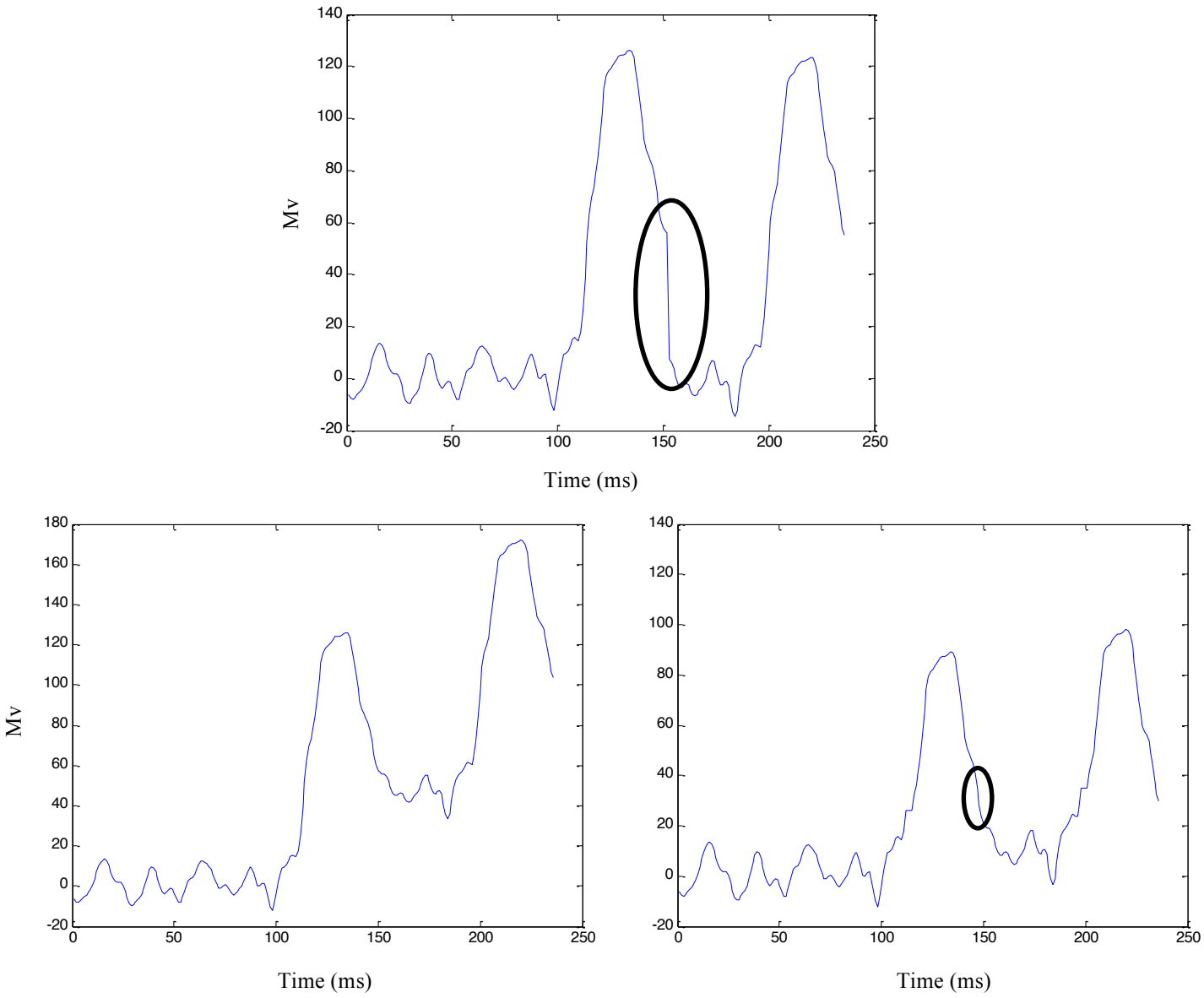

Figure A10.6. All panels show raw time-series data from passive participant 8 in the GSLS condition, trial 76 at ch. 20. Top panel shows raw time-series with discontinuity between time-points 152-154 (circled in black). Bottom right panel shows time-series after version III of our method was applied with first-pass Z-score threshold = 6 and second pass Z-score threshold = 7. Bottom left panel shows time–series after version III of our method was applied with first pass Z-score threshold = 7 and second pass Z-score threshold = 8. One can see that in the bottom right panel, discontinuity appears to have been resolved but in actual fact the smaller of the two jumps remains (circled in black). In the bottom left panel, both jumps have been captured by the Z-score thresholds.

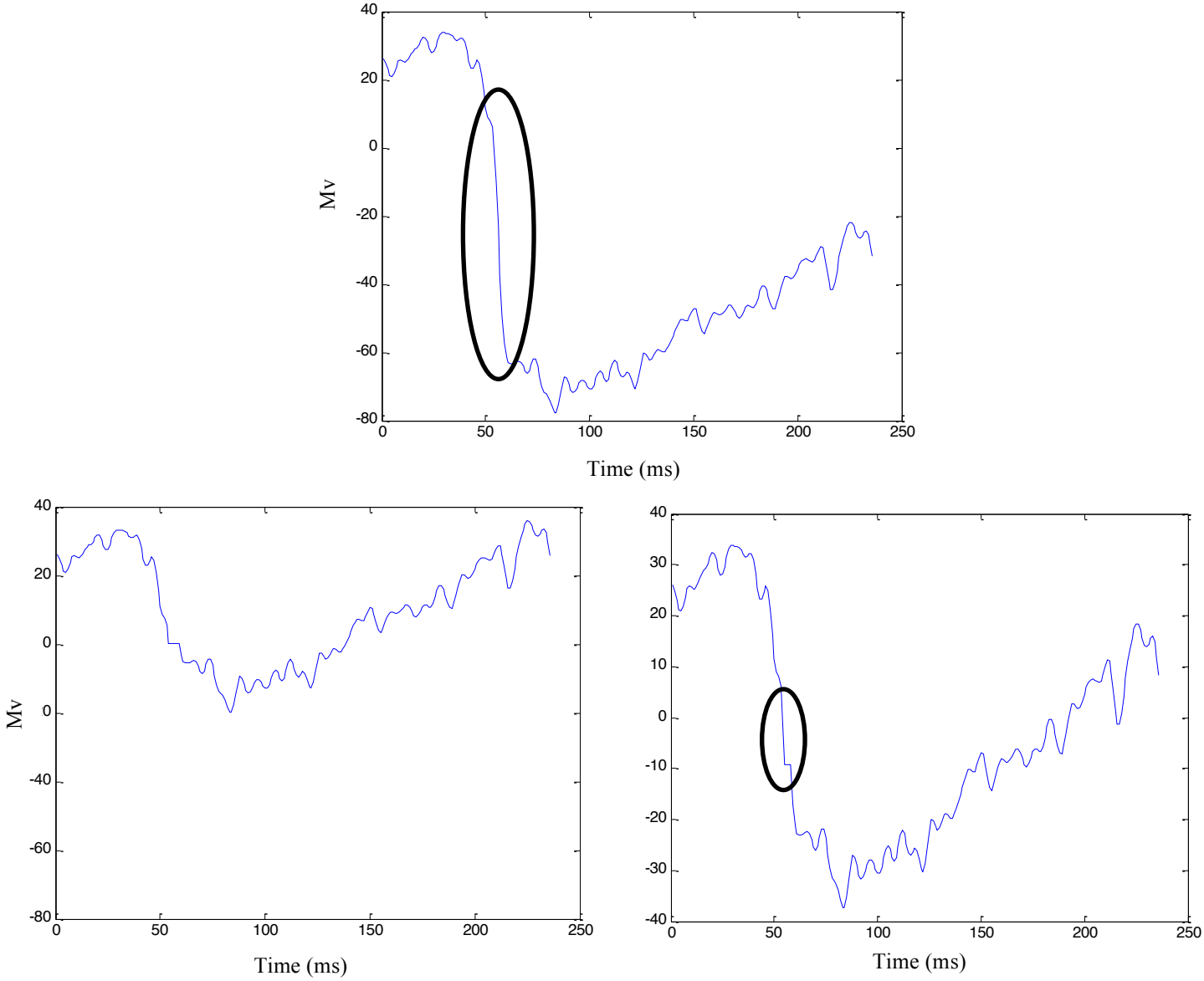

Figure A10.7. All panels show raw time-series data from active participant 8 in the GDLS condition, trial 144 at ch. 53. Top panel shows ra time-series with discontinuity between time-points 16-21 (circled in black). Bottom right panel shows time-series after version III of our method was applied with first-pass Z-score threshold = 7 and second pass Z-score threshold = 7. Bottom left panel shows time–series after version III of our method was applied with first pass Z-score threshold = 7 and second pass Z-score threshold = 8. One can see in the bottom right panel, some jumps have been corrected although there is still discontinuity within the data. The bottom left panel shows that all discontinuity was resolved whilst variance within the data was preserved.

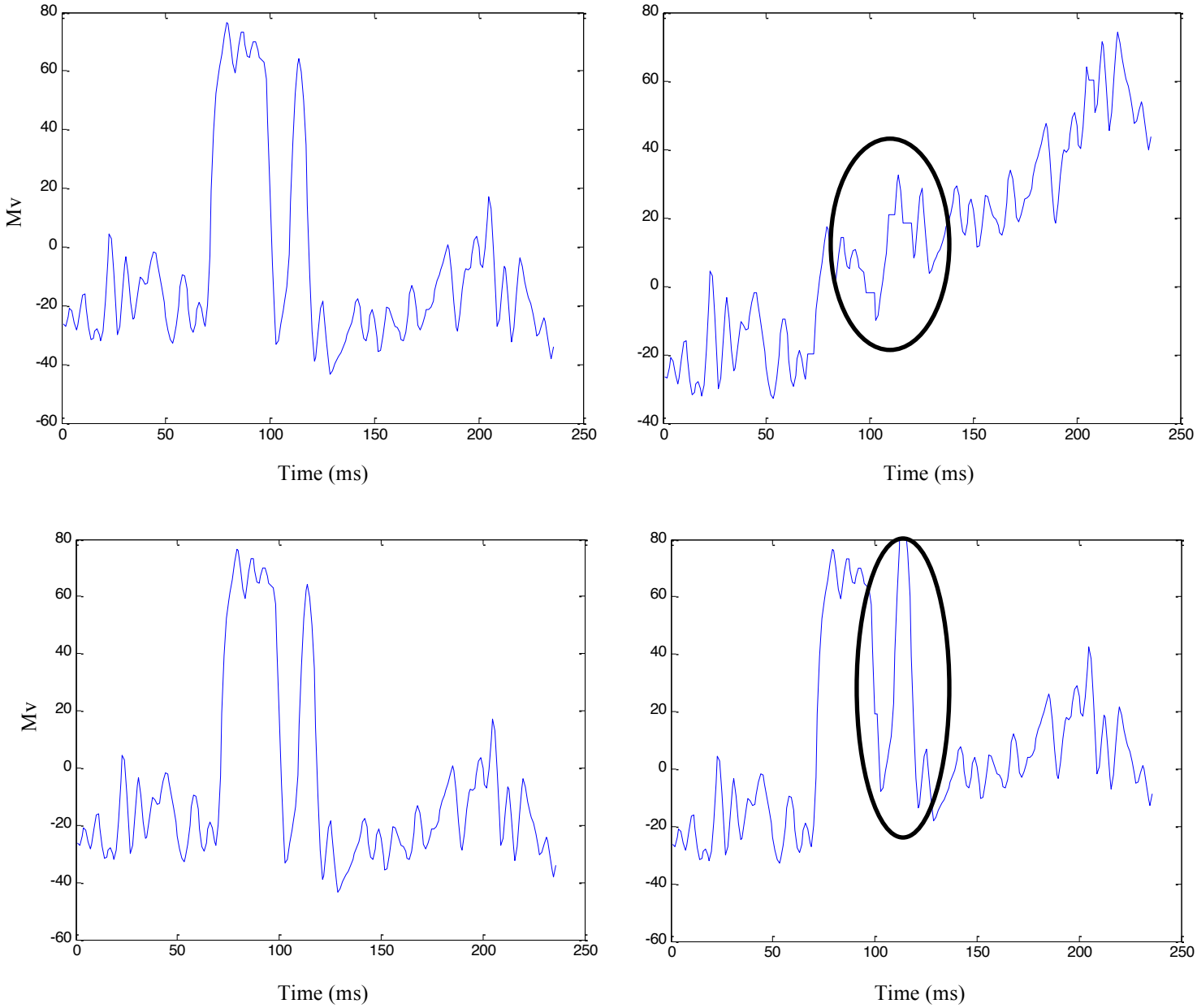

Figure A10.8. All panels show raw time-series data from active participant 9 in the GDLS condition, trial 126 at ch. 24. Top left panel shows raw time-series with a large amount of variance. Top right panel shows time-series after version III of our method was applied with first-pass Z-score threshold = 3 and second pass Z-score threshold = 4. Bottom right panel shows time–series after version III of our method was applied with first pass Z-score threshold = 8 and second pass Z-score threshold = 7. Bottom left panel shows time-series after version III of our method was applied with first pass Z-score threshold = 7 and second pass Z-score threshold = 8. One can see that in the top right panel, low Z-score thresholds have corrected the variance and distorted the shape of the time-series (circled in black). In the bottom right panel, one can see that having a lower secondary Z-score threshold has also distorted the shape of the data (circled in black). The bottom left panel shows the time-series was not distorted with a first pass Z-score threshold of 7 and a secondary threshold of 8; thus in this case the integrity of the raw data was preserved despite there being a high level of variance within the data.

Appendix 11: Histograms of trials representing the Sum Squared Error (SSE) between the raw time-series and the re-aligned time-series for participants in the sedated condition

Here we present histograms of trials for each participant from the sedation dataset. The x-axis represents the size of the Sum Squared Error (SSE) between the raw time-series and the re-aligned time-series after application of Version III of our method for re-aligning discontinuity (discussed in Chapter 8).

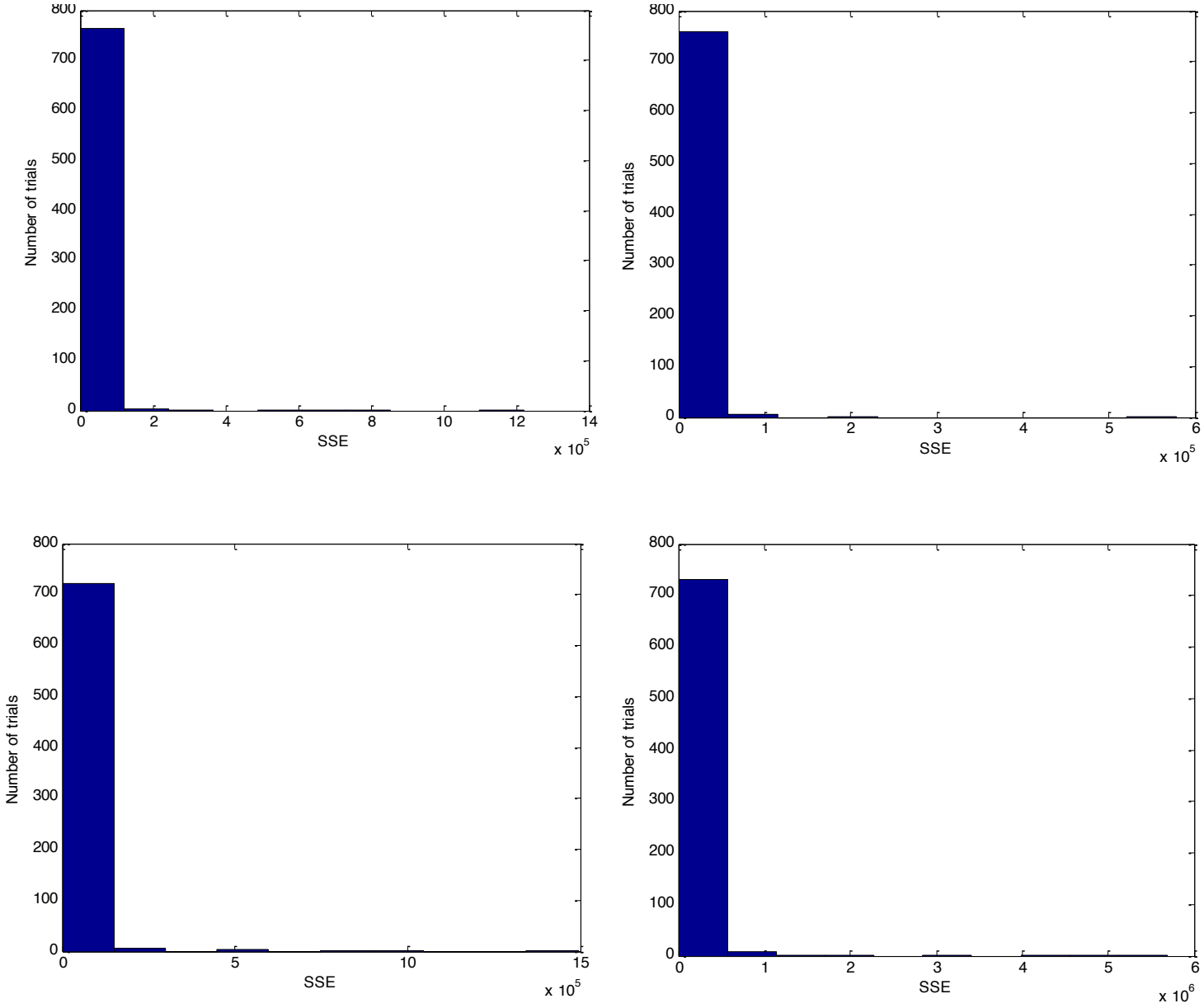

Figure A11.1. Histograms of the error difference between raw data trials and re-aligned trials (after version III of the method for re-alignment) for participants 02 (top left), 05 (top right), 06 (bottom left) and 07 (bottom right) of the sedation study.

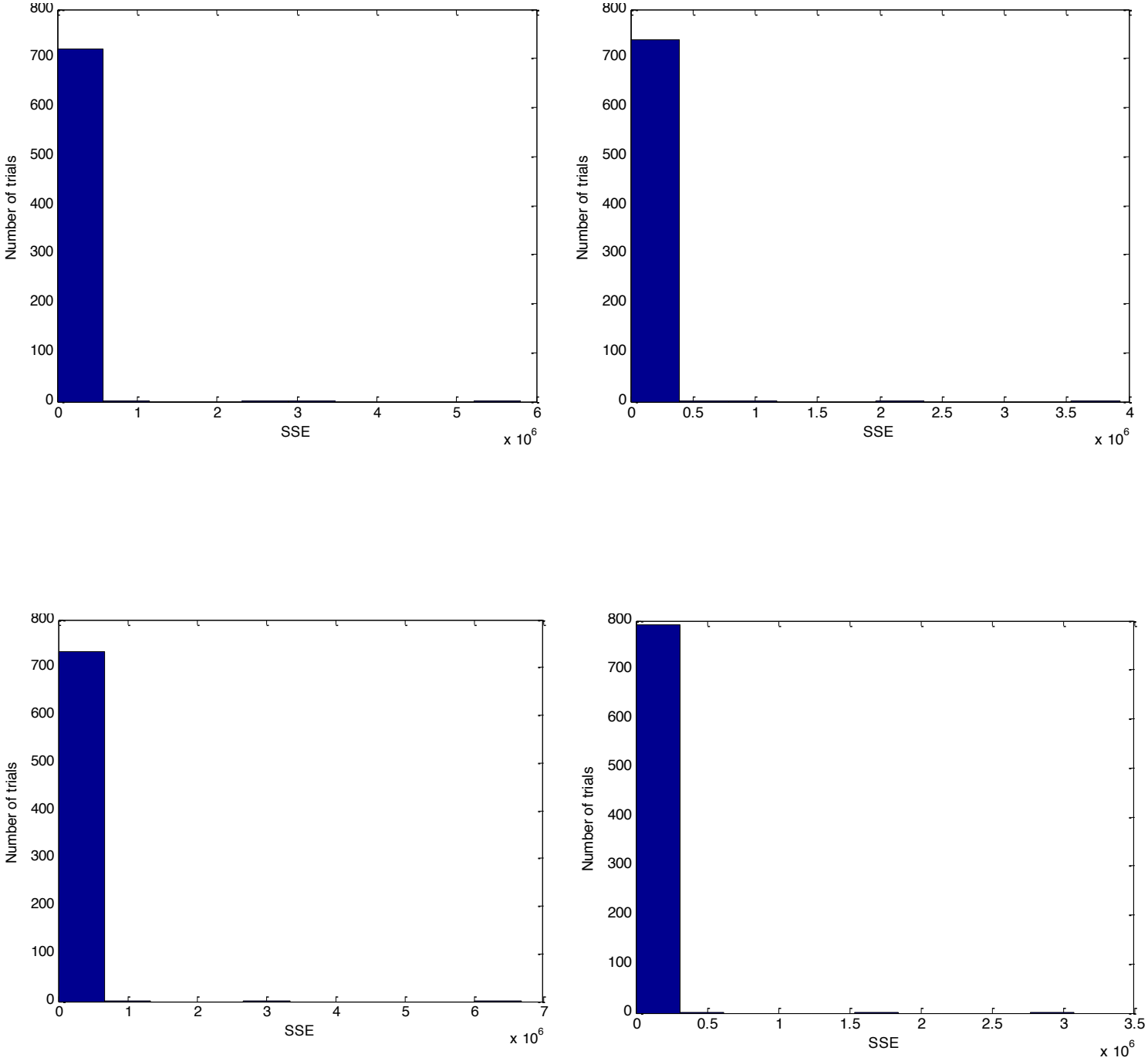

Figure A11.2. Histograms of the error difference between raw data trials and re-aligned trials (after version III of the method for re-alignment) for participants 08 (top left), 09 (top right), 13 (bottom left) and 16 (bottom right) of the sedation study.

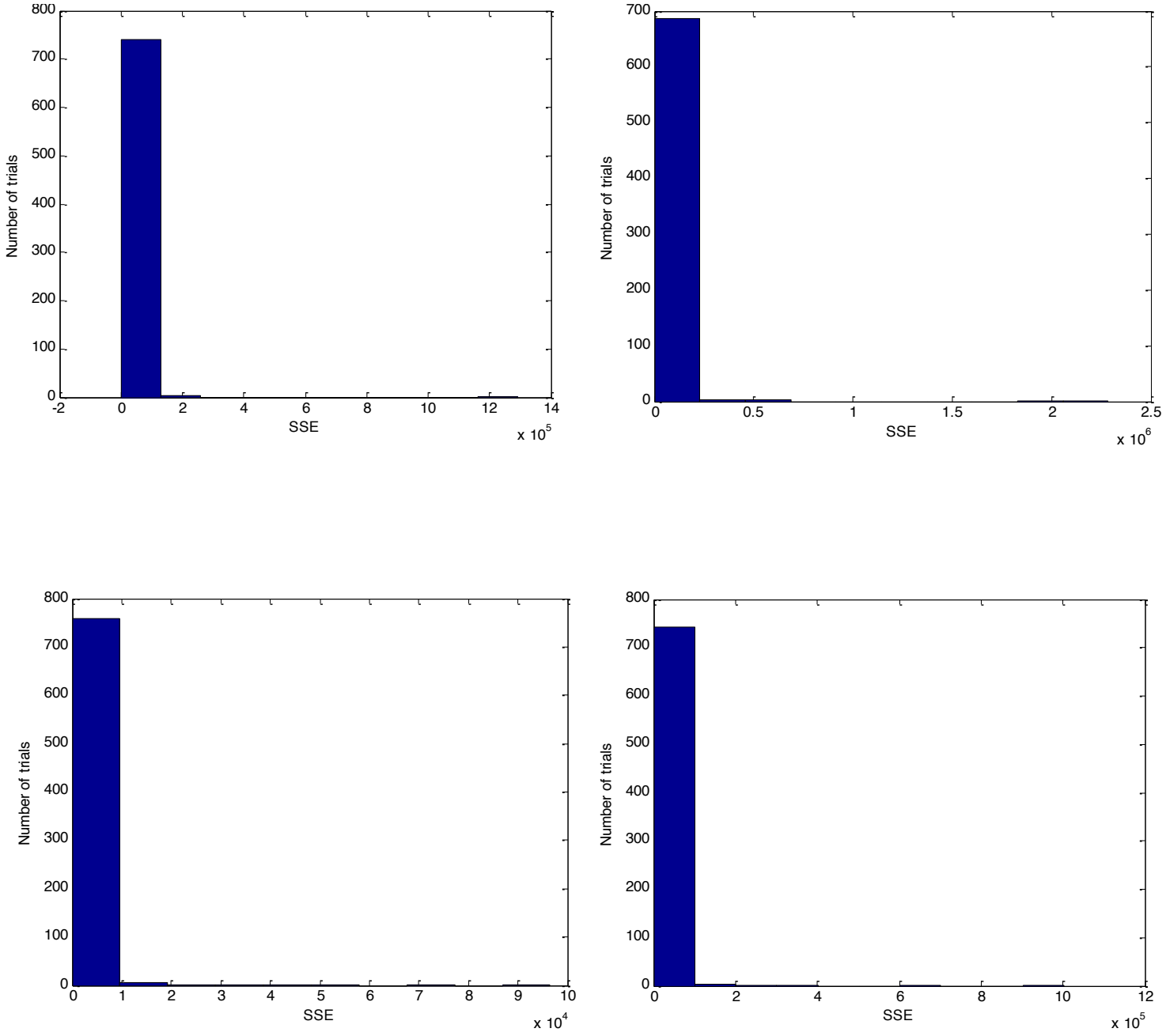

Figure A11.3. Histograms of the error difference between raw data trials and re-aligned trials (after version III of the method for re-alignment) for participants 17 (top left), 18 (top right), 20 (bottom left) and 22 (bottom right) of the sedation study.

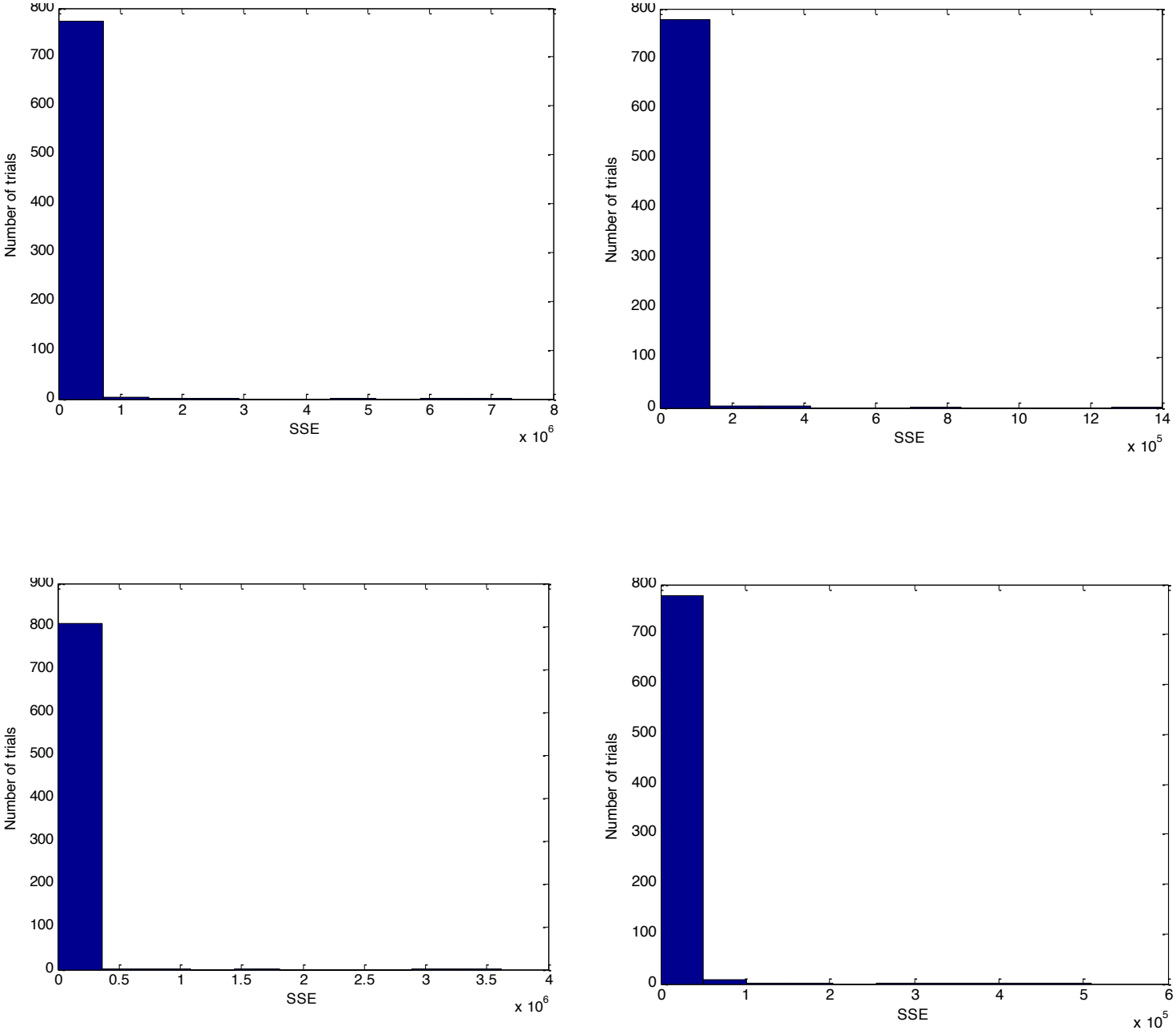

Figure A11.4. Histograms of the error difference between raw data trials and re-aligned trials (after version III of the method for re-alignment) for participants 23 (top left), 24 (top right), 26 (bottom left) and 27 (bottom right) of the sedation study.

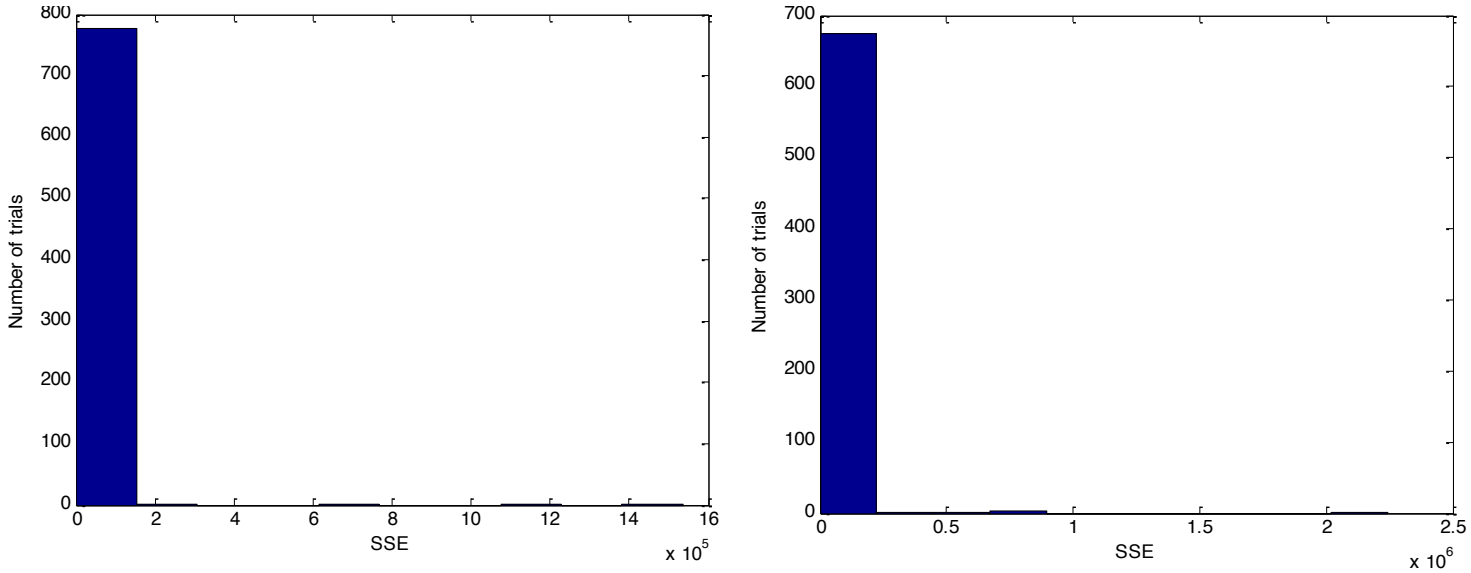

Figure A11.5. Histograms of the error difference between raw data trials and re-aligned trials (after version III of the method for re-alignment) for participants 28 (left) and 29 (right) of the sedation study.

References

Alonso-Nanclares, L., Gonzalez-Soriano, J., Rodriguez, J. R., & DeFelipe, J. (2008). Gender differences in human cortical synaptic density, *Proceedings of the National Academy of Sciences of the United States of America,* 105, (38), 14615-14619.

Altman, D., G. & Bland, J. M. (2005). Standard deviations and standard errors, *British Medical Journal*, 331, 903.

Auksztulewicz, R. & Friston, K. (2015). Attentional Enhancement of Auditory Mismatch Responses: a DCM/MEG Study, *Cerebral Cortex*, 25, (1), 1-11.

Azevedo, F. A., Carvalho, L. R., Grinberg, L. T., Farfel, J. M., Ferretti, R. E., Leite, R. E., et al. (2009). Equal numbers of neuronal and nonneuronal cells make the human brain an isometrically scaled-up primate brain, *Journal of Comparative Neurology,* 513, (5), 532-541.

Baars, B. (1988). A Cognitive Theory of Consciousness, Cambridge University Press, New York.

Baars, B. (1996). Understanding Subjectivity: Global Workspace Theory and the Resurrection of the Observing Self, *Journal of Consciousness Studies*, 3, (3), 211-216.

Baddeley, A., D. & Hitch, G. (1974). Working Memory, *Psychology of Learning and Motivation*, 8, 47-89.

Baluch, F. & Itti, L. (2011) . Mechanisms of top-down attention, *Trends in Neurosciences*, 34, (4), 210-224.

Bauer, R. M. (1984). Autonomic recognition of names and faces in prosopagnosia: A neuropsychological application of the guilty knowledge test, *Neuropsychologia*, 22, (4), 457-469.

Bekinschtein, T., Dehaene, S., Rohaut, B., Tadel, F., Cohen, L., & Naccache, L. (2009). Neural signature of the conscious processing of auditory regularities, *PNAS*, 106, (5), 1672-1677.

Berti, A., & Rizzolatti, G. (1992). Visual Processing without Awareness: Evidence from Unilateral Neglect, *Journal of Cognitive Neuroscience*, 4, (4), 345-351.

Block, N. (2005). Two neural correlates of consciousness, *TRENDS in Cognitive Sciences*, 9, (2), 46-52.

Boly, M., Garrido, M., A., Gosseries, O., Bruno, MA., Boveroux, P., Schnakers, C., Massimini, M., Litvak, V., Laureys, S., & Friston, K. (2011). Preserved Feedforward But Impaired Top-Down Processes in the Vegetative State, *Science*, 332, 858-861.

Boly, M., Faymonville, M. E., Schnakers, C., Peigneux, P., Lambermont, B., Phillips, C., Lancellotti, P., Luxen, A., Lamy, M., Moonen, G., Maquet, P. & Laureys, S. (2008). Perception of pain in the minimally conscious state with PET activation: an observational study, *Lancet Neurology*, 7, 1013-1020.

Boly, M., Faymonville, M. E., Peigneux, P., Lambermont, B., Damas, F., Luxen, A., Lamy, M., Moonen, G., Maquet, P. & Laureys, S. (2005). Cerebral processing of auditory noxious stimuli in severely brain injured patients: Differences between VS and MCS, Neuropsychological Rehabilitation, 15, (3/4), 283-289.

Chalmers, D. (1995). Facing Up to the Problem of Consciousness. *Journal of consciousness studies*, 2, (3), 200-219.

Chennu, S., Noreika, V., Gueorguiev, D., Blenkmann, A., Kochen, S., Ibáñez, A., Owen, A. M., Bekinschtein, T. A. (2013). Expectation and Attention in Hierarchical Auditory Prediction, *The Journal of Neuroscience*, 33, (27), 11194-11205.

Crick, F., & Koch, C. (1990). Towards a neurobiological theory of consciousness, *The Neurosciences*, 2, 263-275.

Crick, F., & Koch, C. (2003). A framework for consciousness, *Nature Neuroscience*, 6, (2), 119-126.

Dehaene, S., Kerszberg, M., & Changeux, JP. (1998). A neuronal model of a global workspace in effortful cognitive tasks, *Neurobiology*, 95, 14529-14534.

Del Cul, A., Baillet, S. & Dehaene, S. (2007). Brain dynamics underlying the nonlinear threshold for access to consciousness, *PLoS Biology*, 5, 260.

Dennett, D. (1978). *Brainstorms*, Bradford Books, New York.

Felleman, D. J., & Van Essen, D. C. (1991). Distributed hierarchical processing in the primate cerebral cortex, *Cerebral Cortex,* 1, (1), 1-47.

Fischer, C., Luaute, J., Adeleine, P., & Morlet, D. (2004). Predictive value of sensory and cognitive evoked potentials for awakening from coma, *Neurology*, 63, 669.

Fisher, R. A. (1925). *Statistical Methods for Research Workers*, University of Michigan Library.

Freidman, D., Cycowicz, Y. M., Gaeta, H. (2001). The novelty P3: an event-related brain potential (ERP) sign of the brain's evaluation of novelty, *Neuroscience and Biobehavioural Reviews*, 25, 355-373.

Friston, K. J. (2010). The free-energy principle: a unified brain theory?, *Nature Neuroscience,* 11, 127-138.

Friston, K. J., Price, C. J., Fletcher, P., Moore, C., Frackowiak, R. S. J. & Dolan, R. J. (1996). The Trouble with Cognitive Subtraction, *Neuroimage*, 4, 97-104.

Friston , K. J., Holmes, A. P., Worsley, K. J., Poline, J.-P., Frith, C. D. & Frackowiak, R. S. J. (1995). Statistical Parametric Maps in Functional Imaging: A General Linear Approach, *Human Brain Mapping*, 2, 189-210.

Giacino, J. T., Ashwal, S., Childs, N., Cranford, R., Jennett, B., Katz, D. I., Kelly, J. P., Rosenberg, J. H., Whyte, J., Zafonte, R. D., & Zasler, N. D. (2002). The Minimally Conscious State – Definition and Diagnostic Criteria, *Neurology*, 58, (3), 349-353.

Goodale, M. A., & Milner, D. A. (1992). Separate visual pathways for perception and action, *Trends in Neuroscience*, 15, (1), 20-25.

Haenschel, C., Vernon, D. J., Dwivedi, P., Gruzelier, J. H., & Baldeweg, T. (2005). Event-Related Brain Potential Correlates of Human Auditory Sensory Memory-Trace Formation, *The Journal of Neuroscience*, 25, (45), 10494-10501.

Holcomb, P. J. (1993). Semantic priming and stimulus degradation: Implications for the role of the N400 in language processing, *Psychophysiology*, 30, 47-61.

Humphreys, G. W., Hodsoll, J., & Campbell, C. (2005). Attending but not seeing: The "other race" effect in face and person perception studied through change blindness, *Visual Cognition*, 12, (1), 249-262.

Johnson-Laird, P. N. (1988). *The Computer and the Mind*, Harvard University Press.

Kilner, J. M. & Friston, K. J. (2010). Topological Inference for EEG and MEG, *The Annals of Applied Statistics*, 4, (3), 1272-1290.

Kilner, J. M., Kiebel, S. J. & Friston, K. J. (2004). Applications of random field theory to electrophysiology, *Neuroscience Letters*, 374, 174-178.

Koch, C. (2004). *The Quest For Consciousness: A Neuroscientific Approach*, Roberts & Co.

Koch, C., & Crick, F. (2001). The zombie within, *Nature*, 411, 893.

Lamme, V., A., F. (2004). Separate neural definitions of visual consciousness and visual attention; a case for phenomenal awareness, *Neural Networks*, 17, 861-872.

Loveman, E., Van Hooff, J. C., & Smith, D. C. (2001). The auditory response as an awareness monitor during anesthesia, *British Journal of Anesthesia*, 86, (4), 513-518.

Marsh, B., White, M., Morton, N., & Kenny, G. N. (1991). Pharmacokinetic model driven infusion of propofol in children, *British Journal of Anaesthesia,* 67, (1), 41-48.

May, P., J., C. & Tiitinen, H. (2010). Mismatch Negativity (MMN), the deviance-elicited auditory deflection, explained, *Psychophysiology*, 27, 66-122.

McIntosh, A. R., Lobaugh, N. J. (2004). Partial least squares analysis of neuroimaging data: applications and advances, *NeuroImage*, 23, 250-263.

Milner, A. D., & Goodale, M. A. (1995). *The Visual Brain in Action*, Oxford University Press, Oxford, United Kingdom.

Morgan, H., Klein, C., Boehm, S. G., Shapiro, K., & Linden, D. (2008). Working Memory for Faces Modulates P300, N170, and N250r, *Journal of Cognitive Neuroscience,* 20, (6), 989-1002.

Näätänen, R., Jacobsen, T., Winkler, I. (2005). Memory-based or afferent processes in mismatch negativity (MMN): A review of the evidence, *Psychophysiology*, 42, 25-32.

Näätänen, R., Tervaniemi, M., Sussman, E., Paavilainen, P., Winkler, I. (2001). "Primitive intelligence" in the auditory cortex, *Trends in Neuroscience*, 24, 283-288.

Näätänen, R., Paavilainen, P., Titinen, H., Jiang, D., Alho, K. (1993). Attention and mismatch negativity, *Psychophysiology*, 30, (5), 436-450.

Näätänen, R. (1992). Attention and Brain Function, Lawrence Erlbaum Associates, Inc Publishers, Hillsdale New Jersey.

O'Reilly, R. C., & Munakata, Y. (2000). *Computational explorations in cognitive neuroscience: Understanding the mind by simulating the brain* MIT press.

Pegado, P., Bekinschtein, T., Chausson, N., Deheane, S., Cohen, L., & Naccache, L. (2010). Probing the lifetimes of auditory novelty detection processes, *Neuropsychologia*, 48, 3145-3154.

Phillips, C., Mattout, J., Rugg, M, D., Maquet, P., & Friston, K. (2005). An empirical Bayesian solution to the source reconstruction problem in EEG, *NeuroImage*, 24, (4), 997-1011.

Polich, J. (2007). Updating P300: An integrative theory of P3a and P3b, *Clinical Neurophysiology*, 118, (10), 2128-2148.

Prinzmetal, W., Nwachuku, I., Bodanski, L., Blumenfeld, L., & Shimizu, N. (1997). The Phenomenology of Attention, *Consciousness and Cognition*, 6, 372-412.

Rémi-King, J., Gramfort, A., Schurger, A., Naccache, L. & Dehaene, S. (2014). Two Distinct Dynamic Modes Subtend the Detection of Unexpected Sounds, PLOS one, 9, (1).

Rosenthal, D. M. (2005). Higher-order thoughts and the appendage theory of consciousness, Philosophical Psychology, 6, (2), 155-167.

Sergent, C., Baillet, S. & Dehaene, S. (2005). Timing of the brain events underlying access to consciousness during the attentional blink, *Nature Neuroscience*, 8, 1391-1400.

Seydell-Greenwald, A., Greenberg, A. & Rauschecker, J. P. (2014). Are You Listening? Brain Activiation Associated With Sustained Nonspatial Auditory Attention in the Presence and Absence of Stimulation, *Human Brain Mapping*, 35, 2233-2252.

Sperry, R. W. (1961). Cerebral Organization and Behaviour, *Science*, 133, 1749-1757.

Tiitinen, H., May, P., Reinikainen, K. & Näätänen, R. (1994). Attentive novelty detection in humans is governed by pre-attentive sensory memory, Letters to Nature, *Nature*, 372, 90-92.

Tudor, M., Tudor, L., & Tudor, K. I. (2005). Hans berger (1873-1941)--the history of electroencephalography. [Hans Berger (1873-1941)--povijest elektroencefalografije] *Acta Medica Croatica : Casopis Hravatske Akademije Medicinskih Znanosti,* 59, (4), 307-313.

Wacongne, C., Changeux, JP., & Dehaene, S. (2012). A Neuronal Model of Predictive Coding Accounting for the Mismatch Negativity, *The Journal of Neuroscience*, 32, (11), 3665-3678.

Wacongne, C., Labyt, E., Wassenhove, V., Bekinschtein, T., Naccache, L., & Dehaene, S. (2011). Evidence for a hierarchy of predictions and prediction errors in human cortex, *PNAS*, 108, (51), 20754-20759.

Yuval-Greenberg, S., Merriam, E. P. & Heeger, D. J. (2014). Spontaneous Microsacades Reflect Shifts in Covert Attention, *The Journal of Neuroscience*, 34, (41), 13693-13700.